

# Compilation of Thermal Properties of Hydrogen in Its Various Isotopic and Ortho-Para Modifications

By Harold W. Woolley, Russell B. Scott, and F. G. Brickwedde

New developments in science and industry are aided by accurate knowledge of the behavior of important substances. The great abundance of chemical processes and compounds in which hydrogen is involved make it of particular interest. The experimental and derived data presented here for hydrogen extend over a large range of temperature. Low temperatures are required for the liquid and solid, and moderate and high temperatures occur in chemical reactions.

The available thermal data for  $H_2$ , HD, and  $D_2$  in solid, liquid, and gaseous states have been brought together, including the distinctive properties of ortho and para forms of  $H_2$  and  $D_2$ . Some data not previously published have been added. The thermal data include thermodynamic functions for the ideal gas state, equilibrium constants, data of state, viscosity, and thermal conductivity with dependence on the pressure, vapor pressure, solid-liquid equilibria, specific heats, and latent heats. Values of state derivatives useful in thermodynamic calculations have been given for normal hydrogen, and the related differences between thermodynamic functions for real and ideal gas states have been evaluated. A temperature entropy diagram for normal  $H_2$  in the range of experimental data is also given. The compiled thermal properties of hydrogen are presented in 38 tables, 33 graphs, and numerous equations. The sources of the data have been given in an extensive bibliography.

## I. Introduction

It was recommended by the National Research Council Committee on Thermal Data for Chemical Industries<sup>1,2</sup> and by others that the thermal data on substances of industrial importance should be reexamined with the intention of preparing consistent tables of thermal data of especial interest to chemical engineers and investigators.

In this paper thermal data on hydrogen in its various isotopic and ortho-para modifications are compiled and correlated. Data on properties of the gaseous, liquid, and solid states are presented in tables and graphs, and by use of formulas. Thermodynamic properties are given for the ideal gas state. In addition, tables based on the PVT data for the real gas furnish the additional information required for the calculation of the thermodynamic properties of the real gas. For the con-

densed phases, directly observable properties are given. Because of the industrial importance of flow and heat-transfer problems, correlations of viscosity and of thermal conductivity are included and their dependence upon pressure discussed briefly. A number of topics are discussed in detail to explain the fundamental principles involved. Most of the data included were taken from published papers. However, a small proportion are based on unpublished measurements made at the Bureau.

The following are the symbols and values of physical constants and conversion factors used in this paper.

### 1. Symbols

Many symbols that are not used extensively in this paper have been omitted from this list.

$A$ , constant in an equation for a PVT isotherm.

$B$ , second virial coefficient in equation of state of gas.

$B_r$ , rotational spectroscopic constant.

<sup>1</sup> Division of Chemistry and Chemical Technology, National Research Council.

<sup>2</sup> F. Enssell Behowsky, Chairman, 1938 to 1947.

- b*, *b*, constant in an equation for a PVT isotherm; also, a constant in an equation of state.
- C*, *C*, constant in an equation for a PVT isotherm; also, the Sutherland constant in a viscosity formula.
- C'*, constant in an equation for a PVT isotherm.
- C<sub>p</sub><sup>o</sup>*, molar heat capacity (molar specific heat) at constant pressure for ideal gas.
- C<sub>s</sub>*, molar heat capacity (molar specific heat) along a saturation curve.
- C<sub>v</sub><sup>o</sup>*, molar heat capacity (molar specific heat) at constant volume for ideal gas.
- c*, *c*, velocity of light; also a constant in an equation for a PVT isotherm.
- c<sub>2</sub>*, radiation constant  $hc/k$ .
- D<sub>r</sub>*, rotational spectroscopic constant.
- E*, a thermodynamic function, internal energy per mole.
- E<sup>o</sup>*, *E* for a substance in the ideal gaseous state.
- E<sub>0</sub><sup>o</sup>*, *E<sup>o</sup>* at the absolute zero of temperature when for each molecule the energy associated with internal degrees of freedom is at its lowest quantized value.
- F*, a thermodynamic function, molar free energy  $F = E + PV - TS$ .
- F<sup>o</sup>*, *F* for a substance in the ideal gaseous state at a pressure of 1 atmosphere.
- F<sub>r</sub>*, rotational spectroscopic constant.
- F<sub>r,s</sub>*, or *F*, term value.
- f*, a thermodynamic function, fugacity.
- G<sub>v</sub>*, vibrational term value.
- g*, statistical weight of a quantum level.
- H*, a thermodynamic function, molar heat content or enthalpy,  $H = E + PV$ .
- H<sup>o</sup>*, *H* for a substance in the ideal gaseous state.
- H<sub>r</sub>*, rotational spectroscopic constant.
- h*, Planck's constant.
- i*, nuclear spin.
- J*, rotational quantum number.
- K*, equilibrium constant.
- k*, *k*, Boltzmann constant; also, thermal conductivity.
- L<sub>v</sub>*, latent heat of vaporization.
- M*, molecular weight.
- m*, reduced mass for molecule.
- N*, total number of molecules considered.
- N<sub>v</sub>*, number of molecules in a given quantum level.
- N<sub>0</sub>*, Avogadro's number.
- P*, pressure.
- P<sub>c</sub>*, pressure at the critical point.
- P<sub>n</sub>*, pressure of 1 standard atmosphere,  $1.01325 \times 10^6$  dynes  $\text{cm}^{-2}$  by definition.
- p*, momentum corresponding to generalized coordinate *q*.
- q*, a generalized coordinate.
- R*, molar gas constant.
- r*, atomic separation.
- r<sub>0</sub>*, atomic separation *r* for minimum potential energy.
- S*, a thermodynamic function, molar entropy.
- S<sup>o</sup>*, *S* for a substance in the ideal gaseous state at a pressure of 1 atmosphere.
- T*, absolute temperature on the Kelvin scale.
- T<sub>c</sub>*, temperature *T* at critical point.
- T<sub>0</sub>*, Kelvin temperature *T* of the ice point, that is, of 0° C.
- U*, intramolecular potential energy.
- U<sub>11</sub>*, ratio of mean free path lengths for diffusion and viscosity.
- V*, molar volume.
- V<sub>c</sub>*, molar volume at the critical point.
- V<sub>v</sub>*, molar volume of gas at 1-atmosphere pressure and the ice point.
- v<sub>l</sub>*, molar volume of liquid at zero pressure.
- v*, vibrational quantum number.
- Z*, abbreviation for  $PV/RT$ .
- $\gamma$ , ratio of specific heats,  $C_p/C_v$ .
- $\epsilon$ , energy for a quantum state.
- $\eta$ , viscosity.
- $\theta$ , a characteristic Kelvin temperature for a crystal lattice in Debye's theory of specific heats.
- $\Lambda$ , length of mean free path.
- $\mu$ , Joule-Thomson coefficient.
- $\xi$ , fractional increase in atomic separation beyond that for minimum potential energy.
- $\rho$ , density in Amagat units.
- $\sigma$ , a correlation function for PVT data.
- $\chi$ , a function in one equation of state.
- $\varphi$ , a correlation function for PVT data.

## 2. Values Used for Some Physical Constants and Conversion Factors

(Numbers in parentheses refer to the references given below)

*c* (velocity of light) =  $2.99776 \times 10^{10}$  cm sec<sup>-1</sup> (1).

*c<sub>2</sub>* (radiation constant) =  $\frac{hc}{k} = \frac{N_0 hc}{R} = 1.4384$  cm deg (2).

*h* (Planck's constant) =  $6.624 \times 10^{27}$  cm sec (1).

*N<sub>0</sub>* (Avogadro number) =  $6.0228 \times 10^{23}$  mole<sup>-1</sup> (1).

$P_0$  (pressure of standard atmosphere) =  $1.01325 \times 10^6$  dynes  $\text{cm}^{-2}$  (3).

$R$  (molar gas constant) =  $N_0 k = 8.3144 \times 10^7$  erg  $\text{mole}^{-1} \text{deg}^{-1}$  (1).

= 1.98714 thermochemical cal  $\text{mole}^{-1} \text{deg}^{-1}$  (4).

$T_0$  (Kelvin temperature of ice point) =  $273.16^\circ \text{K}$  (5).

Atomic weight of hydrogen ( $\text{H}^1$ ) on chemical scale = 1.000786 (1).

Atomic weight of deuterium ( $\text{D}$  or  $\text{H}^2$ ) on chemical scale = 2.01418 (1).

1 thermochemical calorie = 4.1833 international joules (5).

1 international joule (NBS) = 1.000165 absolute joules (6).

(1) Raymond T. Birge, *Rev. Modern Phys.* **13**, 233 (1941).

(2) Birge's value (*Rev. Modern Phys.* **13**, 233 (1941)) adjusted for later NBS value of the ratio international coulomb/absolute coulomb = 0.99985; see also reference (7).

(3) Definition.

(4) Birge's value (*Rev. Modern Phys.* **13**, 233 (1941)) adjusted to thermochemical calorie and NBS value for ratio international joule/absolute joule.

(5) Definition.

(6) NBS Technical News Bulletin **31**, 49 (1947).

(7) R. W. Curtis, R. L. Driscoll, and C. L. Critchfield, *J. Research NBS* **28**, 133 (1942).

## II. Thermodynamic Properties for the Hydrogens in the Ideal Gas State

### 1. General Principles of Calculation

For a gas in a state of extreme rarefaction the energy of interaction between molecules forms a minute part of the total energy of the gas. At such low pressures the thermodynamic properties of the gas may be calculated from the spectroscopically determined energies of the single molecules and the general physical constants without considering the energy of interaction of one molecule with another. Some thermodynamic properties, as for example molar entropy and free energy, do not approach a definite value as the pressure of the gas goes to zero. For this reason, values of thermodynamic functions of a gas at low pressure are often indicated by giving values for a pressure of 1 atm for a fictitious ideal gas having in the limit of low pressure the same thermodynamic functions as the actual gas. The result is then said to be for the gas at a pressure of 1 atmosphere in the hypothetical ideal gas state. Data of state may be used to calculate the differ-

ences between properties in the real and ideal gas states.

The procedure for calculating the thermodynamic properties of a substance in the ideal gas state has been discussed by many writers [3, 30, 31, 32].<sup>3</sup>

In outline, it involves the following ideas: The average number  $n_1$  of molecules in a quantum state of energy  $\epsilon_1$  is related to the average number,  $n_2$ , of molecules in another state of energy  $\epsilon_2$  by the Boltzmann distribution law

$$n_1/n_2 = e^{-\epsilon_1/kT}/e^{-\epsilon_2/kT} = e^{-(\epsilon_1-\epsilon_2)/kT}, \quad (2.1)$$

where  $k$  is the Boltzmann constant, and  $T$  is the absolute temperature.

As there are often several states having the same energy, the number of molecules in a given energy level<sup>4</sup> is also proportional to the number of states,  $g$ . If  $N_1, N_2, N_3, \dots$  are the numbers of molecules in the levels  $\epsilon_1, \epsilon_2, \epsilon_3, \dots$ , respectively, the number of molecules in any one level is

$$N_i = \frac{N g_i e^{-\epsilon_i/kT}}{g_1 e^{-\epsilon_1/kT} + g_2 e^{-\epsilon_2/kT} + \dots} = \frac{N g_i e^{-\epsilon_i/kT}}{\sum_j g_j e^{-\epsilon_j/kT}}, \quad (2.2)$$

where  $N$ , the total number of molecules being considered, is equal to  $\sum N_j$ . If properties are to be expressed on the basis of 1 mole,  $N$  is taken equal to Avogadro's number,  $N_0$ .

The quantum states are specified by means of quantum numbers, the integer values which certain natural variables have when a molecule has a stationary value of energy. The magnitude of the energy is generally expressed in terms of these numbers. In diatomic molecules, the quantum numbers of interest are  $J$ , the rotational quantum number,  $K$ , the rotational quantum number apart from spin, and  $v$ , the vibrational quantum number. The electronic state is also similarly quantized, and quantum numbers appropriate to it may likewise be assigned. The nuclear spins of the two constituent atoms are designated by  $i_1$  and  $i_2$ . In terms of these numbers, the statistical weight,  $g$ , of a level of a diatomic molecule composed of unlike atoms, as for example HD, is  $g_e(2i_1+1)(2i_2+1)(2J+1)$ , where  $g_e$  is the weight of the electronic level of the mole-

<sup>3</sup> Figures in brackets indicate the literature references at the end of this paper.

<sup>4</sup> The term *state* is used in the sense that two states differ if any of *all* the quantum numbers associated with the states are different. The term *level* is used to express the idea that the energy has a definite value. The statistical weight,  $g$ , of a level is the number of states having the energy which define the level. A level with more than one state is said to be degenerate.

cule. The ground electronic level of HD, and of H<sub>2</sub> and D<sub>2</sub>, also, is a singlet state, and accordingly  $g_e$  is 1.

The proton and deuteron spins are  $\frac{1}{2}$  and 1, respectively. For diatomic molecules composed of like atoms, as for example, H<sub>2</sub> and D<sub>2</sub>, there is a division of the rotational levels of the molecule into two groups referred to as the ortho and para series, one of which is composed of the even numbered and the other of the odd numbered rotational levels. Ordinarily, transitions between ortho and para levels are relatively rare, so that the gas can be considered as a mixture of two distinct components. The high temperature equilibrium mixture of the two forms is called the normal mixture, and the more abundant component of the normal mixture is called the ortho component. The statistical weights of the two series depends upon the quantum statistics applicable to the nuclei. For H<sub>2</sub> it is the Fermi-Dirac statistics, for D<sub>2</sub> the Bose-Einstein statistics.

#### Fermi-Dirac statistics:

$$\left. \begin{aligned} g \text{ (para series, even } J\text{'s)} &= \\ g_e (2i+1)i(2J+1) & \\ \\ g \text{ (ortho series, odd } J\text{'s)} &= \\ g_e (2i+1)(i+1)(2J+1) & \end{aligned} \right\} (2.3)$$

#### Bose-Einstein statistics:

$$\left. \begin{aligned} g \text{ (ortho series, even } J\text{'s)} &= \\ g_e (2i+1)(i+1)(2J+1) & \\ \\ g \text{ (para series, odd } J\text{'s)} &= \\ g_e (2i+1)i(2J+1) & \end{aligned} \right\} (2.4)$$

The energy per mole due to molecular rotation and intramolecular vibration is

$$E_{rot} = \sum N_{f, \epsilon} = \frac{N_0 \sum g_f \epsilon e^{-\epsilon/kT}}{\sum g_f e^{-\epsilon/kT}} \quad (2.5)$$

where the  $\epsilon$ 's are the energies of the rotational-vibrational levels relative to the lowest energy level of the molecule. The translational energy,  $3/2 N_0 kT$  or  $3/2 RT$ , is added to this to get  $E^0 - E_0^0$ , the total internal energy per mole for the ideal gas above the chosen zero in which there would be no translational energy and each mole-

cule would be in the lowest energy state available to any form of the molecule.<sup>5</sup>

$$E^0 - E_0^0 = 3/2 RT + N_0 \frac{\sum g_f \epsilon e^{-\epsilon/kT}}{\sum g_f e^{-\epsilon/kT}} \quad (2.6)$$

The superscript zero is used to indicate the ideal gas state.

The enthalpy  $H^0$ , the specific heats  $C_p^0$  and  $C_v^0$ , the entropy  $S^0$ , and the free energy  $F^0$  for the ideal gas state are derivable in accordance with familiar methods of thermodynamics from (1) the internal energy  $E^0 - E_0^0$ , (2) the equation of state  $PV = RT$ , and (3) the translational entropy  $S_t^0$  of an ideal gas of molecular weight  $M$ . The equations for these properties as functions of  $(\epsilon_j/kT)$  are

$$\frac{E^0 - E_0^0}{RT} = \frac{\sum g_j (\epsilon_j/kT) e^{-\epsilon_j/kT}}{\sum g_j e^{-\epsilon_j/kT}} + \frac{3}{2} \quad (2.7)$$

$$\frac{H^0 - E_0^0}{RT} = \frac{E^0 - E_0^0}{RT} + 1 \quad (2.8)$$

$$\frac{C_p^0}{R} = \frac{\sum g_j (\epsilon_j/kT)^2 e^{-\epsilon_j/kT}}{\sum g_j e^{-\epsilon_j/kT}} - \left( \frac{\sum g_j (\epsilon_j/kT) e^{-\epsilon_j/kT}}{\sum g_j e^{-\epsilon_j/kT}} \right)^2 + \frac{3}{2} \quad (2.9)$$

$$\frac{C_v^0}{R} = \frac{C_p^0}{R} + 1 \quad (2.10)$$

$$\frac{S^0}{R} = \ln \sum g_j e^{-\epsilon_j/kT} + \frac{\sum g_j (\epsilon_j/kT) e^{-\epsilon_j/kT}}{\sum g_j e^{-\epsilon_j/kT}} + \frac{S_t^0}{R} \quad (2.11)$$

$$\frac{S_t^0}{R} = \frac{5}{2} \ln T + 3/2 \ln M - \ln(P/P_0) + \ln \frac{(2\pi)^{3/2} R^{3/2}}{h^3 N_0^3 P_0} + \frac{5}{2} \quad (2.12)$$

$$\frac{S_i^0}{R} = \frac{3}{2} \ln T + 3/2 \ln M + \ln V + \ln \frac{(2\pi R)^{3/2}}{h^3 N_0^3} + \frac{5}{2} \quad (2.13)$$

$$\frac{F^0 - E_0^0}{RT} = \frac{H^0 - E_0^0 - TS^0}{RT} = -\ln \sum g_j e^{-\epsilon_j/kT} + \frac{5}{2} \frac{S_t^0}{R} \quad (2.14)$$

<sup>5</sup> Accordingly for orthohydrogen and para-deuterium  $E_0^0$  is not the internal energy at 0° K. For these substances at 0° K the internal energy above the chosen zero ( $J=0, s=0$ ) is the rotational energy per mole of molecules in the rotational level  $J=1$ . At 0° K internal energies of normal hydrogen and normal deuterium are respectively three-fourths the internal energy of orthohydrogen and one-third the internal energy of para-deuterium.

In eq 2.12,  $P$  and  $P_0$  are the pressure of the gas and standard atmospheric pressure, respectively, with both expressed in dynes  $\text{cm}^{-2}$ . The ratio  $P/P_0$  is the pressure expressed in atmospheres.

For a monatomic gas in which the ground state is so far below the others in energy that it alone makes appreciable contribution to the state-sum,  $\sum_j g_j e^{-\epsilon_j/RT}$ , eq 2.7 to 2.14 are simplified considerably. With  $\epsilon_1$ , the energy of the ground state, taken as zero, the state-sum reduces to the constant  $g_1$ .

As a result,  $(E^\circ - E_0^\circ)/RT = 3/2$ ;  $(H^\circ - E_0^\circ)/RT = 5/2$ ;  $C_p^\circ/R = 3/2$ ;  $C_v^\circ/R = 5/2$ ;  $S^\circ/R = \ln g_1 + S_1^\circ/R$ , and  $(F^\circ - E_0^\circ)/RT = -\ln g_1 + 5/2 - S_1^\circ/R$ . When the nuclear spin is included,  $g_1$  contains  $(2i+1)$  as a factor.

Normal hydrogen is a mixture 75 percent of orthohydrogen and 25 percent of parahydrogen, and normal deuterium 66% percent of ortho-deuterium, and 33% percent of paradeuterium. The molar entropy and free energy of a mixture of ideal gases present in the mole fractions  $x_1, x_2, \dots$  are

$$S_{\text{mixture}} = \sum_j x_j S_j^\circ - R \sum_j x_j \ln x_j \quad (2.15)$$

$$F_{\text{mixture}} = \sum_j x_j F_j^\circ + RT \sum_j x_j \ln x_j \quad (2.16)$$

where  $S_j^\circ$  and  $F_j^\circ$ , the molar entropy and free energy of the ideal gas  $j$  in a pure state at the pressure of the mixture, are given by eq 2.11 and 2.14, using eq 2.12 for the evaluation of  $S_j^\circ$ . The summation  $-R \sum_j x_j \ln x_j$  is called the entropy of mixing. Using eq 2.13 for the evaluation of  $S_j$ , and setting  $V$  equal to the molar volume of the constituent, that is, the volume of the mixture divided by the moles of constituent present, is equivalent to using partial pressures in eq 2.12, in which case the entropy and free energy of the mixture are equal simply to  $\sum_j x_j S_j^\circ$  and  $\sum_j x_j F_j^\circ$ .

The functions  $G_s, B_s, D_s, F_s,$  and  $H_s$  for  $\text{H}_2, \text{HD}$  and  $\text{D}_2$  are as follows:

For  $\text{H}_2$ :

$$G_s = 4405.3(v + \frac{1}{2}) - 125.325(v + \frac{1}{2})^2 + 1.9473(v + \frac{1}{2})^3 - 0.11265(v + \frac{1}{2})^4$$

$$B_s = 60.8483 - 3.06635(v + \frac{1}{2}) + 0.068361(v + \frac{1}{2})^2 - 0.0065(v + \frac{1}{2})^3$$

$$D_s = -0.046435 + 0.0014904(v + \frac{1}{2}) - 0.000063648(v + \frac{1}{2})^2$$

$$F_s = 4.93203 \times 10^{-5} + 0.02800 \times 10^{-4}(v + \frac{1}{2})$$

$$H_s = -6.7217 \times 10^{-6}$$

} 2.18

## 2. Energy Values From Spectroscopic Data

The values of  $\epsilon_j$  to be used in evaluating the equations of the preceding section are derived from analysis of molecular spectra. In general, banded electronic absorption and emission spectra, infrared, rotation-vibration absorption spectra, and Raman spectra are considered. But as the  $\text{H}_2$  and  $\text{D}_2$  molecules have no electric dipole moments in their normal states, they have no rotation-vibration absorption spectra. Similarly, no such spectra have been observed for  $\text{HD}$ , although lack of symmetry permits it to have a very weak dipole moment.

The spectroscopic energy level data for hydrogen are represented by a series in which the energies of the levels relative to the ground level,  $v=0, J=0$ , divided by  $hc$  are expressed as a function of the rotational and vibrational quantum numbers  $J$  and  $v$ , see eq 2.17. The quantity  $\epsilon_j/hc$  is called the *term value* of the level and is designated by the symbol  $F$ . Term values are determined experimentally from differences between the wave numbers of spectrum lines and are expressed in terms of reciprocal centimeters as a unit. Here  $F_{v,J}$  is the term value for the level  $v, J$ ;  $F_{0,0}$  for the ground state being zero.

Up to  $25,000 \text{ cm}^{-1}$ , the term values on which tables 4, 7, and 8 are based, can be represented by

$$F_{v,J} = G_v - G_0 + B_v J(J+1) + D_v J^2(J+1)^2 + F_{v,J} J^3(J+1)^3 + H_v J^4(J+1)^4 + \frac{(H_v J^4(J+1)^4)^2}{F_v J^3(J+1)^3 - H_v J^3(J+1)^4} \quad (2.17)$$

where the subscripts used indicate the quantum numbers on which the different symbols depend for their values.

For HD:

$$\left. \begin{aligned} G_v &= 3817.09(v + \frac{1}{2}) - 94.958(v + \frac{1}{2})^2 + 1.4569(v + \frac{1}{2})^3 - 0.07665(v + \frac{1}{2})^4 \\ B_v &= 45.6549 - 1.992721(v + \frac{1}{2}) + 0.038482(v + \frac{1}{2})^2 - 0.00316885(v + \frac{1}{2})^3 \\ D_v &= -0.026136 + 0.00072661(v + \frac{1}{2}) - 0.0000268773(v + \frac{1}{2})^2 \\ F_v &= 2.0827 \times 10^{-5} + 0.01024 \times 10^{-5}(v + \frac{1}{2}) \\ H_v &= -2.1295 \times 10^{-8} \end{aligned} \right\} 2.19$$

For D<sub>2</sub>:

$$\left. \begin{aligned} G_v &= 3118.46(v + \frac{1}{2}) - 64.10(v + \frac{1}{2})^2 + 1.2514(v + \frac{1}{2})^3 - 0.10612(v + \frac{1}{2})^4 + 0.00034(v + \frac{1}{2})^5 \\ B_v &= 30.4286 - 1.04917(v + \frac{1}{2}) + 0.0057934(v + \frac{1}{2})^2 - 0.00027486(v + \frac{1}{2})^3 \\ D_v &= -0.011586 + 0.000151(v + \frac{1}{2}) + 0.000058(v + \frac{1}{2})^2 \\ F_v &= 6.22 \times 10^{-6} + 0.105 \times 10^{-6}(v + \frac{1}{2}) \\ H_v &= -0.442 \times 10^{-8} \end{aligned} \right\} 2.20$$

The numerical values of the coefficients in eq 2.18 to 2.20 are based on the latest available spectroscopic measurements due principally to Rasetti [2], Hyman [5, 6], Jeppesen [6, 7, 12, 15, 24], Beutler [20, 21], and Teal and Mac Wood [22]. The data of Fujioka and Wada [23] were not used and the data of Mie [16] on HD only through its influence on the formula for  $G_v$ . The equations  $G_v$  for H<sub>2</sub> and HD are those given by Teal and Mac Wood [22], and that for D<sub>2</sub> by Jeppesen [24]. The equations for  $B_v$  are essentially Jeppesen's [12, 24] equations expressed for use with  $J(J+1)$ . The constants in the equations for  $D_v$ ,  $F_v$ , and  $H_v$  were obtained from theory using the equations for  $G_v$  and  $B_v$  and the formulas of Dunham [10] without his correction terms.

In the case of hydrogen as for many other substances, extrapolations of spectroscopic formulas have to be made into regions of large rotational quantum numbers for which no wavelength measurements are available in order to obtain values for the energies  $\epsilon_v$  of the higher quantum states. The energy values for large rotational and vibrational quantum numbers are influenced by the law of internuclear force of the molecule for large separations of the nuclei. Special consideration has been given to this point in the present work and two methods were developed whereby more reliable values of the energies of the unobserved higher rotational levels were obtained.

The first improvement was the addition of the

final term in eq 2.17,  $[H_v J^3(J+1)^3] / [(F_v J^3(J+1)^3 - H_v J^4(J+1)^4)]$ . Without the final term, eq 2.17 is of the form in which spectroscopic data have heretofore been represented, but in that form it is not a good approximation for large values of  $J$ . The third, fourth, fifth, and sixth terms of eq 2.17 are of alternate sign and for H<sub>2</sub> the third, fourth, and fifth terms are approximately equal for  $J=28$ . This suggested that the series be extended with successive terms in constant ratio. The final term of eq 2.17 is the sum of the geometric series of added terms in which the term to term ratio is that between the fifth and sixth terms of eq 2.17.

This change in the formula for the energies of the rotational-vibrational levels of the normal ( $1s^1\Sigma$ ) electronic state of hydrogen has only a small effect on the energy values of the observed spectrum lines. Thus the mean difference between Jeppesen's [12] observed and calculated term values for the  $2p^1\Sigma - 1s^1\Sigma$  band for H<sub>2</sub> was  $1.032 \text{ cm}^{-1}$ , whereas using eq 2.17 in place of Jeppesen's equation for the  $1s^1\Sigma$  state the mean difference between observed and calculated values is  $1.030 \text{ cm}^{-1}$ .

As a second improvement, for the calculation of thermodynamic properties above  $2,000^\circ \text{ K}$ , an alternative determination of the highest rotational levels was made. Instead of using the power series eq 2.17, the energies corresponding to any degree of rotation and vibration were determined from the potential energy. This was

carried out in effect by (1) determining the potential energy  $U$  of the nonrotating  $H_2$  molecule as a function of the internuclear separation, (2) adding the rotational energy  $\hbar^2 J(J+1)/8\pi^2 I_e (r/r_e)^2$  to  $U$  to obtain an effective potential energy,  $U'$ , for a molecule with rotational quantum number  $J$ , and

(3) using the quantum condition  $\oint p dq = \int (2m)^{1/2}$

$(\epsilon_{v,J} - U')^{1/2} dr = (v+1/2)\hbar$  to determine the energy  $\epsilon_{v,J}$  of the quantum state  $v, J$ .

The coefficients of a power series used to represent the molecular potential energy were evaluated for the  $H_2$  molecule using Dunham's [10] theoretical relations and the rotational and vibrational data for  $H_2$ :

$$U = 79734\xi^2(1 - 1.6082\xi + 1.8598\xi^2 - 1.8882\xi^3 + 1.7118\xi^4 - 1.450\xi^5 + 1.421\xi^6), \quad (2.21)$$

where  $\xi$  is  $(r-r_e)/r_e$ ,  $r_e$  being the equilibrium value of the internuclear separation, and  $U$  is expressed in reciprocal centimeters. Although this series is a poor representation of  $U$  for internuclear separations twice the equilibrium value (i. e., at  $\xi=1$ ), it is very good for small values of  $\xi$ . Therefore, this series was not used for the potential

energy function finally accepted for internuclear separations much greater than the equilibrium value, but it was used for internuclear separations less than the equilibrium value. At dissociation the minimum value of  $r$  for classical motion is more than half of  $r_e$  (i. e.,  $|\xi| < 0.5$ ), and the series determines the inner portion of the potential energy curve with sufficient reliability for the present purposes.

The ranges of internuclear oscillation,  $\xi_{\max} - \xi_{\min}$ , for different values of the energy needed to fix the outer portion of the potential energy curve, were determined from (1) the vibrational levels of the nonrotating molecule, symbolized by  $G_v$  in eq 2.17 to eq 2.20, which have been accurately measured to within  $140 \text{ cm}^{-1}$  of dissociation [5, 12, 20, 21] and (2) the quantum condition.

$$\oint p dq = (2mr_e^2 \hbar c)^{1/2} \oint (G_v - U)^{1/2} d\xi = (v+1/2)\hbar. \quad (2.22)$$

The method used to obtain  $(\xi_{\max} - \xi_{\min})$  by satisfying eq 2.22 was essentially that of Rydberg [8] and Klein [9]. Calculated values of the potential energy  $U$  in wave numbers are given in table 1.

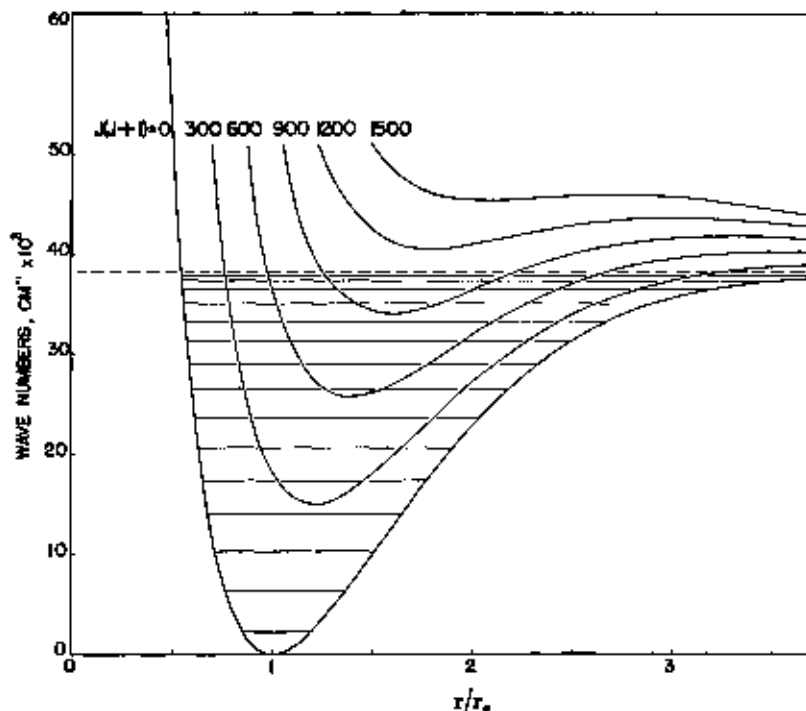


FIGURE 1. Potential-energy curves for  $H_2$ .

TABLE 1. Molecular potential energy  $U$  for  $H_2$  as a function of  $\xi = (r - r_e)/r_e$ , the change in internuclear separation

$\xi$	$U$	$\xi$	$U$	$\xi$	$U$
	cm <sup>-1</sup>		cm <sup>-1</sup>		cm <sup>-1</sup>
-0.5	53,649	0.9	30,540	2.3	36,828
-0.4	27,150	1.0	28,822	2.4	37,160
-0.3	12,899	1.1	24,916	2.5	37,322
-0.2	4,611	1.2	20,910	2.6	37,523
-0.1	942	1.3	16,806	2.7	37,650
0	0	1.4	10,009	2.8	37,770
.1	683	1.6	31,329	2.9	37,867
.2	2,360	1.6	32,472	3.0	37,940
.3	4,628	1.7	33,454	3.1	38,009
.4	7,223	1.8	34,282	3.2	38,061
.5	9,968	1.9	35,001	3.3	38,102
.6	12,744	2.0	35,599	3.4	38,138
.7	15,400	2.1	36,082	3.5	38,163
.8	18,079	2.2	36,496	$\infty$	38,296

$r_e = 0.7414 \times 10^{-8}$  cm

The effective potential energy curves for rotating molecules obtained by adding to  $U$  for the nonrotating molecule the energy of rotation,  $J(J+1)B_e/(1+\xi)^2$ , in cm<sup>-1</sup>, are illustrated in figure 1. By applying the quantum integral,

$$\oint p dq = (2mr_e^2 hc)^{1/2} \oint (F - U')^{1/2} d\xi = (v + 1/2)h, \quad (2.23)$$

to the effective potential energy curves,  $U'$ , a set of corresponding values of energy ( $F$ ) and vibrational quantum number was determined for each

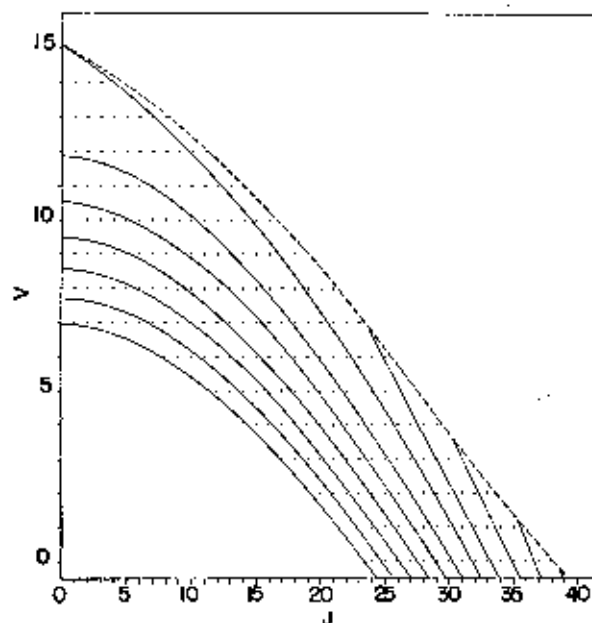


FIGURE 2. Energy contour diagram for  $H_2$ .

of a few large values of the rotational quantum number. In table 2 these corresponding values are given together with the maximum and minimum values of the energy ( $F$ ) for different values of  $J(J+1)$ . The data were used to determine the constant energy lines in the  $v$  versus  $J$  diagram in figure 2.

TABLE 2. Corresponding values of  $v$ ,  $J(J+1)$ , and  $F$

obtained by evaluating  $\oint p dq = (v + 1/2)h$

[The values of  $v$  and  $J$  are not integral and so do not represent stationary states, yet the table values indicate how  $F$  depends on  $v$  and  $J$  over a range including many stationary states.]

$F$ (above $U$ at $\xi=0$ )	$J(J+1)$	$v$
cm <sup>-1</sup>		
38,269	300	8.8483
34,269	300	6.2874
30,269	300	4.5015
26,269	300	2.9381
22,269	300	1.8461
38,269	600	4.6378
34,269	600	2.7292
30,269	600	1.0757
38,269	900	1.4032
42,269	1,200	0.4846
Maximum values of $F$ and $v$ for given values of $J(J+1)$		
38,288	0	15.053
39,058	300	9.919
40,323	600	6.915
41,858	900	3.929
43,712	1,200	1.703
46,980	1,500	-0.072
Minimum values of $F$ and $v$ for given values of $J(J+1)$		
0	0	-0.5
15,027	300	-0.5
25,847	600	-0.5
34,111	900	-0.5
40,606	1,200	-0.5
45,601	1,500	-0.5

Table 3 shows that over a wide range of  $J$  values the results of the numerical integration just described are in good agreement with the rotational energy formula (eq 2.17) when the last term, corresponding to a geometric series continuation, is included. For the larger values of  $J$  there are appreciable differences; yet, when it



### 3. Details of the Calculations and Results

is observed how large the final term of eq 2.17 is in these cases, it seems surprising that the discrepancies between  $F$  (table 2) and  $F$  (eq 2.17) are as small as they are. In another publication [27] a more rapidly converging series representing  $J(J+1)$  as a function of the rotational energy has been suggested.

In the evaluation of the series of section II, 1 for the calculation of the thermal properties, direct summation was employed for temperatures below 2,000° K. The resulting values to 2,000° K for the various thermodynamic functions  $S^\circ$ ,  $H^\circ - E_0^\circ$ ,  $-(F^\circ - E_0^\circ)/T$ , and  $C_p^\circ$  for the ideal gas state at one atmosphere pressure are tabulated in tables 4, 5, and 6, for  $H_2$ , HD, and  $D_2$ . For  $n-H_2$  for temperatures above 2,000° K, the contributions due to levels below 25,000  $cm^{-1}$  were calculated by direct summation, whereas for levels above 25,000  $cm^{-1}$  a less laborious method was used involving the determination of the number of levels within successive equal steps of 2,000  $cm^{-1}$  in the rotational vibrational energy, using the results of the calculations of the last section which led to figures 1 and 2. For these

TABLE 3. Comparison of rotational-vibrational energies  $F$  from table 2 and from equation 2.17

$J(J+1)$	$\epsilon$	$F$ (table 2)	$F$ (table 2) - $F$ (eq 2.17)	Final term of eq 2.17
		$cm^{-1}$	$cm^{-1}$	$cm^{-1}$
300	4.5015	30,269	-54	155
300	6.2574	34,269	-34	164
600	1.0757	30,269	-78	3,904
900	1.4032	33,269	-300	24,182
1,200	0.4545	43,269	761	86,945

TABLE 4. Thermodynamic functions for  $H_2$  in the ideal gaseous state

Values for  $S^\circ$  and  $-(F^\circ - E_0^\circ)/T$  include nuclear spin

Temperature °K	$S^\circ$ , cal mole <sup>-1</sup> deg <sup>-1</sup>			$H^\circ - E_0^\circ$ , cal mole <sup>-1</sup>			$-\frac{F^\circ - F_0^\circ}{T}$ , cal mole <sup>-1</sup> deg <sup>-1</sup>			$C_p^\circ$ , cal mole <sup>-1</sup> deg <sup>-1</sup>		
	$p-H_2$	$o-H_2$	$n-H_2$	$p-H_2$	$o-H_2$	$n-H_2$	$p-H_2$	$o-H_2$	$n-H_2$	$p-H_2$	$o-H_2$	$n-H_2$
10	11.215	16.981	15.607	49.6785	238.337	703.665	6.247	-23.352	-14.760	4.968	4.968	4.968
20	14.668	19.024	19.050	99.357	438.006	353.244	0.690	-2.876	1.382	4.968	4.968	4.968
30	16.672	21.039	21.064	149.036	437.984	403.022	11.706	4.783	7.630	4.968	4.968	4.968
40	17.161	21.537	21.559	194.457	503.065	418.423	12.193	8.328	8.911	4.968	4.968	4.968
50	18.102	22.468	22.494	198.729	537.363	452.705	13.134	9.034	11.178	4.973	4.968	4.969
60	19.214	23.575	23.603	248.581	587.041	502.428	14.243	11.636	13.554	5.007	4.968	4.979
80	20.136	24.492	24.513	398.108	638.722	552.318	15.150	13.670	15.307	6.116	4.969	6.005
100	20.938	25.246	25.258	351.222	696.422	602.622	16.921	16.442	16.679	5.330	4.972	5.061
120	21.669	25.913	25.909	406.015	736.179	653.638	16.694	18.710	17.799	5.648	5.992	5.148
140	22.359	26.500	26.491	464.385	786.086	705.660	17.197	17.786	18.741	6.036	5.003	6.261
160	23.014	27.029	27.142	526.687	836.277	758.910	17.746	18.667	19.554	6.455	5.020	6.368
180	24.259	27.959	28.151	663.782	898.227	860.609	18.729	20.140	20.904	7.304	6.170	6.678
200	25.945	29.143	29.461	890.806	1,067.78	1,045.89	20.007	21.826	22.488	7.907	6.497	6.967
250	28.202	30.808	31.275	1,282.70	1,367.90	1,361.61	21.788	23.889	24.466	7.742	6.110	6.618
300	29.889	32.225	32.758	1,660.40	1,705.80	1,694.47	23.246	26.402	25.981	7.390	6.665	6.770
350	31.108	33.494	33.963	2,009.99	2,028.24	2,023.75	24.426	26.609	27.175	7.158	6.628	6.681
400	31.212	33.446	34.006	2,023.10	2,040.87	2,036.44	24.466	26.643	27.217	7.152	6.608	6.694
500	32.308	34.505	35.073	2,377.84	2,384.39	2,382.73	25.512	27.693	28.285	7.049	6.917	6.951
600	33.244	35.432	36.003	2,729.19	2,731.54	2,730.95	26.421	28.608	29.175	7.010	6.963	6.975
700	34.604	36.990	37.561	3,429.24	3,429.53	3,429.46	27.948	30.131	30.702	6.960	6.992	6.993
800	36.093	38.266	38.638	4,129.48	4,129.52	4,129.61	29.200	31.383	31.955	7.010	7.009	7.009
900	37.165	39.346	39.930	4,621.85	4,631.66	4,631.66	30.263	32.466	33.018	7.037	7.036	7.036
1,000	39.791	41.984	42.455	.....	.....	6,986.23	32.735	34.918	35.490	.....	.....	7.219
1,500	42.720	44.903	46.475	.....	.....	10,697.20	36.389	37.770	38.948	.....	.....	7.730
2,000	45.007	47.190	47.782	.....	.....	14,670.2	37.669	39.861	40.422	.....	.....	8.196
3,000	.....	.....	51.221	.....	.....	23,390.9	.....	.....	43.478	.....	.....	8.869
4,000	.....	.....	53.839	.....	.....	32,345.	.....	.....	45.753	.....	.....	9.342
5,000	.....	.....	55.989	.....	.....	41,826.	.....	.....	47.590	.....	.....	9.746

TABLE 5. Thermodynamic functions for HD in the ideal gas state

Values for  $S^\circ$  and  $-(F^\circ - E_0^\circ)/T$  include nuclear spin

Temperature	$S_0$	$H^\circ - E_0^\circ$	$-\frac{F^\circ - E_0^\circ}{T}$	$C_p^\circ$
$^\circ K$	cal mole <sup>-1</sup> deg <sup>-1</sup>	cal mole <sup>-1</sup>	cal mole <sup>-1</sup> deg <sup>-1</sup>	cal mole <sup>-1</sup> deg <sup>-1</sup>
10	15.982	49.691	11.034	4.971
20	19.497	100.600	14.488	5.365
22.18	20.050	112.254	14.979	5.564
30	21.961	159.270	16.553	6.367
40	23.792	226.510	18.129	6.991
50	25.376	297.472	19.495	7.149
60	26.690	368.910	20.631	7.128
70	27.772	438.914	21.498	7.078
80	28.714	510.484	22.353	7.037
90	29.542	582.706	23.089	7.013
100	30.279	655.733	23.772	6.999
120	31.554	790.592	24.966	6.985
150	33.113	1,002.02	26.445	6.978
200	35.119	1,348.92	28.375	6.975
250	36.076	1,697.62	29.685	6.977
298.16	37.005	2,093.06	31.064	6.979
300	37.006	2,096.30	31.126	6.979
400	39.957	2,734.72	33.095	6.986
500	41.517	3,443.85	34.629	6.999
600	42.795	4,144.90	35.886	7.025
700	43.881	4,849.00	36.953	7.072
1,000	46.443	7,007.20	39.436	7.339
1,500	49.027	10,821.2	42.313	7.909
2,000	51.871	14,898.4	44.421	8.376

higher levels having characteristic temperatures above 36,000° K, the exact placement of each individual level is not important for calculations up to 5,000° K.

Figure 1 shows that the effective potential energy curves for rotational quantum numbers other than 0 have broad potential energy barriers above the minimum dissociation energy, 38,296 cm<sup>-1</sup>, for  $J=0$ . As a result there are above 38,296 cm<sup>-1</sup>, the minimum dissociation energy, quantized rotational-vibrational levels belonging to the sequences of levels below 38,296 cm<sup>-1</sup>. These states are represented by the points in figure 2 between the dashed curve and the full line dissociation energy curve passing through ( $J=0$ ,  $v=15.1$ ) and ( $J=32.5$ ,  $v=-\frac{1}{2}$ ).

It seemed proper to include in the calculations of the thermal properties of hydrogen above 2,000° K these quantized or partially quantized rotational-vibrational states. The values of the thermodynamic functions for  $n$ -H<sub>2</sub> from 2,000° to 5,000° K in table 4 are based on this convention.

The effect of the quantized rotational-vibrational levels above the minimum dissociation energy of H<sub>2</sub> on the most sensitive of the functions calculated, namely the molecular heat capacity, is represented in figure 3. Curve A represents the

TABLE 6. Thermodynamic functions for D<sub>2</sub> in the ideal gaseous state

Values for  $S^\circ$  and  $-(F^\circ - E_0^\circ)/T$  include nuclear spin

Temperature	$S^\circ$ , cal mole <sup>-1</sup> deg <sup>-1</sup>			$H^\circ - E_0^\circ$ , cal mole <sup>-1</sup>			$-\frac{F^\circ - E_0^\circ}{T}$ , cal mole <sup>-1</sup> deg <sup>-1</sup>			$C_p^\circ$ , cal mole <sup>-1</sup> deg <sup>-1</sup>		
	$p$ -D <sub>2</sub>	$o$ -D <sub>2</sub>	$n$ -D <sub>2</sub>	$p$ -D <sub>2</sub>	$o$ -D <sub>2</sub>	$n$ -D <sub>2</sub>	$p$ -D <sub>2</sub>	$o$ -D <sub>2</sub>	$n$ -D <sub>2</sub>	$p$ -D <sub>2</sub>	$o$ -D <sub>2</sub>	$n$ -D <sub>2</sub>
10	17.645	16.839	18.372	220.505	49.679	106.621	-4.408	11.471	7.710	4.966	4.966	4.966
20	21.088	20.283	21.816	270.183	99.364	156.303	7.579	15.315	14.001	4.966	4.972	4.971
22.97	21.904	21.101	22.633	287.919	117.139	174.065	8.689	16.131	15.246	4.966	4.980	4.962
30	23.102	22.315	23.842	319.863	146.614	206.297	12.440	17.831	16.903	4.966	5.106	5.059
40	24.533	23.843	25.368	369.384	202.776	268.378	16.293	18.774	18.879	4.980	5.617	5.404
50	25.649	25.180	25.600	419.699	282.811	316.048	17.297	19.923	20.299	5.033	6.412	5.952
60	26.576	26.418	27.738	470.480	339.843	377.389	18.734	20.904	21.448	5.159	7.163	6.485
70	27.394	27.563	28.786	522.048	405.192	444.444	19.913	21.775	22.419	5.248	7.666	6.887
80	28.114	28.601	29.704	577.589	482.967	514.596	20.893	22.564	23.272	5.336	7.862	7.103
90	28.786	29.527	30.546	634.706	561.671	586.016	21.734	23.287	24.035	5.438	7.860	7.187
100	29.414	30.353	31.304	694.306	639.876	658.018	22.471	23.954	24.794	5.079	7.751	7.193
150	30.569	31.739	32.611	819.996	791.908	801.270	23.726	25.139	25.933	6.460	7.454	7.125
100	32.041	33.968	34.189	1,019.52	1,019.37	1,013.42	25.244	26.629	27.432	6.790	7.149	7.029
200	34.023	35.395	36.202	1,366.03	1,362.00	1,363.29	27.202	28.580	29.388	6.947	6.996	6.980
298.16	36.805	38.162	38.998	2,048.19	2,048.08	2,048.09	29.936	31.313	32.119	6.977	6.978	6.978
300	36.848	38.225	39.031	2,060.93	2,060.92	2,060.92	29.978	31.356	32.161	6.977	6.978	6.978
400	39.857	40.234	41.040	.....	.....	2,759.18	31.959	33.336	34.142	.....	.....	6.969
500	40.419	41.796	42.602	.....	.....	3,459.38	33.500	34.877	35.683	.....	.....	7.019
600	41.704	43.081	43.887	.....	.....	4,104.03	34.763	36.141	36.946	.....	.....	7.079
700	42.892	44.179	44.985	.....	.....	4,676.39	35.836	37.212	38.018	.....	.....	7.173
1,000	45.422	46.800	47.025	.....	.....	7,064.30	38.328	38.718	40.621	.....	.....	7.562
1,500	48.611	49.989	50.794	.....	.....	11,027.3	41.269	42.637	43.442	.....	.....	8.178
2,000	51.027	52.405	53.210	.....	.....	15,229	43.411	44.789	45.694	.....	.....	8.596

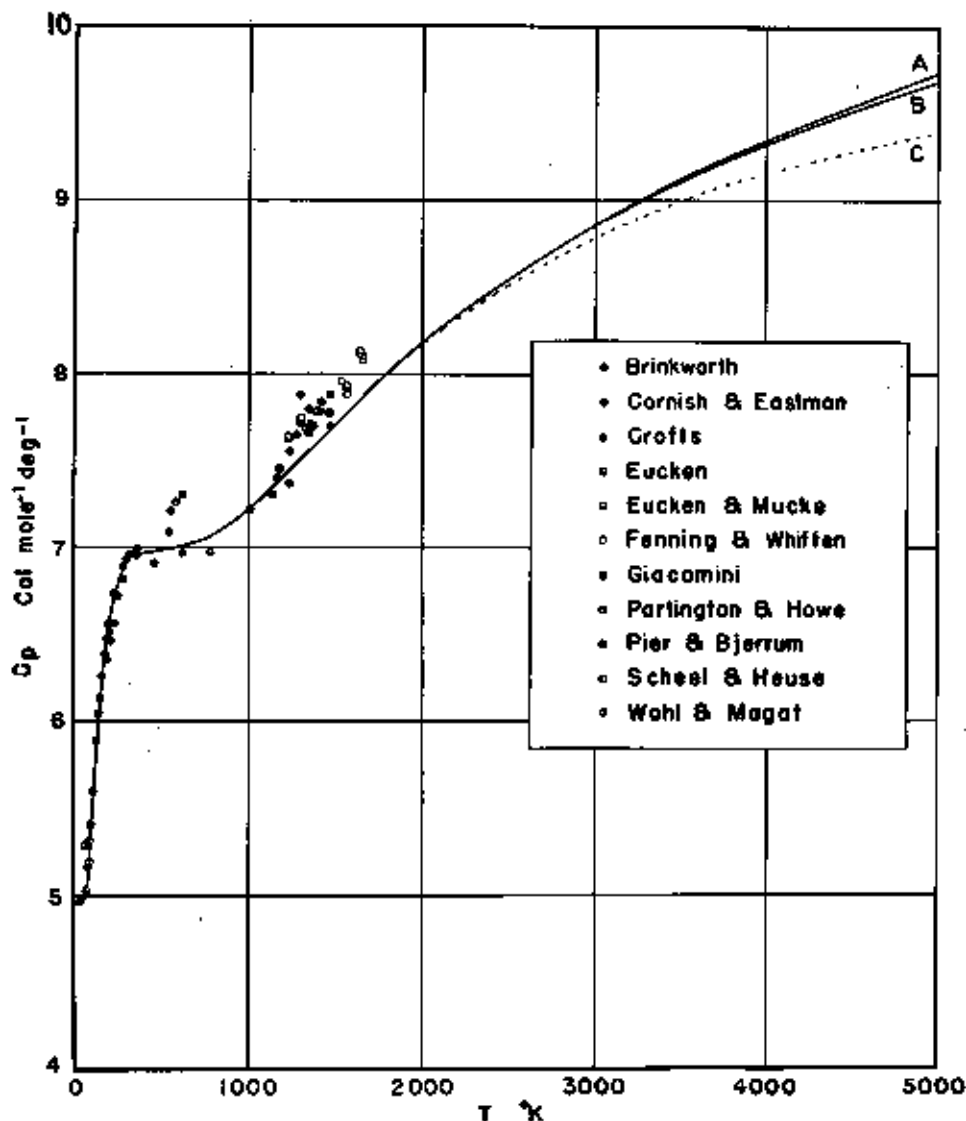


FIGURE 3. Specific heat of normal hydrogen at constant pressure.

TABLE 7. Thermodynamic functions for  $H_2$  in ideal gaseous state

(Based only on levels below minimum dissociation energy)

$T$	Entropy	Enthalpy	$-\frac{F^0 - E_0^0}{T}$	Specific heat
$^{\circ}K$	cal mole $^{-1}$ deg $^{-1}$	cal mole $^{-1}$	cal mole $^{-1}$ deg $^{-1}$	cal mole $^{-1}$ deg $^{-1}$
3,000.....	61.291	23,230.9	43.476	8.696
4,000.....	63.638	32,341	45.763	9.341
5,000.....	65.960	41,854	47.589	9.675

molecular heat capacity if the quantized rotational-vibrational levels above the minimum dissociation energy are included as molecular levels, and curve B represents the molecular heat capac-

ity if the molecular levels are regarded as extending only up to the minimum dissociation energy. In table 7 are tabulated the values of the thermodynamic functions for  $n-H_2$  based on calculations involving only energy levels below the minimum dissociation energy.

For convenience in the calculation of the thermodynamic functions of the real gas  $n-H_2$ , values for  $n-H_2$  in the ideal gas state at all temperatures for which there are entries in the tables of PVT data were obtained from table 4 by interpolation and are tabulated in table 8. The interpolated values of  $S^0$ ,  $-(F^0 - E_0^0)/T$ , and  $C_p^0$  agree to within  $\pm 0.001$  with values that would have been ob-

tained by direct summation. In the case of  $H^\circ - E_0^\circ$ , the agreement is within three in the last digit carried.

TABLE 8. Thermodynamic functions for normal  $H_2$  in the ideal gaseous state

Values for  $S^\circ$  and  $-(F^\circ - E_0^\circ)/T$  include nuclear spin

$T$	$S^\circ$	$H^\circ - E_0^\circ$	$-(F^\circ - E_0^\circ)/T$	$C_p^\circ$
$^\circ K$	cal mole <sup>-1</sup> deg <sup>-1</sup>	cal mole <sup>-1</sup>	cal mole <sup>-1</sup> deg <sup>-1</sup>	cal mole <sup>-1</sup> deg <sup>-1</sup>
16	17.822	333.473	-2.900	4.968
18	18.527	343.406	-0.451	4.968
20	19.050	353.344	1.392	4.968
22	19.594	363.290	3.011	4.968
24	19.966	373.216	4.405	4.968
26	20.343	383.151	5.616	4.968
28	20.722	393.087	6.653	4.968
30	21.094	403.022	7.630	4.968
32	21.385	412.959	8.480	4.968
34	21.686	422.896	9.248	4.968
36	21.970	432.832	9.947	4.968
38	22.329	442.767	10.587	4.968
40	22.494	452.705	11.176	4.969
42	22.737	462.643	11.722	4.970
44	22.966	472.583	12.227	4.971
46	23.189	482.527	12.689	4.973
48	23.400	492.474	13.140	4.975
50	23.603	502.426	13.564	4.978
52	23.798	512.384	13.944	4.982
54	23.986	522.351	14.313	4.986
56	24.168	532.327	14.682	4.991
58	24.343	542.315	14.993	4.996
60	24.513	552.318	15.307	5.005
65	24.915	577.399	16.032	5.029
70	25.288	602.622	16.679	5.061
75	25.639	628.022	17.266	5.101
80	25.969	653.633	17.799	5.148
85	26.283	679.507	18.289	5.202
90	26.581	705.660	18.741	5.261
95	26.868	732.122	19.161	5.325
100	27.142	758.916	19.554	5.393
105	27.406	786.056	19.922	5.463
110	27.664	813.549	20.268	5.534
115	27.911	841.400	20.595	5.606
120	28.151	869.609	20.904	5.678
125	28.384	898.175	21.193	5.746
130	28.610	927.098	21.479	5.816
135	28.831	956.335	21.747	5.883
140	29.047	985.91	22.005	5.947
145	29.257	1,015.80	22.251	6.006
150	29.461	1,045.90	22.483	6.067
155	29.661	1,076.47	22.716	6.123
160	29.856	1,107.22	22.938	6.177
165	30.047	1,138.23	23.149	6.229
170	30.234	1,169.49	23.356	6.276
180	30.505	1,232.71	23.747	6.366
190	30.942	1,307.78	24.116	6.446
200	31.275	1,384.61	24.466	6.518
210	31.594	1,427.10	24.799	6.581
220	31.901	1,493.20	25.115	6.638

TABLE 8. Thermodynamic functions for normal  $H_2$  in the ideal gaseous state—Continued

$T$	$S^\circ$	$H^\circ - E_0^\circ$	$-(F^\circ - E_0^\circ)/T$	$C_p^\circ$
$^\circ K$	cal mole <sup>-1</sup> deg <sup>-1</sup>	cal mole <sup>-1</sup>	cal mole <sup>-1</sup> deg <sup>-1</sup>	cal mole <sup>-1</sup> deg <sup>-1</sup>
230	32.197	1,659.85	25.415	6.688
240	32.463	1,695.96	25.704	6.731
250	32.766	1,694.47	25.981	6.770
260	33.024	1,752.33	26.346	6.803
270	33.282	1,830.49	26.592	6.831
280	33.531	1,896.92	26.749	6.856
300	34.005	2,036.44	27.217	6.904
320	34.462	2,174.63	27.656	6.922
340	34.872	2,313.28	28.066	6.943
360	35.269	2,452.29	28.457	6.957
380	35.646	2,591.63	28.826	6.969
400	36.003	2,730.96	29.175	6.975
420	36.344	2,870.51	29.509	6.980
440	36.669	3,010.14	29.826	6.984
460	36.979	3,149.85	30.131	6.987
480	37.276	3,289.62	30.422	6.990
500	37.561	3,429.46	30.702	6.993
520	37.837	3,569.34	30.973	6.996
540	38.100	3,709.28	31.231	6.999
560	38.356	3,849.30	31.481	7.002
580	38.600	3,989.36	31.722	7.005
600	38.838	4,129.51	31.956	7.009
650	39.359	4,460.19	32.506	7.021

The contributions to the entropy and to the related free energy functions arising from (1) the nuclear spins, (2) the triple degeneracy of the lowest rotational state of *o*- $H_2$  and *p*- $D_2$ , and (3) the mixing of the ortho and para varieties in *n*- $H_2$  and *n*- $D_2$  have been included through eq 2.3, 2.4, 2.15, and 2.16 in all the tables. A comparison of the entropies and free energies of hydrogen and deuterium calculated from calorimetric data with values in the tables must take into account the degeneracies existing in the solid state at the lowest temperature of the calorimetric measurements. There must accordingly be added to the calorimetric values of entropy calculated from data extending from 10° K to higher temperatures, the entropies of table 9. In calculations concerning chemical reactions above room temperature nuclear spin entropies are customarily omitted for all components of the reactions.

To obtain entropies of *n*- $H_2$ , HD, and *n*- $D_2$  suitable for such use above room temperature, there should be subtracted from table values of the entropies  $R \ln (2i_1 + 1) (2i_2 + 2)$  where  $i_1$  and  $i_2$  are the two nuclear spins within the molecule [14]. For *n*- $H_2$  this is equal to  $R \ln 4 = 2.755$

TABLE 2. Low-temperature ( $10^{\circ}$  K) entropy contributions arising from rotational and nuclear-spin degeneracies

Variety.....	$H_2$		HD	$D_2$	
	Para	Ortho		Ortho	Para
Values of $J$ .....	Even	Odd	Only 1	Even	Odd
Weight of lowest rotational level ( $2J+1$ ).....	1	3	Both odd and even	1	3
Nuclear spin weight, see eq 2.3 and 2.4.....	1	3	6	6	3
Total added entropy.....	0	$R \ln 9=4.366$ cal mole $^{-1}$ deg $^{-1}$ .	$R \ln 6=3.560$ cal mole $^{-1}$ deg $^{-1}$ .	$R \ln 6=3.560$ cal mole $^{-1}$ deg $^{-1}$ .	$R \ln 9=4.366$ cal mole $^{-1}$ deg $^{-1}$ .
	$n-H_2$		$n-D_2$		
$-R(x_1 \ln x_1 + x_2 \ln x_2)$ .....	$R(\ln 4 - \frac{3}{4} \ln 3)=1.117$ cal mole $^{-1}$ deg $^{-1}$		$R(\ln 3 - \frac{2}{3} \ln 2)=1.265$ cal mole $^{-1}$ deg $^{-1}$		
$x_1 x_2 + x_2 x_1$ .....	$\frac{3}{4} R \ln 9=3.275$ cal mole $^{-1}$ deg $^{-1}$		$R(\frac{1}{4} \ln 3 + \frac{1}{2} \ln 2)=3.320$ cal mole $^{-1}$ deg $^{-1}$		
Total added entropy ( $x_1 x_2 = R x_1 \ln x_1$ ).....	$R(\ln 4 + \frac{3}{4} \ln 3)=4.392$ cal mole $^{-1}$ deg $^{-1}$		$\frac{3}{4} R \ln 3=6.064$ cal mole $^{-1}$ deg $^{-1}$		

cal mole $^{-1}$  deg $^{-1}$ ; for HD,  $R \ln 6=3.560$  cal mole $^{-1}$  deg $^{-1}$ , and for  $n-D_2$ ,  $R \ln 9=4.366$  cal mole $^{-1}$  deg $^{-1}$ .

The reliability to be expected in thermodynamic functions for the ideal gas state calculated from spectroscopic data has been considered by earlier writers on the basis of the reliability of spectroscopic constants and the gas constant  $R$ . The former estimate of one or two hundredths of a calorie mole $^{-1}$  deg $^{-1}$  for the probable error in the free energy function, specific heat and entropy, appears reasonable. Over much of the temperature range it is probably a more liberal estimate than necessary, as more recent and presumably better spectroscopic data and values for the physical constants have been used. A larger allowance may be necessary for the higher temperatures, however, possibly twice as much at  $5,000^{\circ}$  K.

The results of the present calculations below  $2,000^{\circ}$  K are in fairly close agreement with those of Giauque [4], Johnston and Long [18], Davis and Johnston [17], and Wagman, et al. [28]. Above  $2,000^{\circ}$  K the effect of the new calculations of the high rotational levels of  $H_2$  is apparent.

This can be seen in figure 3 in which the results of Davis and Johnston (curve  $C$ ) for the specific heat of hydrogen, the most sensitive property calculated, are compared with table values of this paper (curves  $A$  and  $B$ ). Curve  $A$ , corresponding to table 4, is based on the inclusion of the quantized rotational-vibrational levels above the minimum dissociation energy as molecular levels, and curve  $B$ , corresponding to table 7, is based only on levels below the minimum dissociation energy.

In figure 3 are plotted also a large number of scattered points representing the experimental observations of many investigators. [33 to 37, 40 to 46, 50, 51, 56]. In cases where mean specific heats were reported, they have been plotted for the mean temperatures of the experimental intervals. At room temperatures and below, the theoretical and experimental specific heats are in good agreement, as has been the case since the correct treatment of the ortho and para forms by Dennison [1] in 1927. Above  $1,200^{\circ}$  K the observations obtained by the explosion method lie above the theoretical curve. The difficulties of the explosion method are great and the accuracy not high [53], consequently the authors feel that the calculated curve and table are more reliable.

At atmospheric pressure and a temperature of  $2,000^{\circ}$  K, there is a small but perceptible dissociation of  $H_2$ , HD, and  $D_2$ . As the heat of dissociation of hydrogen is large there are significant differences between the calculated properties of molecular  $H_2$ , HD, and  $D_2$ , tables 4 to 6, and the properties of the dissociating gases. At  $2,000^{\circ}$  K the table value of  $C_p$  for molecular  $H_2$  is 8.195 cal mole $^{-1}$  deg $^{-1}$ , whereas for an ideal gas mixture of molecular and atomic hydrogen in equilibrium at atmospheric pressure the value is 8.797, a difference of 0.60 cal mole $^{-1}$  deg $^{-1}$ . For HD and  $D_2$  the differences between the two specific heats are 0.41 and 0.57 cal mole $^{-1}$  deg $^{-1}$ , respectively. The effect of pressure upon the specific heat of dissociating hydrogen is illustrated in figure 4 and discussed in section III. At temperatures where there is appreciable dissociation of HD, equilibrium mixtures of  $H_2$ , HD, and  $D_2$ , are established.

### III. Equilibrium Constants for Dissociation, Isotopic Exchange, and Ortho-Para Conversion

The equilibrium constant  $K$  of a gaseous reaction

$$\alpha_1 A_1 + \alpha_2 A_2 + \alpha_3 A_3 \dots = \beta_1 B_1 + \beta_2 B_2 + \beta_3 B_3 \dots, \quad (3.1)$$

in which each of the participating gases  $A_1, A_2, \dots, B_1, B_2, \dots$  has the equation of state  $PV=RT$ , is related to the partial pressures of the gases and to their free energies,  $F^*$ , at unit pressure by the equation

$$RT \ln \frac{P_{B_1}^{\beta_1} P_{B_2}^{\beta_2} P_{B_3}^{\beta_3} \dots}{P_{A_1}^{\alpha_1} P_{A_2}^{\alpha_2} P_{A_3}^{\alpha_3} \dots} = RT \ln K = -(\sum \beta_j F_{B_j}^* - \sum \alpha_j F_{A_j}^*) = -\Delta F^*. \quad (3.2)$$

Equilibrium constants for dissociation, isotopic exchange,\* and ortho-para conversion of hydrogen may be calculated by using the  $-(F^\circ - E_0^\circ)/T$  values of tables 4, 5, and 6.  $E_0^\circ$  is the internal energy per mole of molecules without translational motion in the lowest energy level  $J=0, v=0$  and in the ideal gas state, and  $F^\circ$  is for the ideal

gas state and a pressure of 1 atm; Using  $-(F^\circ - E_0^\circ)/T$  instead of  $F^*$ ,

$$R \ln K = \Delta \frac{-(F^\circ - E_0^\circ)}{T} - \frac{\Delta E_0^\circ}{T}. \quad (3.3)$$

The values of  $\Delta E_0^\circ$  for the reactions considered in this section are given by the spectroscopic data used in the previous section. Using free energy values as given in the tables of this paper, the atmosphere is the unit of pressure for  $K$  and  $P$  in the mass action law,

$$\frac{P_{B_1}^{\beta_1} P_{B_2}^{\beta_2} P_{B_3}^{\beta_3} \dots}{P_{A_1}^{\alpha_1} P_{A_2}^{\alpha_2} P_{A_3}^{\alpha_3} \dots} = K. \quad (3.4)$$

Deviations from the laws of ideal gases can be taken into account by use of fugacities or activities in place of partial pressures and the forms of eq 3.2, 3.3, and 3.4 for  $K$  are retained. When fugacities or activities are substituted for partial pressures,  $F^*$  becomes the free energy at unit fugacity or activity. For a fuller discussion of the use of fugacities and activities the reader is referred to references [29 to 32].

The entropies of monatomic H and D (see p. 383) must include the nuclear and electron spin entropies besides the entropy of translation, eq

\* Equilibrium H<sub>2</sub> and D<sub>2</sub>.

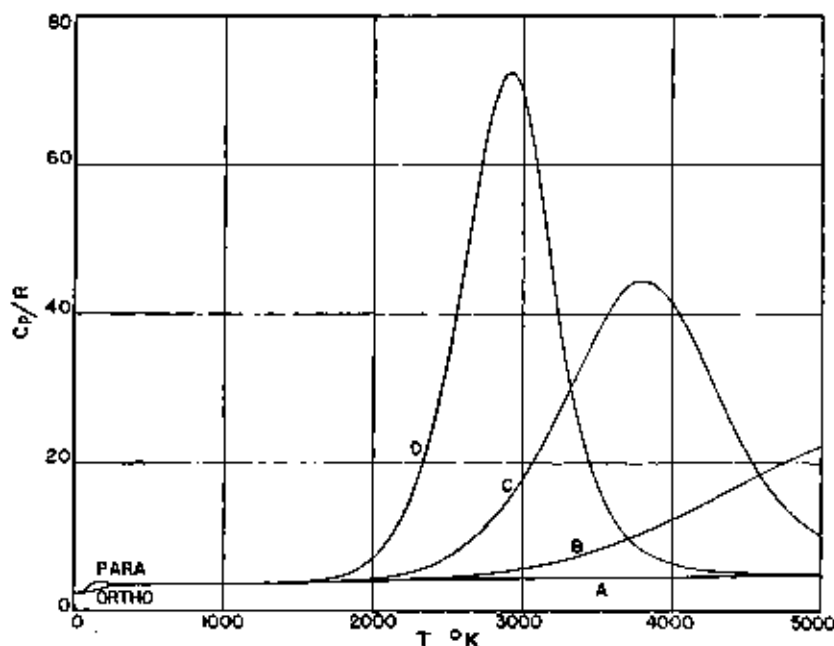


FIGURE 4. Curves showing effect of dissociation on specific heat of H<sub>2</sub>.

2.12, when used with table values of the entropy and free energy of molecular H<sub>2</sub>, HD, and D<sub>2</sub>, in the calculation of equilibrium constants for dissociation. Accordingly for H,

$$-\frac{F^\circ - E_0^\circ}{RT} = \frac{5}{2} \ln T - 2.2663 \text{ and } \frac{S^\circ}{R} = \frac{5}{2} \ln T + 0.2337, \quad (3.5)$$

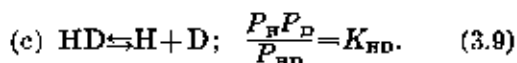
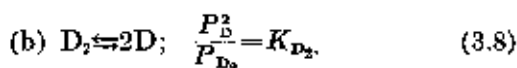
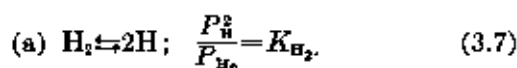
and for D,

$$-\frac{F^\circ - E_0^\circ}{RT} = \frac{5}{2} \ln T - 0.8223 \text{ and } \frac{S^\circ}{R} = \frac{5}{2} \ln T + 1.6777 \quad (3.6)$$

in the ideal gas state at a pressure of 1 atm for the range of temperatures covered by the tables.

### 1. Dissociation of H<sub>2</sub>, D<sub>2</sub>, and HD

The chemical equations for dissociation and the corresponding mass action equations are



For these reactions,  $\Delta E_0^\circ$  of eq 3.3 is the difference between the internal energy of 2 moles of dissociated atoms and 1 mole of molecules in the rotational-vibrational state  $J=0, v=0$ . Beutler's value [21],  $36,116 \pm 6 \text{ cm}^{-1}$ , was accepted for the dissociation of H<sub>2</sub> from its ground state. Assuming that the total depth of the potential energy curve is the same for H<sub>2</sub>, HD, and D<sub>2</sub>, the dissociation energies of HD and D<sub>2</sub> were obtained from the zero-point vibrational energies. These zero point energies were calculated by adding to  $G_0$  (see eq 2.17), the term which Dunham [10] included in the energy of the ground state relative to the bottom of the potential energy curve and designated  $Y_{00}$  in his system. The values thus obtained for the zero point energies of H<sub>2</sub>, HD, and D<sub>2</sub> were respectively 2,179.6, 1,891.0, 1,546.6  $\text{cm}^{-1}$ , and the corresponding energies of dissociation for HD and D<sub>2</sub> from the ground state 36,404.0 and 36,749.0  $\text{cm}^{-1}$ , respectively.

The heats of dissociation of H<sub>2</sub>, HD, and D<sub>2</sub> in the ideal gas state at temperature  $T$  are equal to  $\Delta E_0^\circ + 5RT - (H^\circ - E_0^\circ)$ , where  $(H^\circ - E_0^\circ)$  is the table value of the enthalpy at temperature  $T$ . The heats of dissociation at 0° and 298.16° K are given in table 11. The theoretical value for the heat of dissociation of  $n\text{-H}_2$  at 298° K agrees well with the calorimetric value  $105,000 \pm 3,500 \text{ cal mole}^{-1}$  obtained by Bichowsky and Copeland [47].

On the assumption that the atomic and molecular forms of hydrogen and deuterium are individually ideal gases, the fraction of the originally totally nondissociated hydrogen which has dissociated is  $\sqrt{K/(K+4P)}$ , where  $K$  is the dissociation constant and  $P$  is the total pressure in atmospheres.

The dissociation constants  $K$  and fractions of originally undissociated diatomic molecules, dissociated at 1-atmosphere pressure, are given in table 10 for H<sub>2</sub>, HD, and D<sub>2</sub>.

The experimental values of the equilibrium dissociation constants of H<sub>2</sub> as determined by Langmuir and Mackay [32], and by Langmuir [39], are in agreement with the theoretical values of table 10. Langmuir's  $\alpha$ -values are 0.17 percent at

TABLE 10. Dissociation constants,  $K$ , and fraction dissociated,  $\alpha$ , at 1-atm pressure

For H <sub>2</sub> ⇌ 2H		
T, °K	K	α
atm		
300.....	18.39 × 10 <sup>-22</sup>	21.44 × 10 <sup>-27</sup>
500.....	4.939 × 10 <sup>-19</sup>	3.514 × 10 <sup>-21</sup>
1,000.....	5.174 × 10 <sup>-18</sup>	1.137 × 10 <sup>-16</sup>
1,500.....	3.100 × 10 <sup>-16</sup>	8.675 × 10 <sup>-14</sup>
2,000.....	2.641 × 10 <sup>-14</sup>	8.125 × 10 <sup>-11</sup>
3,000.....	2.480 × 10 <sup>-12</sup>	0.07850
4,000.....	2.526	.6220
5,000.....	41.038	.9646
For HD ⇌ H + D		
300.....	2.732 × 10 <sup>-23</sup>	8.264 × 10 <sup>-28</sup>
500.....	1.265 × 10 <sup>-19</sup>	1.779 × 10 <sup>-21</sup>
1,000.....	1.867 × 10 <sup>-18</sup>	7.048 × 10 <sup>-17</sup>
1,500.....	1.350 × 10 <sup>-16</sup>	5.819 × 10 <sup>-14</sup>
2,000.....	1.215 × 10 <sup>-14</sup>	5.512 × 10 <sup>-11</sup>
For D <sub>2</sub> ⇌ 2D		
300.....	1.319 × 10 <sup>-23</sup>	5.742 × 10 <sup>-27</sup>
500.....	1.171 × 10 <sup>-19</sup>	1.711 × 10 <sup>-21</sup>
1,000.....	2.972 × 10 <sup>-18</sup>	8.420 × 10 <sup>-17</sup>
1,500.....	2.230 × 10 <sup>-16</sup>	7.432 × 10 <sup>-14</sup>
2,000.....	2.227 × 10 <sup>-14</sup>	7.462 × 10 <sup>-11</sup>

2,000° K, 1.6 percent at 2,500° K, 7.2 percent at 3,000° K, and 21 percent at 3,500° K.

TABLE 11. Heats of dissociation of H<sub>2</sub>, HD, and D<sub>2</sub> in cal mole<sup>-1</sup>

T	p-H <sub>2</sub>	o-H <sub>2</sub>	a-H <sub>2</sub>	HD	o-D <sub>2</sub>	p-D <sub>2</sub>	a-D <sub>2</sub>
°K							
0.....	103,239	102,900	103,885	104,064	105,043	104,577	104,891
288.16....	104,191	104,173	104,177	104,992	105,982	105,982	105,982

An equation of state for 1 mole of molecular H<sub>2</sub>, HD, or D<sub>2</sub> capable of forming 2 moles of atoms when completely dissociated, assuming as before that atoms and molecules individually behave as ideal gases, is

$$\frac{PV}{RT} = 1 + \sqrt{\frac{K}{K+4P}} \quad (3.10)$$

or

$$\frac{PV}{RT} = 1 - \frac{KV}{8RT} \left( 1 - \sqrt{1 + 16 \frac{RT}{KV}} \right), \quad (3.11)$$

where  $K$  is a function of  $T$  determined by eq 3.3 and  $V$  is the volume per  $2N_0$  atoms uncombined or combined as molecules.

The thermodynamic properties of an equilibrium mixture of atomic and molecular hydrogen in the ideal gas state can in principle be calculated from the properties of atomic hydrogen at low pressures and the equation of state (eq 3.10) or (eq. 3.11). It is simpler, however, to determine the properties of the mixture from the properties of the atomic and molecular varieties and the fraction dissociated.

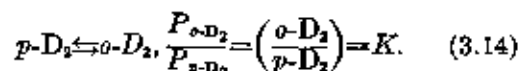
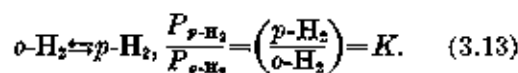
The equation given by Epstein [30] for the heat capacity of a reacting gas mixture, when applied to the heat capacity of an equilibrium mixture of atomic and molecular hydrogen, is

$$\frac{(C_p^0)_{\text{mixture}}}{R} = 2x \frac{(C_p^0)_{\text{atomic}}}{R} + (1-x) \frac{(C_p^0)_{\text{molecular}}}{R} + \frac{(1-x^2)x}{2} \left[ 2 \frac{(H^0)_{\text{atomic}}}{RT} - \frac{(H^0)_{\text{molecular}}}{RT} \right], \quad (3.12)$$

where  $x$  is the fraction of the originally totally nondissociated hydrogen that has dissociated,  $(C_p^0)_{\text{atomic}}$  and  $(C_p^0)_{\text{molecular}}$  are heat capacities per mole of atoms and molecules respectively in the ideal gas state, and  $(C_p^0)_{\text{mixture}}$  is for a mixture

containing  $2N_0$  of atoms combined or uncombined, the components being in the ideal gas state.  $(C_p^0)_{\text{mixture}}$  is a function of  $P$  as well as  $T$  since  $x$  is a function of  $P$ . In figure 4, curves  $D$ ,  $C$ , and  $B$  show the variation of  $(C_p^0/R)_{\text{mixture}}$  for H<sub>2</sub> with temperature for pressures of 0.01, 1, and 100 atmospheres, respectively. Curve  $A$  drawn for comparison is the heat capacity of 1 mole of undissociated H<sub>2</sub>, that is,  $(C_p^0/R)_{\text{molecular}}$ . It appears from these curves that when dissociation has its greatest importance, thermal effects originating in other ways are likely to be dwarfed by comparison. Wildt [19] has calculated the ratio of specific heats of hydrogen at high temperatures using principles similar to those employed here. The results obtained have application to stellar atmospheres.

## 2. Ortho-Para Equilibrium



The equilibrium constants of the ortho-para conversion of H<sub>2</sub> and D<sub>2</sub> in the ideal gas state are independent of  $P$ . Accordingly, pressure does not appreciably change the ortho-para ratio under equilibrium conditions. Although the lowest rotational levels of the ortho and para varieties differ,  $\Delta E_0^0$  for the two reactions (eq 3.13 and eq 3.14) is zero, because in the calculations for both the ortho and para varieties the ground state of the molecule,  $J=0$  and  $v=0$ , was arbitrarily selected as the origin of energies.

In table 12 are given values of the percentage para composition in the ideal gas state of equilibrium mixtures of ortho-para varieties calculated from the state-sums,  $\sum g_i e^{-E_i/RT}$ , see eq 2.2 and eq 2.14. These values are in close agreement with earlier values obtained by Harkness and Deming [11] and are in agreement with the variations in the relative intensities of the ortho-para spectral lines and with estimates of the ortho-para compositions based on measurements of thermal conduction from heated wires. The success in explaining the heat capacity of gaseous hydrogen at moderate and low temperatures is also corroborating evidence for table 12 [48].



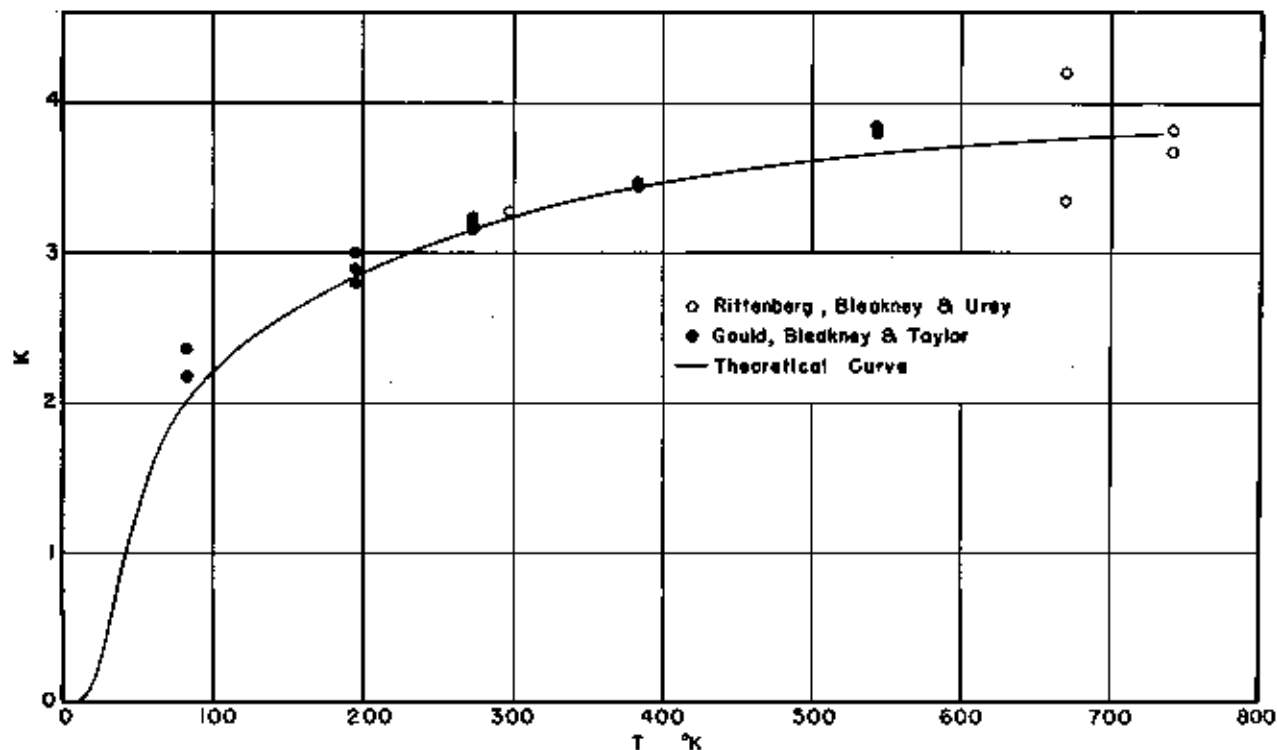


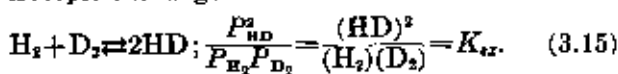
FIGURE 5. The equilibrium constant for  $H_2 + D_2 \rightleftharpoons 2HD$ .

TABLE 12. Ortho-para composition at equilibrium

T	Percentage in para form for $H_2$	Percentage in para form for $D_2$
°K		
10	99.9999	0.0277
20	99.9321	1.996
20.39	99.769	.....
23.57	.....	3.793
30	97.021	7.864
33.10	95.034	.....
40	89.727	14.784
50	77.064	20.718
60	65.580	26.131
70	55.997	28.162
80	48.537	30.141
90	42.382	31.396
100	38.630	32.164
120	32.959	32.916
150	28.003	33.240
200	25.974	33.327
250	25.294	.....
296.16	25.076	33.333
300	25.072	33.333
350	25.019	.....
400	25.005	.....
500	25.000	.....

### 3. Isotopic Exchange

The chemical and mass action equations for isotopic exchange are



The equilibrium constant  $K_{ex}$  of the isotopic exchange reaction (eq 3.15) is related to the dissociation constants  $K$  of eq 3.7, 3.8, and 3.9 by the equation

$$K_{ex} = \frac{K_{H_2} K_{D_2}}{K_{HD}^2}. \quad (3.16)$$

The equilibrium constant  $K_{ex}$  for isotopic exchange in the ideal gas state is independent of  $P$ , and accordingly the relative equilibrium concentrations of  $H_2$ ,  $HD$ , and  $D_2$  are also independent of pressure in the ideal gas state. For this reaction the  $\Delta E_0^\circ$  of eq 3.3, the difference between twice the energy of the ground state of  $HD$  minus the sum of the energies of the ground states of  $H_2$  and  $D_2$ , is equal to twice the zero-point vibrational energy of  $HD$  minus the sum of the zero-point vibrational energies of  $H_2$  and  $D_2$ . Using the values given in section III, 1 for the zero point energies,  $\Delta E_0^\circ$  is 159.5 cal for the formation of 2 moles of  $HD$ .

In figure 5 are plotted experimental values of  $K_{ex}$ , whereas the curve was derived from spectroscopic data as has been indicated. The data of Rittenberg, Bleakney, and Urey [54] were obtained from measurements on hydrogen-deuterium mixtures prepared by the decomposition of mix-

tures of HI and DI, and those of Gould, Bleakney, and Taylor [55] were obtained with mixtures of hydrogen and deuterium that had been adsorbed on various catalysts or had been diffused through palladium. Some of the observations of Gould, Bleakney, and Taylor plotted in figure 5 were not plotted by them in their published article.

Although the theoretical curve of figure 5 is thought to be more reliable than the experimental data, it is to be pointed out that the uncertainties in the zero-point energies of  $H_2$ , HD, and  $D_2$  can give rise to perceptible shifts in the curve. Thus a change in  $\Delta E_0^\circ$  of 3 cal mole<sup>-1</sup>, which is equivalent to about 1 cm<sup>-1</sup> in  $2(G_0)_{HD} - (G_0)_{H_2} - (G_0)_{D_2}$ , changes  $K_{s,2}$  by about 1.5 percent at 100° K. It seems doubtful that  $\Delta E_0^\circ$  is known better than to a very few calories per mole, for while it is plausible, it is apparently not certain that  $D_e$ , the dissociation energy above the minimum of the potential energy curve, is so nearly the same for  $H_2$ , HD, and  $D_2$  [25]. The theoretical values of Urey and Rittenberg [13] are, therefore, practically as reliable as the newly calculated ones.

#### IV. PVT Data and Relations for Hydrogen and Deuterium

In order to calculate the thermodynamic properties of gaseous hydrogen at high densities (in principle at any densities other than very low) from values of the properties for the hypothetical ideal gaseous state, it is necessary to have information concerning the relations between pressure, volume, and temperature for each temperature in question extending from very low to high densities.

##### 1. Hydrogen

The available PVT data for hydrogen fall between 14° and 700° K. They consist, in general, of measurements of volume of known amounts of gas at several different pressures along selected isotherms. The quantities usually reported are values of  $PV$  or  $PV/P_0V_0$  at the measured pres-

ures or densities. In this report this information is presented in the form of tables in which integral values of the variables of state are spaced closely enough to allow accurate interpolation.

The dependent variable  $Z$  appearing in the tables is  $PV/RT$ . Through the definition of  $R$ , this quantity has the value 1 at extremely low densities, and it is of the same order of magnitude over a very extended range of densities. The independent variables chosen are  $T$ , the Kelvin temperature, and  $\rho$ , the Amagat density, which is defined as the ratio of the observed density to the density at standard conditions (0°C and 1 atmosphere). Density was chosen as an independent variable of state in preference to pressure because this resulted in simpler representation of the  $PV/RT$  isotherms. The Amagat density is also the ratio of the volume  $V_0$  of the gas at standard conditions to its observed volume.

$$Z = \frac{\text{observed density}}{\text{density at standard conditions}} = \frac{V_0}{V} \quad (4.1)$$

The best value for  $V_0$ , the molar volume of hydrogen at standard conditions, is 22.4279 liters or 22428.5 cm<sup>3</sup>, according to the values of  $RT_0$  obtained by Cragoe [90] and the value of  $PV/RT$  for hydrogen at standard conditions as given by Cragoe and the present correlation. The density of hydrogen at standard conditions is 0.089888 gram liter<sup>-1</sup>.

Values of  $PV/RT$ , or  $Z$  for  $n$ - $H_2$  are given in table 13 for different values of  $T$  and  $\rho$ . Corresponding values of  $P$  and of the derivatives  $(dZ/dT)_\rho$ ,  $(d^2Z/dT^2)_\rho$  and  $(dZ/d\rho)_T$  needed for the calculation of some of the more important thermal properties of the real gas from ideal gas values (see section V) are given as functions of the same variables of state  $\rho$  and  $T$  in tables 14, 15, 16, and 17, respectively. The temperature intervals used are of graduated size, being as small as 2 degrees at low temperatures and as much as 20 deg above 0° C. The density intervals, except for entries at  $\rho=1, 2, 3, 6,$  and  $10$ , are uniformly equal to 20 Amagats from  $\rho=0$  to  $\rho=500$ .





260	1.00602	1.00126	1.00181	1.00233	1.00277	1.00293	1.00375	1.00445	1.00525	1.00645	1.00738	1.00838	1.00941	1.10016
270	1.00614	1.00131	1.00186	1.00242	1.00286	1.00302	1.00384	1.00454	1.00534	1.00654	1.00747	1.00847	1.00950	1.10025
280	1.00626	1.00143	1.00198	1.00254	1.00298	1.00314	1.00396	1.00466	1.00546	1.00666	1.00759	1.00859	1.00962	1.10037
290	1.00638	1.00155	1.00210	1.00266	1.00310	1.00326	1.00408	1.00478	1.00558	1.00678	1.00771	1.00871	1.00974	1.10049
300	1.00650	1.00167	1.00222	1.00278	1.00322	1.00338	1.00420	1.00490	1.00570	1.00690	1.00783	1.00883	1.00986	1.10061
320	1.00682	1.00189	1.00244	1.00300	1.00344	1.00360	1.00442	1.00512	1.00592	1.00712	1.00805	1.00905	1.01008	1.10085
340	1.00698	1.00205	1.00260	1.00316	1.00360	1.00376	1.00458	1.00528	1.00608	1.00728	1.00821	1.00921	1.01024	1.10101
360	1.00714	1.00221	1.00276	1.00332	1.00376	1.00392	1.00474	1.00544	1.00624	1.00744	1.00837	1.00937	1.01040	1.10117
380	1.00730	1.00237	1.00292	1.00348	1.00392	1.00408	1.00490	1.00560	1.00640	1.00760	1.00853	1.00953	1.01056	1.10133
400	1.00746	1.00253	1.00308	1.00364	1.00408	1.00424	1.00506	1.00576	1.00656	1.00776	1.00869	1.00969	1.01072	1.10149
420	1.00762	1.00269	1.00324	1.00380	1.00424	1.00440	1.00522	1.00592	1.00672	1.00792	1.00885	1.00985	1.01088	1.10165
440	1.00778	1.00285	1.00340	1.00396	1.00440	1.00456	1.00538	1.00608	1.00688	1.00808	1.00901	1.01001	1.01104	1.10181
460	1.00794	1.00301	1.00356	1.00412	1.00456	1.00472	1.00554	1.00624	1.00704	1.00824	1.00917	1.01017	1.01120	1.10197
480	1.00810	1.00317	1.00372	1.00428	1.00472	1.00488	1.00570	1.00640	1.00720	1.00840	1.00933	1.01033	1.01136	1.10213
500	1.00826	1.00333	1.00388	1.00444	1.00488	1.00504	1.00586	1.00656	1.00736	1.00856	1.00949	1.01049	1.01152	1.10229
520	1.00842	1.00349	1.00404	1.00460	1.00504	1.00520	1.00602	1.00672	1.00752	1.00872	1.00965	1.01065	1.01168	1.10245
540	1.00858	1.00365	1.00420	1.00476	1.00520	1.00536	1.00618	1.00688	1.00768	1.00888	1.00981	1.01081	1.01184	1.10261
560	1.00874	1.00381	1.00436	1.00492	1.00536	1.00552	1.00634	1.00704	1.00784	1.00904	1.01007	1.01107	1.01210	1.10277
580	1.00890	1.00397	1.00452	1.00508	1.00552	1.00568	1.00650	1.00720	1.00800	1.00920	1.01023	1.01123	1.01226	1.10293
600	1.00906	1.00413	1.00468	1.00524	1.00568	1.00584	1.00666	1.00736	1.00816	1.00936	1.01039	1.01139	1.01242	1.10309
620	1.00922	1.00429	1.00484	1.00540	1.00584	1.00600	1.00682	1.00752	1.00832	1.00952	1.01055	1.01155	1.01258	1.10325
640	1.00938	1.00445	1.00500	1.00556	1.00600	1.00616	1.00698	1.00768	1.00848	1.00968	1.01071	1.01171	1.01274	1.10341
660	1.00954	1.00461	1.00516	1.00572	1.00616	1.00632	1.00714	1.00784	1.00864	1.00984	1.01087	1.01187	1.01290	1.10357
680	1.00970	1.00477	1.00532	1.00588	1.00632	1.00648	1.00730	1.00800	1.00880	1.01000	1.01103	1.01203	1.01306	1.10373
700	1.00986	1.00493	1.00548	1.00604	1.00648	1.00664	1.00746	1.00816	1.00896	1.01016	1.01119	1.01219	1.01322	1.10389
720	1.00999	1.00509	1.00564	1.00620	1.00664	1.00680	1.00762	1.00832	1.00912	1.01032	1.01135	1.01235	1.01338	1.10405
740	1.01014	1.00525	1.00580	1.00636	1.00680	1.00696	1.00778	1.00848	1.00928	1.01048	1.01151	1.01251	1.01354	1.10421
760	1.01028	1.00541	1.00596	1.00652	1.00696	1.00712	1.00794	1.00864	1.00944	1.01064	1.01167	1.01267	1.01370	1.10437
780	1.01042	1.00557	1.00612	1.00668	1.00712	1.00728	1.00810	1.00880	1.00960	1.01080	1.01183	1.01283	1.01386	1.10453
800	1.01056	1.00573	1.00628	1.00684	1.00728	1.00744	1.00826	1.00896	1.00976	1.01096	1.01199	1.01299	1.01402	1.10469
820	1.01070	1.00589	1.00644	1.00700	1.00744	1.00760	1.00842	1.00912	1.00992	1.01112	1.01215	1.01315	1.01418	1.10485
840	1.01084	1.00605	1.00660	1.00716	1.00760	1.00776	1.00858	1.00928	1.01008	1.01128	1.01231	1.01331	1.01434	1.10501
860	1.01098	1.00621	1.00676	1.00732	1.00776	1.00792	1.00874	1.00944	1.01024	1.01144	1.01247	1.01347	1.01450	1.10517
880	1.01112	1.00637	1.00692	1.00748	1.00792	1.00808	1.00890	1.00960	1.01040	1.01160	1.01263	1.01363	1.01466	1.10533
900	1.01126	1.00653	1.00708	1.00764	1.00808	1.00824	1.00906	1.00976	1.01056	1.01176	1.01279	1.01379	1.01482	1.10549
920	1.01140	1.00669	1.00724	1.00780	1.00824	1.00840	1.00922	1.00992	1.01072	1.01192	1.01295	1.01395	1.01498	1.10565
940	1.01154	1.00685	1.00740	1.00796	1.00840	1.00856	1.00938	1.01008	1.01088	1.01208	1.01311	1.01411	1.01514	1.10581
960	1.01168	1.00701	1.00756	1.00812	1.00856	1.00872	1.00954	1.01024	1.01104	1.01224	1.01327	1.01427	1.01530	1.10597
980	1.01182	1.00717	1.00772	1.00828	1.00872	1.00888	1.00970	1.01040	1.01120	1.01240	1.01343	1.01443	1.01546	1.10613
1000	1.01196	1.00733	1.00788	1.00844	1.00888	1.00904	1.00986	1.01056	1.01136	1.01256	1.01359	1.01459	1.01562	1.10629

TABLE 18. Values of  $Z = PV/RT$  for hydrogen at integral values of  $T$ , the absolute temperature, and  $\rho$ , the density in Amagat units—Continued

Temperature °K	240	260	280	300	340	360	380	400	420	440	460	480	500
42	0.6565	0.6384	0.6221	0.6080	0.5958	0.5853	0.5768	0.5699	0.5643	0.5598	0.5561	0.5531	0.5500
44	0.6874	0.6685	0.6522	0.6380	0.6264	0.6164	0.6084	0.6019	0.5968	0.5928	0.5894	0.5867	0.5840
46	0.7164	0.6968	0.6805	0.6663	0.6553	0.6464	0.6391	0.6330	0.6281	0.6241	0.6207	0.6178	0.6150
48	0.7410	0.7207	0.7044	0.6902	0.6791	0.6704	0.6634	0.6577	0.6532	0.6494	0.6461	0.6431	0.6402
50	0.7644	0.7437	0.7272	0.7130	0.7018	0.6934	0.6871	0.6821	0.6781	0.6746	0.6714	0.6684	0.6654
52	0.7860	0.7648	0.7484	0.7342	0.7230	0.7150	0.7091	0.7044	0.7004	0.6971	0.6941	0.6911	0.6881
54	0.8069	0.7854	0.7690	0.7548	0.7436	0.7360	0.7304	0.7261	0.7224	0.7191	0.7161	0.7131	0.7101
56	0.8262	0.8044	0.7880	0.7738	0.7626	0.7550	0.7500	0.7461	0.7424	0.7391	0.7361	0.7331	0.7301
58	0.8412	0.8190	0.8026	0.7884	0.7772	0.7700	0.7650	0.7611	0.7574	0.7541	0.7511	0.7481	0.7451
60	0.8572	0.8348	0.8184	0.8042	0.7930	0.7860	0.7810	0.7771	0.7734	0.7701	0.7671	0.7641	0.7611
65	0.9225	0.9000	0.8836	0.8694	0.8582	0.8500	0.8441	0.8391	0.8354	0.8321	0.8291	0.8261	0.8231
70	0.9228	0.9224	0.9220	0.9216	0.9212	0.9208	0.9204	0.9200	0.9196	0.9192	0.9188	0.9184	0.9180
75	0.9488	0.9484	0.9480	0.9476	0.9472	0.9468	0.9464	0.9460	0.9456	0.9452	0.9448	0.9444	0.9440
80	0.9711	0.9706	0.9702	0.9698	0.9694	0.9690	0.9686	0.9682	0.9678	0.9674	0.9670	0.9666	0.9662
85	0.9904	0.9895	0.9886	0.9877	0.9868	0.9859	0.9850	0.9841	0.9832	0.9823	0.9814	0.9805	0.9796
90	1.0074	1.0064	1.0055	1.0046	1.0037	1.0028	1.0019	1.0010	1.0001	0.9992	0.9983	0.9974	0.9965
95	1.0224	1.0214	1.0205	1.0196	1.0187	1.0178	1.0169	1.0160	1.0151	1.0142	1.0133	1.0124	1.0115
100	1.0369	1.0359	1.0350	1.0341	1.0332	1.0323	1.0314	1.0305	1.0296	1.0287	1.0278	1.0269	1.0260
105	1.0481	1.0471	1.0462	1.0453	1.0444	1.0435	1.0426	1.0417	1.0408	1.0399	1.0390	1.0381	1.0372
110	1.0589	1.0579	1.0569	1.0560	1.0551	1.0542	1.0533	1.0524	1.0515	1.0506	1.0497	1.0488	1.0479
115	1.0688	1.0678	1.0668	1.0659	1.0650	1.0641	1.0632	1.0623	1.0614	1.0605	1.0596	1.0587	1.0578
120	1.0773	1.0763	1.0753	1.0744	1.0735	1.0726	1.0717	1.0708	1.0699	1.0690	1.0681	1.0672	1.0663
125	1.0854	1.0844	1.0834	1.0825	1.0816	1.0807	1.0798	1.0789	1.0780	1.0771	1.0762	1.0753	1.0744
130	1.0927	1.0917	1.0907	1.0898	1.0889	1.0880	1.0871	1.0862	1.0853	1.0844	1.0835	1.0826	1.0817
135	1.0994	1.0984	1.0974	1.0965	1.0956	1.0947	1.0938	1.0929	1.0920	1.0911	1.0902	1.0893	1.0884
140	1.1055	1.1046	1.1037	1.1028	1.1019	1.1010	1.1001	1.0992	1.0983	1.0974	1.0965	1.0956	1.0947
145	1.1111	1.1101	1.1092	1.1083	1.1074	1.1065	1.1056	1.1047	1.1038	1.1029	1.1020	1.1011	1.1002
150	1.1163	1.1153	1.1144	1.1135	1.1126	1.1117	1.1108	1.1099	1.1090	1.1081	1.1072	1.1063	1.1054
155	1.1212	1.1202	1.1193	1.1184	1.1175	1.1166	1.1157	1.1148	1.1139	1.1130	1.1121	1.1112	1.1103
160	1.1257	1.1247	1.1238	1.1229	1.1220	1.1211	1.1202	1.1193	1.1184	1.1175	1.1166	1.1157	1.1148
165	1.1299	1.1289	1.1280	1.1271	1.1262	1.1253	1.1244	1.1235	1.1226	1.1217	1.1208	1.1199	1.1190
170	1.1337	1.1327	1.1318	1.1309	1.1300	1.1291	1.1282	1.1273	1.1264	1.1255	1.1246	1.1237	1.1228
180	1.1406	1.1396	1.1387	1.1378	1.1369	1.1360	1.1351	1.1342	1.1333	1.1324	1.1315	1.1306	1.1297
190	1.1463	1.1453	1.1444	1.1435	1.1426	1.1417	1.1408	1.1399	1.1390	1.1381	1.1372	1.1363	1.1354
200	1.1514	1.1504	1.1495	1.1486	1.1477	1.1468	1.1459	1.1450	1.1441	1.1432	1.1423	1.1414	1.1405
210	1.1559	1.1549	1.1540	1.1531	1.1522	1.1513	1.1504	1.1495	1.1486	1.1477	1.1468	1.1459	1.1450
220	1.1599	1.1589	1.1580	1.1571	1.1562	1.1553	1.1544	1.1535	1.1526	1.1517	1.1508	1.1499	1.1490
230	1.1635	1.1625	1.1616	1.1607	1.1598	1.1589	1.1580	1.1571	1.1562	1.1553	1.1544	1.1535	1.1526
240	1.1666	1.1656	1.1647	1.1638	1.1629	1.1620	1.1611	1.1602	1.1593	1.1584	1.1575	1.1566	1.1557
250	1.1693	1.1683	1.1674	1.1665	1.1656	1.1647	1.1638	1.1629	1.1620	1.1611	1.1602	1.1593	1.1584
260	1.1716	1.1706	1.1697	1.1688	1.1679	1.1670	1.1661	1.1652	1.1643	1.1634	1.1625	1.1616	1.1607
270	1.1737	1.1727	1.1718	1.1709	1.1700	1.1691	1.1682	1.1673	1.1664	1.1655	1.1646	1.1637	1.1628
280	1.1749	1.1739	1.1730	1.1721	1.1712	1.1703	1.1694	1.1685	1.1676	1.1667	1.1658	1.1649	1.1640
290	1.1768	1.1758	1.1749	1.1740	1.1731	1.1722	1.1713	1.1704	1.1695	1.1686	1.1677	1.1668	1.1659

Properties of Hydrogen

50° C.	1.17865	1.19682	1.21279	1.23083	1.24279	1.26083	1.28079	1.31470	1.34266	1.36762	1.39552	1.42463	1.45400	1.48368	1.51311	1.54235
300	1.17916	1.19690	1.21302	1.23053	1.24309	1.26133	1.28069	1.31500	1.34398	1.36903	1.39679	1.42563	1.45513	1.48538	1.51539	1.54516
320	1.18164	1.20224	1.21844	1.23602	1.24904	1.26780	1.28727	1.32177	1.35144	1.37659	1.39489	1.42344	1.45311	1.48398	1.51399	1.54396
340	1.18385	1.20632	1.22276	1.24082	1.25404	1.27304	1.29267	1.32717	1.35684	1.38199	1.39978	1.42804	1.45789	1.48898	1.51899	1.54886
360	1.18526	1.20892	1.22560	1.24392	1.25730	1.27654	1.29590	1.33040	1.36007	1.38523	1.40292	1.43107	1.46100	1.49181	1.52149	1.55106
380	1.18612	1.21092	1.22780	1.24632	1.26000	1.27954	1.29890	1.33340	1.36307	1.38823	1.40592	1.43397	1.46400	1.49509	1.52506	1.55493
400	1.18751	1.21330	1.23030	1.24892	1.26280	1.28254	1.30217	1.33667	1.36634	1.39150	1.40919	1.43714	1.46707	1.49806	1.52793	1.55770
420	1.18837	1.21516	1.23220	1.25082	1.26480	1.28474	1.30437	1.33887	1.36854	1.39370	1.41139	1.43934	1.46927	1.50026	1.53013	1.55986
440	1.18886	1.21660	1.23370	1.25232	1.26640	1.28654	1.30617	1.34067	1.37034	1.39550	1.41319	1.44114	1.47107	1.50206	1.53193	1.56166
460	1.18930	1.21800	1.23510	1.25372	1.26780	1.28804	1.30767	1.34217	1.37184	1.39700	1.41469	1.44264	1.47257	1.50356	1.53343	1.56316
480	1.18960	1.21916	1.23620	1.25482	1.26890	1.28924	1.30887	1.34337	1.37304	1.39820	1.41589	1.44384	1.47377	1.50476	1.53463	1.56436
500	1.18990	1.21970	1.23670	1.25532	1.26940	1.29004	1.30967	1.34417	1.37384	1.39900	1.41669	1.44464	1.47457	1.50556	1.53543	1.56516
520	1.19000	1.22000	1.23700	1.25562	1.26970	1.29044	1.31007	1.34457	1.37424	1.39940	1.41709	1.44504	1.47497	1.50596	1.53583	1.56556
540	1.19000	1.22020	1.23720	1.25582	1.26990	1.29064	1.31027	1.34477	1.37444	1.39960	1.41729	1.44524	1.47517	1.50616	1.53603	1.56576
560	1.19000	1.22040	1.23740	1.25602	1.27010	1.29084	1.31047	1.34497	1.37464	1.39980	1.41749	1.44544	1.47537	1.50636	1.53623	1.56596
580	1.19000	1.22060	1.23760	1.25620	1.27030	1.29104	1.31067	1.34517	1.37484	1.39990	1.41759	1.44554	1.47547	1.50646	1.53633	1.56606
600	1.19000	1.22080	1.23780	1.25640	1.27050	1.29124	1.31087	1.34537	1.37504	1.39990	1.41769	1.44564	1.47557	1.50656	1.53643	1.56616

TABLE 14. Pressure (in atmospheres) at integral values of  $T$ , the absolute temperature, and  $p$ , the density in Amagat units

Temperature $^{\circ}K$	$p=1$	2	3	6	10	20	40	60	80	100	120	140	160	180	200
16	0.05800	0.11485	0.17083	0.37096	0.66364										
18	0.6835	1.3171	1.9801	4.2166											
20	0.7296	1.4441	2.1516												
22	0.6972	1.5012	2.2729	4.9228	7.9390										
24	0.6736	1.5782	2.3941	5.1285	8.3392	1.59040									
26	0.6496	1.6853	2.5152	5.3038	8.7410	1.79410	3.1448								
28	0.6253	1.8029	2.6362	5.4698	9.1455	1.99805	3.4838	4.7476							
30	0.6010	1.9316	2.7571	5.6281	9.5528	2.20308	3.7800	5.3407	6.8597	7.3966					
32	0.5769	2.0716	2.8778	5.7797	9.9633	2.41028	4.0667	5.7913	7.1193	8.2978	9.3035	9.9442	10.607	10.908	
34	0.5530	2.2232	3.0000	5.9245	1.03751	2.61978	4.3114	6.2201	7.3779	8.1266	10.272	11.296	12.007	12.637	13.133
36	0.5294	2.3868	3.1248	6.0636	1.26336	2.84577	4.5680	6.7099	8.0657	9.0620	11.394	12.490	13.486	14.363	15.063
38	0.5062	2.5629	3.2525	6.1972	1.49502	3.08730	4.8368	7.1994	8.7312	10.049	12.569	13.749	14.875	15.850	17.014
40	0.4834	2.7519	3.3833	6.3255	1.73280	3.33878	5.1186	7.6794	9.3890	11.170	13.438	14.614	15.644	17.746	18.957
42	0.4611	2.9542	3.5175	6.4498	1.97701	3.60292	5.4124	8.1557	10.1445	12.548	14.482	15.653	17.008	18.433	20.846
44	0.4393	3.1703	3.6554	6.5704	2.22800	3.88000	5.7208	8.6200	380	400	420	440	460	480	500
34	12.511	13.790	15.094	14.148	14.274	14.282	14.488	14.884	15.254	15.687	16.090	16.369	16.724	16.223	16.842
36	16.702	18.232	19.894	17.198	17.498	17.800	18.200	18.606	19.019	19.493	20.047	20.706	21.400	22.443	23.642
38	17.874	19.555	21.375	20.051	21.708	21.360	21.960	22.667	23.366	24.162	25.061	26.106	27.320	28.728	30.405
40	20.039	21.966	23.946	22.988	23.910	24.820	25.784	26.726	27.760	28.876	30.188	31.577	33.208	34.966	37.208
42	22.193	24.470	26.702	25.905	27.106	28.213	29.555	30.884	32.186	33.586	35.286	37.105	39.188	41.529	44.084
$p=20$	540	540	560	580	620	680	640	660	680	700					
34	17.960	19.352	21.162	23.266	26.461	30.179	34.908	40.811	48.026	68.702					
36	25.170	27.061	29.460	32.405	36.012	40.372	46.506	51.696							
38	32.453	34.982	38.009	41.664	46.048										
40	39.783	42.840	46.565												
42	47.053	50.690													
$p=1$	2	3	3	6	10	20	40	60	80	100	120	140	160	180	200
42	0.16394	0.30606	0.44814	0.91065	1.50332	2.4494	5.0024	8.1537	10.445	12.548	14.482	16.285	17.906	19.453	20.805
44	0.16997	0.32074	0.46280	0.93498	1.57998	2.5096	5.0789	8.2988	11.106	13.393	15.530	17.511	19.389	21.115	22.766
46	0.17600	0.33542	0.50590	0.96090	1.65900	3.2616	5.2851	8.4170	11.793	14.241	16.508	18.757	20.686	23.792	26.672
48	0.18203	0.35010	0.54931	1.03831	1.75802	3.4624	5.5959	8.9664	12.421	15.085	17.607	20.000	22.279	24.468	26.877
50	0.18806	0.36478	0.59358	1.08792	1.86921	3.5681	5.9062	10.070	13.077	16.088	18.643	21.295	23.791	26.138	28.575
52	0.19409	0.37946	0.63811	1.13721	1.97958	3.7088	7.2162	10.554	13.732	16.768	19.477	22.327	25.180	27.806	30.371
54	0.19997	0.39414	0.68288	1.17853	2.08910	3.8544	7.5900	11.031	14.385	17.605	20.700	23.709	26.622	29.470	32.283
56	0.20584	0.40881	0.72791	1.22079	2.20233	4.0051	7.9599	11.509	15.038	18.443	21.739	24.940	28.060	31.128	34.150
58	0.21167	0.42348	0.77318	1.26406	2.31907	4.1527	8.4045	11.986	15.692	19.290	22.787	26.167	29.407	32.780	36.031
60	0.21750	0.43817	0.81860	1.30833	2.43922	4.3068	8.9048	12.463	16.349	20.114	23.793	27.395	30.968	34.435	37.915
62	0.22302	0.45286	0.86421	1.40002	2.56402	4.4681	9.2908	12.941	17.070	21.000	24.801	28.461	32.004	35.690	40.815
70	0.25893	0.51144	0.99881	1.63066	2.94462	4.80278	9.9979	14.857	19.690	25.277	28.912	32.514	38.101	42.683	47.312





TABLE 14. Pressure (in atmospheres) at integral values of  $T$ , the absolute temperature, and  $\rho$ , the density in Anagat units—Continued

Temperature	$p=230$	210	200	280	300	320	340	360	380	400	420	440	460	480	500
43	22.193	23.470	24.702	25.905	27.105	28.318	29.555	30.824	32.125	33.458	34.824	37.105	38.128	41.429	44.194
44	24.344	25.626	27.352	28.550	30.209	31.804	33.354	34.962	36.634	38.380	40.179	42.975	45.104	47.805	50.829
45	26.638	28.207	30.000	31.732	33.409	35.291	37.189	39.102	41.140	43.319	45.680	48.266	51.087	54.180	57.807
46	29.082	30.941	32.642	34.644	36.678	38.781	40.968	43.325	45.825	48.487	51.307	54.264	57.471	60.971	64.871
50	30.753	33.024	35.276	37.065	39.859	42.264	44.749	47.376	50.105	53.036	56.117	59.449	63.027	66.909	71.132
52	32.897	35.404	37.914	40.463	43.037	46.751	49.558	52.490	55.553	57.820	61.302	64.908	68.678	72.566	77.887
54	35.026	37.780	40.549	43.358	46.242	49.290	52.333	55.588	58.953	62.404	66.449	70.124	74.003	78.292	84.826
56	37.136	40.154	43.180	46.290	49.433	52.692	56.107	59.656	63.397	67.286	71.559	75.629	80.377	85.363	91.207
58	39.250	42.624	45.656	49.174	52.800	56.449	60.187	63.928	67.798	72.066	76.855	81.500	86.659	92.169	98.069
60	41.377	45.097	48.444	52.069	56.779	59.624	63.628	67.320	72.222	76.586	81.787	87.405	92.569	98.497	104.64
65	46.694	50.850	55.041	59.242	63.706	68.352	73.117	78.109	83.246	88.504	94.796	100.90	107.49	114.61	122.02
70	51.993	56.756	61.619	66.610	71.752	77.084	82.625	88.425	94.510	100.92	107.69	114.87	122.48	130.24	138.54
75	57.278	62.661	68.175	73.842	79.692	85.766	92.109	98.723	105.68	112.95	120.65	128.80	137.44	146.62	156.40
80	62.550	68.351	74.691	81.032	87.696	94.609	101.81	109.34	117.23	125.49	134.13	143.25	152.89	162.52	173.42
85	67.750	74.374	81.178	88.189	95.429	103.00	110.86	119.07	127.70	136.76	146.27	156.23	166.67	178.24	190.23
90	72.976	80.165	87.631	95.322	103.29	111.55	120.16	129.16	138.60	148.50	158.94	169.94	181.35	193.85	206.92
95	78.177	86.010	94.081	102.43	111.08	120.08	129.43	139.22	149.47	160.23	171.55	183.40	195.68	208.30	223.64
100	83.378	91.819	100.52	109.62	119.89	129.59	139.67	150.31	161.51	173.29	185.63	198.50	211.55	224.89	240.30
105	88.570	97.618	106.94	116.60	126.82	137.04	147.89	159.38	171.42	183.68	196.66	210.44	224.90	239.34	255.58
110	93.768	103.40	113.35	123.66	134.35	145.83	157.66	169.19	181.88	195.17	208.14	222.82	236.98	250.98	272.95
115	98.912	109.16	119.74	130.70	142.08	153.80	166.22	179.11	192.80	206.72	221.56	237.16	253.61	270.94	299.59
120	104.05	114.90	126.11	137.72	149.77	162.29	175.35	189.90	203.27	218.23	233.94	250.45	267.82	286.16	305.49
125	109.20	120.64	132.46	144.72	157.43	170.87	184.44	198.83	213.81	229.70	246.28	263.46	281.98	301.25	321.61
130	114.34	126.38	138.80	151.70	165.09	179.01	193.52	208.57	224.53	241.14	258.55	276.82	296.08	316.33	337.66
135	119.46	132.08	145.12	158.67	172.71	187.84	202.57	219.47	236.11	253.53	272.77	292.93	313.05	331.29	348.62
140	124.57	137.78	151.44	165.92	180.34	195.94	211.59	228.24	245.85	263.87	283.95	303.99	323.04	346.19	369.50
145	129.68	143.48	157.70	172.57	187.40	202.85	220.81	238.00	256.18	275.15	295.11	316.02	337.68	361.05	386.52
150	134.79	149.10	164.05	179.49	193.34	212.20	229.60	247.73	266.83	286.49	307.24	328.02	349.88	375.37	401.31
155	139.89	154.64	170.34	186.41	203.11	220.46	238.56	257.43	277.14	297.76	319.34	341.06	363.70	390.83	418.53
160	144.97	160.52	176.62	193.55	210.69	228.74	247.51	267.11	287.37	308.96	331.37	354.82	379.43	405.29	432.47
165	150.06	166.19	182.80	200.23	218.23	236.97	255.46	276.30	296.63	320.19	343.34	367.64	393.12	416.94	447.80
170	155.13	171.84	189.15	207.10	225.73	245.12	263.82	284.38	304.84	324.29	348.29	373.82	400.72	434.32	467.30
180	165.24	183.10	200.93	220.79	240.71	261.44	283.02	302.00	320.85	343.45	370.07	400.87	433.98	463.25	494.07
190	175.20	194.31	213.90	234.43	255.63	277.68	300.63	324.05	346.47	375.51	403.72	431.17	460.90	492.05	524.72
200	185.26	205.45	228.26	246.01	270.49	293.88	318.20	343.62	368.95	397.53	428.29	458.37	487.82	520.78	555.26
210	195.36	216.64	241.69	257.57	283.32	310.02	335.73	362.47	390.34	419.43	446.79	481.52	514.68	546.38	583.72
220	205.39	227.81	253.02	273.11	300.14	326.15	352.19	381.38	410.71	441.20	473.24	508.08	541.40	577.80	618.02
230	215.39	238.93	263.63	284.90	314.90	337.22	363.02	401.17	433.97	465.08	498.69	537.57	575.08	608.27	648.21
240	225.36	250.02	275.58	302.08	329.69	349.22	374.99	415.83	451.18	484.70	519.84	558.43	594.09	634.52	676.24
250	235.29	261.07	287.80	316.49	344.26	374.17	405.24	437.90	471.26	506.31	542.06	581.13	620.97	662.08	706.11
260	246.22	272.11	299.98	328.36	358.36	390.05	422.46	456.17	491.27	527.82	565.06	606.72	647.16	690.46	735.73
270	256.126	283.117	312.120	342.219	373.458	406.898	439.629	474.997	511.200	549.220	588.894	630.148	673.268	718.218	765.191
280	266.263	294.102	315.915	346.438	378.048	410.892	446.028	480.630	517.479	555.932	596.044	637.839	681.437	726.937	774.461
290	276.008	304.293	324.293	355.595	387.979	421.985	464.713	498.138	531.041	570.500	611.619	651.455	695.141	745.755	794.448

300	.....	282,903	313,985	346,185	379,394	414,246	450,228	487,607	526,090	566,867	608,920	652,702	698,312	745,850	795,416	847,130
320	.....	284,714	315,997	348,415	382,026	416,903	453,132	490,727	529,826	570,458	612,796	656,830	702,728	750,559	800,425	852,440
340	.....	304,349	337,606	372,470	408,406	446,977	486,361	526,533	568,271	611,628	656,778	703,802	752,802	803,886	855,046	908,288
360	.....	323,921	359,030	396,405	434,699	474,323	515,459	558,109	602,505	648,294	696,478	746,267	798,111	852,047	906,721	963,721
380	.....	343,439	381,204	420,317	460,839	502,945	548,415	591,023	638,663	687,290	737,937	790,671	845,302	902,234	961,484	1,023,16
400	.....	365,235	405,987	448,119	493,007	539,238	586,717	635,585	685,155	735,665	788,092	842,575	899,202	958,000	1,017,943	1,080,063
420	.....	388,904	432,006	474,119	519,916	567,912	617,293	668,144	719,173	772,008	827,172	884,028	942,014	1,001,70	1,064,40	1,129,21
440	.....	413,206	459,666	504,922	552,912	603,380	654,291	706,727	760,300	815,468	872,681	931,488	991,429	1,052,101	1,114,000	1,178,000
460	.....	438,100	486,844	534,822	584,681	636,222	689,586	744,798	800,300	857,640	916,360	976,000	1,037,000	1,099,000	1,162,000	1,226,000
480	.....	463,100	513,287	562,822	613,353	665,378	718,838	773,682	829,360	886,414	945,402	1,005,862	1,068,200	1,132,000	1,196,000	1,261,000
500	.....	488,200	539,833	590,822	643,800	698,778	755,698	814,500	874,830	936,214	1,000,000	1,065,720	1,133,000	1,201,000	1,270,000	1,340,000
520	.....	513,300	566,333	618,822	673,400	729,678	787,600	847,000	907,500	969,600	1,033,000	1,098,000	1,164,000	1,231,000	1,300,000	1,370,000
540	.....	538,400	592,833	646,822	703,800	762,378	822,400	883,800	946,800	1,011,000	1,077,000	1,144,000	1,212,000	1,281,000	1,351,000	1,422,000
560	.....	563,500	618,333	672,822	729,400	788,378	848,800	910,800	974,300	1,039,000	1,105,000	1,172,000	1,240,000	1,309,000	1,379,000	1,450,000
580	.....	588,600	644,833	700,822	758,800	818,378	879,400	941,800	1,005,000	1,070,000	1,136,000	1,203,000	1,271,000	1,340,000	1,410,000	1,481,000
600	.....	613,700	670,333	728,822	788,400	848,378	909,800	972,800	1,037,000	1,103,000	1,170,000	1,238,000	1,307,000	1,377,000	1,448,000	1,520,000
620	.....	638,800	696,833	756,822	816,400	877,378	938,800	1,001,800	1,066,000	1,132,000	1,200,000	1,268,000	1,337,000	1,407,000	1,478,000	1,550,000
640	.....	663,900	722,333	782,822	843,400	905,378	967,800	1,031,800	1,097,000	1,164,000	1,232,000	1,301,000	1,371,000	1,442,000	1,514,000	1,587,000
660	.....	689,000	748,833	809,822	871,400	934,378	998,800	1,064,800	1,132,000	1,200,000	1,269,000	1,339,000	1,410,000	1,482,000	1,555,000	1,629,000
680	.....	714,100	774,333	836,822	899,400	963,378	1,029,800	1,097,800	1,166,000	1,236,000	1,306,000	1,377,000	1,449,000	1,522,000	1,596,000	1,671,000
700	.....	739,200	799,833	862,822	926,400	991,378	1,058,800	1,128,800	1,199,000	1,270,000	1,342,000	1,415,000	1,489,000	1,564,000	1,640,000	1,717,000
720	.....	764,300	825,333	889,822	954,400	1,020,378	1,088,800	1,159,800	1,232,000	1,305,000	1,379,000	1,454,000	1,530,000	1,607,000	1,685,000	1,764,000
740	.....	789,400	850,833	916,822	982,400	1,049,378	1,118,800	1,190,800	1,264,000	1,338,000	1,413,000	1,489,000	1,566,000	1,644,000	1,723,000	1,803,000
760	.....	814,500	876,333	943,822	1,011,400	1,079,378	1,149,800	1,221,800	1,295,000	1,370,000	1,446,000	1,523,000	1,601,000	1,680,000	1,760,000	1,841,000
780	.....	839,600	901,833	970,822	1,040,400	1,109,378	1,180,800	1,253,800	1,328,000	1,404,000	1,481,000	1,559,000	1,638,000	1,718,000	1,799,000	1,881,000
800	.....	864,700	927,333	998,822	1,069,400	1,139,378	1,211,800	1,285,800	1,361,000	1,438,000	1,516,000	1,595,000	1,675,000	1,756,000	1,838,000	1,921,000
820	.....	889,800	952,833	1,024,822	1,094,400	1,165,378	1,238,800	1,313,800	1,390,000	1,468,000	1,547,000	1,627,000	1,708,000	1,790,000	1,873,000	1,957,000
840	.....	914,900	978,333	1,050,822	1,121,400	1,193,378	1,267,800	1,343,800	1,421,000	1,500,000	1,580,000	1,661,000	1,743,000	1,826,000	1,910,000	1,995,000
860	.....	940,000	1,003,833	1,076,822	1,148,400	1,221,378	1,296,800	1,373,800	1,452,000	1,532,000	1,613,000	1,695,000	1,778,000	1,862,000	1,947,000	2,033,000
880	.....	965,100	1,029,333	1,103,822	1,176,400	1,250,378	1,326,800	1,404,800	1,484,000	1,565,000	1,647,000	1,730,000	1,814,000	1,900,000	1,986,000	2,073,000
900	.....	990,200	1,054,833	1,130,822	1,204,400	1,279,378	1,356,800	1,435,800	1,516,000	1,598,000	1,681,000	1,765,000	1,850,000	1,936,000	2,023,000	2,111,000
920	.....	1,015,300	1,080,333	1,157,822	1,232,400	1,308,378	1,386,800	1,466,800	1,548,000	1,631,000	1,715,000	1,800,000	1,886,000	1,973,000	2,061,000	2,150,000
940	.....	1,040,400	1,105,833	1,184,822	1,260,400	1,337,378	1,416,800	1,497,800	1,580,000	1,664,000	1,749,000	1,835,000	1,922,000	2,010,000	2,100,000	2,191,000
960	.....	1,065,500	1,131,333	1,211,822	1,288,400	1,366,378	1,446,800	1,528,800	1,612,000	1,697,000	1,783,000	1,870,000	1,958,000	2,048,000	2,139,000	2,231,000
980	.....	1,090,600	1,156,833	1,238,822	1,316,400	1,395,378	1,476,800	1,559,800	1,644,000	1,730,000	1,817,000	1,905,000	1,994,000	2,084,000	2,175,000	2,267,000
1000	.....	1,115,700	1,182,333	1,264,822	1,343,400	1,423,378	1,505,800	1,589,800	1,675,000	1,762,000	1,850,000	1,939,000	2,029,000	2,120,000	2,212,000	2,305,000

TABLE 15. Values of  $(dZ/dT)$ , at integral values of  $T$ , the

Temperature	1	2	3	4	10	20
$^{\circ}K$	$^{\circ}K^{-1}$	$^{\circ}K^{-1}$	$^{\circ}K^{-1}$	$^{\circ}K^{-1}$	$^{\circ}K^{-1}$	$^{\circ}K^{-1}$
16.....	$8.04 \times 10^{-4}$	$16.1 \times 10^{-4}$	$24.1 \times 10^{-4}$			
18.....	6.07	12.1	18.2	$26.2 \times 10^{-4}$		
20.....	4.76	9.50	14.2	28.4	$47.1 \times 10^{-4}$	
22.....	3.82	7.64	11.4	22.8	37.9	
24.....	3.14	6.28	9.41	18.8	31.2	$59.8 \times 10^{-4}$
26.....	2.62	5.24	7.83	15.7	26.0	51.1
28.....	2.21	4.43	6.65	13.3	22.0	43.7
30.....	1.90	3.80	5.69	11.3	18.8	37.6
32.....	1.64	3.28	4.91	9.79	16.3	32.3
34.....	1.43	2.86	4.27	8.51	14.2	28.1
36.....	1.25	2.50	3.74	7.46	12.4	24.6
38.....	1.10	2.20	3.30	6.59	10.9	21.7
40.....	0.982	1.96	2.94	5.87	9.73	19.4
42.....	.881	1.76	2.64	5.25	8.74	17.4
	220	240	260	280	300	320
34.....	$256 \times 10^{-4}$	$274 \times 10^{-4}$	$291 \times 10^{-4}$	$306 \times 10^{-4}$	$320 \times 10^{-4}$	$331 \times 10^{-4}$
36.....	226	242	257	271	284	296
38.....	200	215	229	242	254	266
40.....	180	193	205	217	228	240
42.....	162	174	185	196	207	218
	1	2	3	4	10	20
43.....	$0.861 \times 10^{-4}$	$1.76 \times 10^{-4}$	$2.64 \times 10^{-4}$	$5.26 \times 10^{-4}$	$8.74 \times 10^{-4}$	$17.4 \times 10^{-4}$
44.....	.794	1.59	2.38	4.76	7.89	16.7
46.....	.719	1.44	2.16	4.30	7.16	14.2
48.....	.653	1.30	1.93	3.93	6.49	12.9
50.....	.596	1.19	1.75	3.58	5.92	11.6
52.....	.546	1.09	1.63	3.26	5.43	10.8
54.....	.502	1.00	1.51	3.01	5.00	9.99
56.....	.466	0.931	1.40	2.79	4.64	9.24
58.....	.434	.867	1.30	2.59	4.30	8.53
60.....	.403	.803	1.20	2.39	3.97	7.84
65.....	.335	.669	1.00	2.00	3.32	6.59
70.....	.281	.561	0.841	1.68	2.79	5.56
75.....	.238	.473	.713	1.42	2.38	4.73
80.....	.205	.411	.616	1.23	2.07	4.09
85.....	.180	.360	.540	1.08	1.80	3.57
90.....	.158	.317	.475	0.949	1.58	3.14
95.....	.140	.279	.418	.836	1.39	2.77
100.....	.124	.247	.371	.742	1.24	2.46
105.....	.110	.220	.331	.662	1.10	2.20
110.....	.098	.198	.297	.593	0.991	1.98
115.....	.089	.182	.272	.544	.904	1.80
120.....	.083	.168	.248	.495	.824	1.64
125.....	.077	.151	.226	.452	.754	1.50
130.....	.069	.139	.206	.416	.692	1.38
135.....	.064	.128	.191	.383	.638	1.27
140.....	.059	.119	.177	.354	.593	1.17
145.....	.054	.109	.163	.328	.543	1.08
150.....	.051	.102	.153	.305	.506	1.01
155.....	.047	.095	.142	.284	.473	0.94
160.....	.044	.089	.133	.265	.442	.88

absolute temperature, and  $\rho$ , the density in Amagat units

40	60	80	100	120	140	160	180	200
$^{\circ}R^{-1}$	$^{\circ}R^{-1}$	$^{\circ}K^{-1}$	$^{\circ}K^{-1}$	$^{\circ}K^{-1}$	$^{\circ}K^{-1}$	$^{\circ}K^{-1}$	$^{\circ}K^{-1}$	$^{\circ}K^{-1}$
$100.5 \times 10^{-4}$								
85.9	$124.8 \times 10^{-4}$							
73.6	108.0	$141.6 \times 10^{-4}$	$173.3 \times 10^{-4}$					
63.4	93.5	122.4	150.1	$176.9 \times 10^{-4}$	$202.3 \times 10^{-4}$	$226.3 \times 10^{-4}$	$249.0 \times 10^{-4}$	
56.1	81.3	108.5	130.8	154.2	178.6	197.7	217.6	$237.1 \times 10^{-4}$
48.3	71.2	93.4	114.6	135.4	156.1	173.9	191.7	208.8
42.7	63.0	82.7	101.6	119.7	137.2	154.0	170.1	184.6
38.1	56.2	73.7	90.5	106.6	122.4	137.5	162.1	166.1
34.2	50.4	66.1	81.3	95.9	110.2	123.8	137.1	149.8
310	350	390	400	420	440	460	480	500
$340 \times 10^{-4}$	$349 \times 10^{-4}$	$358 \times 10^{-4}$	$370 \times 10^{-4}$	$384 \times 10^{-4}$	$401 \times 10^{-4}$	$419 \times 10^{-4}$	$437 \times 10^{-4}$	$455 \times 10^{-4}$
306	315	325	336	349	364	380	396	412
278	287	297	308	320	333	346	360	373
251	262	272	283	294	304	316	328	338
229	240	250	260	270	280	289	298	307
40	60	80	100	120	140	160	180	200
$34.2 \times 10^{-4}$	$60.4 \times 10^{-4}$	$66.1 \times 10^{-4}$	$81.3 \times 10^{-4}$	$95.9 \times 10^{-4}$	$110.2 \times 10^{-4}$	$123.8 \times 10^{-4}$	$137.1 \times 10^{-4}$	$149.8 \times 10^{-4}$
30.9	45.5	50.8	76.6	87.0	99.9	112.3	124.3	134.7
28.0	41.3	44.4	67.0	70.2	80.9	102.1	113.0	123.5
25.4	37.6	40.6	61.1	72.2	83.9	93.2	103.2	113.0
23.3	34.4	45.3	55.9	66.0	78.8	86.4	94.5	103.7
21.3	31.6	41.5	51.2	60.5	69.5	78.3	86.6	95.3
19.7	29.1	38.2	47.1	55.7	63.9	72.0	79.8	87.7
18.2	26.9	36.3	43.5	51.4	59.0	66.5	73.8	81.1
16.8	24.9	32.7	40.3	47.7	54.6	61.6	68.7	75.6
15.5	23.0	30.4	37.6	44.5	51.3	57.9	64.4	70.8
14.0	19.3	25.4	31.3	37.2	43.0	48.7	54.3	60.0
11.0	16.3	21.5	26.6	31.5	36.5	41.5	46.4	51.2
9.40	13.9	18.4	22.8	27.1	31.4	36.6	40.8	44.0
8.13	12.1	16.0	19.8	23.6	27.2	30.8	34.4	38.0
7.00	10.6	14.0	17.3	20.6	23.8	26.9	30.0	33.1
6.23	9.30	12.3	15.3	18.2	21.0	23.7	26.5	29.2
5.60	8.20	10.9	13.5	16.1	18.6	21.1	23.6	26.1
4.89	7.30	9.69	12.0	14.5	16.6	18.9	21.2	23.4
4.33	6.63	8.66	10.7	12.6	14.9	17.0	19.0	21.0
3.96	5.86	7.78	9.63	11.6	13.4	15.3	17.1	18.9
3.57	5.32	7.04	8.73	10.4	12.1	13.8	15.4	17.0
3.25	4.84	6.42	7.97	9.60	11.0	12.5	14.0	15.4
2.98	4.44	5.89	7.32	8.71	10.1	11.5	12.8	14.1
2.74	4.08	5.41	6.73	8.00	9.24	10.4	11.7	12.9
2.52	3.75	4.98	6.19	7.36	8.51	9.58	10.7	11.8
2.32	3.46	4.60	5.71	6.79	7.85	8.84	9.84	10.8
2.15	3.21	4.26	5.28	6.26	7.25	8.18	9.10	9.99
2.00	2.98	3.95	4.89	5.81	6.71	7.57	8.42	9.26
1.96	2.77	3.66	4.53	5.39	6.21	7.02	7.82	8.59
1.74	2.66	3.40	4.20	4.99	5.76	6.51	7.26	7.96

TABLE 15. Values of  $(dZ/dT)_p$  at integral values of  $T$ , the absolute

Temperature	1	2	3	6	10	20
$^{\circ}K$	$^{\circ}K^{-1}$	$^{\circ}K^{-1}$	$^{\circ}K^{-1}$	$^{\circ}K^{-1}$	$^{\circ}K^{-1}$	$^{\circ}K^{-1}$
165.....	$4.1 \times 10^{-9}$	$2.3 \times 10^{-4}$	$12.4 \times 10^{-4}$	$24.8 \times 10^{-6}$	$41.2 \times 10^{-6}$	$83 \times 10^{-4}$
170.....	3.8	7.6	11.5	22.9	28.2	76
180.....	2.3	6.6	9.9	19.9	33.1	66
190.....	2.9	5.8	8.8	17.6	29.3	66
200.....	2.6	5.2	7.7	16.8	26.0	61
210.....	2.3	4.6	6.9	13.9	23.1	46
220.....	2.1	4.1	6.2	12.4	20.4	41
230.....	1.8	3.6	5.4	10.7	18.0	36
240.....	1.6	3.2	4.8	9.5	16.0	32
250.....	1.4	2.9	4.3	8.6	14.4	29
260.....	1.3	2.6	4.0	7.9	12.1	26
270.....	1.200	2.396	3.694	7.167	11.90	23.57
$0^{\circ}C$ .....	1.184	2.325	3.484	5.947	11.53	22.84
280.....	1.089	2.175	3.259	5.499	10.79	21.35
$86^{\circ}C$ .....	0.9169	1.832	2.744	5.470	9.676	17.94
300.....	.9014	1.891	3.006	6.377	8.921	17.64
320.....	.7517	1.502	2.269	4.482	7.431	14.67
340.....	.6800	1.259	1.885	3.757	6.328	12.57
360.....	.5215	1.061	1.600	3.164	5.241	10.32
$100^{\circ}C$ .....	.4769	0.9503	1.423	2.632	4.689	9.219
380.....	.4496	.8977	1.244	2.375	4.427	8.700
400.....	.2914	.7614	1.140	2.267	3.786	7.855
420.....	.3241	.6408	0.9683	1.925	3.181	6.227
440.....	.2758	.5600	.8231	1.635	2.706	5.274
460.....	.2344	.4678	.6995	1.389	2.291	4.464
480.....	.1990	.3970	.5939	1.178	1.941	3.771
500.....	.1687	.3383	.5029	0.9995	1.640	3.176
520.....	.1424	.2838	.4243	.8399	1.389	2.662
540.....	.1190	.2333	.3601	.7069	1.155	2.216
560.....	.0996	.1906	.2997	.5855	0.9368	1.828
580.....	.0824	.1629	.2447	.4819	.7867	1.489
600.....	.0675	.1385	.1991	.3911	.6361	1.193
	220	240	260	280	300	320
42.....	$182 \times 10^{-4}$	$174 \times 10^{-4}$	$155 \times 10^{-4}$	$196 \times 10^{-4}$	$207 \times 10^{-4}$	$218 \times 10^{-4}$
44.....	147	158	168	178	188	196
46.....	134	144	153	162	172	182
48.....	123	131	140	149	158	167
50.....	112	121	129	137	146	153
52.....	103	111	119	126	133	140
54.....	95.3	103	110	116	123	129
56.....	88.3	95.4	102	108	114	120
58.....	82.4	89.0	95.4	101	107	113
60.....	77.2	83.6	89.9	95.9	102	107
65.....	68.4	70.9	76.9	81.5	86.8	91.4
70.....	56.0	60.6	65.1	69.6	73.9	78.3
75.....	48.1	52.0	55.8	59.6	63.4	67.1
80.....	41.6	44.9	48.2	51.5	54.7	57.9
85.....	36.1	39.0	41.9	44.8	47.7	50.4
90.....	31.6	34.4	37.0	39.6	42.0	44.3
95.....	28.5	30.8	33.0	35.2	37.3	39.4
100.....	25.5	27.6	29.6	31.5	33.3	35.1
105.....	23.0	24.8	26.5	28.2	29.8	31.4
110.....	20.7	22.3	23.8	25.3	26.8	28.2
115.....	18.6	20.1	21.6	22.8	24.2	25.4
120.....	16.8	18.2	19.5	20.7	21.9	23.0

40	60	80	100	120	140	160	180	200
$^{\circ}K^{-1}$	$^{\circ}K^{-1}$	$^{\circ}K^{-1}$	$^{\circ}K^{-1}$	$^{\circ}K^{-1}$	$^{\circ}K^{-1}$	$^{\circ}K^{-1}$	$^{\circ}K^{-1}$	$^{\circ}K^{-1}$
$162 \times 10^{-4}$	$240 \times 10^{-4}$	$318 \times 10^{-4}$	$390 \times 10^{-4}$	$452 \times 10^{-4}$	$524 \times 10^{-4}$	$604 \times 10^{-4}$	$672 \times 10^{-4}$	$737 \times 10^{-4}$
151	223	293	361	429	495	559	622	682
131	194	254	312	370	427	483	536	587
114	169	222	273	323	372	419	464	507
101	150	197	242	285	327	367	405	442
91	134	175	215	253	290	325	358	391
81	119	156	192	228	258	289	319	348
71	105	139	170	200	229	257	283	308
63	93	123	151	178	203	228	251	274
56	83	109	134	158	180	209	232	252
51	75	98	120	141	161	180	198	215
46.21	67.90	88.63	108.4	127.0	144.7	161.2	176.6	190.7
44.76	65.74	85.75	104.8	122.8	139.7	155.6	170.3	183.7
41.81	61.34	79.92	97.63	114.1	129.7	144.1	157.6	169.6
35.04	51.26	66.59	80.99	94.42	106.9	118.2	128.5	137.7
34.43	50.36	65.40	78.51	92.66	104.8	115.9	125.9	134.8
28.56	41.63	53.87	65.24	75.70	85.22	93.74	101.2	107.6
23.62	34.61	44.61	53.80	62.13	69.58	76.05	81.62	86.13
19.95	28.89	37.09	44.59	51.16	56.93	61.87	65.87	68.90
17.79	26.09	32.89	39.34	45.04	49.94	53.90	57.16	59.40
16.77	24.19	30.90	36.91	42.16	46.64	50.29	53.05	54.96
14.12	20.27	26.78	30.62	34.75	38.15	40.78	42.69	43.66
11.30	17.00	21.50	25.37	28.58	31.10	32.90	33.93	34.17
10.03	14.25	17.50	20.97	23.41	25.21	26.33	26.73	26.36
8.443	11.92	14.96	17.25	19.06	20.23	20.91	20.70	19.88
7.086	9.926	12.27	14.06	15.36	16.06	16.15	15.82	14.42
6.922	8.221	10.06	11.39	12.21	12.40	12.20	11.32	9.81
4.912	6.753	8.144	9.070	9.510	9.429	8.833	7.685	5.306
4.050	5.484	6.409	7.076	7.192	6.825	5.063	4.649	2.588
3.295	4.382	5.074	5.350	5.190	4.674	3.478	1.380	-0.246
2.636	3.423	3.934	3.852	3.456	2.927	1.345	-0.414	-2.673
2.059	2.585	2.764	2.549	1.951	0.943	-0.496	-2.367	-4.751
340	360	380	400	420	440	460	480	500
$226 \times 10^{-4}$	$240 \times 10^{-4}$	$260 \times 10^{-4}$	$280 \times 10^{-4}$	$270 \times 10^{-4}$	$280 \times 10^{-4}$	$288 \times 10^{-4}$	$289 \times 10^{-4}$	$307 \times 10^{-4}$
209	220	230	240	249	257	265	272	279
192	201	211	220	229	236	243	248	254
175	184	193	202	210	216	223	228	233
161	169	177	185	192	198	204	209	214
149	155	162	169	175	182	188	193	198
136	142	149	156	162	167	173	179	183
126	132	138	144	149	155	160	166	171
118	124	129	134	140	145	150	156	161
112	117	122	126	131	137	143	148	153
99.1	101	105	109	114	116	122	127	132
82.7	86.6	90.6	94.3	98.1	102	106	110	113
70.8	74.5	78.0	81.4	84.7	87.9	91.0	94.1	97.2
61.0	64.1	67.2	70.3	73.2	75.8	78.5	81.0	83.5
53.0	55.6	58.2	60.8	63.2	65.4	67.6	69.8	72.1
46.6	48.8	51.0	53.1	55.2	57.2	59.1	61.0	62.9
41.4	43.3	45.3	47.1	48.9	50.6	52.3	53.9	55.5
36.9	38.7	40.4	42.0	43.6	45.1	46.5	48.0	49.3
33.0	34.5	36.0	37.6	38.9	40.3	41.6	42.8	43.9
29.6	30.9	32.2	33.6	34.8	36.0	37.2	38.2	39.2
26.6	27.8	29.0	30.2	31.3	32.3	33.3	34.2	35.0
24.1	25.1	26.2	27.3	28.3	29.1	29.9	30.5	31.3

TABLE 15. Values of  $(dZ/dT)_p$  at integral values of  $T$ , the absolute

Temperature	220	240	260	280	300	320
$100^{\circ}\text{C}$	$^{\circ}\text{K}^{-1}$	$^{\circ}\text{K}^{-1}$	$^{\circ}\text{K}^{-1}$	$^{\circ}\text{K}^{-1}$	$^{\circ}\text{K}^{-1}$	$^{\circ}\text{K}^{-1}$
125.....	$15.3 \times 10^{-4}$	$18.5 \times 10^{-4}$	$17.7 \times 10^{-4}$	$18.8 \times 10^{-4}$	$19.9 \times 10^{-4}$	$21.9 \times 10^{-4}$
130.....	14.0	15.1	16.2	17.2	18.2	19.3
135.....	12.8	13.8	14.8	15.8	16.7	17.6
140.....	11.7	12.7	13.6	14.5	15.3	16.1
145.....	10.8	11.7	12.5	13.3	14.1	14.9
150.....	10.1	10.9	11.6	12.3	13.0	13.7
155.....	9.36	10.1	10.8	11.4	12.0	12.6
160.....	8.66	9.32	9.96	10.5	11.1	11.7
165.....	8.00	8.60	9.16	9.67	10.3	10.7
170.....	$739 \times 10^{-6}$	$792 \times 10^{-6}$	$841 \times 10^{-6}$	$887 \times 10^{-6}$	$933 \times 10^{-6}$	$980 \times 10^{-6}$
180.....	634	678	719	758	798	831
190.....	547	585	621	655	687	718
200.....	478	512	544	575	604	631
210.....	420	453	482	509	535	559
220.....	373	401	426	450	473	495
230.....	332	354	375	396	415	432
240.....	294	312	330	347	362	376
250.....	260	275	290	304	316	328
260.....	230	243	255	266	276	284
270.....	203.5	215.2	225.4	234.1	241.3	246.8
280.....	180.0	190.9	200.4	208.5	215.0	220.9
290.....	160.5	170.1	178.3	185.1	190.3	195.9
300.....	145.6	152.3	157.6	161.5	164.0	166.8
310.....	142.6	148.9	154.0	157.7	160.9	163.5
320.....	112.0	117.0	121.8	125.2	127.3	129.3
330.....	99.66	103.96	107.96	111.78	115.28	118.36
340.....	70.92	71.87	71.70	70.33	67.70	63.78
350.....	60.67	60.92	60.67	58.69	54.90	50.44
360.....	55.98	55.80	54.68	52.40	48.97	44.28
370.....	43.62	42.76	40.88	37.96	33.94	28.75
380.....	33.56	32.07	29.66	26.24	21.90	16.26
390.....	25.24	23.27	20.42	16.66	11.92	6.157
400.....	18.32	15.97	12.81	8.776	3.834	-2.069
410.....	12.52	9.885	6.479	2.260	-2.216	-8.799
420.....	7.644	4.796	1.201	-3.148	-8.308	-14.30
430.....	3.527	0.496	-3.220	-7.657	-12.36	-18.84
440.....	0.041	-3.122	-6.880	-11.42	-16.62	-22.68
450.....	-2.926	-6.186	-10.06	-14.57	-19.78	-25.66
460.....	-5.466	-8.789	-12.70	-17.29	-22.37	-28.20
470.....	-7.613	-11.00	-14.93	-19.43	-24.54	-30.28



Temperature, and  $\rho$ , the density in Amagat units—Continued

340	360	380	400	420	440	460	480	500
$^{\circ}R^{-1}$	$^{\circ}R^{-1}$	$^{\circ}R^{-1}$	$^{\circ}R^{-1}$	$^{\circ}R^{-1}$	$^{\circ}R^{-1}$	$^{\circ}R^{-1}$	$^{\circ}R^{-1}$	$^{\circ}R^{-1}$
21.9 $\times 10^{-4}$	22.9 $\times 10^{-4}$	23.9 $\times 10^{-4}$	24.8 $\times 10^{-4}$	25.6 $\times 10^{-4}$	26.3 $\times 10^{-4}$	27.0 $\times 10^{-4}$	27.6 $\times 10^{-4}$	28.1 $\times 10^{-4}$
20.1	21.0	21.9	22.6	23.2	23.8	24.4	24.9	25.3
18.4	19.2	19.9	20.5	21.1	21.7	22.1	22.5	22.9
16.9	17.6	18.2	18.8	19.3	19.8	20.2	20.6	20.8
15.5	16.1	16.7	17.2	17.7	18.1	18.5	18.8	19.0
14.3	14.8	15.3	15.8	16.2	16.6	16.9	17.1	17.3
13.2	13.7	14.1	14.6	14.9	15.1	15.3	15.6	15.8
12.2	12.7	13.0	13.3	13.5	13.7	13.9	14.0	14.0
11.2	11.6	11.9	12.1	12.3	12.5	12.6	12.6	12.6
$102_6 \times 10^{-4}$	$105_6 \times 10^{-4}$	$108_6 \times 10^{-4}$	$111_6 \times 10^{-4}$	$113_6 \times 10^{-4}$	$114_6 \times 10^{-4}$	$115_6 \times 10^{-4}$	$116_6 \times 10^{-4}$	$116_6 \times 10^{-4}$
353	392	418	440	458	471	480	485	489
740	771	792	810	825	837	845	852	854
656	678	696	711	722	730	738	743	744
580	598	613	625	634	640	644	648	647
511	527	539	548	554	558	560	561	560
447	460	470	478	480	482	482	481	479
389	399	406	410	412	412	410	407	402
336	344	348	350	350	348	343	337	329
290	295	297	297	294	290	283	273	262
250.6	252.6	252.8	250.5	246.1	239.5	230.2	218.3	200.8
230.0	240.3	236.7	237.0	232.0	224.7	214.9	202.4	187.0
215.7	215.8	212.9	210.0	203.8	195.3	184.3	170.7	154.2
164.0	161.4	157.0	150.5	142.0	131.1	117.9	103.1	83.59
159.5	156.7	152.0	145.4	136.6	125.6	113.2	96.25	77.58
116.8	112.1	105.6	97.22	86.85	74.34	59.57	43.29	22.64
82.95	77.90	70.30	60.85	49.52	35.19	20.73	3.011	-17.11
58.40	51.55	43.14	33.06	21.21	7.491	-8.216	-26.03	-48.09
44.64	37.40	28.67	18.34	6.314	-7.497	-23.21	-40.93	-60.73
36.29	30.90	22.03	11.67	-0.457	-14.28	-29.95	-47.89	-67.30
22.33	14.60	5.500	-5.058	-17.16	-30.68	-46.34	-63.61	-82.82
9.574	1.666	-7.529	-18.08	-30.06	-43.59	-58.70	-75.52	-94.14
-0.687	-8.670	-17.83	-28.21	-40.11	-53.33	-68.04	-84.33	-102.3
-8.984	-16.97	-26.06	-35.27	-47.92	-60.79	-75.06	-90.81	-108.1
-15.73	-23.64	-32.63	-42.72	-53.90	-66.40	-80.30	-95.46	-113.1
-21.20	-29.03	-37.86	-47.72	-60.68	-70.80	-84.14	-98.76	-114.7
-25.87	-32.38	-42.03	-51.65	-62.30	-74.08	-86.91	-101.0	-116.3
-29.32	-36.89	-46.34	-54.73	-64.04	-76.30	-88.82	-102.4	-117.1
-32.80	-39.72	-47.96	-57.08	-67.10	-76.08	-90.06	-103.1	-117.3
-34.72	-41.99	-50.03	-58.89	-68.80	-79.22	-90.78	-103.3	-116.9
-36.99	-43.79	-51.83	-60.24	-69.66	-79.92	-91.08	-103.2	-116.2

TABLE 16. Values of  $(-dZ/dT^2)$ , at integral values of  $T$ .

Temperature	$\mu=1$	2	3	6	10	20
$^{\circ}K$	$^{\circ}K^{-2}$	$^{\circ}K^{-2}$	$^{\circ}K^{-2}$	$^{\circ}K^{-2}$	$^{\circ}K^{-2}$	$^{\circ}K^{-2}$
16.....	$11.4 \times 10^{-4}$	$22.6 \times 10^{-4}$	$33.7 \times 10^{-4}$			
18.....	7.9	16.7	23.5	$47.0 \times 10^{-4}$		
20.....	6.5	11.0	16.5	33.0	$54.0 \times 10^{-4}$	
22.....	4.9	7.9	11.7	23.5	38.6	
24.....	3.9	5.9	8.8	17.4	29.3	$48.6 \times 10^{-4}$
26.....	2.8	4.5	6.8	13.5	22.7	41.6
28.....	1.8	3.5	5.4	10.7	17.9	34.8
30.....	1.4	2.9	4.2	8.6	14.3	28.4
32.....	1.2	2.4	3.5	7.0	11.7	23.3
34.....	0.95	2.0	2.9	5.8	9.7	19.0
36.....	.79	1.7	2.4	4.8	8.0	15.5
38.....	.68	1.4	2.0	4.0	6.6	12.8
40.....	.56	1.1	1.7	3.3	5.5	10.7
42.....	.47	0.92	1.4	2.8	4.6	9.2
	220	240	260	290	300	320
24.....	$167 \times 10^{-4}$	$178 \times 10^{-4}$	$180 \times 10^{-4}$	$190 \times 10^{-4}$	$190 \times 10^{-4}$	$188 \times 10^{-4}$
26.....	136	146	154	160	162	161
28.....	114	121	128	135	138	138
30.....	96	102	108	114	118	119
32.....	82	87	92	97	101	103
	$\mu=1$	2	3	6	10	20
	$^{\circ}K^{-2}$	$^{\circ}K^{-2}$	$^{\circ}K^{-2}$	$^{\circ}K^{-2}$	$^{\circ}K^{-2}$	$^{\circ}K^{-2}$
42.....	$0.47 \times 10^{-6}$	$0.92 \times 10^{-6}$	$1.4 \times 10^{-6}$	$2.8 \times 10^{-6}$	$4.6 \times 10^{-6}$	$9.2 \times 10^{-6}$
44.....	.40	.79	1.2	2.4	4.0	8.0
46.....	.35	.68	1.0	2.1	3.5	6.9
48.....	.31	.61	0.91	1.9	3.1	6.0
50.....	.27	.53	.80	1.6	2.7	5.2
52.....	.23	.46	.69	1.4	2.3	4.6
54.....	.20	.40	.60	1.3	2.0	4.0
56.....	.18	.35	.53	1.1	1.8	3.6
58.....	.16	.32	.48	0.96	1.7	3.3
60.....	.15	.30	.45	.90	1.5	3.0
65.....	.12	.24	.37	.74	1.2	2.4
70.....	.10	.19	.30	.60	0.96	1.9
75.....	.078	.15	.23	.48	.76	1.5
80.....	.063	.12	.19	.38	.61	1.2
85.....	.051	.10	.16	.31	.49	0.97
90.....	.042	.084	.13	.25	.41	.80
96.....	.036	.070	.11	.21	.35	.67
100.....	.030	.059	.091	.18	.29	.57
105.....	.026	.049	.075	.15	.24	.46
110.....	.020	.041	.062	.12	.20	.40
115.....	.017	.035	.052	.10	.17	.34
120.....	.016	.030	.045	.089	.15	.30
125.....	.013	.026	.038	.080	.13	.26
130.....	.012	.023	.035	.071	.12	.23
135.....	.011	.021	.032	.062	.11	.21
140.....	.0095	.019	.028	.055	.093	.19
145.....	.0082	.016	.024	.048	.081	.16
150.....	.0071	.014	.021	.043	.070	.14
155.....	.0063	.013	.019	.039	.062	.13
160.....	.0058	.012	.018	.036	.057	.12
165.....	.0054	.012	.017	.033	.054	.12
170.....	.0050	.011	.016	.031	.050	.11

the absolute temperature, and  $\rho$ , the density in Amagat units

40	60	80	100	120	140	160	180	200
$^{\circ}K^{-1}$	$^{\circ}K^{-2}$	$^{\circ}K^{-1}$	$^{\circ}K^{-1}$	$^{\circ}K^{-2}$	$^{\circ}K^{-2}$	$^{\circ}K^{-2}$	$^{\circ}K^{-2}$	$^{\circ}K^{-2}$
$79.8 \times 10^{-1}$								
67.1	$99.0 \times 10^{-2}$							
55.8	81.9	$106.2 \times 10^{-1}$	$128.0 \times 10^{-2}$					
43.9	67.2	87.2	105.7	$123.0 \times 10^{-2}$	$139.6 \times 10^{-2}$	$156.6 \times 10^{-2}$	$171.0 \times 10^{-1}$	
37.5	55.1	71.9	87.8	102.8	118.9	139.1	142.9	$160.2 \times 10^{-2}$
30.7	45.4	59.6	72.9	85.6	97.5	108.5	118.9	128.0
25.4	37.5	49.4	60.5	71.1	81.1	90.4	98.8	108.6
21.2	31.3	41.0	50.3	59.1	67.5	75.3	82.4	89.3
19.0	28.4	34.3	42.0	49.4	56.5	63.1	69.6	75.9
340	360	380	400	420	440	460	480	500
$182 \times 10^{-2}$	$178 \times 10^{-2}$	$177 \times 10^{-1}$	$181 \times 10^{-2}$	$189 \times 10^{-2}$	$199 \times 10^{-2}$	$210 \times 10^{-2}$	$220 \times 10^{-2}$	$229 \times 10^{-1}$
158	164	152	154	160	170	182	192	204
137	144	132	133	139	147	159	171	183
119	118	117	118	122	130	141	153	166
104	105	106	108	112	118	127	137	148
40	60	80	100	120	140	160	180	200
$^{\circ}K^{-2}$	$^{\circ}K^{-1}$	$^{\circ}K^{-2}$	$^{\circ}K^{-1}$	$^{\circ}K^{-2}$	$^{\circ}K^{-1}$	$^{\circ}K^{-2}$	$^{\circ}K^{-1}$	$^{\circ}K^{-2}$
$19.0 \times 10^{-3}$	$26.4 \times 10^{-2}$	$34.3 \times 10^{-2}$	$42.0 \times 10^{-2}$	$49.4 \times 10^{-2}$	$56.5 \times 10^{-2}$	$63.1 \times 10^{-2}$	$69.6 \times 10^{-2}$	$75.9 \times 10^{-1}$
15.5	22.7	29.3	35.6	41.8	47.9	53.8	59.6	65.9
13.5	19.7	25.4	30.8	36.2	41.5	46.9	52.1	58.9
11.8	17.2	22.4	27.3	32.0	36.6	41.2	45.7	49.7
10.3	15.2	19.9	24.3	28.5	32.5	36.4	40.2	42.7
9.0	13.4	17.6	21.6	25.4	29.0	32.4	35.6	38.7
8.0	11.9	15.6	19.2	22.7	25.9	28.8	31.6	34.4
7.2	10.6	13.9	17.1	20.3	23.1	25.6	28.0	30.5
6.5	9.5	12.4	15.3	18.2	20.7	22.8	24.8	26.9
5.8	8.6	11.3	13.8	16.3	18.5	20.4	22.0	23.6
4.0	6.7	8.9	10.8	12.7	14.5	16.1	17.5	19.0
3.6	5.3	6.9	8.5	10.0	11.5	13.0	14.4	15.7
2.9	4.2	5.5	6.7	8.0	9.3	10.6	11.8	13.0
2.3	3.4	4.5	5.4	6.5	7.6	8.6	9.7	10.7
1.9	2.8	3.7	4.5	5.2	6.1	7.0	7.9	8.8
1.6	2.4	3.1	3.8	4.5	5.2	5.9	6.4	7.2
1.3	2.0	2.6	3.2	3.9	4.4	4.8	5.3	5.9
1.1	1.7	2.2	2.8	3.3	3.7	4.1	4.6	5.0
0.94	1.4	1.9	2.4	2.9	3.2	3.6	4.1	4.4
.80	1.2	1.6	2.0	2.4	2.8	3.2	3.6	3.9
.69	1.0	1.3	1.6	2.0	2.4	2.8	3.1	3.4
.68	0.97	1.1	1.4	1.7	2.0	2.4	2.6	2.9
.61	.77	1.0	1.2	1.5	1.7	2.1	2.3	2.6
.46	.69	0.90	1.1	1.3	1.5	1.8	2.0	2.2
.41	.61	.80	1.0	1.2	1.3	1.6	1.8	2.0
.37	.54	.72	0.91	1.1	1.2	1.4	1.6	1.8
.33	.48	.65	.82	0.97	1.1	1.3	1.4	1.6
.29	.44	.60	.75	.89	1.0	1.2	1.3	1.4
.26	.40	.55	.69	.82	0.93	1.1	1.2	1.3
.26	.37	.51	.65	.75	.87	1.0	1.1	1.2
.24	.35	.47	.58	.70	.81	0.91	1.0	1.1
.22	.32	.43	.53	.64	.74	.84	0.93	1.0

TABLE 16. Values of  $(-d^2Z/dT^2)$ , at integral values of  $T$ , the

Temperature	$\rho=1$	2	3	8	10	20
$^{\circ}K$	$^{\circ}K^{-2}$	$^{\circ}K^{-2}$	$^{\circ}K^{-2}$	$^{\circ}K^{-2}$	$^{\circ}K^{-2}$	$^{\circ}K^{-2}$
170.....	$0.50 \times 10^{-7}$	$1.1 \times 10^{-7}$	$1.6 \times 10^{-7}$	$3.1 \times 10^{-7}$	$5.0 \times 10^{-7}$	$11 \times 10^{-7}$
180.....	.44	0.88	1.3	2.6	4.3	9.3
190.....	.38	.76	1.1	2.2	3.7	7.5
200.....	.33	.66	1.0	2.0	3.2	6.2
210.....	.29	.58	0.87	1.8	2.7	5.4
220.....	.26	.51	.78	1.6	2.4	4.7
230.....	.23	.45	.69	1.4	2.2	4.2
240.....	.20	.40	.60	1.2	2.0	3.7
250.....	.17	.34	.52	1.0	1.7	3.2
260.....	.14	.28	.46	0.86	1.4	2.8
270.....	.1185	.2370	.3554	.7101	1.182	2.358
$0^{\circ}C$ .....	.1140	.2280	.3419	.6830	1.137	2.271
280.....	.10501	.21001	.3149	.6299	1.047	2.095
$25^{\circ}C$ .....	.08510	.1701	.2551	.5094	0.8476	1.691
300.....	.06326	.1265	.1898	.3790	.6302	1.253
320.....	.04706	.0941	.1410	.2813	.4674	1.328
340.....	.03409	.0681	.1026	.2056	.3480	1.079
360.....	.02490	.0498	.0745	.1485	.2463	0.8865
$100^{\circ}C$ .....	.01969	.0393	.0589	.1173	.1945	.7837
380.....	.01727	.0345	.0518	.1036	.1702	.7050
400.....	.01519	.0303	.0454	.0914	.1497	.6143
420.....	.01329	.0265	.0397	.0811	.1299	.5173
440.....	.01161	.0232	.0346	.0723	.1133	.4685
460.....	.01015	.0203	.0304	.0649	.1011	.4239
480.....	.00885	.0177	.0268	.0588	.0900	.3825
500.....	.00768	.0153	.0231	.0536	.0806	.3431
520.....	.00661	.0132	.0201	.0491	.0728	.3056
540.....	.00563	.0113	.0174	.0452	.0663	.2700
560.....	.00474	.0095	.0148	.0418	.0609	.2363
580.....	.00393	.0078	.0125	.0388	.0564	.2044
600.....	.00320	.0064	.0104	.0361	.0528	.1742
	$\rho=250$	240	230	220	200	200
42.....	$82 \times 10^{-6}$	$87 \times 10^{-6}$	$92 \times 10^{-6}$	$97 \times 10^{-6}$	$101 \times 10^{-6}$	$108 \times 10^{-6}$
44.....	71	75	79	84	87	90
46.....	61	65	69	73	76	80
48.....	53	57	61	65	68	72
50.....	47	50	54	58	61	64
52.....	42	44	47	51	54	57
54.....	37	39	41	44	46	49
56.....	33	35	36	38	40	42
58.....	29	31	32	34	36	37
60.....	26	28	30	31	32	34
65.....	21	23	25	26	27	28
70.....	17	19	21	22	23	24
75.....	14	16	17	18	19	20
80.....	12	13	14	15	16	16
85.....	9.7	10	11	12	13	13
90.....	7.8	8.3	8.9	9.5	10	11
95.....	6.4	6.9	7.5	8.1	8.6	9.1
100.....	5.5	6.0	6.5	7.0	7.5	8.0
105.....	4.8	5.3	5.7	6.1	6.5	6.9
110.....	4.3	4.6	5.0	5.3	5.6	6.0
115.....	3.7	4.0	4.3	4.6	4.9	5.2
120.....	3.2	3.5	3.8	4.0	4.3	4.6
125.....	2.8	3.1	3.3	3.5	3.7	3.9
130.....	2.6	2.7	2.9	3.1	3.2	3.3
135.....	2.3	2.4	2.5	2.7	2.9	3.0
140.....	1.9	2.1	2.3	2.4	2.6	2.7

40	60	80	100	120	140	160	180	200
$^{\circ}\text{K}^{-1}$	$^{\circ}\text{K}^{-1}$	$^{\circ}\text{K}^{-1}$	$^{\circ}\text{K}^{-1}$	$^{\circ}\text{K}^{-1}$	$^{\circ}\text{K}^{-1}$	$^{\circ}\text{K}^{-1}$	$^{\circ}\text{K}^{-1}$	$^{\circ}\text{K}^{-1}$
$22 \times 10^{-7}$	$32 \times 10^{-7}$	$42 \times 10^{-7}$	$52 \times 10^{-7}$	$62 \times 10^{-7}$	$72 \times 10^{-7}$	$82 \times 10^{-7}$	$92 \times 10^{-7}$	$102 \times 10^{-7}$
19	27	35	44	53	61	70	79	87
15	22	29	36	43	50	58	65	72
12	18	24	29	35	41	47	53	59
10	15	20	25	29	34	39	44	48
9.8	14	18	22	26	29	33	37	41
8.5	13	17	20	23	26	29	32	36
7.5	11	15	18	20	23	26	29	32
6.8	9.1	13	16	18	20	23	26	29
5.5	8.0	10	13	15	18	20	23	26
4.984	6.998	9.264	11.52	13.76	15.92	18.19	20.38	22.56
4.628	6.766	8.970	11.17	13.35	15.51	17.66	19.79	21.91
4.142	6.171	8.175	10.15	12.11	14.05	16.06	17.85	19.74
3.558	5.001	6.820	8.216	9.788	11.33	12.94	14.56	16.31
3.278	4.872	6.440	7.981	9.496	10.98	12.45	13.99	15.50
2.828	3.900	5.145	6.262	7.553	8.716	9.851	10.96	12.03
2.132	3.180	4.190	5.235	6.082	7.002	7.893	8.758	9.588
1.749	2.487	3.400	4.159	4.951	5.687	6.395	7.075	7.725
1.546	2.296	3.004	3.697	4.366	5.008	5.624	6.211	6.768
1.448	2.138	2.806	3.450	4.069	4.664	5.232	5.773	6.285
1.208	1.706	2.202	2.666	3.173	3.657	4.117	4.551	5.158
1.016	1.496	1.957	2.397	2.810	3.214	3.596	3.939	4.266
0.8602	1.266	1.651	2.019	2.368	2.696	3.004	3.289	3.550
.7326	1.075	1.402	1.711	2.008	2.276	2.529	2.762	2.973
.6271	0.9198	1.196	1.456	1.708	1.931	2.141	2.332	2.503
.5396	.7897	1.026	1.246	1.455	1.646	1.821	1.978	2.116
.4662	.6814	0.8839	1.073	1.249	1.410	1.556	1.688	1.797
.4045	.5903	.7645	0.9265	1.078	1.212	1.332	1.440	1.531
.3622	.5132	.6735	.8026	0.9269	1.046	1.147	1.238	1.309
.3277	.4475	.5777	.6975	.8063	0.9058	0.9992	1.0867	1.1521
.2996	.3916	.5045	.6078	.7011	.7838	.8554	0.9152	0.9620
340	360	380	400	420	440	460	480	500
$104 \times 10^{-7}$	$105 \times 10^{-7}$	$106 \times 10^{-7}$	$108 \times 10^{-7}$	$112 \times 10^{-7}$	$118 \times 10^{-7}$	$127 \times 10^{-7}$	$137 \times 10^{-7}$	$148 \times 10^{-7}$
93	95	98	101	104	109	115	122	132
84	87	91	95	98	102	106	111	116
76	80	84	89	92	96	97	99	101
68	73	77	81	85	87	87	87	88
61	65	69	73	76	77	77	77	76
53	57	61	64	66	67	67	67	65
45	48	51	54	56	56	57	57	56
39	40	42	45	47	47	48	49	49
36	38	37	39	41	42	44	45	46
29	30	31	32	33	34	36	38	39
25	26	27	28	29	30	31	32	34
21	22	23	24	25	26	27	28	30
17	18	19	20	22	23	23	24	25
14	15	16	17	18	19	19	20	20
11	12	13	14	14	15	15	16	16
9.6	10	10	11	11	12	12	13	13
8.4	8.8	9.1	9.5	9.8	10	11	11	11
7.3	7.7	8.0	8.4	8.7	9.1	9.4	10	10
6.4	6.7	7.0	7.3	7.6	8.0	8.3	8.6	8.9
5.5	5.8	6.0	6.3	6.6	6.9	7.3	7.6	7.9
4.7	4.9	5.2	5.5	5.8	6.0	6.3	6.6	6.9
4.0	4.2	4.4	4.6	5.1	5.3	5.6	6.0	6.0
3.5	3.7	4.0	4.2	4.4	4.6	4.8	5.0	5.2
3.2	3.4	3.6	3.7	3.9	4.0	4.2	4.4	4.5
2.9	3.1	3.2	3.3	3.4	3.5	3.7	3.8	3.9

TABLE 16. Values of  $(-d^2Z/dT^2)_p$  at integral values of  $T$ , the

Temperature	$\rho=220$	240	260	280	300	320
$^{\circ}K$	$^{\circ}K^{-2}$	$^{\circ}K^{-2}$	$^{\circ}K^{-2}$	$^{\circ}K^{-2}$	$^{\circ}K^{-2}$	$^{\circ}K^{-2}$
145.....	$1.7 \times 10^{-4}$	$1.8 \times 10^{-4}$	$2.0 \times 10^{-4}$	$2.1 \times 10^{-4}$	$2.3 \times 10^{-4}$	$2.4 \times 10^{-4}$
150.....	1.6	1.6	1.8	1.9	2.1	2.2
155.....	1.4	1.5	1.6	1.8	1.9	2.0
160.....	1.3	1.4	1.5	1.7	1.8	1.9
165.....	1.2	1.4	1.5	1.6	1.8	1.8
170.....	$110 \times 10^{-7}$	$130 \times 10^{-7}$	$130 \times 10^{-7}$	$140 \times 10^{-7}$	$160 \times 10^{-7}$	$160 \times 10^{-7}$
180.....	96	100	110	120	120	130
190.....	78	83	87	93	96	99
200.....	63	67	70	73	78	81
210.....	50	50	59	63	66	69
220.....	46	49	53	56	59	62
230.....	40	44	48	51	53	56
240.....	36	40	43	46	48	51
250.....	32	35	38	40	43	46
260.....	29	31	33	35	37	40
270.....	24.73	26.89	29.03	31.17	33.30	35.42
$0^{\circ}C$ .....	24.01	26.08	28.15	30.20	32.23	34.24
280.....	21.60	23.44	25.26	27.07	28.85	30.62
$20^{\circ}C$ .....	17.25	18.06	20.04	21.33	22.69	23.96
300.....	16.69	18.04	19.37	20.67	21.94	23.17
320.....	15.08	14.09	15.08	16.03	16.66	17.80
340.....	10.39	11.16	11.89	12.68	13.24	13.91
360.....	8.343	8.929	9.480	9.994	10.47	10.90
$100^{\circ}C$ .....	7.283	7.785	8.242	8.682	9.043	9.383
380.....	6.767	7.218	7.635	8.017	8.380	8.684
400.....	5.536	5.895	6.202	6.485	6.733	6.942
420.....	4.564	4.834	5.076	5.285	5.461	5.601
440.....	3.787	3.908	4.181	4.335	4.458	4.547
460.....	3.161	3.225	3.494	3.575	3.658	3.709
480.....	2.659	2.780	2.884	2.962	3.014	3.038
500.....	2.236	2.264	2.411	2.464	2.493	2.496
520.....	1.892	1.967	2.022	2.056	2.067	2.059
540.....	1.606	1.662	1.701	1.720	1.718	1.699
560.....	1.367	1.409	1.434	1.441	1.429	1.396
580.....	1.186	1.196	1.211	1.208	1.188	1.149
600.....	0.997	1.018	1.023	1.014	0.988	0.944

TABLE 17. Values of  $(dZ/d\rho)_T$  at integral values of  $T$ , the

Temperature	$\rho=0$	1	2	3	4	10	20
$^{\circ}K$							
18.....	$-9.108 \times 10^{-4}$	$-9.087 \times 10^{-4}$	$-9.070 \times 10^{-4}$	$-9.062 \times 10^{-4}$			
18.....	-7.709	-7.694	-7.679	-7.664	$-7.620 \times 10^{-4}$		
20.....	-6.633	-6.621	-6.609	-6.595	-6.567	$-6.506 \times 10^{-4}$	
22.....	-5.781	-5.770	-5.759	-5.748	-5.714	-6.670	
24.....	-5.087	-5.077	-5.067	-5.058	-5.029	-4.990	$-4.892 \times 10^{-4}$
26.....	-4.512	-4.503	-4.494	-4.485	-4.460	-4.426	-4.338
28.....	-4.037	-4.019	-4.011	-4.003	-3.980	-3.949	-3.871
30.....	-3.615	-3.608	-3.601	-3.594	-3.573	-3.544	-3.474
32.....	-3.292	-3.285	-3.279	-3.272	-3.253	-3.197	-3.132
34.....	-2.965	-2.949	-2.943	-2.937	-2.919	-2.865	-2.800
36.....	-2.688	-2.682	-2.676	-2.671	-2.654	-2.602	-2.537
38.....	-2.453	-2.446	-2.442	-2.438	-2.422	-2.402	-2.350
40.....	-2.245	-2.240	-2.235	-2.230	-2.216	-2.197	-2.149
42.....	-2.059	-2.054	-2.050	-2.045	-2.032	-2.014	-1.968



TABLE 17. Values of  $(dZ/dp)_T$  at integral values of  $T$ , the absolute

Temperature	$p=220$	240	260	280	300	320	340
°K							
34.....	$-1.650 \times 10^{-4}$	$-1.528 \times 10^{-4}$	$-1.392 \times 10^{-4}$	$-1.254 \times 10^{-4}$	$-1.121 \times 10^{-4}$	$-998 \times 10^{-5}$	$-884 \times 10^{-5}$
36.....	-1.477	-1.360	-1.239	-1.117	-1.001	-892	-798
38.....	-1.323	-1.210	-1.100	-990	-882	-782	-694
40.....	-1.181	-1.077	-973	-870	-778	-690	-615
42.....	-1.064	-956	-857	-758	-658	-568	-481
$p=520$							
34.....	$387 \times 10^{-4}$	$654 \times 10^{-4}$	$941 \times 10^{-4}$	$1.255 \times 10^{-3}$	$1.637 \times 10^{-3}$	$2.080 \times 10^{-3}$	$2.638 \times 10^{-3}$
36.....	538	795	1.077	1.400	1.750	2.130	2.504
38.....	681	961	1.260	1.657			
40.....	812	1,135					
42.....	940						
$p=0$							
	I	2	3	5	10	20	
42.....	$-2.050 \times 10^{-4}$	$-2.054 \times 10^{-4}$	$-2.050 \times 10^{-4}$	$-2.045 \times 10^{-4}$	$-2.032 \times 10^{-4}$	$-2.014 \times 10^{-4}$	$-1.988 \times 10^{-4}$
44.....	-1.892	-1.887	-1.883	-1.879	-1.866	-1.849	-1.829
46.....	-1.746	-1.736	-1.732	-1.728	-1.716	-1.700	-1.680
48.....	-1.603	-1.599	-1.596	-1.591	-1.580	-1.564	-1.545
50.....	-1.473	-1.474	-1.470	-1.467	-1.456	-1.441	-1.424
52.....	-1.355	-1.360	-1.357	-1.353	-1.342	-1.328	-1.313
54.....	-1.259	-1.256	-1.252	-1.249	-1.239	-1.225	-1.211
56.....	-1.182	-1.179	-1.176	-1.172	-1.162	-1.149	-1.136
58.....	-1.072	-1.069	-1.065	-1.063	-1.053	-1.040	-1.029
60.....	-986	-985	-982	-979	-970	-958	-948
65.....	-907	-894	-891	-890	-890	-779	-751
70.....	-654	-661	-649	-646	-636	-628	-601
75.....	-524	-522	-519	-516	-509	-499	-474
80.....	-412	-410	-407	-405	-398	-388	-364
85.....	-315	-313	-310	-308	-301	-292	-269
90.....	-231	-229	-227	-224	-218	-209	-186
95.....	-157	-155	-153	-150	-144	-135	-113
100.....	-90	-88	-86	-84	-77	-69	-48
105.....	-34	-32	-30	-28	-21	-12	+9
110.....	+19	+21	+23	+25	+32	+40	61
115.....	67	69	71	73	79	87	108
120.....	111	113	115	117	123	131	151
125.....	151	153	156	157	159	171	190
130.....	187	189	191	193	199	206	226
135.....	221	223	226	227	232	240	256
140.....	252	254	256	258	263	271	289
145.....	281	283	285	286	292	297	317
150.....	307	309	311	312	318	325	343
155.....	331	333	335	336	342	349	367
160.....	353	355	357	358	364	371	389
165.....	373	375	377	378	384	391	409
170.....	393	395	397	398	404	411	429
180.....	429	431	433	434	439	446	464
190.....	469	462	463	465	470	477	494
200.....	489	490	491	492	498	504	521
210.....	512	514	516	517	522	529	545
220.....	534	536	538	539	544	550	566
230.....	553	555	557	558	563	569	585
240.....	571	573	574	576	580	586	602
250.....	587	589	590	592	596	602	617
260.....	602	604	605	606	610	616	631
270.....	613.9	615.3	616.8	618.2	622.6	628.3	642.8



temperature, and  $\rho$ , the density in Amagat units—Continued

380	390	400	420	440	460	480	500	
$-774 \times 10^{-4}$	$-667 \times 10^{-4}$	$-562 \times 10^{-4}$	$-460 \times 10^{-4}$	$-357 \times 10^{-4}$	$-254 \times 10^{-4}$	$-68 \times 10^{-4}$	$+148 \times 10^{-4}$	
-690	-564	-442	-318	-194	-62	+99	302	
-577	-458	-324	-188	-51	+89	247	487	
-467	-347	-213	-73	+60	218	374	550	
-358	-241	-111	+29	178	321	475	639	
600	660							
$3.227 \times 10^{-4}$	$3.848 \times 10^{-4}$							
40	60	80	100	120	140	160	180	200
$-1.678 \times 10^{-6}$	$-1.798 \times 10^{-6}$	$-1.626 \times 10^{-6}$	$-1.608 \times 10^{-6}$	$-1.617 \times 10^{-6}$	$-1.427 \times 10^{-6}$	$-1.337 \times 10^{-6}$	$-1.245 \times 10^{-6}$	$-1.151 \times 10^{-6}$
-1.721	-1.636	-1.550	-1.465	-1.379	-1.294	-1.209	-1.123	-1.033
-1.678	-1.487	-1.416	-1.335	-1.254	-1.173	-1.092	-1.011	-926
-1.448	-1.371	-1.294	-1.216	-1.139	-1.062	-985	-908	-827
-1.330	-1.258	-1.182	-1.106	-1.034	-961	-887	-813	-736
-1.222	-1.151	-1.080	-1.009	-938	-868	-797	-725	-652
-1.128	-1.054	-986	-918	-849	-781	-713	-645	-573
-1.031	-965	-899	-834	-768	-702	-635	-570	-500
-946	-883	-820	-757	-693	-628	-565	-499	-428
-867	-807	-745	-685	-623	-561	-497	-431	-361
-694	-637	-580	-523	-465	-407	-348	-289	-210
-648	-496	-447	-388	-330	-273	-214	-156	-81
-424	-374	-323	-269	-215	-160	-100	-37	+30
-317	-269	-219	-168	-115	-60	-2	+59	124
-223	-177	-129	-80	-29	+26	+82	142	204
-141	-86	-30	-2	+48	100	156	215	275
-89	-25	+20	+67	116	167	222	279	339
-5	+28	82	126	176	227	281	338	397
+32	95	139	183	221	261	305	352	409
103	145	188	233	280	329	380	433	495
149	191	233	277	324	373	426	481	538
191	232	274	318	364	413	465	518	573
230	270	311	356	401	449	500	552	608
266	306	346	390	434	481	531	583	636
297	337	379	421	466	511	560	611	663
328	368	409	450	493	538	586	637	688
354	394	435	476	519	566	610	660	711
380	419	459	500	543	589	632	681	731
404	442	482	523	565	608	653	701	750
426	464	503	544	588	633	677	719	768
446	484	523	565	604	646	690	736	786
466	503	541	581	622	664	707	752	800
489	526	564	603	643	684	726	780	826
509	545	582	620	659	701	741	804	849
529	565	602	640	679	719	761	824	868
550	590	626	663	701	741	782	824	868
578	613	648	684	721	760	800	842	885
599	633	667	703	739	777	816	867	900
618	651	684	719	755	792	831	872	913
634	666	699	734	770	806	844	884	925
648	680	713	747	782	818	856	894	935
661	692	725	758	792	826	866	903	943
672.6	703.4	735.2	768.1	802.0	837.2	873.0	911.4	950.4

TABLE 17. Values of  $(dZ/d_p)_T$  at integral values of  $T$ , the

Temperature	$\rho=0$	1	2	3	5	10	20
$6^\circ C$	$617.7 \times 10^{-6}$	$619.1 \times 10^{-6}$	$620.5 \times 10^{-6}$	$621.9 \times 10^{-6}$	$623.2 \times 10^{-6}$	$624.9 \times 10^{-6}$	$626.4 \times 10^{-6}$
280	625.4	626.8	628.2	629.6	631.0	632.5	633.8
$85^\circ C$	643.5	644.9	646.3	647.6	651.5	657.3	671.2
300	645.2	646.6	647.9	649.3	653.4	658.9	672.8
320	651.7	653.0	654.4	655.7	659.7	675.0	688.5
340	675.5	676.8	678.1	679.4	683.2	688.4	701.6
360	687.1	688.4	689.6	690.9	694.6	699.7	712.5
$100^\circ C$	693.7	695.0	696.2	697.4	701.1	706.1	718.7
280	696.9	698.1	699.4	700.6	704.2	709.2	721.6
400	706.2	707.4	707.0	708.8	712.4	717.2	729.3
420	712.3	713.4	714.6	715.8	719.3	724.0	735.8
440	718.3	719.4	720.5	721.7	725.1	730.7	741.3
460	725.4	726.5	727.6	728.7	732.1	737.6	747.9
480	727.7	728.8	729.9	731.0	734.3	739.7	749.8
500	731.4	732.5	733.5	734.6	737.8	742.1	752.0
520	734.5	735.6	736.6	737.6	740.8	745.0	755.6
540	737.1	738.2	739.2	740.2	743.3	747.5	758.0
560	739.3	740.3	741.4	742.4	745.4	749.6	759.8
580	741.2	742.2	743.1	744.1	747.1	751.2	761.3
600	742.7	743.6	744.6	745.6	748.6	752.6	762.6
Temperature	$\rho=220$	240	260	280	300	320	
42	$-1.064 \times 10^{-4}$	$-0.950 \times 10^{-4}$	$-0.867 \times 10^{-4}$	$-0.758 \times 10^{-4}$	$-0.658 \times 10^{-4}$	$-0.558 \times 10^{-4}$	
44	-941	-847	-761	-653	-563	-459	
46	-837	-747	-653	-555	-464	-351	
48	-742	-654	-562	-464	-362	-258	
50	-655	-569	-477	-380	-277	-174	
52	-573	-489	-398	-301	-200	-96	
54	-496	-413	-324	-229	-131	-31	
56	-423	-342	-255	-163	-68	+30	
58	-353	-274	-190	-102	-10	+86	
60	-287	-211	-131	-45	+44	128	
65	-137	-62	+15	+94	177	264	
70	-9	+94	137	213	299	376	
75	+69	169	241	316	393	473	
80	191	290	331	406	480	560	
85	270	338	406	480	555	633	
90	340	408	475	548	620	696	
95	402	467	534	604	670	751	
100	457	520	586	655	725	798	
105	507	568	632	699	768	840	
110	552	611	673	739	807	878	
115	592	650	711	775	841	911	
120	628	685	745	807	872	941	
125	660	716	775	836	900	968	
130	689	744	802	862	925	992	
135	718	770	827	886	948	1,014	
140	740	794	850	906	970	1,034	
145	762	816	871	930	990	1,053	
150	783	836	891	948	1,006	1,070	
155	802	854	906	965	1,024	1,085	
160	819	871	924	980	1,038	1,099	
165	836	888	938	993	1,051	1,111	
170	849	909	951	1,005	1,062	1,121	

40	60	80	100	120	140	160	180	200
$675.1 \times 10^{-4}$	$706.7 \times 10^{-4}$	$738.4 \times 10^{-4}$	$771.0 \times 10^{-4}$	$804.9 \times 10^{-4}$	$839.8 \times 10^{-4}$	$876.1 \times 10^{-4}$	$913.6 \times 10^{-4}$	$952.6 \times 10^{-4}$
683.2	713.5	744.8	777.1	810.8	846.2	881.1	918.2	956.7
686.8	726.2	759.7	791.2	825.7	867.4	902.3	928.4	965.8
701.3	732.7	761.0	792.4	824.9	858.6	893.2	929.2	966.5
716.2	744.7	774.2	804.7	836.2	868.6	902.5	937.4	973.5
728.4	756.2	784.8	814.5	845.1	878.7	909.5	943.3	978.4
738.6	766.6	793.5	822.3	852.1	882.9	914.7	947.6	981.6
744.4	770.9	796.4	826.8	856.9	886.1	917.3	949.6	983.0
747.1	773.4	800.6	828.6	857.6	887.0	918.6	950.5	983.6
754.2	779.9	806.4	833.7	861.9	891.1	921.2	952.4	984.5
760.1	785.2	811.0	837.7	865.2	893.7	923.0	953.4	984.7
765.1	789.5	814.8	840.8	867.7	895.5	924.1	953.7	984.2
769.2	793.1	817.8	843.3	869.5	896.6	924.6	953.5	983.3
772.6	796.0	820.2	845.1	870.8	897.3	924.6	952.8	981.9
775.4	798.3	822.0	846.4	871.6	897.5	924.2	951.8	980.2
777.6	800.2	823.4	847.3	871.9	897.3	923.5	950.4	978.2
779.5	801.6	824.4	847.8	871.9	896.8	922.4	948.9	976.1
780.9	802.6	825.0	848.0	871.7	896.1	921.2	947.1	973.8
782.1	803.4	825.3	847.9	871.2	895.1	919.8	945.2	971.3
782.9	803.9	825.4	847.6	870.5	894.0	918.2	943.1	968.7
340	360	380	400	420	440	460	480	500
$-481 \times 10^{-6}$	$-356 \times 10^{-6}$	$-241 \times 10^{-6}$	$-111 \times 10^{-6}$	$+29 \times 10^{-6}$	$178 \times 10^{-6}$	$321 \times 10^{-6}$	$475 \times 10^{-6}$	$630 \times 10^{-6}$
-352	-249	-139	-15	+120	209	403	563	707
-250	-149	-42	+76	203	336	471	612	759
-157	-57	+48	162	291	404	551	694	804
-73	+27	130	240	353	468	588	715	849
+2	102	204	310	418	528	643	765	891
+46	168	270	373	478	585	697	815	939
128	228	329	431	534	640	760	864	964
163	282	382	484	587	692	800	913	1,031
204	332	431	532	636	740	848	961	1,079
355	450	547	647	752	861	973	1,089	1,210
464	556	652	751	856	963	1,075	1,191	1,312
561	651	745	842	944	1,050	1,160	1,274	1,394
644	733	824	919	1,018	1,122	1,231	1,345	1,465
715	802	892	984	1,081	1,183	1,291	1,406	1,526
776	860	948	1,039	1,134	1,234	1,340	1,454	1,576
829	911	997	1,086	1,180	1,279	1,384	1,498	1,618
876	956	1,041	1,129	1,221	1,318	1,422	1,531	1,648
916	996	1,080	1,167	1,259	1,355	1,456	1,561	1,670
958	1,032	1,115	1,201	1,291	1,387	1,486	1,587	1,693
996	1,064	1,146	1,231	1,320	1,414	1,511	1,611	1,715
1,014	1,082	1,173	1,257	1,345	1,437	1,533	1,633	1,736
1,041	1,117	1,197	1,280	1,366	1,457	1,552	1,652	1,754
1,064	1,140	1,216	1,299	1,384	1,473	1,567	1,667	1,768
1,085	1,159	1,236	1,316	1,399	1,487	1,580	1,678	1,779
1,103	1,176	1,252	1,331	1,413	1,500	1,591	1,686	1,785
1,120	1,191	1,265	1,345	1,426	1,511	1,600	1,693	1,790
1,136	1,205	1,278	1,356	1,436	1,520	1,607	1,699	1,796
1,150	1,218	1,290	1,366	1,444	1,526	1,612	1,704	1,799
1,162	1,229	1,300	1,374	1,451	1,531	1,616	1,707	1,801
1,173	1,240	1,309	1,381	1,457	1,536	1,619	1,707	1,800
1,183	1,248	1,317	1,389	1,462	1,539	1,620	1,708	1,797

TABLE 17. Values of  $(dZ/d_r)_T$  at integral values of  $T$ , the absolute

Temperature	$\rho=220$	240	260	280	300	320
180.....	$874 \times 10^{-4}$	$922 \times 10^{-4}$	$972 \times 10^{-4}$	$1.025 \times 10^{-4}$	$1.081 \times 10^{-4}$	$1.140 \times 10^{-4}$
190.....	895	943	992	1,043	1,098	1,156
200.....	913	961	1,009	1,060	1,113	1,169
210.....	929	976	1,024	1,074	1,126	1,180
220.....	943	990	1,037	1,086	1,137	1,190
230.....	956	1,001	1,049	1,098	1,148	1,198
240.....	967	1,011	1,057	1,104	1,154	1,205
250.....	976	1,020	1,065	1,111	1,160	1,211
260.....	984	1,027	1,072	1,117	1,165	1,215
270.....	991.0	1,033.1	1,078.2	1,122.1	1,169.3	1,218.3
.....	$0^\circ C$	1,034.7	1,078.2	1,123.3	1,170.2	1,219.0
280.....	998.6	1,038.0	1,081.0	1,125.6	1,172.0	1,220.2
.....	$10^\circ C$	1,044.5	1,044.7	1,088.4	1,129.7	1,174.7
300.....	1,005.2	1,045.3	1,086.6	1,130.0	1,174.8	1,221.4
320.....	1,011.0	1,049.8	1,090.1	1,131.8	1,176.1	1,220.1
340.....	1,014.7	1,052.3	1,091.3	1,131.7	1,175.6	1,217.1
360.....	1,016.9	1,053.4	1,091.2	1,130.8	1,174.9	1,215.9
.....	$100^\circ C$	1,017.6	1,053.4	1,090.4	1,128.8	1,169.5
380.....	1,017.8	1,053.2	1,089.9	1,127.9	1,167.2	1,207.9
400.....	1,017.8	1,052.2	1,087.8	1,124.7	1,163.9	1,202.4
420.....	1,017.1	1,050.6	1,085.2	1,121.0	1,159.0	1,196.4
440.....	1,015.8	1,048.4	1,082.1	1,116.9	1,154.9	1,190.2
460.....	1,014.0	1,045.8	1,078.6	1,112.6	1,147.6	1,183.8
480.....	1,011.9	1,042.9	1,074.9	1,108.0	1,142.1	1,177.4
500.....	1,009.5	1,039.8	1,071.0	1,103.3	1,136.6	1,171.0
520.....	1,006.9	1,036.6	1,067.0	1,098.6	1,131.0	1,164.6
540.....	1,004.2	1,033.1	1,062.9	1,093.7	1,125.4	1,158.2
560.....	1,001.2	1,029.8	1,058.7	1,088.8	1,119.9	1,151.9
580.....	998.2	1,026.0	1,054.6	1,084.0	1,114.4	1,145.7
600.....	995.1	1,022.3	1,050.3	1,079.2	1,108.9	1,139.5

340	380	390	400	420	440	460	480	400
$1.201 \times 10^{-4}$	$1.254 \times 10^{-4}$	$1.330 \times 10^{-4}$	$1.399 \times 10^{-4}$	$1.471 \times 10^{-4}$	$1.546 \times 10^{-4}$	$1.623 \times 10^{-4}$	$1.702 \times 10^{-4}$	$1.794 \times 10^{-4}$
1,215	1,276	1,341	1,408	1,478	1,550	1,626	1,707	1,792
1,227	1,287	1,350	1,418	1,484	1,559	1,638	1,708	1,790
1,237	1,296	1,358	1,422	1,489	1,559	1,632	1,708	1,788
1,245	1,304	1,365	1,428	1,493	1,561	1,633	1,708	1,787
1,253	1,310	1,370	1,432	1,496	1,562	1,633	1,708	1,786
1,259	1,315	1,373	1,434	1,497	1,563	1,633	1,708	1,783
1,264	1,319	1,375	1,436	1,498	1,563	1,631	1,702	1,778
1,267	1,321	1,378	1,438	1,497	1,561	1,628	1,697	1,771
1,269.3	1,322.4	1,377.8	1,435.2	1,495.1	1,557.6	1,622.8	1,690.6	1,761.8
1,269.7	1,322.5	1,377.4	1,434.6	1,494.9	1,556.3	1,621.1	1,688.6	1,759.1
1,270.3	1,322.4	1,378.6	1,433.1	1,491.9	1,553.2	1,617.1	1,683.7	1,753.1
1,269.9	1,320.3	1,372.8	1,427.3	1,484.1	1,543.3	1,604.8	1,669.0	1,735.9
1,269.7	1,320.0	1,372.3	1,426.6	1,483.2	1,542.2	1,603.5	1,667.4	1,734.0
1,266.8	1,315.3	1,363.7	1,418.1	1,472.5	1,529.2	1,588.1	1,649.5	1,713.4
1,262.2	1,309.0	1,357.7	1,408.2	1,460.6	1,515.1	1,571.6	1,630.6	1,692.0
1,256.6	1,301.8	1,348.9	1,397.5	1,448.0	1,500.6	1,555.1	1,611.6	1,670.7
1,252.4	1,294.7	1,342.6	1,390.2	1,439.6	1,490.9	1,544.1	1,599.4	1,656.8
1,250.2	1,293.9	1,339.3	1,386.4	1,435.2	1,485.8	1,538.4	1,593.0	1,649.7
1,242.3	1,285.6	1,329.6	1,375.1	1,422.3	1,471.2	1,521.9	1,574.6	1,629.2
1,236.1	1,277.2	1,319.7	1,363.8	1,409.4	1,456.7	1,505.8	1,556.6	1,609.3
1,229.7	1,268.6	1,309.9	1,352.8	1,398.8	1,442.6	1,489.0	1,539.2	1,590.1
1,221.3	1,260.1	1,300.1	1,341.8	1,384.6	1,428.9	1,474.8	1,522.4	1,571.6
1,213.9	1,251.6	1,290.5	1,330.6	1,372.4	1,415.5	1,460.1	1,506.2	1,553.9
1,205.5	1,243.2	1,281.1	1,320.2	1,360.7	1,402.6	1,445.8	1,490.6	1,538.9
1,199.2	1,234.9	1,271.8	1,310.0	1,349.4	1,390.1	1,432.1	1,475.6	1,520.5
1,192.0	1,226.3	1,262.9	1,300.0	1,338.4	1,378.0	1,419.9	1,461.2	1,504.6
1,184.9	1,218.9	1,254.0	1,290.3	1,327.7	1,366.3	1,406.2	1,447.3	1,489.6
1,177.9	1,211.2	1,245.5	1,280.0	1,317.4	1,355.0	1,393.9	1,434.0	1,475.4
1,171.1	1,203.4	1,237.2	1,271.7	1,307.4	1,344.1	1,382.0	1,421.2	1,461.5

Many thermodynamic equations involve derivatives in which  $P$ ,  $V$ , and  $T$  are the variables of state. Applications of the tables of this paper in which the variables are  $Z$ ,  $\rho$ , and  $T$  to calculations of properties involving derivatives in which the variables are  $P$ ,  $V$ , and  $T$  may be facilitated by means of equations relating the  $P$ ,  $V$ ,  $T$  and the  $Z$ ,  $\rho$ ,  $T$  derivatives. The following are adequate for many ordinary uses:

$$\frac{T}{P} \left( \frac{dP}{dT} \right)_V = \frac{T}{P} \left( \frac{dP}{dT} \right)_\rho = \frac{T}{P} \left( \frac{dS}{dV} \right)_T = 1 + \frac{T}{Z} \left( \frac{dZ}{dT} \right)_\rho \quad (4.2)$$

$$-\frac{V}{P} \left( \frac{dP}{dV} \right)_T = \frac{\rho}{P} \left( \frac{dP}{d\rho} \right)_T = 1 + \frac{\rho}{Z} \left( \frac{dZ}{d\rho} \right)_T \quad (4.3)$$

$$-\frac{T}{V} \left( \frac{dV}{dT} \right)_P = \frac{T}{\rho} \left( \frac{d\rho}{dT} \right)_P = \frac{T}{V} \left( \frac{dS}{dP} \right)_T; \quad -\frac{1 + \frac{T}{Z} \left( \frac{dZ}{dT} \right)_\rho}{1 + \frac{\rho}{Z} \left( \frac{dZ}{d\rho} \right)_T} \quad (4.4)$$

The Joule-Thomson coefficient  $\mu$  may be utilized to illustrate the use of these formulas. Thus for purposes of calculations with the tables of this paper, the familiar equation

$$\mu = \left( \frac{dT}{dP} \right)_H = \frac{V}{C_p} \left[ \frac{T}{V} \left( \frac{dV}{dT} \right)_P - 1 \right] \quad (4.5)$$

is put in the form

$$\mu = \left( \frac{dT}{dP} \right)_H = \frac{V_0}{\rho C_p} \left[ \frac{1 + \frac{T}{Z} \left( \frac{dZ}{dT} \right)_\rho}{1 + \frac{\rho}{Z} \left( \frac{dZ}{d\rho} \right)_T} - 1 \right] \quad (4.6)$$

where  $V_0$  is the molar volume of hydrogen at standard conditions and  $C_p$  is the molar heat capacity at the given conditions of  $T$  and  $P$  or  $T$  and  $\rho$ .

In correlating the PVT data for hydrogen the function

$$\sigma = \frac{T}{T_0} \frac{V}{V_0} \log_{10} \frac{PV}{RT} \quad (4.7)$$

was used, where  $T_0$  is the Kelvin temperature of the ice point. Reported temperatures were reduced wherever possible to a thermodynamic scale having the ice point temperature  $273.16^\circ$ . All available data were considered in this work but only those appearing most reliable were used and these were weighted according to their apparent

precision. The data used [59, 61, 63, 65, 66, 67, 70 to 74, 76, 79, 81, 85, 88, 91, 177] are plotted in figure 6 with the exception of a few observations at temperatures below  $29^\circ$  K and at densities lower than  $\rho=10$ , which were omitted because in these regions of low precision the scattering is so great that the points would be confusing.

A lower boundary to the  $\sigma$  versus  $\rho$  gas-liquid diagram in figure 6 is furnished by the vapor-liquid saturation line and the freezing curve. These are represented in figure 6 by dashed lines. The saturation line for the vapor rises steeply onto the diagram at low densities and with decreasing slope approaches tangency to the critical isotherm at the critical point which is indicated by an asterisk. The saturation line for liquid hydrogen is a nearly straight and horizontal line from a density somewhat greater than the critical to the triple point. The freezing curve, which represents the values of  $\sigma$  for liquid when for a given temperature the pressure is great enough to cause the liquid to freeze, rises nearly vertically from the triple point and bends towards higher densities.

The saturation curve on the vapor side was obtained with the help of the vapor pressure equation (eq 7.2) and the PVT representation given by eq 4.14 and table 19. On the liquid side it was obtained from the same vapor pressure equation and the volumes of the liquid at saturation pressure, given in table 31 and discussed in section VIII. The freezing curve was obtained from the melting point-pressure relations given in table 30 combined with extrapolations based on the higher density observations of Bartholomé for the isotherms of the liquid which are given in table 32.

The isothermal curves of figure 6 represent final table values. The curves are not necessarily the best fit for the experimental data for each individual isotherm inasmuch as the curves and table values are the result of correlating all the data and include the temperature dependence which, while it does not affect the relative position of points on one isotherm, may shift the whole isotherm somewhat. Isotherms that depended upon only a few individual observations and covered only a small range of densities were given less weight than others. For a given isotherm, data at higher densities, corresponding to larger deviations from the ideal gas law, were usually given

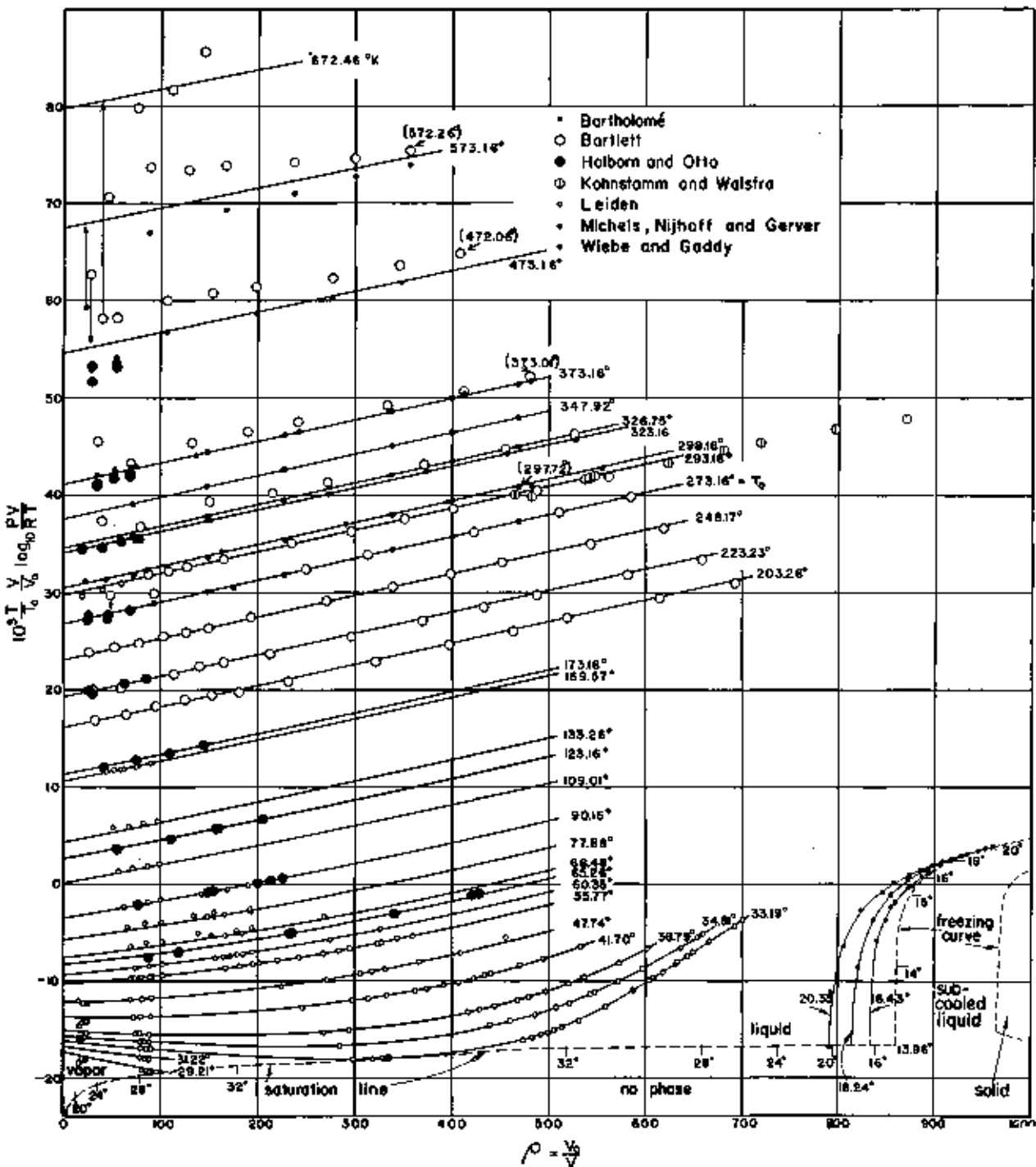


FIGURE 6. Plot of PVT data for  $H_2$  in the fluid states.

greater weight than data at low densities. In fact in some instances the low density data were given zero weight. Data at the highest temperatures do not appear to be very reliable, probably because

of penetration of the containers by hydrogen. At very low temperatures the deviations from the ideal gas law have not been measured very precisely because the pressure range over which

measurements can be made is limited by condensation.

Cragoe has shown that for densities up to  $\rho=500$  the 0° C isotherm is fitted to within experimental accuracy by the equation  $\sigma=b+c\rho$ . Figure 6 shows that, although this linear relation between  $\sigma$  and  $\rho$  fails at low temperatures, it is valid within experimental error over a considerable range of temperatures above 200° K. This relation was made the basis for the correlation of the PVT data above 0° C. The different method used for correlating the data below 0° C is described under (b).

(a) Region Above 0° C

Above 0° C, equations of the form  $\sigma=b+c\rho$  were fitted to the PVT data plotted in figure 6, and  $b$  and  $c$ , the intercept and slope of an isothermal line, were determined as functions of  $T$ . The quantity  $Z=PV/RT$  thus obtained as a function of  $T$  and  $\rho$ ,

$$PV/RT = \exp 2.30259 \frac{T_0}{T} [b(T)\rho + c(T)\rho^2] = \exp [B(T)\rho + C(T)\rho^2], \quad (4.8)$$

was used for the calculation of the tables of  $Z$ ,  $P$ ,  $(dZ/d\rho)_T$ ,  $(dZ/dT)_\rho$ , and  $(d^2Z/dT^2)_\rho$ .

Before fitting functions of  $T$  to  $b$  and  $c$ , small corrections were applied to some of the data. A constant error in  $T$  and constant factor errors along an isotherm in  $P$ ,  $V$ , and the number of moles of gas, cause deviations from the true isotherm that are very nearly proportional to  $1/\rho$ . Such hyperbolic deviations from a straight line are most easily detected in data extending from low to high densities. A change in  $V$  by 0.2 percent is sufficient to considerably straighten the 573.16° K (300° C) isotherm of Wiebe and Gaddy, and raise the line drawn through their adjusted data so that it intersects the  $\sigma$  axis of figure 6 only 0.7 unit below the table line for 573.16° K and crosses the table line at  $\rho=550$ . Wiebe and Gaddy call attention in their paper to an estimated error of 0.05 to 0.10 percent in the volume of their high pressure steel pipette at 200° and 300° C. It would seem that some part of the 0.2-percent adjustment, which straightens the 300° C isotherm of Wiebe and Gaddy, might be attributed to small temperature and pressure errors and to some loss of hydrogen in the steel.

Hyperbolic adjustments proportional to  $1/\rho$  of

Bartlett's higher temperature data straighten the isotherms and improve their agreement with the lines representing the tables. A comparison of the observations of Michels, Nijhoff, and Gerber [79] at different temperatures for nearly constant values of  $\rho$ , revealed apparent small hyperbolic trends of the data for the separate isotherms superposed on one larger though small random pattern of scattering common to all their isotherms. Using their 0° C isotherm as a reference line, their other data were adjusted to remove the hyperbolic deviations. The points of figure 6 represent reported data adjusted only to the Kelvin scale having 273.16° at the ice point.

Least square determinations were made of the straight lines fitting the adjusted  $\sigma$  versus  $\rho$  isothermal data for the different observers separately. From these, values of intercept  $b$  and slope  $c$  were obtained for the different observers at each temperature of measurement. Holborn's data above 0° C, however, were used only for obtaining intercepts, the slopes of adjacent isotherms of other observers being used with his data.

Expanding the exponential of eq 4.8,

$$PV/RT = 1 + B\rho + [(1/2)B^2 + C]\rho^2 + [(1/6)B^3 + BC]\rho^3 + [(1/24)B^4 + (1/2)C^2 + (1/2)B^2C]\rho^4 + \dots \quad (4.9)$$

shows that  $B(T)$  is the second virial coefficient and that a correlation of intercepts  $b$  of  $\sigma$ -isotherms is essentially a correlation of values of the second virial coefficients of hydrogen. Formulas expressing the dependence of the second virial coefficient on temperature have been derived theoretically on the assumption of simple laws of intermolecular forces. One of the most satisfactory formulas is based on a law of intermolecular force of the form  $\lambda_n r^{-n} - \lambda_m r^{-m}$  and is due to Lennard-Jones. For  $n=13$  and  $m=7$ , the Lennard-Jones formula for  $B$  is

$$B = B_1 T^{-1/4} + B_2 T^{-3/4} + B_3 T^{-5/4} + \dots, \quad (4.10)$$

where all the coefficients  $B_i$  of this infinite series are determined by  $\lambda_n$  and  $\lambda_m$ . Following essentially a procedure used successfully by F. G. Keyes [89], we used only the first three terms of this series and selected values for  $B_1$ ,  $B_2$ , and  $B_3$  which resulted in the best fit of a three constant equation with the intercepts of the  $\sigma$ -isotherms. Our formula,

$$B = 0.0055478 T^{-1/4} - 0.036877 T^{-3/4} - 0.22004 T^{-5/4}, \quad (4.11)$$



intended for use above 0° C, passes through the intercept of the -50° C isotherm determined by the correlation below 0° C.

The slopes of the  $\sigma$ -isotherms were represented by a two term empirical formula without theoretical justification, except that it involves powers of  $T$  which make  $C$  go to zero as  $T$  grows very large.

$$C = 0.004788T^{-3/2} - 0.04053T^{-2}. \quad (4.12)$$

The exponents of  $T$  were chosen so as to simplify the temperature function coefficients in the power series in  $\rho$  of eq 4.9.

The tables from 270° to 600° K have been computed on the basis of these formulas, and in

0.06 percent for the 100° C isotherm, and for the other isotherms it is of this approximate magnitude or smaller. At low densities the deviation for the 0° C isotherm does not appear to be systematic. On the other hand, it will be seen that there is a systematic deviation at densities greater than 500 with the experimental values for  $\sigma$  less than those obtained by linear extrapolation from the intermediate densities. This trend is supported by the high pressure data of Kohnstamm and Walstra [61, 81], also shown in the figure. If the representation of the  $\sigma$  isotherm by an equation is extended beyond  $\rho = 500$ , it will be necessary to include a small quadratic term in the expression for  $\sigma$ .

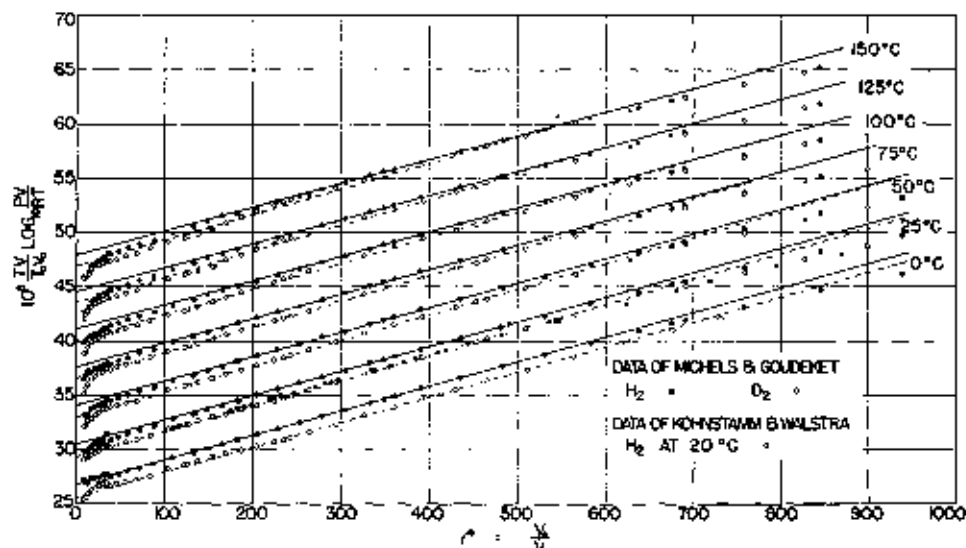


FIGURE 7. A plot of part of the PVT data for  $H_2$  and  $D_2$  from 0° C to 150° C.

this temperature range the various derivatives tabulated have been calculated analytically.

It was not until considerably after the preparation of the tables on hydrogen that we were able to examine the data of Michels and Goudekot published in *Physica* 1941 [91]. Values of  $\sigma$  for these data on  $H_2$  are shown as solid circles in figure 7 with the tables represented by the solid straight lines. The agreement for  $H_2$  is not complete but seems fairly satisfactory at moderate densities. At low densities there are discrepancies, roughly hyperbolic, which have the appearance of the hyperbolic deviations resulting from small systematic errors discussed earlier in this section. If the hyperbolic deviation is attributed to a systematic error in the volume, the error amounts to

#### (b) Region Below 0° C

At low temperatures the  $\sigma$  versus  $\rho$  isotherms are curved; making it difficult to decide how the isotherm should be drawn at low densities where the data were meager and the precision was low.

Another function,  $T^{3/2}V/V_0 \left(1 - \frac{PV}{RT}\right)$ , plotted against  $\rho = V_0/V$  as abscissa gave lines which appeared to be straight at low densities for temperatures below 56°K, though there is considerable curvature at high densities. In figure 8,  $T^{3/2}V/V_0 \left(1 - \frac{PV}{RT}\right) + 0.0006\rho = \psi$  is plotted against  $\rho$ , the term  $0.0006\rho$  being added to make isotherms nearly horizontal at low densities and thus increase the scale of the plot. The sensitivity to

small changes of  $PV/RT$  at  $\rho=200$  and  $T=55^\circ\text{K}$  is 18 times greater in figure 8 than in figure 6 and 14 times greater at  $\rho=200$  and  $T=33^\circ\text{K}$ . The curves of figure 8 were drawn to fit the data for each particular isotherm considered independently, and though the curves do not represent the tables exactly they agree closely with them. Below  $31^\circ\text{K}$  the data were not sufficient and precise enough to determine consistent isothermal curves when the isotherms were considered independently. The data lower than  $29^\circ\text{K}$  were not plotted because the double valued nature of  $\psi$  causes the data below  $29^\circ\text{K}$  to fall in the same region on the diagram as is covered by the data above  $29^\circ\text{K}$ .

At first it appeared that the critical isotherm in figure 8 could be represented by a straight line from  $\rho$  equal to zero to  $\rho$  greater than the critical density. However, the conditions that  $(dP/dV)_T$  and  $(d^2P/dV^2)_T$  be zero at the critical point impose upon the slope and curvature of the isotherm at the critical point the conditions

$$\left. \begin{aligned} \left(\frac{d\psi}{d\rho}\right)_{T_c} &= \frac{T_c^{3/2}}{\rho_c^2} \left( 2 \frac{P_c V_c}{RT_c} - 1 \right) + 0.0006, \\ \left(\frac{d^2\psi}{d\rho^2}\right)_{T_c} &= \frac{2T_c^{3/2}}{\rho_c^2} \left( 1 - 3 \frac{P_c V_c}{RT_c} \right). \end{aligned} \right\} \quad (4.13)$$

In addition, values for the critical temperature and pressure should satisfy the vapor-pressure equation.

Only a single determination has been made of the critical temperature and pressure of hydrogen [62]. The critical isotherm was located somewhere between the 2 measured isotherms at  $32.94^\circ$  and  $33.29^\circ\text{K}$ , and was at the time (1917) considered to be  $33.19^\circ\text{K}$  with a certainty of about  $0.1^\circ$ , though in 1925 it was stated in a footnote to Leiden Communication 172a that  $T_c$  should be about  $0.1^\circ$  lower. The critical pressure inferred from the  $P$  versus  $V$  isotherms in 1917 was 12.80 atm. Later in 1917 [142] the vapor pressure equation of  $\text{H}_2$  above the boiling point was determined and the value 12.75 atm deduced for  $P_c$  using  $T_c=33.18^\circ\text{K}$  (on basis of  $T_0=273.09$ ). Two determinations [62] were made of the critical density based on the extrapolation of the rectilinear diameter. These gave  $\rho_c=345$ . The values reported in later Leiden Communications have not in all cases been the latest determined values. The most recently reported Leiden values [69] are

<sup>1</sup> Unless otherwise stated, temperatures are expressed on the Kelvin Scale with  $T_0=273.16^\circ$ .

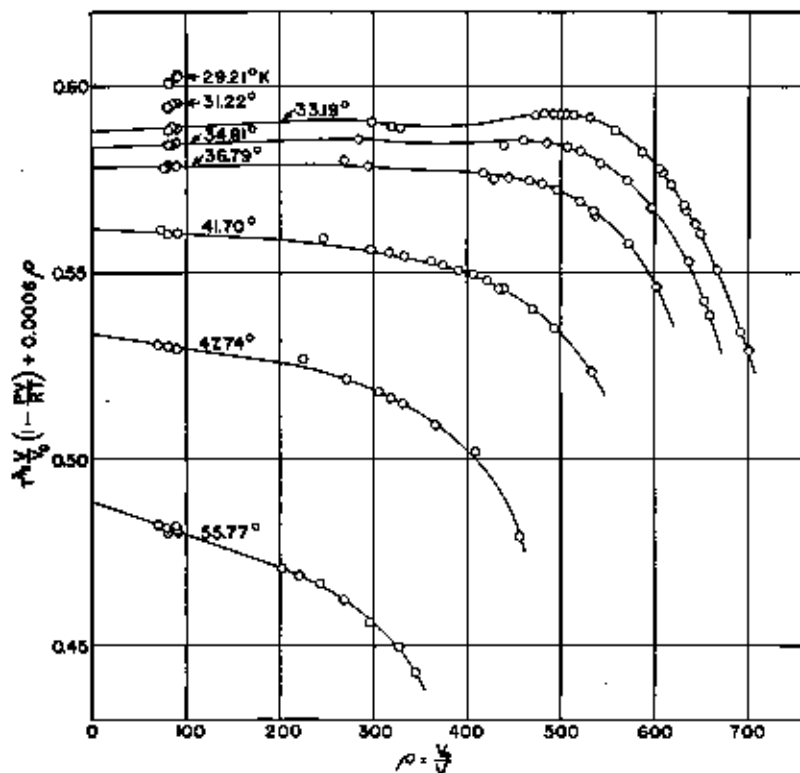


FIGURE 8. Plot of PVT data for  $\text{H}_2$  at low temperatures.

$T_c=33.19^\circ K$  (on basis of  $T_0=273.16$ ),  $P_c=12.751$  atm and  $1/\rho_c=0.02909$  or  $\rho_c=344$ . The lower critical temperature  $33.1^\circ K$  inferred from Leiden Communication 172a is supported by the agreement of the vapor pressure 12.81 atm, calculated from vapor pressure equation (eq 7.2) with the critical pressure determined in 1917 from the  $P$  versus  $V$  isotherms.

Difficulties are encountered in obtaining agreement with the experimental PVT data (fig. 8)

vapor pressure equation (7.2). These critical constants are listed in table 18.

TABLE 18. Critical constants of hydrogen

$T_c$	$P_c$	$\rho_c = \frac{V_0}{V_c}$	$V_c$	$\frac{P_c V_c}{RT_c}$
$^\circ K$ 33.19	atm 12.98	335	$cm^3/mole^{-1}$ 96.97	0.3191

It seemed reasonable to assume that the iso-

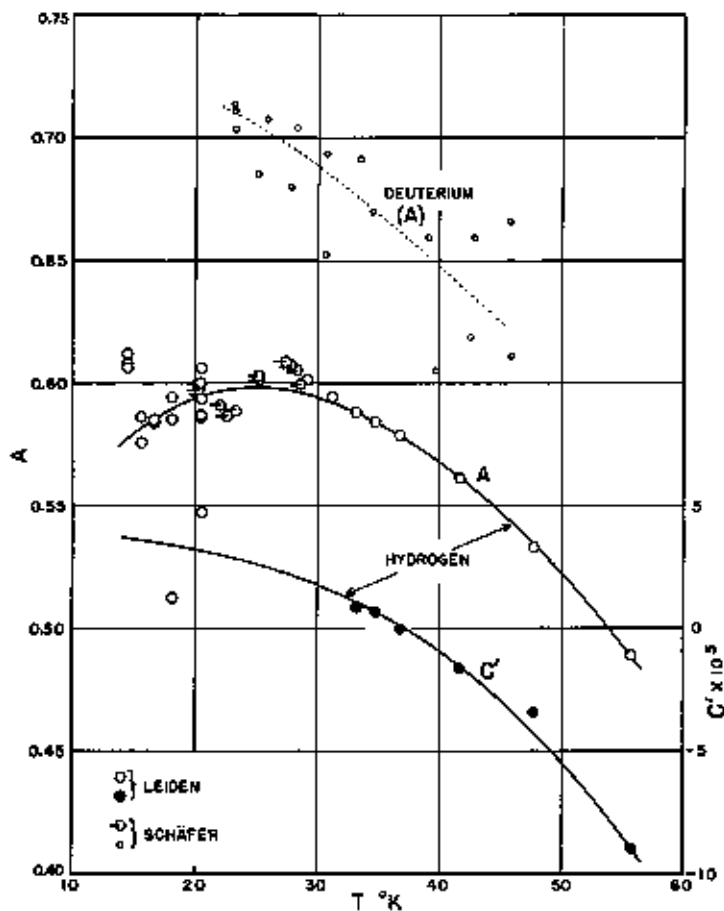


FIGURE 9. Intercepts and slopes from figure 8.

on the basis of  $T_c=33.1^\circ$  and  $P_c=12.81$  atm, however, unless the critical density is inferred to be about 320, in Amagat units, instead of the reported values 345 or 344. This difference in critical density seemed too large on the basis of the probable precision of the density measurements. The adjustment has instead been so made and the critical isotherm in figure 8 so drawn that  $T_c=33.19^\circ$ ,  $P_c=12.98$  atm, and  $\rho_c=335$ . This value of  $P_c$  is consistent with the PVT data and with

therms of figure 8 are straight lines up to  $\rho=200$ . This assumption was used in correlating the observed data below the critical temperature where the data were scarce and the precision low. In figure 9 the intercepts  $A$  and the slopes  $C'$  of the isotherms of figure 8 are plotted as functions of the temperature. The curve for the slope was extrapolated smoothly to lower temperatures as slopes could not be obtained from the data below  $33^\circ K$ .

Also shown in figure 9 are values for  $A$  calculated from second virial coefficients determined experimentally by Schäfer [85]. Schäfer reported the results of his PVT measurements as virial coefficients  $B'(T) = d(PV/RT)/dP$  at constant temperature and at  $P=0$ . The values of  $A = -(RT^{3/2}/V_0)B'(T)$  obtained from Schäfer's results agree well with those obtained from data of the Leiden Laboratory as shown by figure 9. Schäfer observed no consistent difference between the second virial coefficients of para hydrogen, normal hydrogen, and a one to one mixture of ortho and para varieties.

The equation for the straight part of the  $\psi$ -isotherms of figure 8 may be written

$$\frac{T^{3/2}}{\rho} \left(1 - \frac{PV}{RT}\right) = A + C\rho, \quad (4.14)$$

where  $C = C' - 0.0006$ ,  $C'$  being the slopes plotted in figure 9 of the  $\psi$ -isotherms in figure 8. Values of  $A$  and  $C$  and their derivatives are given for hydrogen in table 19. The values of  $PV/RT$  from  $\rho=0$  to  $\rho=200$  and from  $T=14^\circ$  to  $T=56^\circ$  K in

TABLE 19. Hydrogen values of  $A$  and  $C$  (and derivatives) in the equation for isotherms

$$T^{3/2} \frac{V}{V_0} \left(1 - \frac{PV}{RT}\right) = A + C\rho$$

[Applicable at Amagat densities less than 200]

$T$	$A$	$C$	$dA/dT$	$dC/dT$
$^\circ K$	$^\circ K^{3/2}$	$^\circ K^{3/2}$	$^\circ K^{1/2}$	$^\circ K^{1/2}$
14.....	0.5754	$-3.621 \times 10^{-7}$	0.00388	$-76 \times 10^{-8}$
16.....	.5927	-5.686	.00330	-82
18.....	.5987	-5.653	.00284	-90
20.....	.5933	-5.672	.00192	-100
22.....	.5865	-5.693	.00118	-112
24.....	.5861	-5.716	.00040	-127
26.....	.5961	-5.748	-.00032	-145
28.....	.5926	-5.774	-.00097	-165
30.....	.5940	-5.809	-.00154	-187
32.....	.5904	-5.848	-.00202	-213
34.....	.5858	-5.892	-.00243	-245
36.....	.5805	-5.943	-.00280	-282
38.....	.5746	-6.003	-.00317	-320
40.....	.5679	-6.071	-.00356	-368
42.....	.5604	-6.146	-.00397	-426
44.....	.5521	-6.229	-.00438	-486
46.....	.5429	-6.320	-.00476	-547
48.....	.5320	-6.420	-.00509	-622
50.....	.5225	-6.529	-.00540	-705
52.....	.5114	-6.640	-.00572	-803
54.....	.4996	-6.770	-.00608	-926
56.....	.4871	-6.900	-.00650	-1084

TABLE 20. Pressure, density, and  $PV/RT$  for saturated  $H_2$  vapor

$T$	$P$	$\rho$	$PV/RT$
$^\circ K$	atm	Amagats	
14.....	0.0728	1.445	0.98415
16.....	.2018	3.262	.96798
18.....	.4661	7.321	.94306
20.....	.8691	13.311	.91263
22.....	1.6045	22.235	.87420
24.....	2.6455	35.017	.82783
26.....	3.8686	53.02	.77298
28.....	5.395	78.55	.70778
30.....	8.010	116.33	.62732
32.....	10.593	180.04	.53554
33.19.....	12.98	335	.4191

table 13 were calculated using eq 4.14 with table 19. Table 20, giving the pressure, density, and value of  $PV/RT$  for saturated  $H_2$  vapor, was prepared similarly using the vapor pressure equation for  $n-H_2$  (eq 7.2). For certain uses eq 4.14 with table 19 may be more convenient than the tables of  $PV/RT$  and its derivatives.

For temperatures below  $56^\circ$  K and densities greater than  $\rho=200$  where  $\psi$  could not be represented by a simple function of  $\rho$ , a table was made of values of  $\psi$  for each  $\rho$  and  $T$  entry in the  $Z$ -table. The  $\psi$ -values of this table were obtained from figure 8 by graphical interpolation. Large plots of  $\psi$ -isochores, 20 Amagat units apart, on  $\psi$  versus  $T$  graphs were made of values of  $\psi$  read from figure 8. Values of  $\psi$  at 2-degree intervals were read from the isochores. A  $Z(\rho, T)$  table was calculated from the  $\psi(\rho, T)$  table.

From  $56^\circ$  to  $273^\circ$  K, the  $\sigma$ -function rather than the  $\psi$ -function was used because above  $56^\circ$  K the  $\sigma$ -isotherms approach linear functions of the density. The method of graphical interpolation used below  $56^\circ$  K was used above, also, to obtain a table of  $\sigma$ -values for the  $\rho$  and  $T$  entries of the  $Z$ -table. The accuracy of graphical interpolation was improved by using more sensitive plots than figure 6 of modified  $\sigma$ -functions obtained by adding to  $\sigma$  simple functions of  $T$  and  $\rho$ , which brought the isotherms and isochores closer together so that they could be easily plotted to a large scale. Values of  $\sigma$  were obtained at densities as high as  $\rho=500$ , although between  $70^\circ$  and  $200^\circ$  K measurements were not available at densities this high. This region was filled in by extrapolation of  $\sigma$ -curves to higher densities along isotherms and by interpolation along isochores between the upper

and lower temperature regions where there were data to determine the trend. From the  $\sigma(\rho, T)$  table a  $Z(\rho, T)$  table was obtained by calculation.

The  $Z(\rho, T)$  table obtained through graphical interpolation of the  $\psi$  and  $\sigma$  isotherms as has just been described was smoothed along isotherms and along isochores by inspection of second differences. In general the  $Z$ -tables are smooth to one unit in the last digit.

The tables of  $(dZ/dT)_\rho$  and  $(dZ/d\rho)_T$  below  $0^\circ\text{C}$  were for the most part calculated from the smoothed  $Z$  table by the method of Rutledge [179] for the calculation of derivatives from smooth sets of tabular values of data.<sup>6</sup> In the region below  $56^\circ\text{K}$  and  $\rho=200$ , where the  $\psi$  versus  $\rho$  isotherms are straight lines, the following equations, obtained by differentiating eq 4.14, were used with table 19 to calculate the derivatives

$$\left(\frac{dZ}{dT}\right)_\rho = \frac{3}{2} \frac{(1-Z)}{T} - \frac{\rho}{T^{3/2}} \frac{dA}{dT} - \frac{\rho^2}{T^{3/2}} \frac{dC}{dT} \quad (4.15)$$

$$\left(\frac{dZ}{d\rho}\right)_T = -\frac{1}{T^{3/2}} [A + 2(C' - 0.0006)\rho]. \quad (4.16)$$

Where the derivatives could be obtained both by the method of Rutledge and by eq 4.15 and 4.16, the agreement was very satisfactory. The  $(dZ/d\rho)_T$  and  $(dZ/dT)_\rho$  tables were also smoothed along isotherms and isochores by inspection of second differences.

The  $(d^2Z/dT^2)_\rho$  table below  $0^\circ\text{C}$  was obtained throughout by the method of Rutledge from the smoothed  $(dZ/dT)_\rho$  table and was also smoothed. The equation for  $(d^2Z/dT^2)_\rho$  corresponding to eq 4.15 for the first derivative was considered too involved for easy computation.

In general, the tables of derivatives are smooth to the last digit recorded.

#### (c) Reliability of Tables of PVT Data

By inspecting figures 6 to 8 it is possible to arrive at some general conclusions regarding the deviations of the observed data from the  $Z(\rho, T)$  table. It may be noted that, except at low densities, the deviations of the observational values of  $\sigma$  from the curves representing the table are of about the same magnitude at different densities along a given isotherm up to  $\rho=500$ .<sup>7</sup> This means that deviations of  $(PV/RT)-1$

along an isotherm are approximately proportional to the density. At low densities the deviations are large because the sensitivity of the  $\sigma$  and  $\psi$  plots approaches infinity as  $\rho$  approaches zero. It is difficult to make an estimate of the probable error in  $PV/RT$  based on the deviations because, as is seen, the greatest deviations are the systematic differences between the results of different observers and are not accidental errors as should be the case if error theory were to apply. The user of the tables can make an estimate of the mean difference between the observed and tabulated values of  $PV/RT$ , in any particular region of temperature and density by noting the deviations shown on the graph and from these calculating the corresponding deviations in  $PV/RT$ . For temperatures below  $60^\circ\text{K}$  it would be best to use figure 8 for this purpose as it is plotted to a larger scale than is figure 6.

In constructing the tables for the intermediate temperature regions where analytical equations of state were not used, just enough digits were retained so that changes made in smoothing would be confined to the last digit. As a considerable amount of smoothing resulted from the graphical methods used, many of the irregularities in the measured values were not apparent in the unsmoothed tables.

It is believed that throughout the table the values were carried out to at least as many significant figures as were at all justified by the data, and that the last digit recorded should be considered very uncertain. In that part of the table between  $77^\circ$  and  $200^\circ\text{K}$  which was filled in by interpolation and extrapolation the last two digits should be considered uncertain, the last recorded digit being retained to achieve continuity with the rest of the table.

The tables are thought to be most reliable for temperatures between  $273^\circ$  and  $373^\circ\text{K}$  ( $0^\circ$  and  $100^\circ\text{C}$ ), because at these temperatures the experimental difficulties encountered are not as great as at higher and lower temperatures. Also, as is shown by figure 6 the results of several different investigators are in agreement at these temperatures. Above  $373^\circ\text{K}$  the experimental data are not as self-consistent as at temperatures immediately below. As the values of  $PV/RT$  given in the tables for these higher temperatures are derived largely from an extrapolation based on the temperature region between  $273^\circ$  and  $373^\circ\text{K}$ ,

<sup>6</sup> Assuming that differences of higher order than the fourth are negligible.

<sup>7</sup> For still greater densities larger deviations occur as shown by figure 7.

an estimate of reliability of the high temperature portion of the tables involves both the applicability of the correlating function, eq 4.8, and the precision of the experimental data. Considering the differences between the isothermal lines determined by different sets of experimental data of different observers and the same observer at different temperatures, it seems probable that the extrapolation is more reliable than the experimental data at temperatures above 473° K.

It is doubted that  $PV/RT$  is known to better than 0.2 percent for densities as high as 100 Amagats near 33° K, the critical temperature.

Below the critical temperature, the data are not very satisfactory. In addition to the difficulties of making measurements at low temperatures, there exists the circumstance that below the critical temperature the range of vapor densities that can be covered is limited by the density of saturated vapor. At low densities the deviations  $(1-Z)$  from the ideal gas law are small and hence difficult to measure precisely.

There is another method of obtaining values of second virial coefficients which may be advantageous for the low temperature region. It involves the determination of the velocity of sound, which has been carried out for gaseous hydrogen at liquid-hydrogen temperatures and various pressures by van Itterbeek and Keesom [77], using a resonance method. The change of the velocity of sound with pressure at very low pressures is related to the value of the second virial coefficient and to its first and second derivatives. Because of this relationship, it is possible to determine the second virial coefficient from the velocity of sound if the second virial coefficient is already known in an adjacent range of temperature. Van Itterbeek and Keesom concluded that the agreement between their own measurements and the PVT data was "rather good", although for both types of data the scattering was quite appreciable.

In calculating the tables of derivatives by the method of Rutledge, the criterion for retaining significant figures in the recorded values was the same as that previously mentioned, namely, enough places were carried so that the changes resulting from the smoothing were in general confined to the last digit. As in the case of the tables of  $PV/RT$ , it is believed that the tabulated values of the derivatives are given to as many significant figures as are justified by the data.

The interesting features of the PVT data for deuterium are most evident when deuterium is compared with hydrogen. The difference between the second virial coefficients of  $H_2$  and  $D_2$  has been investigated theoretically [86, 87], though a complete treatment of the problem has not been made.

Assuming the same intermolecular forces for  $H_2$  and  $D_2$ , classical mechanics and statistics lead to the same equation of state for  $H_2$  and  $D_2$ . The quantum theory of virial coefficients leads to effective volumes of molecules and to second virial coefficients that are larger than the classical values, the differences being small at ordinary temperatures but becoming large at low temperatures.<sup>10</sup>

In table 21 are given ratios between quantum mechanical and classical values of second virial coefficients, for gases whose molecules are rigid nonattracting spheres. They may also be considered as ratios between apparent molecular volumes for the two treatments. These ratios are based on formulas derived by Uhlenbeck and Beth [84]. Columns 2 and 3 are for gases with molecular weights 2 and 4, respectively. The value of the ratio depends, among other things, upon the diameters of the rigid spheres. Here the size of the spheres was taken to be the same for the two

TABLE 21. Ratio between quantum mechanical and classical second virial coefficients for nonattracting rigid spherical molecules \* of molecular weight  $M$

$T$ ° K	$B_{\text{quantum}}/B_{\text{classical}}$ for $M=2$	$B_{\text{quantum}}/B_{\text{classical}}$ for $M=4$
600.....	1.21	1.16
300.....	1.30	1.21
100.....	1.52	1.37
25.....	2.7	2.0
5.....	4.6	2.0

\* With diameters calculated from the van der Waals'  $b$  for hydrogen.

<sup>10</sup> The application of quantum mechanics instead of ordinary mechanics has as one effect for rigid spherical molecules the removal of the classical discontinuity in the calculated distribution of molecules for pair separations corresponding to contact between the spheres. As smaller separations are prevented by the impenetrability of the spheres, the continuity is established by a reduction of the molecular density for separations greater than that corresponding to contact. The effect is large for separations of sphere surfaces up to a considerable fraction of the de Broglie wavelength (for which  $h/\sqrt{2mE}$  is a representative value) and depends through this upon the temperature. This reduction of molecular density beyond the minimum separation could be represented roughly in a classical description as an increase of the volume from which 1 molecule causes the centers of other molecules to be excluded. In classical theory the second virial coefficient for nonattracting rigid spheres is proportional to the excluded volume.

gases and to be equal to the size calculated from the van der Waals  $b$  for  $H_2$ .

Although it would scarcely be expected that the results of calculations for rigid nonattracting spheres would apply to real  $H_2$  and  $D_2$  molecules, it would seem likely that qualitative indications would be correct, at least at higher temperatures where the excluded volume predominates over the intermolecular attractive forces in determining the magnitude of the second virial coefficient. This is borne out by experiment, the difference in second virial coefficients ( $B_{H_2} - B_{D_2}$ ), being positive, though smaller than would be indicated by table 21 for rigid spheres by a factor of about 2.6 at  $300^\circ K$ . Uhlenbeck and Beth derived an approximate quantum mechanical representation for the second virial coefficient applicable at high

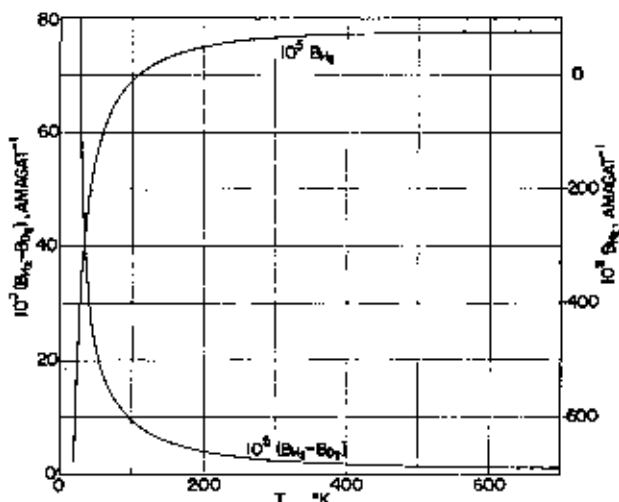


FIGURE 10. Second virial coefficient for  $H_2$  and the difference between second virial coefficients for  $H_2$  and  $D_2$ .

temperatures for molecules with radially symmetrical force fields. Their formulas were applied to hydrogen and deuterium by de Boer and Michels [87] upon the assumption that the intermolecular forces were the same for  $H_2$  and  $D_2$ . They obtained differences between the virial coefficients for  $H_2$  and  $D_2$  represented by the upper temperature portion of one of the curves of figure 10. In a later paper by Michels and Goudekot [92] attention was called to the fact that the intermolecular forces of hydrogen and deuterium do differ a little because the mean internuclear separations of  $H_2$  and  $D_2$  molecules are different as a result of the different zero point vibrations of their nuclei.

The effect of the intermolecular attractive forces overbalances the effect of the excluded volume or the repulsive forces of the molecules in determining the magnitude of the second virial coefficient at low temperatures, and makes the coefficient negative. Nevertheless, at low temperatures, as at high temperatures, the difference in second virial coefficients  $B_{H_2} - B_{D_2}$  is positive, partly for the reason already discussed in the case of high temperatures, namely the larger apparent quantum-mechanical volume of  $H_2$  molecules, and partly for another reason. There is a closer spacing of the discrete negative energy states and smaller zero point energy for pairs of  $D_2$  molecules than for pairs of  $H_2$  molecules because of the mass difference, so that by reason of the Boltzmann factor,  $\exp[-\text{energy}/kT]$ , there is a greater degree of association or clustering together of  $D_2$  molecules than of  $H_2$  molecules. Without a consideration of the Boltzmann factors for these negative energy levels the effect of the difference of mass would be less clear, as the quantum treatment for the continuum would require that the spacing of the levels there be smaller for  $D_2$  than for  $H_2$  in essentially the same ratio as in the case of the discrete negative energy levels. With these or similar ideas in mind, Schäfer [86] derived a formula for the difference in second virial coefficients for  $H_2$  and  $D_2$  at low temperatures, which involved a constant whose magnitude he so chose as to obtain a fit with his experimental values for the difference in the second virial coefficients.

Figure 9 shows values of  $A$  in the equation of state (eq 4.14) calculated from the second virial coefficients of deuterium for the temperature range  $23^\circ$  to  $45^\circ$  determined experimentally by Schäfer [85].

$$A = -T^{3/2}(dZ/d\rho)_{T,\rho \rightarrow 0} = -T^{3/2}B_1, \quad (4.17)$$

where  $B_1$  is the second virial coefficient in the equation of state  $PV = RT(1 + B_1\rho + B_2\rho^2 + \dots)$ . The dashed line curve in figure 9 was obtained by adding to the  $A$ 's for  $H_2$  the differences between the  $A$ 's calculated from the differences between the second virial coefficients of  $H_2$  and  $D_2$  which Schäfer determined partly theoretically and partly empirically. Schäfer's measurements were made on deuterium at low densities and hence do not give information on higher virial coefficients. Approximate values of  $PV$  for deuterium at low

temperatures may be found by using values of  $A$  from figure 9 in eq 4.14, and either neglecting the  $C$  term or preferably using the corresponding value of  $C$  for  $H_2$ .

Values of the function  $\sigma = (TV/T_0V_0) \log_{10}(PV/RT)$  calculated from the data of Michels and Goudekot [92] for  $D_2$  are shown as open circles in figure 7. The dashed straight lines for deuterium are obtainable from the equation

$$PV/RT = \exp[B(T)\rho + C(T)\rho^2], \quad (4.18)$$

where

$$B(T) = 0.0055298T^{-1/4} - 0.036040T^{-3/4} - 0.25878T^{-5/4}$$

and

$$C(T) = 0.00580T^{-3/2} - 0.0565T^{-2}$$

The constants in the formula for  $B$  have been so chosen that the difference between  $D_2$  and  $H_2$  intercepts on the  $\sigma$ -axis is in close agreement with the theoretical result of de Boer and Michels [87] from 250° to 450° K.

In figure 10, a curve marked  $10^5(B_{H_2} - B_{D_2})$  shows the trend of differences between second virial coefficients based on the theoretical calculations above 150° K and on the results of Schäfer below 50° K with an interpolation between. It may be inferred that the differences between the PVT data for  $H_2$  and  $D_2$  decrease rather rapidly with increase of temperature. For comparison, the curve marked  $10^5 B_{H_2}$ , in figure 10, shows on a different scale the magnitude of the corresponding second virial coefficient for  $H_2$  at the same temperatures.

If it is assumed that the  $\sigma$  or  $(TV/T_0V_0) \log(PV/RT)$  isotherms for  $D_2$  and  $H_2$  are parallel, values of  $PV/RT$  for  $D_2$  may be obtained from those tabulated for  $H_2$  by (1) calculating the  $\sigma_{H_2}$  or  $\sigma$  for  $H_2$ , from the values of  $PV/RT$ ,  $T$  and  $\rho$ , (2) subtracting the difference  $(\sigma_{H_2} - \sigma_{D_2})_{\rho=0}$  to get  $\sigma_{D_2}$ , and then (3) calculating the corresponding value of  $PV/RT$  for  $D_2$ . A plot of the difference  $10^5(\sigma_{H_2} - \sigma_{D_2})_{\rho=0}$  which may be used for this purpose is shown in figure 11. An alternative method based on the assumption that only the second term of the series expansion eq 4.9 for  $PV/RT'$  is to be changed is as follows.  $10^5$

$(B_{H_2} - B_{D_2})$ , obtained from figure 11 by multiplying  $10^5(\sigma_{H_2} - \sigma_{D_2})_{\rho=0}$  by 2.302585  $T_0/T$  or obtained directly from figure 10, is multiplied by  $10^{-5}$  and the product subtracted from  $PV/RT$  for  $H_2$  to give  $PV/RT$  for  $D_2$ . This alternative method is simpler than the other method and may be as reliable.

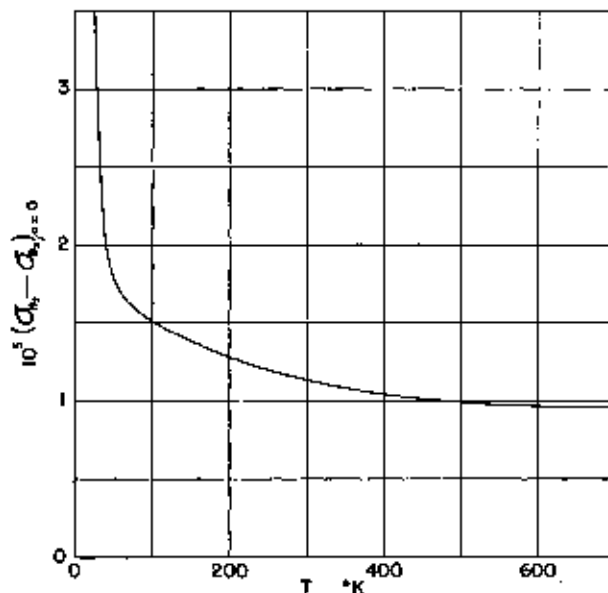


FIGURE 11. Difference between intercepts of  $\sigma$  versus  $\rho$  isotherms for  $H_2$  and  $D_2$ .

## V. Calculation of Thermal Properties of the Real Gas

The calculation of thermodynamic properties of a real gas from values of these properties for the ideal gas rests upon the principle that the difference between values of a thermodynamic function at different densities for the same temperature may be determined from data of state for the gas at the given temperature.

The entropy and free energy of a gas are dependent upon the pressure, even in the ideal state, and in tables 4 to 8 they are given for the hydrogens in the ideal gas state at a pressure of 1 standard atm. On the other hand, the internal energy, enthalpy, and specific heat in the ideal gas state are independent of density at constant temperature.

Equations 5.1 to 5.8 show how, using the data of state expressed in the form,  $Z = Z(\rho, T)$ , the thermodynamic properties of the real gas at a temperature  $T$  and an Amagat density  $\rho$  may be calculated from properties for the ideal gas state



at a pressure of 1 atm, given for the hydrogens in tables 4 to 8.

$$\frac{S_{p,T}(\text{real gas})}{R} = \frac{S_{p=1,T}^{\circ}(\text{ideal})}{R} + \ln \frac{P_0 V_0}{R T_0} - \ln \frac{T}{T_0} - \ln \rho - \int_0^{\rho} [(Z-1)/\rho] d\rho - \int_0^{\rho} [T(dZ/dT)_{\rho}/\rho] d\rho \quad (5.1)$$

This can be expressed in a slightly different form by using the identity

$$\int_0^{\rho} [(Z-1)/\rho] d\rho + \int_0^{\rho} [T(dZ/dT)_{\rho}/\rho] d\rho = \left( d \left\{ T \int_0^{\rho} [(Z-1)/\rho] d\rho \right\} / dT \right) \quad (5.2)$$

$$\frac{H_{p,T}(\text{real gas})}{RT} = \frac{H_T^{\circ}(\text{ideal})}{RT} - \int_0^{\rho} [T(dZ/dT)_{\rho}/\rho] d\rho + (Z-1) \quad (5.3)$$

$$\frac{F_{p,T}(\text{real gas})}{RT} = \frac{F_{p=1,T}^{\circ}(\text{ideal})}{RT} - \ln \frac{P_0 V_0}{R T_0} + \ln \frac{T}{T_0} + \ln \rho + \int_0^{\rho} [(Z-1)/\rho] d\rho + (Z-1) \quad (5.4)$$

$$\ln [f(\text{fugacity of real gas})/P] = \int_0^{\rho} (Z-1)/\rho d\rho - \ln Z + (Z-1) \quad (5.5)$$

$$\frac{E_{p,T}(\text{real gas})}{RT} = \frac{E_T^{\circ}(\text{ideal})}{RT} - [T(dZ/dT)_{\rho}/\rho] d\rho \quad (5.6)$$

$$\frac{(C_p)_{p,T}(\text{real gas})}{R} = \frac{(C_p)_{p,T}^{\circ}(\text{ideal})}{R} - 2 \int_0^{\rho} [T(dZ/dT)_{\rho}/\rho] d\rho - \int_0^{\rho} [T^2(d^2Z/dT^2)_{\rho}/\rho] d\rho \quad (5.7)$$

$$\frac{(C_p)_{p,T}(\text{real gas})}{R} = \frac{(C_p)_{p,T}^{\circ}(\text{ideal})}{R} - \left. \begin{aligned} &2 \int_0^{\rho} [T(dZ/dT)_{\rho}/\rho] d\rho - \int_0^{\rho} [T^2(d^2Z/dT^2)_{\rho}/\rho] d\rho + \\ &\{ [Z + T(dZ/dT)_{\rho}]^2 / [Z + \rho(dZ/d\rho)_T] \} - 1. \end{aligned} \right\} \quad (5.8)$$

In order to facilitate the calculation of the thermodynamic properties of hydrogen in the real gas state, tables 22 and 23 were computed.<sup>11</sup> Lagrangian four point formulas [181] were used for the tabular integrations.

Table 22 is intended for use in the calculation of

<sup>11</sup> For the calculation of these tables the authors are indebted to Messrs Roger F. Clapp, Kingsley Elder, Jr., and Robert Mann, who worked as student assistants at the National Bureau of Standards during the summer of 1941.

entropies. The values in the second column, headed  $(S_{p=1}^{\circ} - S_{p=1}^{\circ})/R$ , are for the difference between entropies of hydrogen in the ideal gas state at 1-atm pressure and at unit Amagat density, divided by  $R$ .

$$\frac{S_{p=1,T}^{\circ}(\text{ideal})}{R} - \frac{S_{p=1,T}^{\circ}(\text{ideal})}{R} = -\ln \frac{P_0 V_0}{R T_0} + \ln \frac{T}{T_0} - 0.000618 + \ln T/T_0 \quad (5.9)$$

The row at the bottom of the table, headed  $(S_{p=1}^{\circ} - S^{\circ})/R$ , is for the difference between entropies in the ideal gas states at Amagat densities one and  $\rho$ , divided by  $R$ .

$$\frac{S_{p=1,T}^{\circ}(\text{ideal})}{R} - \frac{S_{\rho,T}^{\circ}(\text{ideal})}{R} = \ln \rho \quad (5.10)$$

The other rows and columns of table 22 headed  $(S^{\circ} - S)/R$  give the differences between the entropies in the ideal and real gas states at the same temperature and density, divided by  $R$ .

$$\frac{S_{p,T}^{\circ}(\text{ideal})}{R} - \frac{S_{p,T}(\text{real})}{R} = \int_0^{\rho} [(Z-1)/\rho] d\rho + \int_0^{\rho} [T(dZ/dT)_{\rho}/\rho] d\rho \quad (5.11)$$

In order, then, to get  $S/R$  for the real gas hydrogen at a temperature  $T$  and Amagat density  $\rho$ , one subtracts from  $S^{\circ}/R$ , obtained from  $S^{\circ}$  given in table 8, the sum of three numbers for the appropriate values of  $T$  and  $\rho$  to be obtained from table 22: one comes from the second column, headed  $(S_{p=1}^{\circ} - S_{p=1}^{\circ})/R$ ; another from the bottom row of the table, headed  $(S_{p=1}^{\circ} - S^{\circ})/R$ ; and the third from the rows and columns of the table headed  $(S^{\circ} - S)/R$ .

Table 23 is for the difference between the enthalpy of hydrogen in the ideal and real gas states at temperature  $T$  and Amagat density  $\rho$ , divided by  $RT$ .

$$\frac{H_T^{\circ}(\text{ideal})}{RT} - \frac{H_{p,T}(\text{real})}{RT} = \int_0^{\rho} [T(dZ/dT)_{\rho}/\rho] d\rho - (Z-1) \quad (5.12)$$

Hence to obtain  $H/RT$  for hydrogen in the real gas state, one subtracts the appropriate value of  $(H^{\circ} - H_{\rho})/RT$  in table 23 from the value of  $H^{\circ}/RT$  obtained from  $H^{\circ}$  given in table 8 for the deal gas state.

TABLE 22. Entropy differences divided by  $R$ , for normal  $H_2$ .

$\frac{S^0 - S^1}{R}$ , Entropy of ideal gas minus entropy of real gas at same  $T$  and  $p$ , divided by  $R$ .  
 $\frac{S^0_{p=1} - S^1_{p=1}}{R}$ , Entropy of ideal gas at pressure of 1 atmosphere minus entropy of ideal gas at density of 1 Atmosphere, divided by  $R$ .  
 $\frac{S^0_{p=1} - S^0_{p=1}}{R}$ , Entropy of ideal gas at density of 1 Atmosphere minus entropy of ideal gas at density of  $p$  Atmosphere, divided by  $R$ .

Temperature °K	$\frac{S^0_{p=1} - S^1_{p=1}}{R}$	$\frac{S^0_{p=1} - S^0_{p=1}}{R}$	2	3	5	10	20	40	60	80	100	120	140	160	180	200
16	-2.68809	0.00773	0.01117	0.01803	0.0287											
18	-2.72050	0.00723	0.00615	0.00684	0.01284											
20	-2.61494	0.00796	0.00784	0.01724	0.0287											
22	-2.51863	0.00754	0.00792	0.01563	0.0283											
24	-2.43202	0.00840	0.00849	0.01453	0.0245											
26	-2.35235	0.00830	0.00839	0.01378	0.0230											
28	-2.27847	0.00818	0.00818	0.01301	0.0218											
30	-2.20948	0.00838	0.00815	0.01245	0.0208											
32	-2.14494	0.00888	0.00895	0.01189	0.0198											
34	-2.08432	0.00910	0.00929	0.01137	0.0190											
36	-2.02716	0.00915	0.00943	0.01088	0.0181											
38	-1.97358	0.00917	0.00949	0.01047	0.0174											
40	-1.92180	0.00916	0.00956	0.01014	0.0169											
42	-1.87201	0.00925	0.00964	0.00986	0.0165											
44	-1.82549	0.00930	0.00980	0.00960	0.0160											
46	-1.78204	0.00936	0.00989	0.00958	0.0156											
48	-1.73949	0.00945	0.00999	0.00959	0.0153											
50	-1.69865	0.00950	0.01001	0.00962	0.0150											
52	-1.65943	0.00956	0.01013	0.00976	0.0148											
54	-1.62189	0.00961	0.01021	0.00983	0.0146											
56	-1.58532	0.00967	0.01031	0.00982	0.0144											
58	-1.54921	0.00973	0.01042	0.00981	0.0142											
60	-1.51333	0.00980	0.01050	0.00980	0.0140											
62	-1.47829	0.00985	0.01055	0.00981	0.0138											
64	-1.44321	0.00991	0.01061	0.00982	0.0136											
66	-1.40828	0.00996	0.01066	0.00983	0.0134											
68	-1.37349	0.00999	0.01071	0.00984	0.0132											
70	-1.33884	0.01001	0.01076	0.00985	0.0130											
72	-1.30431	0.01002	0.01081	0.00986	0.0128											
74	-1.26989	0.01003	0.01086	0.00987	0.0127											
76	-1.23568	0.01004	0.01091	0.00988	0.0125											
78	-1.20167	0.01005	0.01096	0.00989	0.0124											
80	-1.16786	0.01006	0.01101	0.00990	0.0123											
82	-1.13424	0.01007	0.01106	0.00991	0.0122											
84	-1.10081	0.01008	0.01111	0.00992	0.0121											
86	-1.06757	0.01009	0.01116	0.00993	0.0120											
88	-1.03452	0.01010	0.01121	0.00994	0.0119											
90	-1.00166	0.01011	0.01126	0.00995	0.0118											
92	-0.96898	0.01012	0.01131	0.00996	0.0117											
94	-0.93648	0.01013	0.01136	0.00997	0.0116											
96	-0.90415	0.01014	0.01141	0.00998	0.0115											
98	-0.87198	0.01015	0.01146	0.00999	0.0114											
100	-0.84000	0.01016	0.01151	0.00999	0.0113											
102	-0.80819	0.01017	0.01156	0.01000	0.0112											
104	-0.77654	0.01018	0.01161	0.01001	0.0111											
106	-0.74504	0.01019	0.01166	0.01002	0.0110											
108	-0.71369	0.01020	0.01171	0.01003	0.0109											
110	-0.68248	0.01021	0.01176	0.01004	0.0108											
112	-0.65141	0.01022	0.01181	0.01005	0.0107											
114	-0.62048	0.01023	0.01186	0.01006	0.0106											
116	-0.58969	0.01024	0.01191	0.01007	0.0105											
118	-0.55904	0.01025	0.01196	0.01008	0.0104											
120	-0.52852	0.01026	0.01201	0.01009	0.0103											
122	-0.49813	0.01027	0.01206	0.01010	0.0102											
124	-0.46787	0.01028	0.01211	0.01011	0.0101											
126	-0.43774	0.01029	0.01216	0.01012	0.0100											
128	-0.40774	0.01030	0.01221	0.01013	0.0099											
130	-0.37786	0.01031	0.01226	0.01014	0.0098											
132	-0.34809	0.01032	0.01231	0.01015	0.0097											
134	-0.31844	0.01033	0.01236	0.01016	0.0096											
136	-0.28890	0.01034	0.01241	0.01017	0.0095											
138	-0.25947	0.01035	0.01246	0.01018	0.0094											
140	-0.23015	0.01036	0.01251	0.01019	0.0093											
142	-0.20094	0.01037	0.01256	0.01020	0.0092											
144	-0.17184	0.01038	0.01261	0.01021	0.0091											
146	-0.14284	0.01039	0.01266	0.01022	0.0090											
148	-0.11394	0.01040	0.01271	0.01023	0.0089											
150	-0.08514	0.01041	0.01276	0.01024	0.0088											
152	-0.05644	0.01042	0.01281	0.01025	0.0087											
154	-0.02784	0.01043	0.01286	0.01026	0.0086											
156	0.00076	0.01044	0.01291	0.01027	0.0085											
158	0.02936	0.01045	0.01296	0.01028	0.0084											
160	0.05806	0.01046	0.01301	0.01029	0.0083											
162	0.08686	0.01047	0.01306	0.01030	0.0082											
164	0.11576	0.01048	0.01311	0.01031	0.0081											
166	0.14476	0.01049	0.01316	0.01032	0.0080											
168	0.17386	0.01050	0.01321	0.01033	0.0079											
170	0.20306	0.01051	0.01326	0.01034	0.0078											
172	0.23236	0.01052	0.01331	0.01035	0.0077											
174	0.26176	0.01053	0.01336	0.01036	0.0076											
176	0.29126	0.01054	0.01341	0.01037	0.0075											
178	0.32086	0.01055	0.01346	0.01038	0.0074											
180	0.35056	0.01056	0.01351	0.01039	0.0073											
182	0.38036	0.01057	0.01356	0.01040	0.0072											
184	0.41026	0.01058	0.01361	0.01041	0.0071											
186	0.44026	0.01059	0.01366	0.01042	0.0070											
188	0.47036	0.01060	0.01371	0.01043	0.0069											
190	0.50056	0.01061	0.01376	0.01044	0.0068											
192	0.53086	0.01062	0.01381	0.01045	0.0067											
194	0.56126	0.01063	0.01386	0.01046	0.0066											
196	0.59176	0.01064	0.01391	0.01047	0.0065											
198	0.62236	0.01065	0.01396	0.01048	0.0064											
200	0.65306	0.01066	0.01401	0.01049	0.0063											



TABLE 22. Entropy differences divided by  $R$ , for normal  $H_2$ —Continued

Temperature	$\frac{S^{\circ}(T_2) - S^{\circ}(T_1)}{R}$	$\frac{S^{\circ} - S}{R}$														
		220	240	260	280	300	320	340	360	380	400	420	440	460	480	500
16																
18																
20																
22																
24																
26																
28																
30																
32																
34	-2.0649	0.391	0.424	0.457	0.486	0.509	0.531	0.551	0.568	0.583	0.598	0.604	0.625	0.633	0.646	0.656
36	-2.0272	0.370	0.408	0.441	0.470	0.494	0.515	0.535	0.552	0.568	0.582	0.592	0.612	0.622	0.632	0.642
38	-1.9731	0.364	0.395	0.427	0.458	0.480	0.500	0.519	0.535	0.551	0.564	0.574	0.592	0.602	0.612	0.622
40	-1.9218	0.365	0.386	0.417	0.448	0.478	0.509	0.539	0.569	0.601	0.632	0.664	0.698	0.728	0.752	0.778
42	-1.8750	0.348	0.379	0.409	0.439	0.470	0.501	0.531	0.563	0.594	0.625	0.658	0.691	0.721	0.753	0.782
44	-1.8265	0.343	0.374	0.404	0.434	0.465	0.495	0.526	0.557	0.589	0.622	0.655	0.688	0.721	0.755	0.789
46	-1.7820	0.338	0.368	0.398	0.428	0.458	0.488	0.518	0.548	0.578	0.608	0.640	0.672	0.705	0.739	0.784
48	-1.7305	0.333	0.363	0.393	0.423	0.453	0.483	0.513	0.543	0.573	0.603	0.633	0.663	0.693	0.723	0.771
50	-1.6837	0.328	0.358	0.388	0.417	0.447	0.478	0.508	0.538	0.571	0.603	0.633	0.663	0.693	0.726	0.769
52	-1.6394	0.325	0.354	0.383	0.413	0.443	0.472	0.502	0.531	0.561	0.590	0.621	0.651	0.681	0.714	0.762
54	-1.6217	0.320	0.350	0.379	0.409	0.438	0.467	0.497	0.526	0.556	0.585	0.615	0.645	0.675	0.708	0.754
56	-1.5853	0.317	0.346	0.375	0.405	0.434	0.464	0.494	0.523	0.553	0.582	0.611	0.641	0.671	0.704	0.749
58	-1.5602	0.314	0.343	0.373	0.402	0.432	0.462	0.492	0.521	0.551	0.580	0.610	0.640	0.670	0.703	0.749
60	-1.5183	0.312	0.341	0.371	0.401	0.431	0.461	0.491	0.520	0.550	0.580	0.610	0.640	0.670	0.703	0.751
62	-1.4833	0.305	0.334	0.363	0.393	0.423	0.453	0.483	0.512	0.542	0.571	0.601	0.631	0.661	0.694	0.749
70	-1.3622	0.298	0.326	0.354	0.382	0.410	0.438	0.466	0.494	0.522	0.550	0.578	0.606	0.634	0.662	0.709
76	-1.2672	0.291	0.319	0.346	0.373	0.400	0.428	0.455	0.482	0.509	0.536	0.563	0.590	0.617	0.644	0.727
80	-1.2298	0.286	0.314	0.342	0.370	0.397	0.425	0.452	0.479	0.506	0.533	0.560	0.587	0.614	0.641	0.714
85	-1.1650	0.281	0.308	0.335	0.364	0.392	0.421	0.450	0.478	0.506	0.534	0.562	0.590	0.618	0.646	0.700
90	-1.1109	0.275	0.304	0.332	0.359	0.387	0.415	0.443	0.471	0.500	0.528	0.556	0.584	0.612	0.640	0.691
95	-1.0628	0.274	0.301	0.328	0.355	0.383	0.411	0.440	0.468	0.495	0.523	0.551	0.579	0.607	0.635	0.684
100	-1.0055	0.270	0.297	0.324	0.351	0.379	0.407	0.435	0.463	0.491	0.519	0.547	0.575	0.603	0.631	0.677
105	-0.9507	0.267	0.294	0.320	0.347	0.375	0.402	0.430	0.458	0.485	0.513	0.541	0.569	0.597	0.625	0.670
110	-0.9102	0.264	0.290	0.317	0.344	0.371	0.398	0.425	0.452	0.479	0.506	0.533	0.560	0.587	0.614	0.658
115	-0.8657	0.262	0.287	0.313	0.340	0.367	0.394	0.421	0.448	0.475	0.502	0.529	0.556	0.583	0.610	0.653
120	-0.8252	0.259	0.285	0.311	0.337	0.364	0.390	0.418	0.445	0.473	0.501	0.528	0.556	0.583	0.610	0.649
125	-0.7824	0.258	0.284	0.309	0.335	0.361	0.388	0.415	0.442	0.470	0.498	0.525	0.552	0.580	0.608	0.644
130	-0.7431	0.257	0.282	0.307	0.333	0.359	0.385	0.412	0.438	0.465	0.491	0.518	0.545	0.572	0.600	0.640
135	-0.7044	0.255	0.280	0.305	0.331	0.357	0.383	0.409	0.436	0.463	0.490	0.517	0.544	0.571	0.600	0.634
140	-0.6690	0.253	0.278	0.303	0.329	0.354	0.380	0.407	0.433	0.460	0.487	0.514	0.541	0.568	0.595	0.630
145	-0.6359	0.252	0.277	0.301	0.327	0.352	0.378	0.404	0.431	0.457	0.483	0.510	0.537	0.564	0.591	0.626
150	-0.6000	0.251	0.275	0.300	0.325	0.351	0.376	0.402	0.428	0.454	0.480	0.506	0.532	0.558	0.584	0.622



TABLE 23. Enthalpy of ideal gas minus enthalpy of real gas at the same  $T$  and  $p$ , divided by  $RT$ , for normal  $H_2$

Temperature °K	$\frac{H^0 - H}{RT}$														
	$p=1$ Atmosat	2	3	0	10	20	40	60	80	100	120	140	160	180	200
16	0.02133	0.04381	0.06508	0.11144											
18	0.01899	0.03725	0.05393	0.08456											
20	0.01814	0.03226	0.04335	0.06456	0.1004										
22	0.01620	0.02839	0.03853	0.05469	0.0811										
24	0.01423	0.02463	0.03283	0.04761	0.0704	0.2494									
26	0.01232	0.02090	0.02839	0.04185	0.0626	0.2377	0.4430								
28	0.01023	0.01616	0.02183	0.03481	0.0517	0.2323	0.4694	0.591							
30	0.00831	0.01180	0.01746	0.02584	0.0397	0.1830	0.3657	0.535	0.708	0.872					
32	0.00651	0.00701	0.01040	0.01669	0.0246	0.051	0.1318	0.21	0.344	0.497	0.643	1.085	1.222	1.355	
34	0.00481	0.00516	0.00737	0.01096	0.0177	0.0281	0.043	0.071	0.103	0.141	0.185	0.232	0.281	0.331	1.361
36	0.00319	0.00346	0.00493	0.00714	0.0110	0.016	0.024	0.036	0.051	0.068	0.086	0.106	0.128	0.153	1.253
38	0.00165	0.00179	0.00246	0.00376	0.0051	0.007	0.010	0.014	0.019	0.025	0.032	0.040	0.049	0.059	1.180
40	0.00017	0.00024	0.00032	0.00044	0.00059	0.00082	0.0011	0.0015	0.0020	0.0026	0.0034	0.0043	0.0053	0.0064	1.078
42	0.00076	0.00101	0.00137	0.00184	0.00252	0.00345	0.0045	0.0058	0.0074	0.0092	0.0112	0.0134	0.0159	0.0188	1.006
44	0.00388	0.00517	0.00673	0.00865	0.0109	0.0135	0.0164	0.0195	0.0229	0.0265	0.0303	0.0343	0.0385	0.0429	0.942
46	0.00504	0.00666	0.00853	0.01076	0.0133	0.0162	0.0193	0.0226	0.0261	0.0298	0.0337	0.0378	0.0421	0.0465	0.883
48	0.00473	0.00646	0.00840	0.01072	0.0133	0.0161	0.0191	0.0222	0.0255	0.0290	0.0326	0.0363	0.0401	0.0440	0.829
50	0.00445	0.00628	0.00829	0.01065	0.0132	0.0159	0.0188	0.0218	0.0249	0.0281	0.0313	0.0345	0.0378	0.0411	0.779
52	0.00419	0.00602	0.00800	0.01036	0.0127	0.0151	0.0175	0.0200	0.0225	0.0250	0.0274	0.0298	0.0321	0.0344	0.734
54	0.00396	0.00578	0.00773	0.00991	0.0118	0.0139	0.0160	0.0181	0.0202	0.0222	0.0242	0.0262	0.0281	0.0300	0.692
56	0.00376	0.00556	0.00748	0.00983	0.0114	0.0133	0.0152	0.0171	0.0189	0.0207	0.0224	0.0241	0.0258	0.0274	0.654
58	0.00356	0.00534	0.00722	0.00962	0.0109	0.0126	0.0142	0.0157	0.0171	0.0184	0.0197	0.0209	0.0221	0.0232	0.616
60	0.00337	0.00514	0.00699	0.00921	0.0102	0.0116	0.0129	0.0141	0.0151	0.0161	0.0170	0.0178	0.0186	0.0193	0.586
65	0.02946	0.05062	0.07087	0.11771	0.20443	0.3284	0.4813	0.656	0.852	1.068	1.294	1.529	1.774	2.028	2.291
70	0.02611	0.04522	0.06322	0.10542	0.20085	0.3151	0.4503	0.6033	0.7743	0.953	1.139	1.331	1.528	1.731	1.941
75	0.02231	0.03911	0.05492	0.09382	0.17297	0.2704	0.3861	0.5103	0.6433	0.7843	0.933	1.089	1.251	1.418	1.591
80	0.02085	0.03411	0.04819	0.08239	0.15643	0.2464	0.3513	0.4703	0.5933	0.7203	0.8513	0.9863	1.1253	1.2683	1.4153
86	0.0184	0.03018	0.04151	0.07161	0.13628	0.2162	0.3113	0.4203	0.5333	0.6503	0.7713	0.8963	1.0253	1.1583	1.2953
90	0.0168	0.02739	0.03739	0.06487	0.12539	0.2004	0.2864	0.3834	0.4904	0.5974	0.7044	0.8114	0.9184	1.0254	1.1324
95	0.0148	0.02401	0.03301	0.05644	0.11009	0.1804	0.2564	0.3434	0.4404	0.5374	0.6344	0.7314	0.8284	0.9254	1.0224
100	0.0132	0.02165	0.02965	0.04963	0.10116	0.1661	0.2361	0.3161	0.4031	0.4901	0.5771	0.6641	0.7511	0.8381	0.9251
105	0.0119	0.02028	0.02787	0.04512	0.09182	0.1518	0.2168	0.2868	0.3668	0.4468	0.5268	0.6068	0.6868	0.7668	0.8468
110	0.0107	0.01916	0.02632	0.04142	0.08065	0.1356	0.1956	0.2606	0.3256	0.3906	0.4556	0.5206	0.5856	0.6506	0.7156
115	0.0097	0.01794	0.02469	0.03879	0.07490	0.1249	0.1799	0.2399	0.3049	0.3699	0.4349	0.4999	0.5649	0.6299	0.6949
120	0.00898	0.01675	0.02293	0.03593	0.06957	0.1171	0.1641	0.2161	0.2711	0.3261	0.3811	0.4361	0.4911	0.5461	0.6011
125	0.00839	0.01581	0.02148	0.03348	0.06473	0.1063	0.1473	0.1933	0.2413	0.2893	0.3373	0.3853	0.4333	0.4813	0.5293
130	0.00771	0.01453	0.02013	0.03113	0.05904	0.1034	0.1394	0.1814	0.2234	0.2654	0.3074	0.3494	0.3914	0.4334	0.4754
135	0.00704	0.01316	0.01863	0.02863	0.05452	0.0945	0.1255	0.1615	0.1965	0.2315	0.2665	0.3015	0.3365	0.3715	0.4065
140	0.00644	0.01206	0.01723	0.02623	0.04942	0.0844	0.1194	0.1544	0.1894	0.2244	0.2594	0.2944	0.3294	0.3644	0.3994
145	0.00587	0.01115	0.01593	0.02413	0.04512	0.0741	0.1031	0.1321	0.1611	0.1901	0.2191	0.2481	0.2771	0.3061	0.3351
150	0.00531	0.01002	0.01439	0.02159	0.03958	0.0635	0.0875	0.1115	0.1355	0.1595	0.1835	0.2075	0.2315	0.2555	0.2795

155	.....	000103	000770	01144	0204	0254	028	035	036	035
160	.....	000104	000771	0120	0174	0214	021	028	027	025
165	.....	000105	000772	0125	0179	0219	021	028	027	025
170	.....	000106	000773	0130	0184	0224	021	028	027	025
175	.....	000107	000774	0135	0189	0229	021	028	027	025
180	.....	000108	000775	0140	0194	0234	021	028	027	025
185	.....	000109	000776	0145	0199	0239	021	028	027	025
190	.....	000110	000777	0150	0204	0244	021	028	027	025
195	.....	000111	000778	0155	0209	0249	021	028	027	025
200	.....	000112	000779	0160	0214	0254	021	028	027	025
205	.....	000113	000780	0165	0219	0259	021	028	027	025
210	.....	000114	000781	0170	0224	0264	021	028	027	025
215	.....	000115	000782	0175	0229	0269	021	028	027	025
220	.....	000116	000783	0180	0234	0274	021	028	027	025
225	.....	000117	000784	0185	0239	0279	021	028	027	025
230	.....	000118	000785	0190	0244	0284	021	028	027	025
235	.....	000119	000786	0195	0249	0289	021	028	027	025
240	.....	000120	000787	0200	0254	0294	021	028	027	025
245	.....	000121	000788	0205	0259	0299	021	028	027	025
250	.....	000122	000789	0210	0264	0304	021	028	027	025
255	.....	000123	000790	0215	0269	0309	021	028	027	025
260	.....	000124	000791	0220	0274	0314	021	028	027	025
265	.....	000125	000792	0225	0279	0319	021	028	027	025
270	.....	000126	000793	0230	0284	0324	021	028	027	025
275	.....	000127	000794	0235	0289	0329	021	028	027	025
280	.....	000128	000795	0240	0294	0334	021	028	027	025
285	.....	000129	000796	0245	0299	0339	021	028	027	025
290	.....	000130	000797	0250	0304	0344	021	028	027	025
295	.....	000131	000798	0255	0309	0349	021	028	027	025
300	.....	000132	000799	0260	0314	0354	021	028	027	025
305	.....	000133	000800	0265	0319	0359	021	028	027	025
310	.....	000134	000801	0270	0324	0364	021	028	027	025
315	.....	000135	000802	0275	0329	0369	021	028	027	025
320	.....	000136	000803	0280	0334	0374	021	028	027	025
325	.....	000137	000804	0285	0339	0379	021	028	027	025
330	.....	000138	000805	0290	0344	0384	021	028	027	025
335	.....	000139	000806	0295	0349	0389	021	028	027	025
340	.....	000140	000807	0300	0354	0394	021	028	027	025
345	.....	000141	000808	0305	0359	0399	021	028	027	025
350	.....	000142	000809	0310	0364	0404	021	028	027	025
355	.....	000143	000810	0315	0369	0409	021	028	027	025
360	.....	000144	000811	0320	0374	0414	021	028	027	025
365	.....	000145	000812	0325	0379	0419	021	028	027	025
370	.....	000146	000813	0330	0384	0424	021	028	027	025
375	.....	000147	000814	0335	0389	0429	021	028	027	025
380	.....	000148	000815	0340	0394	0434	021	028	027	025
385	.....	000149	000816	0345	0399	0439	021	028	027	025
390	.....	000150	000817	0350	0404	0444	021	028	027	025
395	.....	000151	000818	0355	0409	0449	021	028	027	025
400	.....	000152	000819	0360	0414	0454	021	028	027	025
405	.....	000153	000820	0365	0419	0459	021	028	027	025
410	.....	000154	000821	0370	0424	0464	021	028	027	025
415	.....	000155	000822	0375	0429	0469	021	028	027	025
420	.....	000156	000823	0380	0434	0474	021	028	027	025
425	.....	000157	000824	0385	0439	0479	021	028	027	025
430	.....	000158	000825	0390	0444	0484	021	028	027	025
435	.....	000159	000826	0395	0449	0489	021	028	027	025
440	.....	000160	000827	0400	0454	0494	021	028	027	025
445	.....	000161	000828	0405	0459	0499	021	028	027	025
450	.....	000162	000829	0410	0464	0504	021	028	027	025
455	.....	000163	000830	0415	0469	0509	021	028	027	025
460	.....	000164	000831	0420	0474	0514	021	028	027	025
465	.....	000165	000832	0425	0479	0519	021	028	027	025
470	.....	000166	000833	0430	0484	0524	021	028	027	025
475	.....	000167	000834	0435	0489	0529	021	028	027	025
480	.....	000168	000835	0440	0494	0534	021	028	027	025
485	.....	000169	000836	0445	0499	0539	021	028	027	025
490	.....	000170	000837	0450	0504	0544	021	028	027	025
495	.....	000171	000838	0455	0509	0549	021	028	027	025
500	.....	000172	000839	0460	0514	0554	021	028	027	025
505	.....	000173	000840	0465	0519	0559	021	028	027	025
510	.....	000174	000841	0470	0524	0564	021	028	027	025
515	.....	000175	000842	0475	0529	0569	021	028	027	025
520	.....	000176	000843	0480	0534	0574	021	028	027	025
525	.....	000177	000844	0485	0539	0579	021	028	027	025
530	.....	000178	000845	0490	0544	0584	021	028	027	025
535	.....	000179	000846	0495	0549	0589	021	028	027	025
540	.....	000180	000847	0500	0554	0594	021	028	027	025
545	.....	000181	000848	0505	0559	0599	021	028	027	025
550	.....	000182	000849	0510	0564	0604	021	028	027	025
555	.....	000183	000850	0515	0569	0609	021	028	027	025
560	.....	000184	000851	0520	0574	0614	021	028	027	025
565	.....	000185	000852	0525	0579	0619	021	028	027	025
570	.....	000186	000853	0530	0584	0624	021	028	027	025
575	.....	000187	000854	0535	0589	0629	021	028	027	025
580	.....	000188	000855	0540	0594	0634	021	028	027	025
585	.....	000189	000856	0545	0599	0639	021	028	027	025
590	.....	000190	000857	0550	0604	0644	021	028	027	025
595	.....	000191	000858	0555	0609	0649	021	028	027	025
600	.....	000192	000859	0560	0614	0654	021	028	027	025
605	.....	000193	000860	0565	0619	0659	021	028	027	025
610	.....	000194	000861	0570	0624	0664	021	028	027	025
615	.....	000195	000862	0575	0629	0669	021	028	027	025
620	.....	000196	000863	0580	0634	0674	021	028	027	025
625	.....	000197	000864	0585	0639	0679	021	028	027	025
630	.....	000198	000865	0590	0644	0684	021	028	027	025
635	.....	000199	000866	0595	0649	0689	021	028	027	025
640	.....	000200	000867	0600	0654	0694	021	028	027	025
645	.....	000201	000868	0605	0659	0699	021	028	027	025
650	.....	000202	000869	0610	0664	0704	021	028	027	025
655	.....	000203	000870	0615	0669	0709	021	028	027	025
660	.....	000204	000871	0620	0674	0714	021	028	027	025
665	.....	000205	000872	0625	0679	0719	021	028	027	025
670	.....	000206	000873	0630	0684	0724	021	028	027	025
675	.....	000207	000874	0635	0689	0729	021	028	027	025
680	.....	000208	000875	0640	0694	0734	021	028	027	025
685	.....	000209	000876	0645	0699	0739	021	028	027	025
690	.....	000210	000877	0650	0704	0744	021	028	027	025
695	.....	000211	000878	0655	0709	0749	021	028	027	025
700	.....	000212	000879	0660	0714	0754	021	028	027	025
705	.....	000213	000880	0665	0719	0759	021	028	027	025
710	.....	000214	000881	0670	0724	0764	021	028	027	025
715	.....	000215	000882	0675	0729	0769	021	028	027	025
720	.....	000216	000883	0680	0734	0774	021	028	027	025
725	.....	000217	000884	0685	0739	0779	021	028	027	025
730	.....	000218	000885	0690	0744	0784	021	028	027	025
735	.....	000219	000886	0695	0749	0789	021	028	027	025
740	.....	000220	000887	0700	0754	0794	021	028	027	025
745	.....	000221	000888	0705	0759	0799	021	028	027	025
750	.....	000222	000889	0710	0764	0804	021	028	027	025
755	.....	000223	000890	0715	0769	0809	021	028	027	025
760	.....	000224	000891	0720	0774	0814	021	028	027	025
765	.....	000225	000892	0725	0779	0819	021	028	027	025
770	.....	000226	000893	0730						

TABLE 28. Enthalpy of ideal gas minus enthalpy of real gas at the same T and p, divided by RT, for normal H<sub>2</sub>—Continued

Temperature °K	$\frac{H^0 - H}{RT}$														
	p=220	240	260	280	300	320	340	360	380	400	420	440	460	480	500
16															
18															
20															
22															
24															
26															
28															
30															
32															
34	1.475	1.562	1.662	1.753	1.850	1.953	2.071	2.184	2.284	2.310	2.382	2.453	2.521	2.586	2.647
36	1.369	1.461	1.559	1.653	1.743	1.830	1.912	1.991	2.065	2.136	2.204	2.269	2.331	2.390	2.446
38	1.267	1.361	1.449	1.534	1.612	1.683	1.770	1.844	1.914	1.981	2.044	2.104	2.161	2.215	2.265
40	1.168	1.266	1.349	1.421	1.489	1.554	1.646	1.715	1.781	1.843	1.902	1.958	2.010	2.059	2.104
42	1.069	1.171	1.250	1.325	1.398	1.467	1.634	1.699	1.661	1.719	1.774	1.826	1.874	1.919	1.970
44	1.021	1.097	1.170	1.241	1.308	1.373	1.435	1.496	1.553	1.605	1.660	1.707	1.752	1.792	1.838
46	0.957	1.038	1.097	1.153	1.226	1.286	1.344	1.400	1.453	1.504	1.561	1.607	1.657	1.707	1.757
48	0.898	0.965	1.029	1.091	1.150	1.206	1.260	1.311	1.361	1.407	1.451	1.492	1.530	1.564	1.594
50	0.844	0.907	0.968	1.025	1.080	1.131	1.183	1.231	1.275	1.319	1.359	1.396	1.430	1.461	1.489
52	0.796	0.855	0.911	0.965	1.017	1.066	1.112	1.156	1.198	1.237	1.273	1.307	1.338	1.365	1.391
54	0.750	0.806	0.860	0.910	0.958	1.003	1.046	1.087	1.125	1.161	1.195	1.225	1.253	1.279	1.301
56	0.708	0.761	0.811	0.859	0.904	0.947	0.987	1.025	1.060	1.093	1.123	1.151	1.177	1.200	1.219
58	0.670	0.720	0.767	0.812	0.855	0.896	0.934	0.969	1.002	1.033	1.061	1.087	1.110	1.130	1.148
60	0.635	0.682	0.727	0.770	0.811	0.849	0.886	0.919	0.950	0.979	1.005	1.029	1.049	1.069	1.085
62	0.605	0.650	0.694	0.736	0.776	0.813	0.848	0.881	0.912	0.940	0.967	0.992	1.015	1.035	1.051
64	0.585	0.628	0.670	0.711	0.750	0.787	0.822	0.855	0.886	0.915	0.942	0.968	0.992	1.013	1.030
66	0.565	0.606	0.646	0.685	0.723	0.759	0.793	0.825	0.855	0.883	0.909	0.934	0.958	0.978	0.994
68	0.547	0.587	0.626	0.663	0.699	0.734	0.767	0.798	0.828	0.856	0.882	0.908	0.932	0.952	0.968
70	0.531	0.570	0.608	0.644	0.679	0.713	0.745	0.776	0.806	0.834	0.860	0.886	0.910	0.929	0.944
72	0.517	0.555	0.592	0.627	0.661	0.694	0.726	0.757	0.787	0.815	0.841	0.867	0.891	0.910	0.925
74	0.505	0.541	0.577	0.611	0.644	0.676	0.707	0.737	0.766	0.793	0.819	0.845	0.869	0.887	0.900
76	0.495	0.529	0.564	0.597	0.629	0.660	0.690	0.719	0.747	0.773	0.799	0.825	0.850	0.867	0.880
78	0.487	0.519	0.553	0.585	0.616	0.646	0.675	0.703	0.730	0.756	0.781	0.807	0.832	0.849	0.861
80	0.481	0.511	0.544	0.575	0.605	0.634	0.662	0.689	0.715	0.740	0.765	0.790	0.815	0.831	0.843
82	0.476	0.505	0.537	0.567	0.596	0.624	0.651	0.677	0.702	0.727	0.751	0.776	0.799	0.815	0.826
84	0.472	0.500	0.531	0.560	0.588	0.615	0.641	0.666	0.690	0.714	0.738	0.762	0.785	0.800	0.810
86	0.469	0.496	0.526	0.554	0.581	0.607	0.632	0.656	0.679	0.702	0.725	0.748	0.770	0.784	0.793
88	0.467	0.493	0.522	0.549	0.575	0.600	0.624	0.647	0.669	0.691	0.713	0.735	0.756	0.769	0.776
90	0.466	0.491	0.519	0.545	0.570	0.594	0.617	0.639	0.660	0.681	0.701	0.721	0.741	0.753	0.759
92	0.465	0.489	0.516	0.541	0.565	0.588	0.610	0.631	0.651	0.671	0.690	0.709	0.728	0.739	0.744
94	0.465	0.488	0.514	0.538	0.561	0.583	0.604	0.624	0.643	0.662	0.680	0.698	0.716	0.726	0.730
96	0.464	0.487	0.512	0.535	0.557	0.578	0.598	0.617	0.635	0.653	0.670	0.687	0.704	0.713	0.716
98	0.464	0.486	0.510	0.532	0.554	0.575	0.594	0.612	0.629	0.646	0.662	0.678	0.694	0.702	0.705
100	0.464	0.485	0.508	0.529	0.549	0.568	0.586	0.603	0.619	0.635	0.650	0.665	0.680	0.687	0.690
102	0.464	0.484	0.506	0.526	0.545	0.563	0.580	0.596	0.611	0.626	0.640	0.654	0.668	0.674	0.676
104	0.464	0.483	0.504	0.523	0.541	0.558	0.574	0.589	0.603	0.617	0.630	0.643	0.656	0.661	0.662
106	0.464	0.482	0.502	0.520	0.537	0.553	0.568	0.582	0.595	0.608	0.620	0.632	0.644	0.648	0.649
108	0.464	0.481	0.500	0.517	0.533	0.548	0.562	0.575	0.587	0.599	0.610	0.621	0.632	0.635	0.635
110	0.464	0.480	0.498	0.514	0.529	0.543	0.556	0.568	0.579	0.589	0.599	0.608	0.617	0.619	0.619
112	0.464	0.479	0.496	0.511	0.525	0.538	0.550	0.561	0.571	0.580	0.589	0.597	0.605	0.606	0.606
114	0.464	0.478	0.494	0.508	0.521	0.533	0.544	0.554	0.563	0.571	0.579	0.586	0.593	0.594	0.594
116	0.464	0.477	0.492	0.505	0.517	0.528	0.538	0.547	0.555	0.562	0.569	0.575	0.581	0.582	0.582
118	0.464	0.476	0.490	0.502	0.513	0.523	0.532	0.540	0.547	0.554	0.560	0.566	0.571	0.572	0.572
120	0.464	0.475	0.488	0.499	0.509	0.518	0.526	0.533	0.539	0.545	0.550	0.555	0.560	0.561	0.561
122	0.464	0.474	0.486	0.496	0.505	0.513	0.520	0.526	0.531	0.536	0.540	0.544	0.548	0.549	0.549
124	0.464	0.473	0.484	0.493	0.501	0.508	0.514	0.519	0.523	0.527	0.530	0.533	0.536	0.537	0.537
126	0.464	0.472	0.482	0.490	0.497	0.503	0.508	0.512	0.515	0.518	0.520	0.522	0.524	0.525	0.525
128	0.464	0.471	0.480	0.487	0.493	0.498	0.502	0.505	0.508	0.510	0.512	0.514	0.515	0.516	0.516
130	0.464	0.470	0.478	0.484	0.489	0.493	0.496	0.498	0.500	0.501	0.502	0.503	0.504	0.504	0.504
132	0.464	0.469	0.476	0.481	0.485	0.488	0.491	0.493	0.494	0.495	0.495	0.496	0.496	0.496	0.496
134	0.464	0.468	0.474	0.478	0.481	0.483	0.485	0.486	0.487	0.487	0.487	0.487	0.487	0.487	0.487
136	0.464	0.467	0.472	0.475	0.477	0.478	0.479	0.479	0.479	0.479	0.479	0.479	0.479	0.479	0.479
138	0.464	0.466	0.470	0.472	0.473	0.474	0.474	0.474	0.474	0.474	0.474	0.474	0.474	0.474	0.474
140	0.464	0.465	0.468	0.469	0.470	0.470	0.470	0.470	0.470	0.470	0.470	0.470	0.470	0.470	0.470
142	0.464	0.464	0.466	0.466	0.466	0.466	0.466	0.466	0.466	0.466	0.466	0.466	0.466	0.466	0.466
144	0.464	0.464	0.465	0.465	0.465	0.465	0.465	0.465	0.465	0.465	0.465	0.465	0.465	0.465	0.465
146	0.464	0.464	0.464	0.464	0.464	0.464	0.464	0.464	0.464	0.464	0.464	0.464	0.464	0.464	0.464
148	0.464	0.464	0.464	0.464	0.464	0.464	0.464	0.464	0.464	0.464	0.464	0.464	0.464	0.464	0.464
150	0.464	0.464	0.464	0.464	0.464	0.464	0.464	0.464	0.464	0.464	0.464	0.464	0.464	0.464	0.464



166	.....	.032	.029	.011	.002	-.009	-.040	-.083	-.048	-.066	-.064	-.105	-.128	-.154
167	.....	.022	.017	.005	-.013	-.024	-.038	-.061	-.067	-.084	-.104	-.126	-.150	-.176
168	.....	.011	.006	-.003	-.028	-.040	-.053	-.068	-.080	-.103	-.124	-.146	-.171	-.197
170	.....	.001	-.005	-.021	-.031	-.042	-.050	-.065	-.083	-.103	-.123	-.143	-.169	-.198
180	.....	-.017	-.035	-.044	-.063	-.092	-.098	-.113	-.134	-.154	-.178	-.200	-.225	-.253
180	.....	-.023	-.042	-.052	-.076	-.105	-.122	-.140	-.161	-.181	-.204	-.228	-.255	-.285
200	.....	-.046	-.056	-.063	-.083	-.125	-.142	-.161	-.181	-.203	-.227	-.262	-.279	-.309
210	.....	-.057	-.068	-.078	-.098	-.141	-.160	-.179	-.200	-.223	-.247	-.282	-.290	-.320
220	.....	-.068	-.080	-.107	-.122	-.166	-.176	-.196	-.218	-.241	-.268	-.292	-.320	-.350
230	.....	-.079	-.091	-.105	-.126	-.172	-.191	-.212	-.235	-.258	-.284	-.311	-.340	-.370
240	.....	-.088	-.101	-.118	-.132	-.185	-.206	-.227	-.250	-.275	-.301	-.328	-.356	-.388
250	.....	-.095	-.111	-.128	-.142	-.198	-.219	-.241	-.265	-.290	-.316	-.344	-.374	-.405
260	.....	-.104	-.119	-.131	-.151	-.209	-.230	-.253	-.277	-.303	-.330	-.358	-.388	-.420
270	.....	-.110	-.128	-.142	-.161	-.220	-.240	-.263	-.288	-.314	-.341	-.370	-.401	-.436
280	.....	-.116	-.135	-.149	-.169	-.230	-.250	-.273	-.298	-.325	-.353	-.382	-.414	-.450
290	.....	-.121	-.141	-.155	-.175	-.237	-.257	-.280	-.305	-.332	-.360	-.390	-.422	-.458
300	.....	-.127	-.147	-.161	-.181	-.243	-.263	-.286	-.311	-.338	-.366	-.396	-.428	-.464
310	.....	-.132	-.152	-.166	-.186	-.249	-.269	-.292	-.317	-.344	-.372	-.402	-.434	-.470
320	.....	-.137	-.157	-.171	-.191	-.254	-.274	-.297	-.322	-.349	-.377	-.407	-.439	-.475
330	.....	-.142	-.162	-.176	-.196	-.260	-.280	-.303	-.328	-.355	-.383	-.413	-.445	-.481
340	.....	-.147	-.167	-.181	-.201	-.265	-.285	-.308	-.333	-.360	-.388	-.418	-.450	-.486
350	.....	-.152	-.172	-.186	-.206	-.270	-.290	-.313	-.338	-.365	-.393	-.423	-.455	-.491
360	.....	-.157	-.177	-.191	-.211	-.275	-.295	-.318	-.343	-.370	-.398	-.428	-.460	-.496
370	.....	-.162	-.182	-.196	-.216	-.280	-.300	-.323	-.348	-.375	-.403	-.433	-.465	-.501
380	.....	-.167	-.187	-.201	-.221	-.285	-.305	-.328	-.353	-.380	-.408	-.438	-.470	-.506
390	.....	-.172	-.192	-.206	-.226	-.290	-.310	-.333	-.358	-.385	-.413	-.443	-.475	-.511
400	.....	-.177	-.197	-.211	-.231	-.295	-.315	-.338	-.363	-.390	-.418	-.448	-.480	-.516
410	.....	-.182	-.202	-.216	-.236	-.300	-.320	-.343	-.368	-.395	-.423	-.453	-.485	-.521
420	.....	-.187	-.207	-.221	-.241	-.305	-.325	-.348	-.373	-.400	-.428	-.458	-.490	-.526
430	.....	-.192	-.212	-.226	-.246	-.310	-.330	-.353	-.378	-.405	-.433	-.463	-.495	-.531
440	.....	-.197	-.217	-.231	-.251	-.315	-.335	-.358	-.383	-.410	-.438	-.468	-.500	-.536
450	.....	-.202	-.222	-.236	-.256	-.320	-.340	-.363	-.388	-.415	-.443	-.473	-.505	-.541
460	.....	-.207	-.227	-.241	-.261	-.325	-.345	-.368	-.393	-.420	-.448	-.478	-.510	-.546
470	.....	-.212	-.232	-.246	-.266	-.330	-.350	-.373	-.398	-.425	-.453	-.483	-.515	-.551
480	.....	-.217	-.237	-.251	-.271	-.335	-.355	-.378	-.403	-.430	-.458	-.488	-.520	-.556
490	.....	-.222	-.242	-.256	-.276	-.340	-.360	-.383	-.408	-.435	-.463	-.493	-.525	-.561
500	.....	-.227	-.247	-.261	-.281	-.345	-.365	-.388	-.413	-.440	-.468	-.498	-.530	-.566
510	.....	-.232	-.252	-.266	-.286	-.350	-.370	-.393	-.418	-.445	-.473	-.503	-.535	-.571
520	.....	-.237	-.257	-.271	-.291	-.355	-.375	-.398	-.423	-.450	-.478	-.508	-.540	-.576
530	.....	-.242	-.262	-.276	-.296	-.360	-.380	-.403	-.428	-.455	-.483	-.513	-.545	-.581
540	.....	-.247	-.267	-.281	-.301	-.365	-.385	-.408	-.433	-.460	-.488	-.518	-.550	-.586
550	.....	-.252	-.272	-.286	-.306	-.370	-.390	-.413	-.438	-.465	-.493	-.523	-.555	-.591
560	.....	-.257	-.277	-.291	-.311	-.375	-.395	-.418	-.443	-.470	-.498	-.528	-.560	-.596
570	.....	-.262	-.282	-.296	-.316	-.380	-.400	-.423	-.448	-.475	-.503	-.533	-.565	-.601
580	.....	-.267	-.287	-.301	-.321	-.385	-.405	-.428	-.453	-.480	-.508	-.538	-.570	-.606
590	.....	-.272	-.292	-.306	-.326	-.390	-.410	-.433	-.458	-.485	-.513	-.543	-.575	-.611
600	.....	-.277	-.297	-.311	-.331	-.395	-.415	-.438	-.463	-.490	-.518	-.548	-.580	-.616
610	.....	-.282	-.302	-.316	-.336	-.400	-.420	-.443	-.468	-.495	-.523	-.553	-.585	-.621
620	.....	-.287	-.307	-.321	-.341	-.405	-.425	-.448	-.473	-.500	-.528	-.558	-.590	-.626
630	.....	-.292	-.312	-.326	-.346	-.410	-.430	-.453	-.478	-.505	-.533	-.563	-.595	-.631
640	.....	-.297	-.317	-.331	-.351	-.415	-.435	-.458	-.483	-.510	-.538	-.568	-.600	-.636
650	.....	-.302	-.322	-.336	-.356	-.420	-.440	-.463	-.488	-.515	-.543	-.573	-.605	-.641
660	.....	-.307	-.327	-.341	-.361	-.425	-.445	-.468	-.493	-.520	-.548	-.578	-.610	-.646
670	.....	-.312	-.332	-.346	-.366	-.430	-.450	-.473	-.498	-.525	-.553	-.583	-.615	-.651
680	.....	-.317	-.337	-.351	-.371	-.435	-.455	-.478	-.503	-.530	-.558	-.588	-.620	-.656
690	.....	-.322	-.342	-.356	-.376	-.440	-.460	-.483	-.508	-.535	-.563	-.593	-.625	-.661
700	.....	-.327	-.347	-.361	-.381	-.445	-.465	-.488	-.513	-.540	-.568	-.598	-.630	-.666
710	.....	-.332	-.352	-.366	-.386	-.450	-.470	-.493	-.518	-.545	-.573	-.603	-.635	-.671
720	.....	-.337	-.357	-.371	-.391	-.455	-.475	-.498	-.523	-.550	-.578	-.608	-.640	-.676
730	.....	-.342	-.362	-.376	-.396	-.460	-.480	-.503	-.528	-.555	-.583	-.613	-.645	-.681
740	.....	-.347	-.367	-.381	-.401	-.465	-.485	-.508	-.533	-.560	-.588	-.618	-.650	-.686
750	.....	-.352	-.372	-.386	-.406	-.470	-.490	-.513	-.538	-.565	-.593	-.623	-.655	-.691
760	.....	-.357	-.377	-.391	-.411	-.475	-.495	-.518	-.543	-.570	-.598	-.628	-.660	-.696
770	.....	-.362	-.382	-.396	-.416	-.480	-.500	-.523	-.548	-.575	-.603	-.633	-.665	-.701
780	.....	-.367	-.387	-.401	-.421	-.485	-.505	-.528	-.553	-.580	-.608	-.638	-.670	-.706
790	.....	-.372	-.392	-.406	-.426	-.490	-.510	-.533	-.558	-.585	-.613	-.643	-.675	-.711
800	.....	-.377	-.397	-.411	-.431	-.495	-.515	-.538	-.563	-.590	-.618	-.648	-.680	-.716
810	.....	-.382	-.402	-.416	-.436	-.500	-.520	-.543	-.568	-.595	-.623	-.653	-.685	-.721
820	.....	-.387	-.407	-.421	-.441	-.505	-.525	-.548	-.573	-.600	-.628	-.658	-.690	-.726
830	.....	-.392	-.412	-.426	-.446	-.510	-.530	-.553	-.578	-.605	-.633	-.663	-.695	-.731
840	.....	-.397	-.417	-.431	-.451	-.515	-.535	-.558	-.583	-.610	-.638	-.668	-.700	-.736
850	.....	-.402	-.422	-.436	-.456	-.520	-.540	-.563	-.588	-.615	-.643	-.673	-.705	-.741
860	.....	-.407	-.427	-.441	-.461	-.525	-.545	-.568	-.593	-.620	-.648	-.678	-.710	-.746
870	.....	-.412	-.432	-.446	-.466	-.530	-.550	-.573	-.598	-.625	-.653	-.683	-.715	-.751
880	.....	-.417	-.437	-.451	-.471	-.535	-.555	-.578	-.603	-.630	-.658	-.688	-.720	-.756
890	.....	-.422	-.442	-.456	-.476	-.540	-.560	-.583	-.608	-.635	-.663	-.693	-.725	-.761
900	.....	-.427	-.447	-.461	-.481	-.545	-.565	-.588	-.613	-.640	-.668	-.698	-.730	-.766

Values of  $F/RT$ ,  $E/RT$ , and  $\ln(f/P)$  may be obtained rather simply from values of  $S/R$  and  $H/RT$  and the  $Z$ -table in accordance with the following equations:

$$F/RT = (H/RT) - (S/R) \quad (5.13)$$

$$\ln \frac{f}{P} = \frac{F_{p,T(\text{real})} - F_{p,T(\text{ideal})}}{RT} - \ln Z \quad (5.14)$$

$$E/RT = (H/RT) - Z \quad (5.15)$$

The value of  $[F_{p,T(\text{real})} - F_{p,T(\text{ideal})}]/RT$  may be obtained by subtracting  $(S^\circ - S)/R$ , given in table 22, from  $(H^\circ - H)/RT$ , given in table 23.

The calculation of the heat capacities of the real gas involves the evaluation of

$$\int_0^p [T^2(d^2Z/dT^2)_{p/\rho}] d\rho.$$

$$[C_{p(\text{real,ans})} - C_{p(\text{ideal})}]/R = T \left\{ \left( \frac{d}{d\rho} \left[ \frac{H^\circ - H}{RT} \right] \right)_p \left( \frac{dP}{dT} \right)_p \left/ \left( \frac{dP}{d\rho} \right)_T - \left( \frac{d}{dT} \left[ \frac{H^\circ - H}{RT} \right] \right)_p \right\} - \frac{H^\circ - H}{RT} \quad (5.17)$$

$$= -T \left( \frac{d}{dT} \left[ \frac{H^\circ - H}{RT} \right] \right)_p - \frac{H^\circ - H}{RT} + \left[ Z + T \left( \frac{dZ}{dT} \right)_p \right] \left[ T \left( \frac{dZ}{dT} \right)_p - \rho \left( \frac{dZ}{d\rho} \right)_T \right] \left/ \left[ Z + \rho \left( \frac{dZ}{d\rho} \right)_T \right] \right. \quad (5.17a)$$

The derivatives in eq 5.17 may be calculated from tables 14 and 23, using a method of tabular differentiation. Except for the first term, the derivatives in eq 5.17a are given in tables 15 and 17.

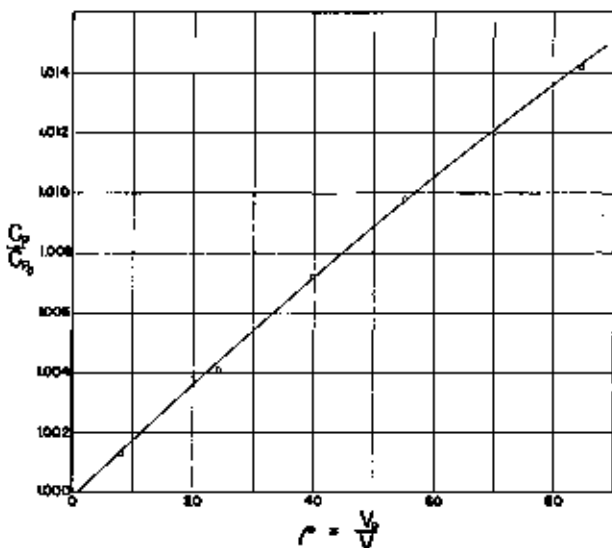


FIGURE 12. Effect of density on specific heat of  $H_2$  at  $50^\circ C$ .

Figure 12 shows the dependence of the specific heat at constant pressure for hydrogen at  $50^\circ C$  upon the Amagat density  $\rho$ . The curve represents the results of the evaluation of formula 5.8, using

This may be carried out using the  $(d^2Z/dT^2)_p$  table (table 16), and a method of tabular integration. Table 23 may be used to obtain  $\int_0^p [T(dZ/dT)_{p/\rho}] d\rho$ , since from eq 5.12 it follows that

$$\int_0^p [T(dZ/dT)_{p/\rho}] d\rho = \frac{H^\circ - H}{RT} \text{ (from table 23)} + (Z - 1). \quad (5.16)$$

In the temperature and density ranges where  $Z$  may be represented by an analytic expression,<sup>12</sup> these two integrals may be evaluated by using series expansions for  $Z$  and its derivatives in the integrands. The difference between the specific heats at constant pressure for the real and ideal gas states may be calculated using the equation

the PVT correlation of this paper. The plotted points are observations by Workman [49]. No other direct experimental data on the effect of pressure upon the specific heat at constant pressure are available for hydrogen.

An indirect indication of the effect of pressure on the specific heat of hydrogen is found in the work of van Itterbeek [78], who used the results of van Itterbeek and Keesom [77] on the effect of pressure on the velocity of sound in hydrogen at liquid hydrogen temperatures. The results of van Itterbeek at a pressure of one-tenth of an atmosphere indicate that the increase of  $C_p$  with pressure above the zero-pressure value agrees with the PVT prediction within 3 percent at  $17.5^\circ K$  and at  $19.0^\circ K$ , but is lower by more than 30 percent at  $20.5^\circ K$ . At pressures above  $\frac{1}{2}$  atm at  $20.5^\circ K$ , this difference in heat capacity has become approximately  $0.1 \text{ cal deg}^{-1} \text{ mole}^{-1}$ , but this discrepancy is reduced by roughly 50 percent if the data of van Itterbeek and Keesom are evaluated with values of  $C_p - C_v$  based on the PVT tables of this paper.

<sup>12</sup> Up to  $\rho = 600$  at temperatures above  $0^\circ C$ , the equation  $Z = \exp(B\rho + C\rho^2)$  has been used. This is eq 4.8 and eq 4.9 is its series expansion. The symbols stand for functions of  $T$ , which are given by eq 4.11 and 4.12.

From  $\rho = 0$  to  $\rho = 200$  and  $T = 14^\circ$  to  $56^\circ K$   $Z$  can be expressed by  $Z = 1 - (A/T^2)\rho - (C/T^2)\rho^2$ , which is equivalent to eq 4.14. The symbols  $A$  and  $C$  stand for functions of  $T$ , whose values are tabulated in table 18.

The specific heat of hydrogen at constant volume has been determined by Eucken [169] for various combinations of temperature and density in the ranges 35° to 110° K and 60 to 150 Amagats.

Joule-Thomson coefficients of hydrogen may be of interest. These may be calculated from eq 4.6. For this calculation there are required: the value of  $C_p$ , which may be calculated using eq 5.8 or 5.17. Values of  $Z$ ,  $(dZ/dT)_p$ , and  $(dZ/d\rho)_T$  are given explicitly in tables 13, 15, and 17. By using values of  $C_p$  for  $H_2$  at 50° C derived from figure 12, the following values of  $\mu$  for 50° C were obtained by calculation: at  $\rho=20$ ,  $\mu=-0.0350$  deg atm<sup>-1</sup>;  $\rho=40$ ,  $\mu=-0.0364$ ;  $\rho=60$ ,  $\mu=-0.0378$ ;  $\rho=80$ ,  $\mu=-0.0390$ , and  $\rho=100$ ,  $\mu=-0.0402$ . By extrapolation, one obtains for  $\mu$  at  $\rho=0$  the value  $-0.0335$ .

There are no accurate measured Joule-Thomson data for hydrogen for 50° C with which these calculated values of  $\mu$  may be compared.

Results of measurements on Joule-Thomson effects in hydrogen and deuterium at liquid air and room temperatures have been published recently by Johnston and coworkers [57, 58], with curves showing calculated values for hydrogen based on the tables of this paper.\* Considering that the Joule-Thomson coefficients are not obtained with great simplicity from the PVT data and depend sensitively on the trends of the representation, the agreement is considered fairly satisfactory.

The location of the inversion curve for the Joule-Thomson effect in hydrogen on a  $\rho$ - $T$  graph may be determined from tables 15 and 17 by finding values of  $\rho$  and  $T$  for which  $T(dZ/dT)_p = \rho(dZ/d\rho)_T$ , in accordance with eq. 4.6.

An expression for  $\mu$  in terms of derivatives of the enthalpy,  $H$ , is

$$\mu = \frac{(dH/d\rho)_T}{\left(\frac{dH}{d\rho}\right)_T \left(\frac{dP}{dT}\right)_p - \left(\frac{dH}{dT}\right)_p \left(\frac{dP}{d\rho}\right)_T} \quad (5.18)$$

In accordance with this equation the inversion curve may be determined by inspection of the  $(H^\circ - H)/RT$  table (table 23), since  $\mu=0$  where

$$\left(\frac{d(H^\circ - H)/RT}{d\rho}\right)_T = 0. \quad (5.19)$$

The heavy curve in figure 13 is the inversion curve of hydrogen as given by the correlation of this paper. In locating it, values of  $P$  were determined with the help of table 14. For temperatures below 75° K some extrapolation beyond the limit of the tables was necessary. In this extrapolated region the  $\sigma$  versus  $\rho$  diagram, figure 6, was worked with, and the relation for the inversion curve on this diagram was used to get the extrapolated part of the inversion curve directly from the  $\sigma$  versus  $\rho$  diagram.

In a Joule-Thomson expansion of hydrogen at constant temperature from a high to a very low

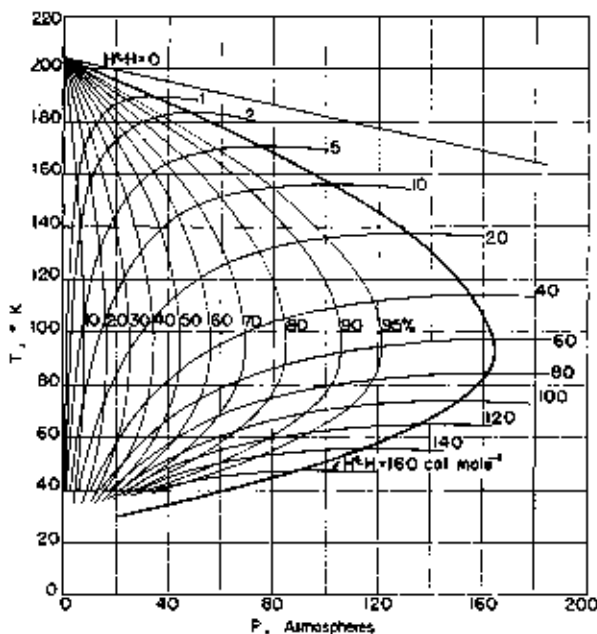


FIGURE 13. Curves related to the Joule-Thomson cooling of  $H_2$ .

density, approaching zero density, there is a change in enthalpy equal to  $(H^\circ - H)$ . In figure 13 the curves that cross the inversion curve horizontally are curves of constant  $H^\circ - H$ . As  $H^\circ$  is a function of temperature, these constant  $(H^\circ - H)$  curves are not isenthalpics.

The horizontal crossing of the inversion curve by the  $(H^\circ - H)$  curve is related to the fact that  $\mu$ , which is zero along the inversion curve, is equal to  $(dH/dP)_T/C_p$ , which means that along the inversion curve  $(dH/dP)_T$  is zero. The enthalpy change  $(H^\circ - H)$  is equal, very nearly, to the amount of refrigeration, per mole of gas, available for the liquefaction of hydrogen in a Hampson or Linde low pressure type of hydrogen liquefier in which a

\*The tables of this paper were completed before the papers by Johnston and coworkers [57, 58] on the Joule-Thomson coefficients of  $H_2$  and  $D_2$  appeared. Our correlation of PVT data would doubtless have been better if these Joule-Thomson data had been available at the time the correlation was made.

continuous flow of gaseous hydrogen is allowed to expand from a high to a low pressure without doing work against an external force system. The fraction  $x$  of the high pressure hydrogen flow that might, theoretically, be liquefied is

$$x = \frac{H' - H}{H' - H_{10}} = \frac{H' - H}{(H' - H_{10}) + L_v} \quad (5.20)$$

where  $H$  and  $H'$  are the enthalpies of the compressed and expanded hydrogen at the temperature at which the compressed hydrogen leaves the precooler and enters the last stage interchanger before expansion;  $L_v$  is the heat of vaporization of liquid hydrogen at the boiling temperature determined by the pressure of the expanded hydrogen; and  $(H_{10} - H_{10}) = L_v$  is the difference in enthalpies of saturated vapor and liquid in equilibrium at the pressure of the expanded hydrogen. Only a relatively small error is made in  $x$  if in place of  $H'$  and  $H_{10}$  for the real gas at atmospheric pressure one uses the enthalpies  $H^\circ$  and  $H^\circ_{10}$  of hydrogen in the ideal gas state at the same temperatures as would be used for  $H'$  and  $H_{10}$ .

$$x = \frac{H^\circ - H}{H^\circ - H^\circ_{10} + L_v} \quad (5.21)$$

For a temperature of precooling equal to 65° K, the error introduced by the approximation is about 0.5 percent.

The lines of figure 13 that are roughly parallel to the inversion curve and converge with it at the inversion point, 204.6° K, are lines showing the pressure at which  $H^\circ - H$  has reached a given fraction of its maximum value for the given temperature. As the inversion curve is the line of maximum values of  $(H^\circ - H)$  it is also the 100-percent line in this family of constant percentage lines.

In the free expansion of a continuous flow of gas not doing work against an external force system, the maximum refrigeration is obtained by expanding from the inversion pressure for the given temperature of the compressed gas. The curves of constant percentage of maximum values of  $(H^\circ - H)$  are also curves of constant percentage of the maximum available refrigeration in an expansion to low pressure.

Figure 13 makes apparent how greatly the refrigeration and the fraction of hydrogen liquefied (eq 5.21) by a Hampson type liquefier are increased

by lowering the temperature of the compressed hydrogen before it enters the final interchanger from which expansion of the hydrogen takes place. It is also seen that the condition of highest inversion pressure (92° K and 165 atm) is by no means the most favorable condition for liquefaction; a further cooling of the compressed hydrogen by 32 degrees nearly doubles the refrigeration produced and more than doubles the fraction liquefied. It is also seen from figure 13 that for the usual range of temperatures (55° to 90° K) to which compressed hydrogen is precooled before expansion in a Hampson-type liquefier, about 95 percent of the maximum refrigeration is obtained when the pressure of the compressed gas is only 75 percent of the inversion pressure.

## VI. Viscosity and Thermal Conductivity

### 1. Viscosity and Thermal Conductivity of the Gas Near Atmospheric Pressure

#### (a) Hydrogen

Values for the viscosity of gaseous normal hydrogen at atmospheric pressure for temperatures above the boiling point and at saturation pressure for two temperatures below the boiling point are given in table 24. These were calculated using the empirical equation

$$\eta = 85.558 \times 10^{-7} \frac{T^{3/2}}{T + 19.55} \frac{T + 650.39}{T + 1175.9} \text{ poises} \quad (6.1)$$

for the viscosity at very low pressure,<sup>13</sup> together with values for the small differences between viscosities at atmospheric or saturation pressure and at very low pressure (see eq 6.17 and 6.16). The four constants of eq 6.1 were chosen on the basis of experimental data near 20°, 90°, 300°, and 685° K. The value used for the viscosity of hydrogen at 685° K was 0.55 percent larger than the experimental values of Trautz and Zink [99], as their value was based on Millikan's value for the viscosity of air which is now known to be low by about this amount.

In figure 14 are plotted deviations of recent experimental viscosity data from eq 6.1. No changes were made in the experimental data for

<sup>13</sup> This viscosity at very low pressure is a true or bulk viscosity. The pressure effect mentioned here is not the familiar low pressure effect on the apparent experimental viscosity involving the accommodation coefficient and the limited size of experimental apparatus.

TABLE 24. Viscosity of gaseous hydrogen (H<sub>2</sub>)

<i>T</i>	$\eta$	<i>T</i>	$\eta$	<i>T</i>	$\eta$
°K	Poises	°K	Poises	°K	Poises
10.....	61.0×10 <sup>-4</sup>	260.....	843.6×10 <sup>-4</sup>	620.....	1.461×10 <sup>-1</sup>
20.....	109.3	270.....	834.6	640.....	1.493
30.....	160.7	280.....	855.3	660.....	1.524
40.....	206.6	290.....	875.6	680.....	1.555
50.....	248.9	300.....	895.0	700.....	1.585
60.....	287.6	310.....	916.0	720.....	1.616
70.....	323.8	320.....	935.8	740.....	1.646
80.....	367.9	330.....	953.4	760.....	1.675
90.....	399.3	340.....	974.8	780.....	1.705
100.....	421.1	350.....	994.0	800.....	1.734
110.....	450.8	360.....	1,013	820.....	1.763
120.....	479.3	370.....	1,032	840.....	1.792
130.....	507.0	380.....	1,051	860.....	1.820
140.....	533.8	390.....	1,069	880.....	1.848
150.....	559.8	400.....	1,087	900.....	1.876
160.....	585.2	420.....	1,124	920.....	1,904
170.....	610.0	440.....	1,160	940.....	1,932
180.....	634.3	460.....	1,195	960.....	1,959
190.....	658.1	480.....	1,230	980.....	1,986
200.....	681.4	500.....	1,264	1,000.....	2,013
210.....	704.3	520.....	1,298	1,020.....	2,040
220.....	726.9	540.....	1,331	1,040.....	2,068
230.....	749.0	560.....	1,364	1,060.....	2,092
240.....	770.9	580.....	1,397	1,080.....	2,118
250.....	792.4	600.....	1,429	1,100.....	2,144

the differences in density. Deviations of table 24 values from eq 6.1 are represented in figure 14 by the peaked curve, which is appreciably above the zero line between 10° K and 100° K and in very close agreement with it at higher temperatures. This peaked curve represents the viscosity at atmospheric pressure above the boiling point and at saturation vapor pressure below the boiling point. Different reported values of viscosity at low temperatures are so poorly in agreement that their comparison does not indicate the magnitude of the peak, which has accordingly been obtained from theory, using data of state. To limit the crowding of experimental points in the figure, those plotted represent only data published since 1928, but a few data obtained after 1928 have been omitted. The data of Trautz and co-workers [94 to 102] would be in better agreement with the zero line if increased by about one half percent for the revision in the value for the viscosity of air.

It has been pointed out by others that the Sutherland formula

$$\eta = \eta' \left( \frac{T}{T'} \right)^{3/2} \frac{T' + C}{T + C} \quad (6.2)$$

does not fit the data for hydrogen over an extended range of temperature. This may be seen in figure 14 in which the deviations of the Sutherland formula from eq 6.1 are represented by the curve below the zero line. The constant *C* was evaluated at 300° K to represent the trend of the best data.

Values of the thermal conductivity of gaseous normal hydrogen are given in table 25.

TABLE 25. Thermal conductivity of gaseous hydrogen at 1 atm

<i>T</i>	<i>K</i>	<i>T</i>	<i>K</i>
°K	cal cm <sup>-1</sup> sec <sup>-1</sup> °C <sup>-1</sup>	°K	cal cm <sup>-1</sup> sec <sup>-1</sup> °C <sup>-1</sup>
10.....	14.3×10 <sup>-4</sup>	260.....	367.0×10 <sup>-1</sup>
20.....	34.0	270.....	406.7
30.....	53.5	280.....	422.1
40.....	70.7	290.....	434.2
50.....	88.5	300.....	446.3
60.....	101.4	320.....	469.8
70.....	118.1	340.....	493.8
80.....	130.6	360.....	515
90.....	145.9	380.....	537
100.....	161.3	400.....	559
110.....	177.0	420.....	580
120.....	192.9	440.....	601
130.....	208.8	460.....	622
140.....	224.6	480.....	643
150.....	240.4	500.....	664
160.....	256.0	620.....	664
170.....	271.4	640.....	705
180.....	286.6	660.....	725
190.....	301.1	680.....	746
200.....	315.4	600.....	706
210.....	329.6		
220.....	343.5		
230.....	357.2		
240.....	370.7		
250.....	384.0		

They were calculated from the equation

$$k = [1.8341 - 0.004458T + (1.1308 + 0.0008973T)C_p^0] \frac{\eta}{M} \frac{1}{\left(1 + \frac{3.2}{T}\right)} \quad (6.3)$$

In principle, a correction from low pressure to one atmosphere would be applicable, but it has been omitted because the uncertainty of the experimental values is much greater. In eq 6.3, *M* is the molecular weight,  $\eta$  the viscosity given by eq 6.1, *C<sub>p</sub><sup>0</sup>* the specific heat in calories per mole per degree at constant pressure, and *T* the temperature in degrees Kelvin. This equation is an empirical representation of the data and was

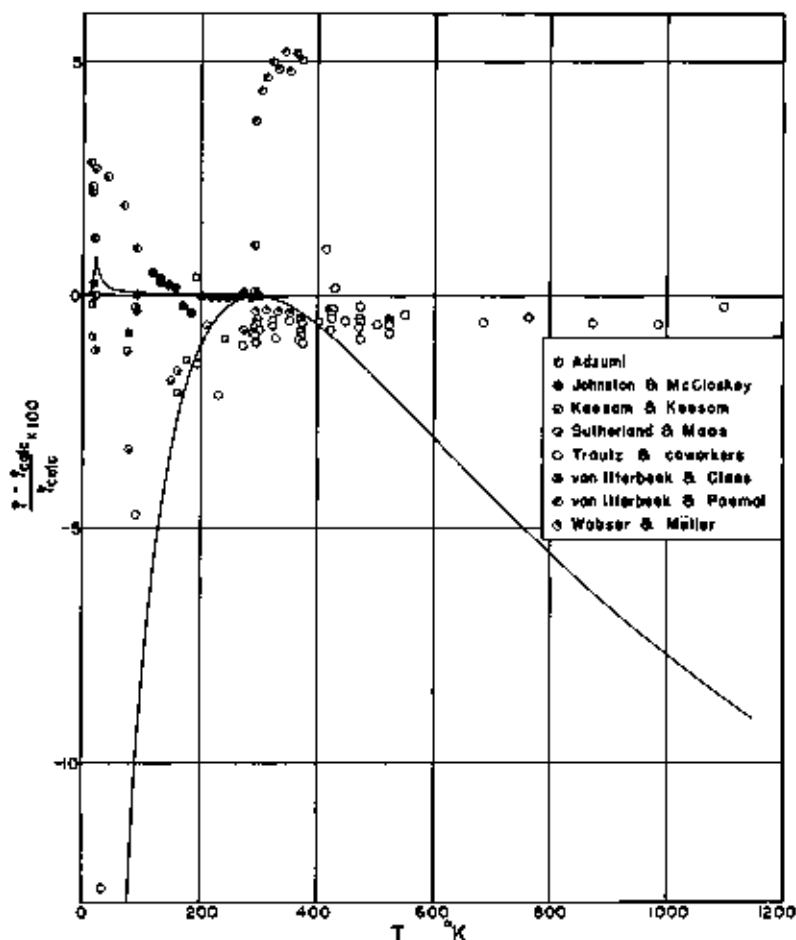


FIGURE 14. Viscosity of hydrogen.

obtained in several steps, which will be explained in the discussion that follows.

In figure 15, curve *A* represents eq 6.3, whereas curves *B* and *C* are theoretical and are given for comparison. Curve *C* is for Eucken's relation

$$k = (9\gamma - 5)C_v^0 \eta / (4M), \quad (6.4)$$

or its equivalent

$$k = (C_v^0 + 1.25R)\eta / M. \quad (6.5)$$

Chapman and Cowling [137] proposed the formula

$$k = \left[ \frac{15}{4}(\gamma - 1) + \frac{1}{2} U_{11}(5 - 3\gamma) \right] \eta C_v^0 / M, \quad (6.6)$$

which is equivalent to

$$k = [U_{11}C_v^0 + (3.75 - 2.5U_{11})R]\eta / M. \quad (6.7)$$

The transport of internal molecular energy of a gas is supposed to be represented better theoret-

ically as a result of including the quantity  $U_{11}$ , which is the ratio of mean free path lengths for diffusion and viscosity.

$U_{11}$  is a pure number whose value was determined theoretically for (1) smooth elastic spheres and (2) for molecules repelling as the inverse fifth power of the distance (Maxwellian molecules), the values being 1.204 and 1.55, respectively.

For  $U_{11}$  equal to 1, curve *C* is obtained, as eq 6.6 and 6.7 then reduce to eq 6.4 and 6.5. Curve *B* of figure 15 is a graph of eq 6.7 with  $U_{11} = 1.4$ , a value indicated by a group of measurements of the conductivity near 300° K. It is evident that the main body of the experimental data is not consistent with a constant value of  $U_{11}$ . On the basis of a value of 1.4 for  $U_{11}$  near 300° K and a higher value at 700° K, as indicated by a curve representing the data, the relation

$$U_{11} = 1.1308 + 0.0008973T \quad (6.8)$$

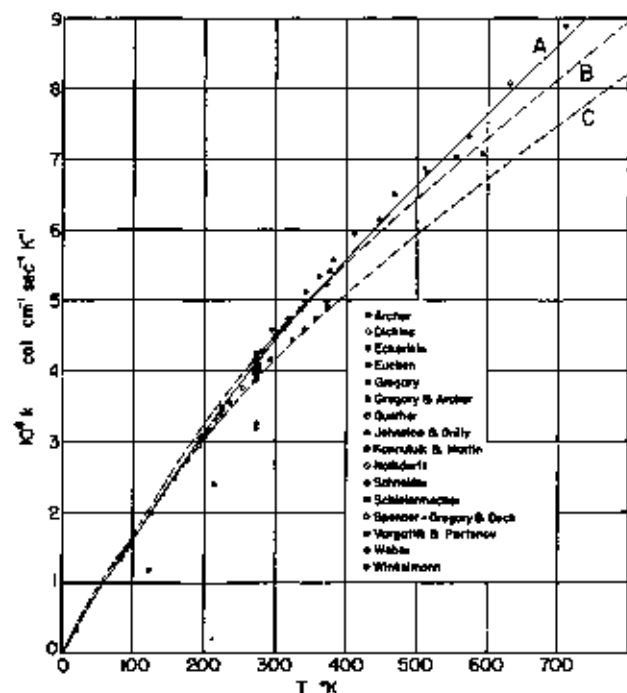


FIGURE 15. Thermal conductivity of hydrogen.

was adopted. It was found that the curve was not critically dependent on the functional form of  $U_{11}$  as a change to  $U_{11}=a+b\sqrt{T}$  altered the final curve negligibly between 300° and 700° K.

At temperatures somewhat below 100° K, the ideal gas specific heat of hydrogen at constant pressure approaches the value  $(5/2)R$  characteristic of a monatomic gas. For this value of  $C_p$ , the  $U_{11}$  terms in eq 6.7 cancel and eq 6.4 to 6.7 reduce to

$$k = \frac{5}{2} \eta (C_v/M). \quad (6.9)$$

This equation has been derived exactly for a force that at all distances is repulsive and proportional to  $1/r^5$ . Enskog [132] has shown that for attracting rigid spheres (Sutherland molecules),

$$k = [2.522/1(1 + 0.03C/T)] \eta C_v/M,$$

where  $C$  is the Sutherland constant in eq 6.2. Thermal conductivities of hydrogen measured at liquid air temperatures are a few percent lower than equations 6.4 to 6.9 would indicate. No theoretical explanation of this is at hand, but the agreement of the three independent investigations in this region indicates that the lower value is to be accepted. To take account of this, a correction

factor  $1/(1+3.2/T)$  has been included, having a form suggested by Enskog's theoretical result for attracting rigid spheres but with the constant chosen to fit these experimental data. The inclusion of this factor also brings the final curve closer to Eucken's experimental value at 20.96° K, which is still almost 12 percent lower than the curve.

The curve as chosen to fit the thermal conductivity data is not regarded as completely satisfactory. In the temperature range 270° to 400° K, the experimental data appear to fall into two groups, one quite close to the curve adopted and the other lower by about 7 percent. The lower group includes the most recent data.

Equation 6.4 to 6.9 make it evident that at low-temperatures where the specific heats of ortho and para hydrogen differ, their thermal conductivities differ also. This difference in thermal conductivity was the basis of the method of ortho-para analysis used by Bonhoeffer and Hardeck [121]. The temperature or electrical resistance of an electrically heated wire carrying a given current determines, after calibration, the ortho-para composition of the hydrogen that surrounds the wire in a tube externally thermostated at liquid air temperature. A small difference is to be expected in the viscosities of ortho and para hydrogen by reason of small differences in their intermolecular forces manifested by small differences in vapor pressure, and density of the condensed states.

This difference in viscosities is small and was not detected in the experiment undertaken by Hardeck and Schmidt [122], in which an accuracy of 1 percent was attained. In later developments of the so-called thermal conductivity method of ortho-para analysis, the pressure of the gas was reduced to make the mean free path large compared with the diameter of the heated wire. For this condition the ordinary thermal conductivity is not the controlling factor.

#### (b) Deuterium

Several investigations have been made of the viscosity of deuterium at atmospheric pressure, the most recent being that of Van Itterbeek and Van Paemel [106, 107], published in 1940. Table 26, which gives values for the ratio between viscosities of deuterium and hydrogen for several temperatures, was taken from the paper by Van Itterbeek and Van Paemel.

TABLE 28. Ratio of viscosities for gaseous D<sub>2</sub> and H<sub>2</sub>

T	$\eta(\text{D}_2)/\eta(\text{H}_2)$
°K	
293.....	1.40
80.....	1.38
50.....	1.37
70.....	1.36
30.....	1.24
16.....	1.24
12.5.....	1.24

The ratio of the thermal conductivity of deuterium at 0° C to the thermal conductivity of hydrogen also at 0° was determined by C. T. Archer [127] and by W. G. Kannuluik [130], who obtained respectively, the values 0.736<sub>2</sub> and 0.732<sub>4</sub>. By using the mean of these values with appropriate values of  $C_p$  and  $\eta$ , one obtains for  $U_{11}$  in eq 6.7 for the thermal conductivity of D<sub>2</sub> at 0° C the value 1.55. Archer also measured the thermal conductivity of various equilibrium mixtures of H<sub>2</sub>, HD, and D<sub>2</sub>.

For two isotopic gases with identically the same intermolecular forces, the classical theory values for the ratio of their viscosities, and the ratio of their thermal conductivities at temperatures where their heat capacities are equal are

$$\eta_1/\eta_2 = \sqrt{M_1/M_2} \text{ and } k_1/k_2 = \sqrt{M_2/M_1} \quad (6.10)$$

For H<sub>2</sub> and D<sub>2</sub> these ratios have the values:  $\eta_{\text{D}_2}/\eta_{\text{H}_2} = 1.414$  and  $k_{\text{D}_2}/k_{\text{H}_2} = 0.707$ , and are independent of the intermolecular force field so long as it is the same for the two isotopes. The difference between the rotational heat capacities of H<sub>2</sub> and D<sub>2</sub> at low temperatures by itself makes the ratio  $k_{\text{D}_2}/k_{\text{H}_2}$  larger and thus has an effect opposite to but less than that of the smaller mean velocity of D<sub>2</sub> molecules caused by the greater mass. Using Eucken's eq 6.4 for  $k$  and making allowance for the difference in heat capacities of H<sub>2</sub> and D<sub>2</sub>, one obtains 0.718 for  $k_{\text{D}_2}/k_{\text{H}_2}$  at 0° C. The classical theory values for these ratios of thermal conductivities and viscosities are approached closely at room temperatures. The effect of quantum mechanical interaction in transport phenomena can be described in terms of increase in the apparent size of the molecules. In classical theory the size of the molecule plays an important role, the viscosity and thermal conductivity decreasing as the size increases. For

hydrogen and deuterium, the quantum mechanical increase in apparent size is small at room temperature but becomes large at low temperature. The increase depends also upon the masses of the colliding molecules and is larger for H<sub>2</sub> than for D<sub>2</sub> at the same temperature. It was pointed out in the section on the PVT data for deuterium that the quantum theory of second virial coefficients includes an effect interpretable classically as an increase in apparent size of molecules, becoming very large at low temperatures. The quantum mechanically obtained increase in apparent size with lowering of temperature is not the same for viscosity as that associated with the second virial coefficient, however. This is not surprising when one considers that the increase in the mean de Broglie wave length with decreasing temperature increases the diffraction behind a scattering molecule; an effect that does not enter in the determination of the second virial coefficient, but which taken by itself would decrease the apparent size of a scattering molecule for viscosity.

## 2. Viscosity and Thermal Conductivity of the Gas at High Pressures

There are no experimental data on the thermal conductivity of gaseous H<sub>2</sub> at high pressures. For viscosity, however, experimental data obtained by Boyd [134] and Gibson [135] are available. Gibson's data, which are for 25° C, are more precise than those of Boyd and are plotted in figure 16. It will be seen that there is fairly good agreement between these better experimental data and the curve representing the theoretical formula due to Enskog. Differing approaches to the problem of relating viscosity and variables of state will be found elsewhere [133, 136].

In elementary theory, the viscosity and thermal conductivity for a given gas are proportional to the product of  $V$ ,  $\rho$ , and  $\Lambda$ , where  $V$  is the mean molecular velocity,  $\rho$  is the density, and  $\Lambda$  is a suitable mean path length for the transfer of momentum or energy. Although  $\Lambda$  is often taken as identical with the ordinary free path of molecular motion, it is actually greater by a small distance of the order of magnitude of a molecular diameter, as at each collision the momenta and energies are transferred an additional distance related to the diameters of the molecules involved. Thus instead of  $\Lambda$  decreasing as  $1/\rho$  when  $\rho$  is increased, which would make  $\rho\Lambda$  independent of



$\rho$ ,  $\Delta$  decreases a little less slowly so as to make  $\rho\Delta$  increase slightly as  $\rho$  is increased. Accordingly, both the thermal conductivity and the viscosity of a gas would be expected to increase with increasing density, particularly when multiple encounters between molecules occur frequently as in the case of high densities.

Enskog's theory was developed for a gas whose molecules were assumed to be mutually attracting rigid spheres, for which the equation of state has the form

$$P + a\rho^2 = RT\rho(1 + b\rho\chi), \quad (6.11)$$

used by Enskog takes account of simultaneous encounters of three and four molecules as treated by Boltzmann and Clausius.

According to Enskog's theory, the viscosity and thermal conductivity of a compressed gas are related to the viscosity  $\eta_0$  and conductivity  $k_0$  at low pressure by the equations

$$\eta/\eta_0 = b\rho[1/(b\rho\chi) + 0.8 + 0.7614b\rho\chi \dots] \quad (6.14)$$

and

$$k/k_0 = b\rho[1/(b\rho\chi) + 1.2 + 0.7574b\rho\chi \dots] \quad (6.15)$$

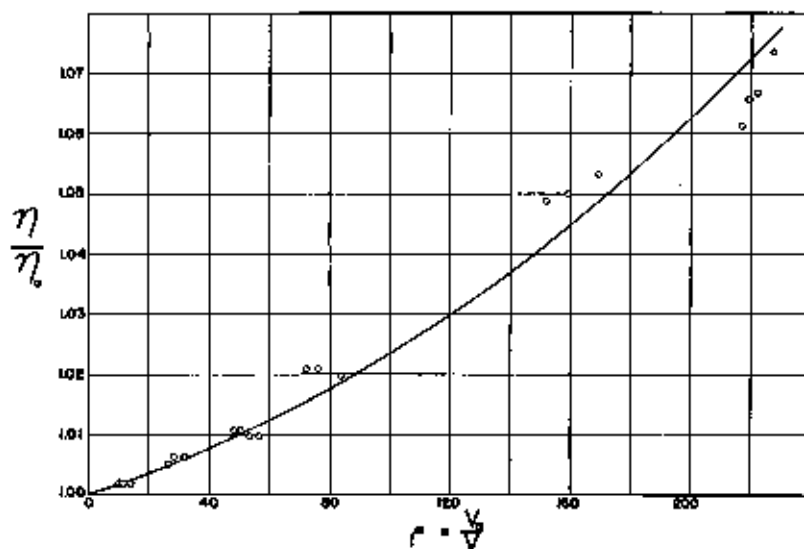


FIGURE 16. Effect of density on viscosity of hydrogen at 25° C.

where the constants  $a$  and  $b$  are assumed to be independent of  $T$  and  $\rho$ , and  $\chi$  is a function of  $\rho$  expressed in the form of a power series in  $b\rho$ . The equation of state that was used is thus almost the same as the Van der Waals equation

$$P + a\rho^2 = RT\rho(1 - b\rho)^{-1} = RT\rho [1 + b\rho(1 + b\rho + b^2\rho^2 + \dots)] \quad (6.12)$$

except for the details of the dependence of  $\chi$  upon  $\rho$ . The Van der Waals equation is derived on the basis that simultaneous encounters of three or more molecules are rare enough to be neglected. Only at low pressures is this valid and under this condition terms of the second degree and higher in  $b\rho$  are neglected in the derivation. The function

$$\chi = 1 + 0.625b\rho + 0.2869b^2\rho^2 + \dots \quad (6.13)$$

It follows from eq 6.11, the equation of state assumed for Enskog's theory, that

$$b\rho\chi = \frac{T}{P} \left( \frac{dP}{dT} \right)_\rho \left( \frac{PV}{RT} \right) - 1 = Z - 1 + T \left( \frac{dZ}{dT} \right)_\rho \quad (6.16)$$

Thus, the value of  $b\rho\chi$  may be calculated from the tables of  $Z$  and  $(dZ/dT)_\rho$  and the value of  $b\rho$  may then be found with the help of eq 6.13.

Over the range of Gibson's experimental viscosity data very little change is made in the values predicted if simple power series expansions in  $b\rho\chi$ , obtained from equations 6.14 and 6.15, are used:

$$\eta/\eta_0 = 1 + 0.175b\rho\chi + 0.7557(b\rho\chi)^2 - 0.405(b\rho\chi)^3 \quad (6.17)$$

$$k/k_0 = 1 + 0.575b\rho\chi + 0.5017(b\rho\chi)^2 - 0.204(b\rho\chi)^3 \quad (6.18)$$

The coefficient of the last term of each equation would be changed if higher order terms were added to eq 6.13, 6.14, and 6.15. Dropping the last term of eq 6.17 for  $\eta/\eta_0$  does not significantly change the agreement with Gibson's experimental data.

In order to show the general magnitude of the theoretical effect of pressure on the viscosity and thermal conductivity of hydrogen the preceding equations have been evaluated for several additional combinations of temperature and pressure, using data from the PVT tables. Table 27 gives the values thus obtained. It is seen that the calculated relative change in  $\eta$  and  $k$  with pressure is much more pronounced at the lower temperatures, for which large deviations from the ideal gas law occur even at moderate pressures.

TABLE 27. Effect of pressure on viscosity and thermal conductivity of hydrogen

$T$	$P$	$\eta/\eta_0$	$k/k_0$
$^{\circ}\text{K}$	atm		
18	0.455	1.0045	1.0138
20	0.899	1.0077	1.0225
22	1.365	1.0125	1.0317
30	1	1.0057	1.0114
30	2.04	1.0088	1.0248
38	30.4	1.53	1.76
40	1	1.0021	1.0068
40	2.80	1.0067	1.0199
40	37.2	1.53	1.70
50	1	1.0015	1.0048
50	3.55	1.0060	1.0178
50	50	1.31	1.49
60	1	1.0012	1.0037
70	1	1.0009	1.0030
70	6.05	1.0051	1.0155
70	30	1.11	1.22
80	1	1.00075	1.0024
90	1	1.00065	1.0021
90	6.50	1.0047	1.0144
90	60.0	1.05	1.13
100	1	1.00058	1.0018
110	1	1.00049	1.0016
150	1	1.00034	1.0011
250	1	1.00018	1.0006
400	1	1.00010	1.0003
600	1	1.00006	1.0002

### 3. The Viscosity of Liquid Hydrogen

The first determination of the viscosity of liquid hydrogen was made in 1917 by Verschaffelt and Nicaise [133] from measurements of the logarithmic decrement of the oscillatory rotation of a sphere in liquid hydrogen at 20.36° K.

Later, determinations were made of the viscosity of liquid hydrogen from 15° to 20° K, in 1938 by Keesom and Mac Wood [139] from measurements of the logarithmic decrement of an oscillating disc, and in 1939 by Johns [140], using the capillary flow method. The reported viscosities are

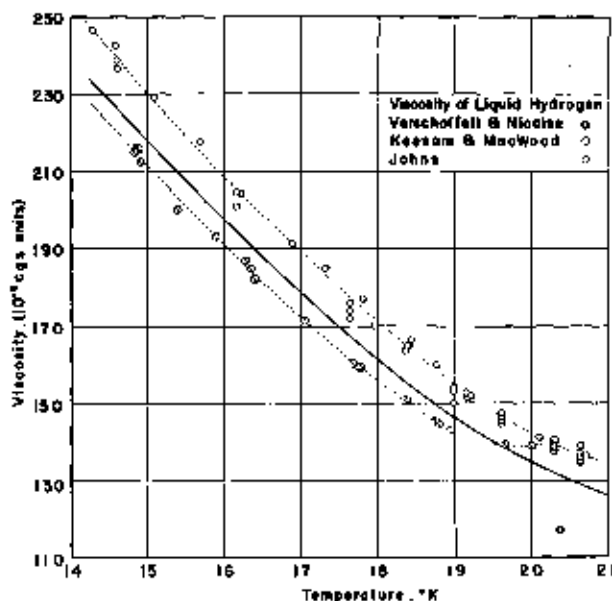


FIGURE 17. Viscosity of liquid hydrogen.

shown in figure 17. The values obtained by Johns are roughly 10 percent greater than those of Keesom and Mac Wood except near the boiling point, 20.4° K. There seems to be no clear indication in the papers reporting the measurements that either of these two later sets is less dependable than the other. Accordingly a curve to represent the present most probable values of the viscosity of liquid hydrogen was drawn principally between the two sets. Near the boiling point the curve was drawn approximately parallel to that of Johns because it was felt that the lower value of Verschaffelt and Nicaise supported the more regular variation of viscosity with temperature as reported by Johns.

### VII. Pressure Temperature Relations for Two-Phase Equilibria for H<sub>2</sub>, HD, and D<sub>2</sub> as Single Components

In this section are presented data on (1) vapor pressures of solid and liquid H<sub>2</sub>, HD, and D<sub>2</sub> with such derived constants as normal boiling temperatures and triple-point temperatures and pres-

tures; differences between the vapor pressures of different mixtures of *o*- and *p*-H<sub>2</sub>; and changes in vapor pressures of ortho-para H<sub>2</sub> mixtures resulting from self conversion; (2) the pressure-temperature relations for the solid-liquid equilibrium of H<sub>2</sub>, HD, and D<sub>2</sub>. The data are presented in the form of equations, tables, and graphs.

is used in this section as the unit of vapor pressure. Temperatures are on the Kelvin Scale.

In tables 28 and 29 the vapor pressures, boiling points, and triple points of the different isotopic and ortho-para modifications of hydrogen are compared.

(a) H<sub>2</sub>

The differences between the hydrogen vapor-pressure data reported in the literature [143 to 146, 148] are the result, principally, of differences in the temperature scales used by different observers and of unknown differences in the ortho-para composition of the hydrogen.

The vapor-pressure data recently obtained [146] at the National Bureau of Standards are on the low-temperature scale established at the National Bureau of Standards and are for known ortho-

1. Vapor Pressures, Boiling, and Triple Points<sup>14</sup>

The present vapor-pressure data on the hydrogens can be fitted with equations of the form

$$\log_{10} P = A + B/T + CT \quad (7.1)$$

to within the accuracy of the experimental data. The millimeter of Hg at 0° C and standard gravity

<sup>14</sup> Boiling-point and triple-point data from this section have been used in advance of publication in the "Tables of Selected Values of Chemical Thermodynamic Properties" prepared by the National Bureau of Standards in conjunction with the Office of Naval Research of the U. S. Navy Department.

TABLE 28. Vapor pressures of the several isotopic varieties of hydrogen at integral temperatures and at their triple points and boiling points.

[Values marked (\*) were obtained by extrapolation of the vapor-pressure equation to temperatures at which no data were available. The *o*-H<sub>2</sub> table is based on an extrapolation with respect to composition.]

T	20.4° K Equilibrium hydrogen 0.21 percent <i>o</i> -H <sub>2</sub>		Normal hydrogen 75 percent <i>o</i> -H <sub>2</sub>		Orthohydrogen 100 percent <i>o</i> -H <sub>2</sub>		Normal deuterium 85.57 percent <i>o</i> -D <sub>2</sub>		20.4° K Equilibrium deuterium 97.8 percent <i>o</i> -D <sub>2</sub>		Hydrogen deuteride	
	P	State	P	State	P	State	P	State	P	State	P	State
° K	mm Hg		mm Hg		mm Hg		mm Hg		mm Hg		mm Hg	
10	1.93	Solid*	1.72	Solid*			0.95	Solid*	0.09	Solid*	0.28	Solid*
11	5.62	Solid	5.06	Solid			.20	do	.21	do	.99	Solid
12	13.9	do	12.7	do			.73	do	.75	do	2.04	Do.
13	30.2	do	27.9	do			2.14	do	2.20	do	7.46	Do.
13.81 <sub>5</sub>	52.8	Triple point	49.1	do			4.61	do	4.73	do	14.5	Do.
13.95	57.4	Liquid	54.0	Triple point			5.24	do	5.37	do	16.3	Do.
14	58.6	do	55.4	Liquid			5.44	Solid	5.57	Solid	16.8	Do.
14.05	60.5	do	57.0	do	65.1	Triple point*	5.68	do	5.82	do	17.5	Do.
15	100.4	do	95.0	do	92.2	Liquid*	12.3	do	12.6	do	34.4	Do.
16	161.3	do	163.3	do	149.1	do	25.4	do	26.0	do	65.2	Do.
16.60	209.3	do	199.7	do	194.4	do	37.9	do	38.7	do	92.3	Triple point
17	246.2	do	235.2	do	229.2	do	48.6	do	49.8	do	112.5	Liquid
18	360.6	do	345.9	do	337.8	do	87.2	do	89.7	do	176.4	Do.
18.69	459.8	do	442.0	do	432.3	do	128.3	do	129.5	Triple point	234.5	Do.
18.73	464.9	do	448.9	do	437.1	do	128.5	Triple point	130.3	Liquid	237.5	Do.
19	510.1	do	490.2	do	480.7	do	145.1	Liquid	147.2	do	264.7	Do.
20	700.3	do	675.7	do	662.6	do	319.9	do	323.1	do	382.8	Do.
20.37 <sub>5</sub>	760	do	733.9	do	720.0	do	344.9	do	348.4	do	421.9	Do.
20.39	758.8	do	730	do	715.7	do	286.2	do	289.9	do	438.1	Do.
20.45	801.7	Liquid*	774.4	Liquid*	760	do	262.6	Liquid*	266.2	Liquid*	447.7	Liquid*
21	937.0	do	906.4	do	890.6	do	322.2	do	326.9	do	532.2	Do.
22	1226.0	do	1189.0	do	1170.4	do	458.5	do	466.1	do	730.5	Do.
22.13 <sub>5</sub>	1269.4	do	1230.8	do	1211.8	do	479.6	do	486.5	do	760	Do.
23	1674.9	do	1629.0	do	1598.4	do	638.2	do	646.3	do	972.0	Do.
23.52 <sub>7</sub>	1784.4	do	1734.5	do	1712.2	do	749.3	do	760	do	1121.1	Do.
23.57 <sub>5</sub>	1808.6	do	1753.3	do	1730.6	do	760	do	770.6	do	1133.9	Do.

TABLE 29. Boiling points and triple points of the hydrogens

	Boiling point		Triple point	
			T	P
	° K	° K	mm Hg	
20.4° K equilibrium hydrogen (0.21% <i>o</i> -H <sub>2</sub> )	20.27 <sub>3</sub>	13.81 <sub>1</sub>	52.8	
38 percent <i>o</i> -H <sub>2</sub> , 62 percent <i>p</i> -H <sub>2</sub>	20.32	13.96	53.0	
Normal hydrogen (75% <i>o</i> -H <sub>2</sub> )	20.36 <sub>6</sub>	13.97 <sub>7</sub>	54.0	
Orthohydrogen	20.45	14.05	55.1	
Normal deuterium (96.87% <i>o</i> -D <sub>2</sub> )	23.57 <sub>3</sub>	18.72 <sub>4</sub>	128.5	
20.4° K equilibrium deuterium (97.8% <i>o</i> -D <sub>2</sub> )	23.57 <sub>7</sub>	18.69 <sub>6</sub>	128.5	
Paradeuterium	23.58	18.78	128.5	
Hydrogen deuteride	22.13 <sub>2</sub>	18.60 <sub>1</sub>	92.8	

para compositions. Only the NBS results are given here.

Normal hydrogen (75 percent *o*-H<sub>2</sub>, 25 percent *p*-H<sub>2</sub>):

$$\text{Liquid: } \log_{10} P(\text{mm Hg}) = 4.66687 - \frac{44.9569}{T} + 0.020537 T. \quad (7.2)$$

$$\text{Solid: } \log_{10} P(\text{mm Hg}) = 4.56488 - \frac{47.2059}{T} + 0.03939 T. \quad (7.3)$$

20.4° K-equilibrium hydrogen (99.79 percent *p*-H<sub>2</sub>, 0.21 percent *o*-H<sub>2</sub>):

$$\text{Liquid: } \log_{10} P(\text{mm Hg}) = 4.64392 - \frac{44.3450}{T} + 0.02093 T. \quad (7.4)$$

$$\text{Solid: } \log_{10} P(\text{mm Hg}) = 4.62438 - \frac{47.0172}{T} + 0.03635 T. \quad (7.5)$$

The triple-point temperatures and pressures were determined experimentally with a low-temperature calorimeter with a platinum resistance thermometer for the temperature measurements. Equations 7.2 to 7.5 were made to fit these triple points, and are based on vapor pressure data extending from 10.5° to 20.4° K. Although the equation for liquid normal H<sub>2</sub> is based only on National Bureau of Standards data below 20.4° K, the equation represents, within the limits of experimental accuracy, the Leiden data that extend nearly to the critical point, 33.19° K. As mentioned in section IV, the vapor-pressure equation for normal hydrogen was used in constructing the PVT relations for hydrogen. The experimentally determined triple-point temperatures and pres-

ures for *n*-H<sub>2</sub> and *e*-H<sub>2</sub> are given in tables 28 and 29.

Figure 18 is a diagram of differences between the vapor pressures of a 20.4° K equilibrium mixture of *o*- and *p*-H<sub>2</sub> (0.21 percent *o*-H<sub>2</sub>) and five different mixtures of *o*- and *p*-H<sub>2</sub> in the liquid state. The vapor pressure of the 20.4° K equilibrium mixture is denoted by  $P_{(o-H_2)}$ , and that of any other mixture by  $P_{(mixture)}$ . Each curve of the graph is for a single mixture whose composition is indicated on the graph by its *o*-H<sub>2</sub> composition. The 75 percent curve is for normal hydrogen. The vapor pressure differences  $\Delta P$  are plotted as a function of the vapor pressure of the 20.4° K equilibrium hydrogen. The circles represent the experimental data.

Figure 19 shows the vapor pressure differences of figure 18 extended into the solid range, for mixtures of 38 and 75 percent ortho composition. At the extreme right of the figure, these mixtures and the *e*-H<sub>2</sub> with which they are compared are all liquid. Passing to the left, the first sharp break encountered on either curve corresponds to the triple point of the mixture. The second sharp break corresponds to the triple point of *e*-H<sub>2</sub>. To the left of the last break, both materials are solid. Between the two breaks on either curve, the mixture is solid but the *e*-H<sub>2</sub> is liquid.

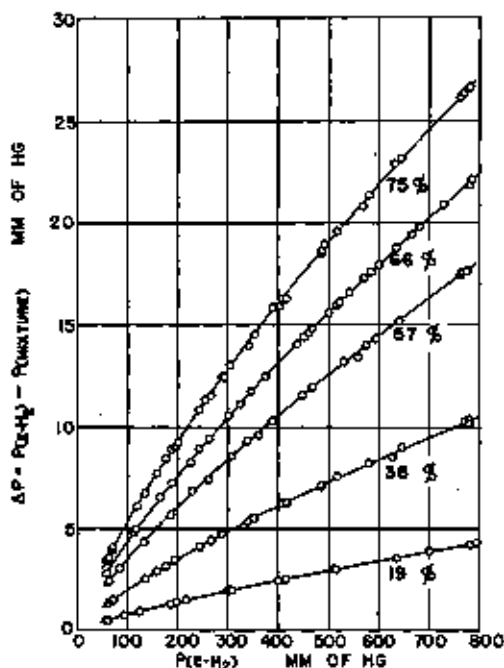


FIGURE 18. Vapor pressure differences for liquid ortho-para H<sub>2</sub> mixtures.

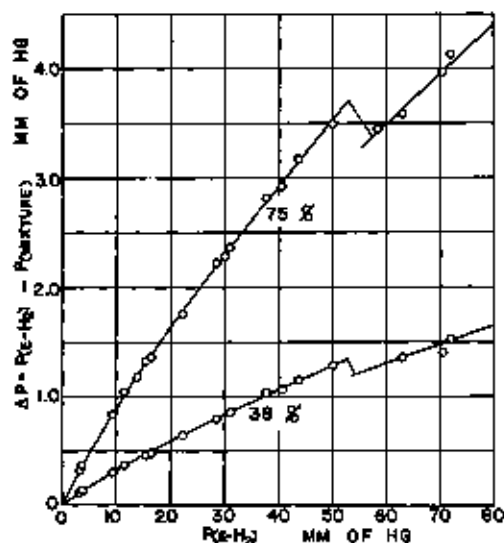


FIGURE 19. Vapor pressure differences for solid ortho-para  $H_2$  mixtures.

A comparison of the  $\Delta P$ 's for different mixtures of *o*- and *p*- $H_2$  in figures 18 and 19 shows that the  $\Delta P$ 's are not proportional to their corresponding differences in composition.

For ideal solutions the ratio  $\Delta P/\Delta x$ , where  $\Delta x$  is the difference in composition, is independent of the composition at constant temperature. In figure 20 this ratio is plotted for four temperatures, the circles representing the experimental vapor pressure data as given by points on the smooth curves of figure 18. Figure 20 shows that the vapor pressures of ortho-para mixtures differ greatly from ideal solution predictions.

The vapor pressure differences ( $P_{e-H_2} - P_m$ ) for mixtures of *o*- and *p*- $H_2$  of any composition at 14.00°, 16.00°, 18.00° and 20.39° K may be calculated from the isotherms of figure 20. Other isotherms may be determined with the help of figures 18 and 19. By extending the isotherms of figure 20 to 100 percent *o*- $H_2$ , the vapor pressure of pure liquid *o*- $H_2$  was determined. The following equation represents the vapor pressures of pure liquid *o*- $H_2$  obtained in this way:

$$\text{liquid: } \log_{10} P(\text{mm Hg}) = 4.65009 - \frac{45.0439}{T} + 0.021168T \quad (7.6)$$

The triple-point temperature and pressure of *o*- $H_2$  were determined by a quadratic extrapolation of the triple point temperatures and pressures of

*e*- $H_2$  (20.4° K), *m*- $H_2$  (38 percent *o*- $H_2$ ) and *n*- $H_2$ . The values thus obtained for *o*- $H_2$  were 14.05° K and 55.1 mm Hg. These are in agreement with eq 7.6 for the vapor pressure of liquid *o*- $H_2$ .

If linear extrapolation is used, omitting the values for *m*- $H_2$ , one obtains 14.00° K and 54.4 mm Hg as lower limiting values of the triple point constants for *o*- $H_2$ . The triple point constants of *m*- $H_2$  were obtained by reading the values  $P(e-H_2)$  and  $\Delta P$  corresponding to the upper break in the 38 percent curve. The difference of these is the triple point pressure of *m*- $H_2$ . By substituting  $P(e-H_2)$  into the vapor pressure equation (eq 7.4) for liquid *e*- $H_2$ , the triple point temperature of *m*- $H_2$  is obtained. The uncertainties in these derived triple point constants of *m*- $H_2$  and *o*- $H_2$  are greater than for the experimentally determined values for *e*- $H_2$  and *n*- $H_2$ .

The vapor pressure of a nonequilibrium mixture of *o*- and *p*- $H_2$  changes slowly with time because of the slow conversion of a nonequilibrium mixture, liquid or solid, to the equilibrium composition. At its normal boiling point, the vapor pressure of *n*- $H_2$  changes at the rate of 0.23 mm Hg per hour [148]. Paramagnetic substances increase the rate of conversion. The rate of increase of the vapor pressure at 20.4° K of a sample of hydrogen containing 0.01 percent oxygen was about three times that for pure hydrogen.

The interconversion of ortho and parahydrogen in the absence of molecular dissociation is the result of an intra-molecular rearrangement of pro-

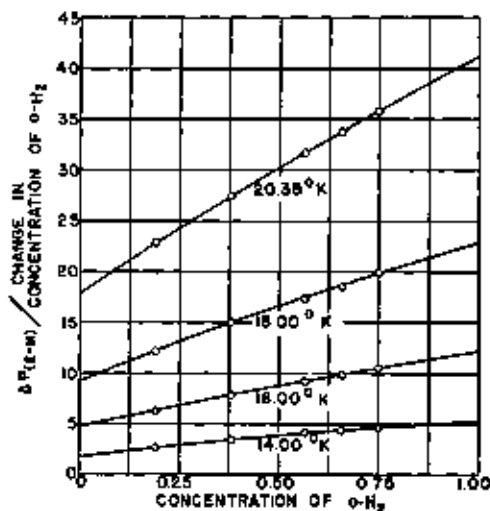


FIGURE 20. Deviations of vapor pressure of ortho-para  $H_2$  mixtures from law of ideal solutions.

tons in the presence of a strong magnetic field, inhomogeneous on a scale of molecular dimensions.

As  $p\text{-H}_2$  has no net nuclear magnetic moment, the self conversion of nonequilibrium mixtures results only from the interaction of  $o\text{-H}_2$  molecules, which do have a nuclear magnetic moment, with each other and with  $p\text{-H}_2$  molecules. Hence, the ortho-para conversion in liquid and solid  $\text{H}_2$  is a bimolecular change.

$$-d[o\text{-H}_2]/dt = k_1[o\text{-H}_2]^2 - k_2[o\text{-H}_2][p\text{-H}_2] \quad (7.7)$$

The velocity constant  $k_2$  is much smaller than  $k_1$  in accord with the small equilibrium proportion of  $o\text{-H}_2$ . At equilibrium, where  $d[o\text{-H}_2]/dt$  is zero,  $k_2/k_1 = [o\text{-H}_2]/[p\text{-H}_2]$ . Values of equilibrium concentrations are given in table 12. For liquid hydrogen the velocity constant  $k_1$  for conversion is 0.0114 per hour when concentrations are expressed in mole fractions. The value of  $k_1$  for solid  $\text{H}_2$ , 0.019  $\text{hr}^{-1}$  [147], is larger than for liquid  $\text{H}_2$  but decreases with time due to the immobility of molecules in the solid. The initial value of  $k_1$  is restored however by melting and freezing.

#### (b) $\text{D}_2$

The vapor pressures of normal and equilibrium deuterium were measured [149] relative to the vapor pressure of liquid  $n\text{-H}_2$  from 14° to 20.4° K. As these measurements are independent of a temperature scale their functional relations are given. Vapor pressures are expressed in terms of mm of Hg at standard conditions.

*Normal deuterium* (66.67 percent  $o\text{-D}_2$ , 33.33 percent  $p\text{-D}_2$ ):

$$\text{Liquid: } \log_{10} P(n\text{-D}_2) = -1.3376 + 1.3004 \log_{10} \frac{P(n\text{-H}_2)}{P(n\text{-H}_2)} \quad (7.8)$$

$$\text{Solid: } \log_{10} P(n\text{-D}_2) = -1.9044 + 1.5143 \log_{10} P(n\text{-H}_2) \quad (7.9)$$

*20.4°K Equilibrium deuterium* (97.8 percent  $o\text{-D}_2$ , 2.2 percent  $p\text{-D}_2$ ):

$$\text{Liquid: } \log_{10} P(o\text{-D}_2) = -1.3302 + 1.3000 \log_{10} P(n\text{-H}_2) \quad (7.10)$$

$$\text{Solid: } \log_{10} P(o\text{-D}_2) = -1.8873 + 1.5106 \log_{10} P(n\text{-H}_2) \quad (7.11)$$

Substituting for  $\log_{10} P(n\text{-H}_2)$  values given by eq. 7.2 for liquid  $n\text{-H}_2$  the following equations for  $\log_{10} P(\text{D}_2)$  are obtained:

*Normal deuterium* (66.67 percent  $o\text{-D}_2$ , 33.33 percent  $p\text{-D}_2$ ):

$$\text{Liquid: } \log_{10} P(\text{mm Hg}) = 4.7312 - \frac{58.4619}{T} + 0.02671T \quad (7.12)$$

$$\text{Solid: } \log_{10} P(\text{mm Hg}) = 5.1626 - \frac{68.0782}{T} + 0.03110T \quad (7.13)$$

*20.4°K equilibrium deuterium* (97.8 percent  $o\text{-D}_2$ , 2.2 percent  $p\text{-D}_2$ ):

$$\text{Liquid: } \log_{10} P(\text{mm Hg}) = 4.7367 - \frac{58.4440}{T} + 0.02670T \quad (7.14)$$

$$\text{Solid: } \log_{10} P(\text{mm Hg}) = 5.1625 - \frac{67.9119}{T} + 0.03102T \quad (7.15)$$

The triple-point temperatures and pressures for  $\text{D}_2$  given in tables 28 and 29 were obtained by simultaneous solution of the vapor pressure equations for solid and liquid.

The self conversion of nonequilibrium mixtures of  $o$ - and  $p\text{-D}_2$  proceeds at a very much slower rate than for  $\text{H}_2$ . Thus no increase in the vapor pressure of liquid  $n\text{-D}_2$  resulting from self conversion was observed at 20.4° K over a period of 100 hours [149]. The estimated probable error of two observations extending over 100-hour periods was  $\pm 0.27$  mm Hg. The small rate of self conversion of  $\text{D}_2$ , compared with  $\text{H}_2$ , is a result of the smaller magnetic moment of the deuteron compared with the proton. The ratio of nuclear magnetic moments  $\text{D}/\text{H}$  is 0.26. The relative rate of self conversion for the same displacements of  $\text{D}_2$  and  $\text{H}_2$  from the equilibrium ortho-para composition is proportional, as to order of magnitude only, to the fourth power of their relative magnetic moments, that is to 0.005. Allowing for the smaller displacement of  $n\text{-D}_2$  from equilibrium composition and the smaller difference between the vapor pressures of the ortho and para varieties of  $\text{D}_2$ , the expected ratio of the rates of vapor pressure change,  $n\text{-D}_2$  to  $n\text{-H}_2$ , is of the order of  $10^{-3}$ . For a more detailed discussion see reference [149].

#### (c) HD

As the two nuclei of the HD molecule are dissimilar, hydrogen deuteride does not have ortho and para varieties. Measurements of the vapor

pressure of HD extend from 10.4° to 20.4° K [150]. The following vapor-pressure equations were made to fit the triple-point temperature 16.604° K measured with a platinum resistance thermometer in a calorimeter in which the solid and liquid phases were in equilibrium.

HD:

$$\text{Liquid: } \log_{10} P \text{ (mm Hg)} = 5.04964 - \frac{55.2495}{T} + 0.01479 T \quad (7.16)$$

$$\text{Solid: } \log_{10} P \text{ (mm Hg)} = 4.70260 - \frac{56.7154}{T} + 0.04101 T \quad (7.17)$$

The triple-point pressure of HD given in tables 28 and 29 can be obtained from either of these equations.

#### (d) HT and DT

Tritium, T, the hydrogen isotope of atomic weight 3 is radioactive and has a half-lifetime of  $31 \pm 8$  years [151]. Its disintegration products are a negative  $\beta$ -particle and  $\text{He}^3$ . Because of its comparatively short half-life, the natural abundance of T in hydrogen is extremely small. Libby and Barter [152] determined the vapor pressures of HT and DT using T made by the irradiation of a block of metallic Li with neutrons ( $\text{Li}^6 + n \rightarrow \text{He}^4 + \text{T}^3$ ). The tritium held by the Li as LiT was liberated by the reaction of  $\text{H}_2\text{O}$  or  $\text{D}_2\text{O}$  with the Li block. Gaseous  $\text{H}_2$  or  $\text{D}_2$  with a trace of HT or DT was obtained. The gas was liquefied and then evaporated, and the radioactivity of the evaporated vapor was measured as a function of the volume of the remaining unevaporated liquid. From a comparison of the radioactivity of the vapor leaving the liquid during different periods of the evaporation, Libby and Barter calculated the vapor pressures of HT and DT, making use of ideal solution laws for this purpose. They obtained for the vapor pressures of HT and DT,  $254 \pm 16$  and  $123 \pm 6$  mm Hg, respectively, at the normal boiling temperature of hydrogen (20.39° K). By extrapolation, they estimated that the vapor pressure of  $\text{T}_2$  at 20.39° K is  $45 \pm 10$  mm Hg.

## 2. Pressure-Temperature Relations for Solid-Liquid Equilibrium

The melting, or freezing pressures, of  $n\text{-H}_2$ , HD, and  $n\text{-D}_2$  given in table 30 are based on

smooth curves drawn through the experimental data ( $\text{H}_2$ , [153 to 157]; HD [150];  $\text{D}_2$  [174]) and cover the same ranges of pressure and temperature as the data. Figure 21 is a diagram of the deviations of the data for  $n\text{-H}_2$  from the table. The dashed line shows a 1-percent deviation from the table and the full-line curve represents the deviation from the table of the equation

$$\log_{10}(237.1 + P) = 1.85904 \log_{10} T + 0.24731, \quad (7.18),$$

where  $P$  is in  $\text{kg cm}^{-2}$ .

TABLE 30. Melting temperature-pressure relations for  $n\text{-H}_2$ , HD, and  $n\text{-D}_2$

T	$\Gamma$		
	$n\text{-H}_2$	HD	$n\text{-D}_2$
$^{\circ}\text{K}$	$\text{kg cm}^{-2}$	$\text{kg cm}^{-2}$	$\text{kg cm}^{-2}$
13.06.....	0.07	.....	.....
14.....	1.4	.....	.....
16.....	33.2	.....	.....
18.....	67.3	.....	.....
16.60.....	.....	0.13	.....
17.....	103.5	14.2	.....
18.....	142.3	52.6	.....
16.72.....	.....	.....	0.17
19.....	183.8	92.9	13.9
20.....	227.1	.....	36.0
21.....	272.3	.....	100.0
22.....	318.6	.....	.....
23.....	368.0	.....	.....
24.....	415.0	.....	.....
25.....	466.6	.....	.....
26.....	518	.....	.....
27.....	579	.....	.....
28.....	638	.....	.....
29.....	695	.....	.....
30.....	744	.....	.....
32.....	867	.....	.....
34.....	996	.....	.....
36.....	1,131	.....	.....
38.....	1,274	.....	.....
40.....	1,422	.....	.....
45.....	1,821	.....	.....
50.....	2,258	.....	.....
55.....	2,735	.....	.....
60.....	3,249	.....	.....
65.....	3,801	.....	.....
70.....	4,389	.....	.....
75.....	5,014	.....	.....
80.....	5,674	.....	.....

Figure 22 is intended to show the relation between the melting pressures of  $n\text{-H}_2$ , HD, and  $n\text{-D}_2$ . The curve for  $n\text{-H}_2$  is a graph of table values. The curves through the experimental

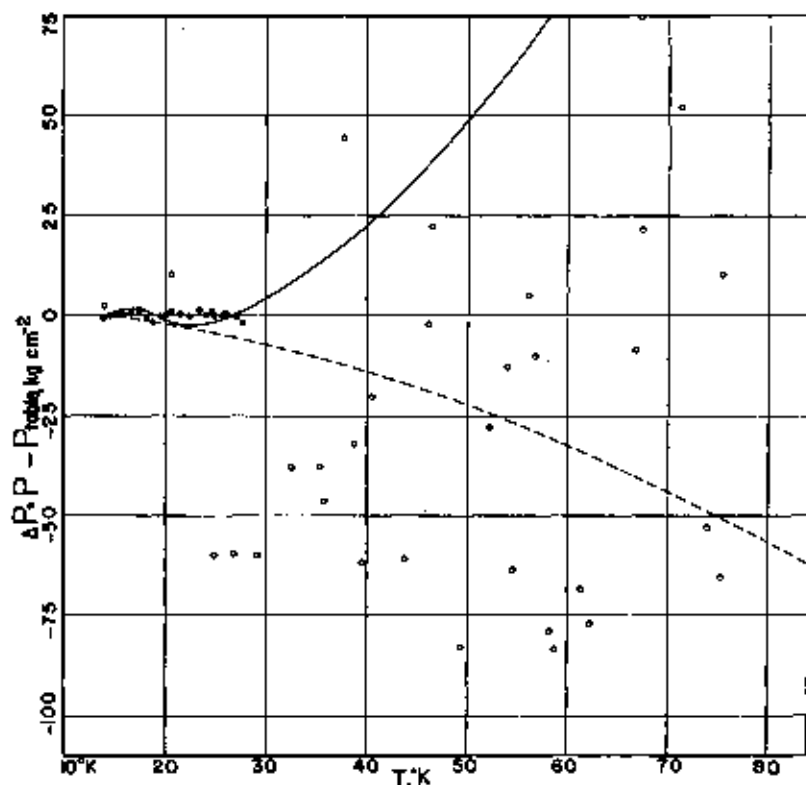


FIGURE 21. Melting pressure of  $n\text{-H}_2$  as a function of temperature.

data for HD and  $\text{D}_2$  were obtained by a simple vertical displacement of the  $\text{H}_2$  curve and show that the differences in melting pressures of the three isotopic varieties are only slightly dependent upon the temperature. These differences in pressure are  $89.6 \text{ kg cm}^{-2}$  for  $\text{H}_2$  and HD and  $170.6 \text{ kg cm}^{-2}$  for  $\text{H}_2$  and  $\text{D}_2$ . As the change of melting pressure with temperature,  $dP/dT$ , has nearly the same value for  $\text{H}_2$ , HD, and  $\text{D}_2$ , if compared at the same temperature, it follows from the Clapeyron equations that  $L_f/\delta V$ , the ratio of the heat of fusion to the change in volume on melting, also has nearly the same value for the three isotopes when compared at the same value of  $T$ . A similar statement can be made for  $S_f/\delta V$ , the ratio of the entropy of fusion to the change in volume on melting.

The table values of melting pressure for HD

and  $\text{D}_2$  were obtained from curves drawn through the experimental data and not from the curves of figure 22.

## VIII. PVT Data for the Condensed States

The available data of state for the condensed phases of  $\text{H}_2$ , HD, and  $\text{D}_2$  are meager [158 to 166] and in general not accurate enough for the calculation of reliable values of thermodynamical properties. The data on the liquid, however, were used in the construction of the liquid regions of the  $\sigma$  versus  $\rho$  diagrams, figure 6, and the  $T$  versus  $S$  diagram, figures 31, 32, and 33.

### 1. Liquid $\text{H}_2$ , HD, and $\text{D}_2$

In table 31 are given the molar volumes of liquid  $n\text{-H}_2$ ,  $p\text{-H}_2$ , HD, and  $n\text{-D}_2$  in equilibrium



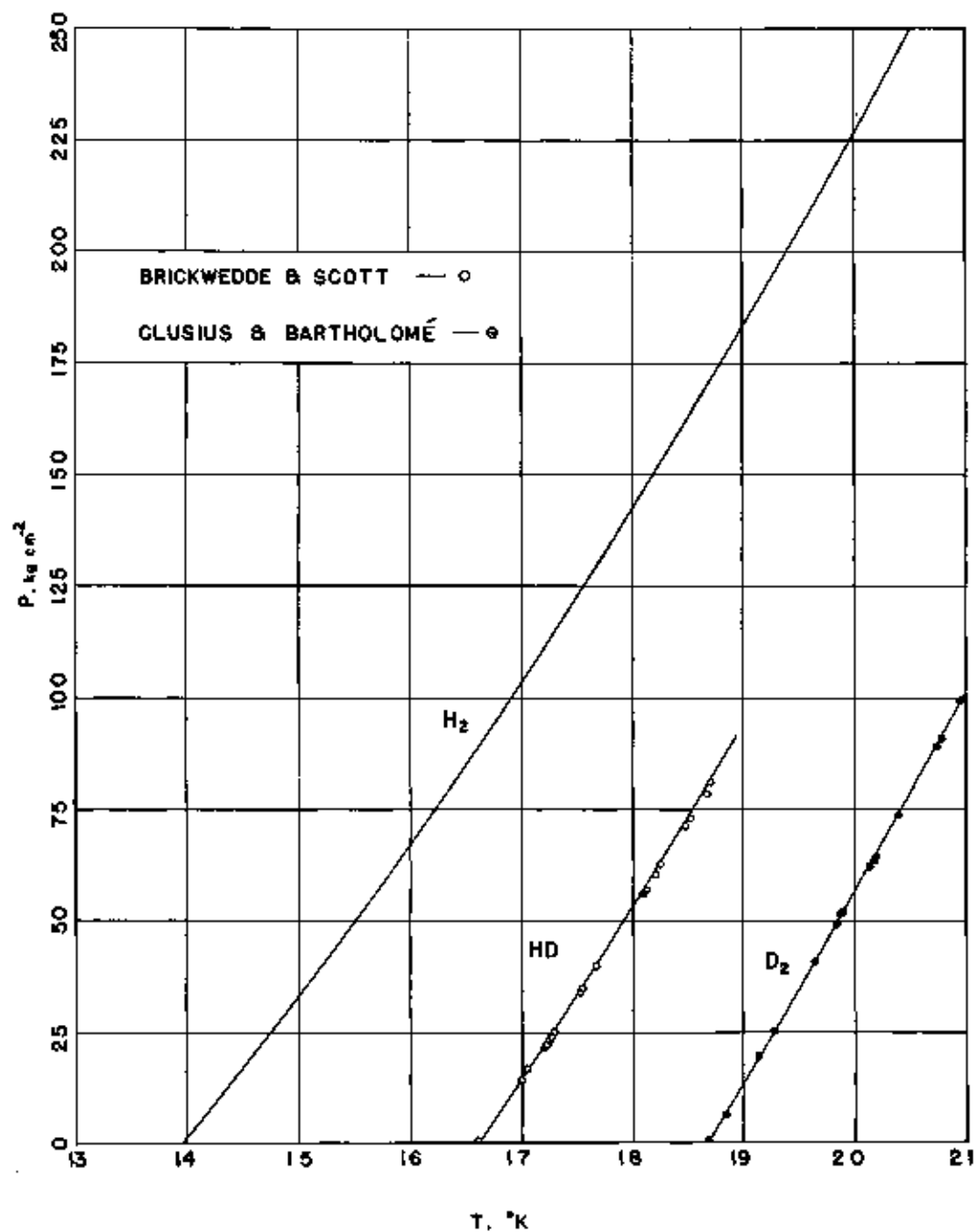


FIGURE 22. Melting pressures of  $n\text{-H}_2$ , HD, and  $n\text{-D}_2$ .

TABLE 31. Molar volumes of normal hydrogen, parahydrogen, normal deuterium, and hydrogen deuteride, in the liquid state

T	Volume of liquid at saturation pressure			
	n-H <sub>2</sub>	p-H <sub>2</sub>	n-D <sub>2</sub>	HD
°K	cm <sup>3</sup> mole <sup>-1</sup>	cm <sup>3</sup> mole <sup>-1</sup>	cm <sup>3</sup> mole <sup>-1</sup>	cm <sup>3</sup> mole <sup>-1</sup>
13.813	.....	25.176	.....	.....
13.96	25.168	.....	.....	.....
14	26.119	25.227	.....	.....
15	26.407	25.513	.....	.....
16	26.721	25.858	.....	.....
16.804	.....	.....	.....	24.487
17	27.081	27.178	.....	24.584
18	27.426	27.549	.....	24.885
18.723	.....	.....	23.162	.....
19	27.816	27.945	23.237	25.211
20	28.232	28.368	23.525	25.572
20.39	28.401	.....	.....	.....
22	29.235	.....	.....	.....
24	30.451	.....	.....	.....
26	31.925	.....	.....	.....
28	34.056	.....	.....	.....
30	37.138	.....	.....	.....
32	43.211	.....	.....	.....
33.19	66.95	.....	.....	.....

with vapor from the triple point to the highest temperature of measurement. From the triple point to 20.4° K, these equilibrium molar volumes have been represented by the following equations, in which temperatures are on the Kelvin scale:

Normal hydrogen [163]:

$$V(\text{cm}^3 \text{ mole}^{-1}) = 24.747 - 0.08005T + 0.012716T^2 \quad (8.1)$$

Parahydrogen [163]:

$$V(\text{cm}^3 \text{ mole}^{-1}) = 24.902 - 0.0888T + 0.013104T^2 \quad (8.2)$$

Hydrogen deuteride [150]:

$$V(\text{cm}^3 \text{ mole}^{-1}) = 24.886 - 0.30911T + 0.01717T^2 \quad (8.3)$$

Normal deuterium [174]:

$$V(\text{cm}^3 \text{ mole}^{-1}) = 22.965 - 0.2460T + 0.0137T^2 \quad (8.4)$$

Table values at 20.39° K and lower were calculated from these equations. Values of the molar volume of liquid normal hydrogen above 20.4° K were obtained from the experimental data of Mathias, Crommelin, and Onnes [161] with the help of a sensitive interpolation method based upon the use

of an empirical equation and a deviation graph. A change was made in the experimental data because the value used by Mathias, Crommelin, and Onnes for the density of gaseous hydrogen at standard conditions differs from that recommended in this paper on page 396.

Bartolomé [177] measured the molar volumes of liquid n-H<sub>2</sub> and n-D<sub>2</sub> as a function of pressure at three temperatures between 16° and 21° K. The measurements extended from the vapor pressure to nearly the freezing pressure. Smoothed values of molar volumes are given in tables 32 and 33. Bartholomé showed that isothermal changes in volume to about 9 percent of the volume of "saturated" liquid can be represented to within the precision of his measurements, ±0.05 cm<sup>3</sup> mole<sup>-1</sup> by Eucken's equation

$$\frac{1}{V^2} = \frac{1}{2} \left[ \frac{1}{v_0^2} + \sqrt{\frac{1}{v_0^2} + \alpha P} \right], \quad (8.5)$$

in which V, the molar volume of the liquid, is expressed as a function of the pressure P. v<sub>0</sub> is the molar volume extrapolated to zero pressure, and α is an empirical constant dependent upon the temperature. Tables 32 and 33 include values of the molar volumes of liquid n-H<sub>2</sub> and n-D<sub>2</sub> at freezing pressure for the three temperatures of Bartholomé's measurements.

TABLE 32. Molar volumes of liquid n-H<sub>2</sub> for various temperatures and pressures.

Pressure	T=16.43° K	T=18.24° K	T=20.33° K
lg cm <sup>-1</sup>	cm <sup>3</sup> mole <sup>-1</sup>	cm <sup>3</sup> mole <sup>-1</sup>	cm <sup>3</sup> mole <sup>-1</sup>
0°	26.87	27.54	28.43
10	26.59	27.18	27.97
26	26.20	26.72	27.40
50	25.66	26.10	26.63
75	25.20	25.59	25.96
82.6	25.08	.....	.....
100	.....	25.14	25.42
125	.....	24.71	24.91
150	.....	24.30	24.47
151.98	.....	24.27	.....
175	.....	.....	24.09
200	.....	.....	23.76
225	.....	.....	23.48
241.63	.....	.....	23.31
	$\alpha = 3.90 \times 10^{-11} \frac{\text{mole}^2}{\text{cm}^4 \text{kg}}$	$\alpha = 3.93 \times 10^{-11} \frac{\text{mole}^2}{\text{cm}^4 \text{kg}}$	$\alpha = 4.16 \times 10^{-11} \frac{\text{mole}^2}{\text{cm}^4 \text{kg}}$

\* The values at zero pressure were obtained by extrapolation consistent with the molar volumes at saturation vapor pressure given by eq. 8.1.

TABLE 33. Molar volumes of liquid  $n\text{-D}_2$  for various temperatures and pressures

Pressure	$T=19.70^\circ\text{K}$	$T=20.31^\circ\text{K}$	$T=20.97^\circ\text{K}$
$l_g\text{ cm}^{-2}$	$\text{cm}^3\text{ mole}^{-1}$	$\text{cm}^3\text{ mole}^{-1}$	$\text{cm}^3\text{ mole}^{-1}$
0 <sup>a</sup> .....	23.44	23.33	23.34
10.....	23.24	23.37	23.50
20.....	23.05	23.15	23.35
30.....	22.89	22.97	23.14
40.....	22.74	22.79	22.95
43.18.....	22.70	.....	.....
50.....	.....	22.63	22.77
60.....	.....	22.49	22.50
69.46.....	.....	22.36	.....
70.....	.....	.....	22.45
80.....	.....	.....	22.30
90.....	.....	.....	22.16
98.67.....	.....	.....	22.05
	$\alpha=5.75\times 10^{-11}\frac{\text{mole}^2}{\text{cm}^3\text{ kg}}$	$\alpha=7.20\times 10^{-11}\frac{\text{mole}^2}{\text{cm}^3\text{ kg}}$	$\alpha=7.37\times 10^{-11}\frac{\text{mole}^2}{\text{cm}^3\text{ kg}}$

<sup>a</sup> The values at zero pressure were obtained by extrapolation consistent with the molar volumes at saturation vapor pressure given by eq 8.4.

## 2. Solid $\text{H}_2$ , HD, and $\text{D}_2$

The crystal structure of solid hydrogen is thought to be hexagonal close-packed, on the basis of an X-ray investigation of solid parahydrogen by the Debye-Scherrer method at the temperature of liquid helium, conducted by Keesom, de Smedt, and Mooy [162].

Tables 34 and 35 contain all the available experi-

mental data of state on solid  $\text{H}_2$ , HD, and  $\text{D}_2$ . Molar volumes at  $0^\circ\text{K}$  were obtained by calculation.

Molar volumes of the solid at the triple point given in table 34 were obtained by subtracting the volume changes on fusion from the triple point volumes of the liquid calculated from eq 8.1, 8.3, and 8.4. The volume changes on fusion, given in table 34, were calculated using the Clapeyron equation with the calorimetrically measured heats of fusion (section IX, 3), and  $dP/dT$  for the solid-liquid equilibrium at the triple point (section VII, 2).

Molar volumes of the solid in table 34 above the triple-point temperature were obtained from Bartholome's measurements of the change in volume on fusion at the temperatures given in table 34, and the volumes of the liquid at melting pressure given in tables 32 and 33.

The molar volumes of solid  $\text{H}_2$  and  $\text{D}_2$  at  $4.2^\circ\text{K}$  in table 34 were measured by Megaw [165] with a pycnometer in which the solid  $\text{H}_2$  or  $\text{D}_2$  was surrounded with liquid helium, the volume of which had previously been measured as a function of pressure at this temperature. The compressibilities of solid  $\text{H}_2$  and  $\text{D}_2$  at  $4.2^\circ\text{K}$ , given in table 35, were calculated by Miss Megaw from the results of these measurements.

TABLE 34. Molar volumes of solid  $n\text{-H}_2$ , HD and  $n\text{-D}_2$  and volume changes upon fusion

T	P	$n\text{-H}_2$		HD		$n\text{-D}_2$		Remarks
		Volume of solid	Volume change on fusion	Volume of solid	Volume change on fusion	Volume of solid	Volume change on fusion	
$^\circ\text{K}$	$\text{kg/cm}^2$	$\text{cm}^3/\text{mole}$	$\text{cm}^3/\text{mole}$	$\text{cm}^3/\text{mole}$	$\text{cm}^3/\text{mole}$	$\text{cm}^3/\text{mole}$	$\text{cm}^3/\text{mole}$	
20.97.....	98.7	.....	.....	.....	.....	20.67	1.96	T and P for solid-liquid equilibrium.
20.31.....	99.5	.....	.....	.....	.....	20.20	2.15	
18.72.....	0.17 <sub>1</sub>	.....	.....	.....	.....	20.48	2.65	$n\text{-D}_2$ triple point.
16.60.....	.126	.....	.....	21.94	2.65	.....	.....	HD triple point.
14.24.....	102.0	22.24	2.03	.....	.....	.....	.....	T and P for solid-liquid equilibrium.
16.43.....	82.6	22.78	2.30	.....	.....	.....	.....	
12.96.....	0.07 <sub>1</sub>	23.25	2.85	.....	.....	.....	.....	$n\text{-H}_2$ triple point.
4.2.....	.....	22.55	.....	.....	.....	19.66	.....	Solid-vapor equilibrium.
4.2.....	0	22.85	.....	.....	.....	19.56	.....	Smoothed values based on direct experimental determination.
4.2.....	10	23.49	.....	.....	.....	19.50	.....	
4.2.....	25	23.30	.....	.....	.....	19.41	.....	
4.2.....	50	23.03	.....	.....	.....	19.28	.....	
4.2.....	75	21.80	.....	.....	.....	19.15	.....	
4.2.....	100	21.60	.....	.....	.....	19.06	.....	
0.....	0	22.57	.....	.....	.....	19.49	.....	By calculation.

TABLE 35. Experimentally determined compressibilities,

$$\frac{1}{V} \left( \frac{dV}{dP} \right)_T, \text{ of solid H}_2 \text{ and D}_2 \text{ at } 4.2^\circ \text{ K}$$

Compressibility	H <sub>2</sub> compressibility	D <sub>2</sub> compressibility
At pressure 0 kg cm <sup>-2</sup> .....	kg <sup>-1</sup> cm <sup>3</sup> (5.8 ± 1.5) × 10 <sup>-4</sup>	kg <sup>-1</sup> cm <sup>3</sup> (4.5 ± 2) × 10 <sup>-4</sup>
At pressure 100 kg cm <sup>-2</sup> .....	3.2 × 10 <sup>-4</sup>	2.1 × 10 <sup>-4</sup>
Average for range 0 to 100 kg cm <sup>-2</sup> .	(5.0 ± 0.5) × 10 <sup>-4</sup>	(3.3 ± 0.7) × 10 <sup>-4</sup>

Miss Megaw calculated the expansivities of solid H<sub>2</sub> and D<sub>2</sub> at 4.2° and 11° K, given in table 36, using the formula

$$C_p - C_v = TV \left( \frac{dV}{dT} \right)_P^2 / \left( \frac{dV}{dP} \right)_T, \quad (8.6)$$

with the calorimetrically determined specific heats at constant pressure and volume, and the compressibility measured at 4.2° K (table 35).

TABLE 36. Expansivities,  $\frac{1}{V} \left( \frac{dV}{dT} \right)_P$ , of solid H<sub>2</sub> and D<sub>2</sub> calculated from  $C_p - C_v$

T	H <sub>2</sub>	D <sub>2</sub>
° K	° K <sup>-1</sup>	° K <sup>-1</sup>
4.2	0.24 × 10 <sup>-2</sup>	0.17 × 10 <sup>-2</sup>
11	.51 × 10 <sup>-2</sup>	.37 × 10 <sup>-2</sup>

The compressibilities and expansivities of solid H<sub>2</sub> and D<sub>2</sub> are large when compared with values of these properties for other substances. This is ascribed to the zero-point vibrational energy of the lattice which for hydrogen is an unusually large fraction of the negative potential energy of the lattice. This accounts also for an unusually large variation in the compressibilities of H<sub>2</sub> and D<sub>2</sub> with pressure (see table 35), and for the variation with  $T$  and  $V$  of  $d \ln \theta / d \ln V$ , which derivative of the Debye  $\theta$  is usually regarded as a constant for other solids [165].

## IX. The Thermal Properties of the Condensed Phases

In this section are included the calorimetrically measured properties: specific heats and heats of fusion and vaporization.

### 1. Specific Heats of the Solids and Liquids

#### (a) Hydrogen

The specific heats at saturation pressure of solid and liquid hydrogen were measured (1923) by

Simon and Lange [171] between 10° and 20° K, before the discovery of parahydrogen. Clusius and Hiller [172] measured (1929) the specific heats of solid and liquid parahydrogen over the same range of temperatures and obtained the same values, within experimental error, for the specific heats of parahydrogen as had been obtained by Simon and Lange for supposedly normal hydrogen. Mendelsohn, Ruhemann, and Simon [173] measured (1931) the specific heats of several mixtures of ortho- and parahydrogen between 2.5° and 11.5° K. Their results on pure parahydrogen were in agreement with the earlier measurements of Clusius and Hiller, the data from 2.5° to

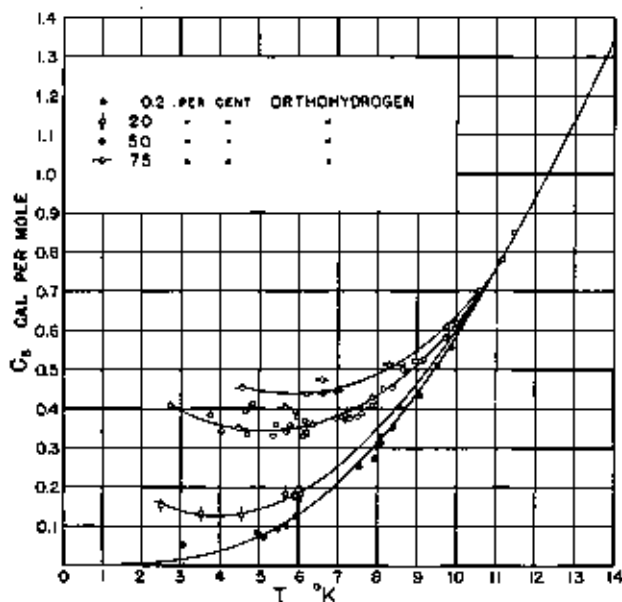


FIGURE 23. Specific heat,  $C_p$ , of solid H<sub>2</sub> for various ortho-para compositions.

14° K fitting rather closely a Debye function with  $\theta = 91^\circ \text{ K}$ .

The data of Mendelsohn, Ruhemann, and Simon are shown in figure 23. It is seen that, at temperatures below 11° K, the specific heats of mixtures containing orthohydrogen are larger than for pure parahydrogen. This difference in specific heats is connected with the multiplicity of states belonging to the lowest  $\sigma$ -H<sub>2</sub> rotational level,  $J=1$ . The different states, three in number, correspond to three different orientations of the angular momentum vector of an  $\sigma$ -H<sub>2</sub> molecule relative to the electric field in the hydrogen crystal. At 0° K, all  $\sigma$ -H<sub>2</sub> molecules are in the orientation state of lowest energy. At tempera-

tures of the order of  $\Delta E/k$ , where  $\Delta E$  is the difference in the energy of the states, the distribution of  $o\text{-H}_2$  molecules over the three states changes rapidly with change of temperature. Along with this there is an absorption of energy and an increase in specific heat. As temperatures are approached that are high compared with  $\Delta E/k$ , the distribution of  $o\text{-H}_2$  molecules becomes uniform over the three orientation states, and the specific heat of orientation approaches zero. It may be seen from figure 23 that  $12^\circ\text{K}$  is effectively a high temperature for this distribution, and that at temperatures above  $12^\circ\text{K}$  the distribution over the three  $J=1$  states must be practically uniform.

The specific heats,  $C_s$ , of liquid and solid hydrogen along the saturated vapor lines are given in table 37. The  $C_s$  curves of figures 24, 25, and 26 for  $n\text{-H}_2$  at temperatures above  $11^\circ\text{K}$  represent this table.

In figures 25 and 26 the heat capacity,  $C_s$ , of

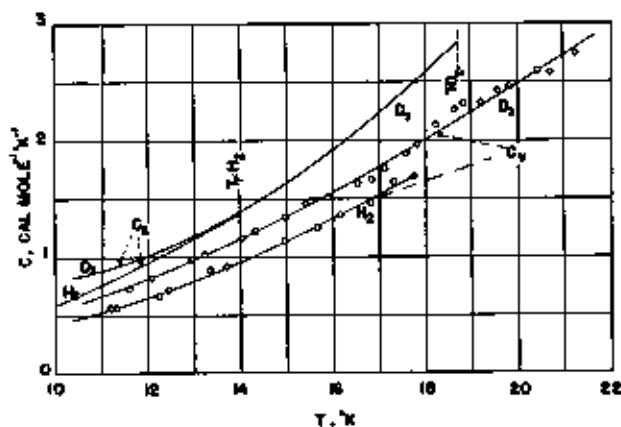


FIGURE 25. Specific heats,  $C_s$  and  $C_l$ , of solid  $\text{H}_2$  and  $\text{D}_2$ .

solid and of liquid  $n\text{-H}_2$  at constant specified values of the density are compared with the heat capacity,  $C_s$ , of solid and liquid  $n\text{-H}_2$  in equilibrium with saturated vapor. It is to be noted that the  $C_s$  curves of these two figures are not for  $C_s$  of solid and liquid  $\text{H}_2$  along a line of equilibrium of vapor and condensed phase. The  $C_s$  measurements on the solid were made by Bartholomé and Eucken [176] at the density of solid  $\text{H}_2$  at a melting temperature of about  $19^\circ\text{K}$ . The  $C_s$  measurements for the liquid were made by Eucken [169] and by Bartholomé and Eucken at densities ranging from  $0.034$  to  $0.077\text{ g cm}^{-3}$  (380 Amagats to 860 Amagats). The density of liquid  $n\text{-H}_2$  at its normal boiling point is  $0.07097\text{ g cm}^{-3}$  (789.7 Amagats).

The difference between  $C_s$  in figure 25 for the solid at constant density and  $C_s$  at densities of the solid along the solid-vapor equilibrium line is small. The corresponding difference for the liquid is larger and, at the critical temperature  $33.19^\circ\text{K}$ , is of the order of 1 or 2  $\text{cal mole}^{-1}\text{K}^{-1}$

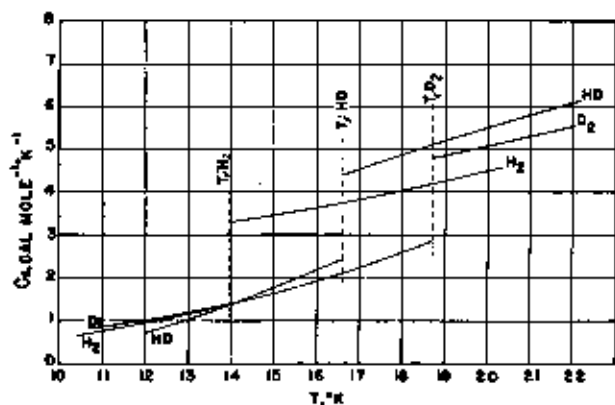


FIGURE 24. Specific heat,  $C_s$ , of solid and liquid  $\text{H}_2$ , HD, and  $\text{D}_2$ .

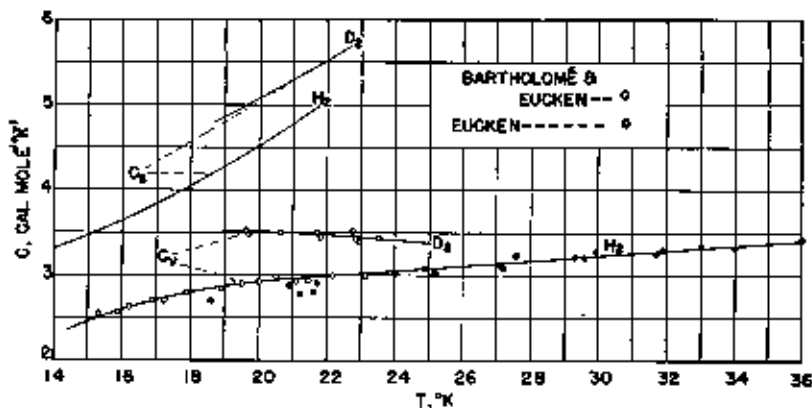


FIGURE 26. Specific heats,  $C_s$  and  $C_l$ , of liquid  $\text{H}_2$  and  $\text{D}_2$ .

TABLE 37. Specific heats at saturation pressure of normal hydrogen, normal deuterium, and hydrogen deuteride in the solid and liquid states

T	Hydrogen		Deuterium		Hydrogen deuteride	
	$C_p$	State	$C_p$	State	$C_p$	State
$^{\circ}K$	cal mole <sup>-1</sup> deg <sup>-1</sup>		cal mole <sup>-1</sup> deg <sup>-1</sup>		cal mole <sup>-1</sup> deg <sup>-1</sup>	
10	0.68	Solid				
11	.78	do	0.88	Solid		
12	.95	do	1.00	do	0.69	Solid
13	1.18	do	1.19	do	1.03	Do.
13.96	1.37	do				
13.96	3.31	Liquid				
14	3.31	do	1.39	do	1.39	Do.
15	3.45	do	1.63	do	1.76	Do.
16	3.63	do	1.90	do	2.17	Do.
16.00					2.42	Do.
16.00					4.40	Liquid
17	3.83	do	2.21	do	4.53	Do.
18	4.04	do	2.56	do	4.88	Do.
18.72			2.84	do		
18.72			4.80	Liquid		
19	4.27	do	4.98	do	5.20	Do.
20	4.50	do	5.08	do	5.49	Do.
21			5.30	do	5.79	Do.
22			5.52	do	6.09	Do.

$C_p$  along the liquid-vapor line being greater [176].

The difference between  $C_p$  and  $C_v$  for hydrogen is large when compared with the differences for other substances having higher boiling temperatures. In general,  $(C_p - C_v)$  is large for low-boiling substances because of their larger expansivities.

The Debye  $\Theta$  in the Debye specific heat function that fits the  $C_p$  data on solid  $H_2$  is  $105^{\circ}K$ . This may be compared with  $91^{\circ}K$  for  $C_v$ .

The specific heats at constant pressure of compressed liquid hydrogen and gaseous hydrogen were measured by Gutsche [178] for temperatures from  $16^{\circ}K$  to  $38^{\circ}K$  and for pressures of about 10, 25, 40, 60, 80, and 100 kg cm<sup>-2</sup>, using a calorimeter so arranged that approximate constancy of pressure was maintained by manual operation of valves permitting fluid to pass from the calorimeter. As a result of this experimental procedure, the mass of hydrogen in the calorimeter was smaller at the higher temperatures, and consequently the accuracy of measurement is probably lower at the higher temperatures.

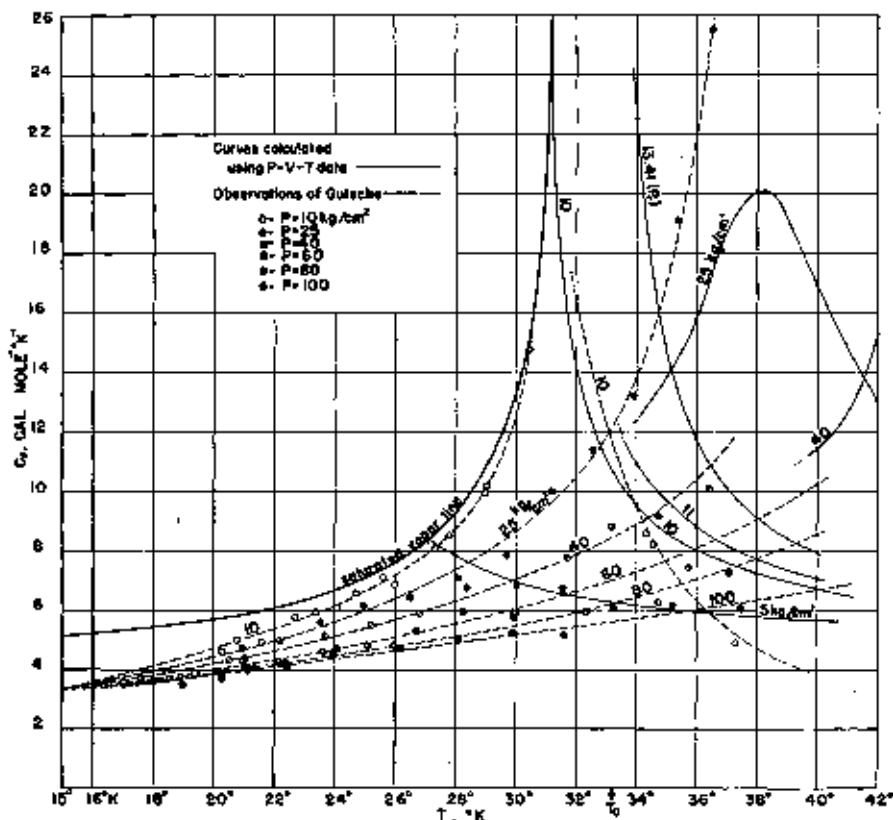


FIGURE 27. Specific heat,  $C_p$ , of compressed liquid and gaseous  $H_2$ .

In figure 27 are plotted Gutsche's experimental data with dotted curves as drawn by Gutsche in his paper to represent the experimental data. The full line curves apply only to the vapor and were obtained by calculation from the PVT correlations of preceding sections of the paper and specific heats in the ideal gas state, table 8. The heavy curve shows  $C_p$  for saturated vapor. The full-line curves beginning on this heavy curve, or saturated vapor line, sloping downward toward the right represent the specific heats,  $C_p$ , for the vapor at pressures of 5 and 10 kg cm<sup>-2</sup>. Parts of similar curves also based on the PVT data are shown for 11 and for 13.41 kg cm<sup>-2</sup>, the critical pressure.

For temperatures above the critical, the dashed curves of Gutsche for 10, 25, and 40 kg cm<sup>-2</sup> are quite different from the full line curves based on PVT data. The dashed curve for the gas at 10 kg cm<sup>-2</sup> is certainly incorrect at the highest temperatures, as the actual deviation from the ideal gas law for hydrogen is such as to increase  $C_p$  above the approximately 5 cal deg<sup>-1</sup> mole<sup>-1</sup> of the ideal gas at these temperatures.

It is seen in figure 27 that Gutsche's experimental values for the liquid scatter considerably. It is believed that Gutsche's recommended values of  $C_p$  for liquid hydrogen, represented by the dashed lines in figure 27, are too high. In figure 30 are shown two sets of isobars,  $E$  and  $E'$ , on a temperature-entropy diagram for liquid hydrogen. The full-line curves,  $E$ , were calculated from Gutsche's  $C_p$  data; the dashed curves,  $E'$ , are the best fit for all the thermal and state data on liquid hydrogen and are the ones used in the construction of the temperature-entropy diagram. As  $(dS/dT)_E = C_p/T$ , the two sets of isobars,  $E$  and  $E'$ , imply different  $C_p$ 's and show that Gutsche's values of  $C_p$  are too high to be consistent with the other data on liquid hydrogen. The differences are of the order of 15 percent in the  $C_p$ 's of liquid hydrogen. The ratio  $C_p/C_v$  for liquid hydrogen in equilibrium with vapor was calculated from the velocity of sound in liquid hydrogen, and  $C_p$  was obtained by combining this calculated value of the ratio ( $C_p/C_v$ ), with  $C_v$  from figure 26. Pitt and Jackson [175] obtained the value 1,127 m sec<sup>-1</sup> for the velocity of sound in liquid hydrogen at 20.46° K. Using this with a value of  $(dV/dP)$  extrapolated from Bartholomé's data (VIII), one obtains a value of 5.07 cal deg<sup>-1</sup> mole<sup>-1</sup> for  $C_p$ ,

for liquid hydrogen in equilibrium with vapor ( $\sim 1$  atm) at 20.46° K.

This is slightly lower than would probably be obtained by extrapolating Gutsche's curves to 1 atm.

#### (b) D<sub>2</sub> and HD

In figure 24 the specific heats  $C_p$  at saturation pressure of liquid and solid *n*-D<sub>2</sub> and HD are compared with  $C_p$  for H<sub>2</sub>. The D<sub>2</sub> measurements were made by Clusius and Bartholomé [174] and the HD measurements by Brickwedde and Scott [150]. The solid D<sub>2</sub> data are fitted, within experimental accuracy, by a Debye function with  $\Theta = 89^\circ$ . The data on solid HD, however, can not be fitted over the range of measurement with a single value of  $\Theta$ . Thus  $\Theta$  for  $C_p$  of HD at 16.3° K is 79°, whereas for 12.5° K,  $\Theta$  is 98°. As the Debye function is intended to represent  $C_p$ , this failure to fit the  $C_p$  data is not surprising.

In figures 25 and 26 the specific heat  $C_p$  at constant volume of solid and liquid D<sub>2</sub> is compared with  $C_p$  for D<sub>2</sub> and  $C_p$  for H<sub>2</sub>. A Debye function with  $\Theta = 97^\circ$  fits within experimental accuracy the  $C_p$  data for solid D<sub>2</sub>. This value of  $\Theta$  for solid D<sub>2</sub> may be compared with 105° for solid H<sub>2</sub>. According to the simple theory of lattice vibrations, which assumes simple harmonic restoring forces in the lattice,  $\Theta$  would be proportional to  $1/\sqrt{M}$  and the  $\Theta$ 's for H<sub>2</sub> and D<sub>2</sub> would be in the ratio  $\sqrt{4/2} = 1.41$ . The ratio of the experimental values however, is 1.08. This is evidence that the lattice restoring forces in solid H<sub>2</sub> and D<sub>2</sub> are strongly anharmonic.

## 2. Latent Heats of Vaporization

#### (a) Normal Hydrogen

Simon and Lange [171] measured the heat of vaporization of normal hydrogen at several temperatures between the triple point and the boiling point. They found that heat of vaporization, in calories per mole, was given by

$$L_v = 219.7 - 0.27(T - 16.6)^2, \quad (9.1)$$

where  $T$  is the Kelvin temperature.

#### (b) Mixtures of *o*-H<sub>2</sub> and *p*-H<sub>2</sub>

As orthohydrogen and parahydrogen are very closely related, it might be expected that their mixtures would have properties related very simply to those of the pure components. Never-

theless, the  $H_2$  vapor-pressure data of Brickwedde and Scott [146] given by the equations and graphs of Section 7 show that the ortho-para  $H_2$  mixtures do not follow Raoult's law for ideal solutions. A simple application of the Clapeyron equation in the form applying to a pure substance indicates that the latent heat of vaporization and the internal energy of the liquid and solid do not follow a linear, but rather an approximately quadratic dependence upon the composition. This same qualitative result is obtained when account is taken of change of composition by fractionation during vaporization. Functions approximately linear in  $x$ , the ortho mole fraction, are obtained when  $L_{mix} - L_{eq}$ , the difference in latent heats, and  $E_{eq} - E_{mix}$ , the difference in the internal energy, are divided by  $x_{mix} - x_{eq}$ , the corresponding difference in the ortho mole fraction. The subscript "eq" indicates the ortho-para mixture that is at equilibrium at 20.4° K, containing 0.21 percent of ortho- and 99.79 percent of parahydrogen. The subscript "mix" refers to any other mixture for which data were obtained. When the line for  $\Delta E/\Delta x$  is horizontal, it indicates that ideal solution laws apply. The line has a clear indication of slope, as shown by the continuous lines in figure 28, indicating that ideal solution laws do not apply. In the graph for  $\Delta E/\Delta x$ , the points for the liquid include a contribution of about 7 percent related to change of composition due to fractionation. The lower dashed line shows the result when this correction is omitted. For the solid it was thought proper to omit the correction for this effect because departure from equilibrium due to slowness of diffusion in the solid would make it too uncertain. The upper dashed line shows the result for the solid when such a correction for fractionation is included.

The use of straight lines for  $\Delta E/\Delta x$ , the divided difference of the internal energy, has a theoretical justification apart from the fact that the scattering of individual values is so great as to obscure the exact shape of the curve for the liquid. If the internal energy of the liquid is a simple sum of independent energies of different molecular pairs, all of essentially equal probability of formation, then the energy has the form

$$E = x^2 E_{oo} + 2x(1-x) E_{op} + (1-x)^2 E_{pp} \quad (9.2)$$

In this case, the differences  $E_{eq} - E_{mix}$  divided by the corresponding differences in  $x$  for the mix-

tures of different compositions will be linearly dependent on  $x$ . The slope of this line is  $2E_{op} - E_{oo} - E_{pp}$  and the value of the ordinate at  $x = x_{eq}$  is  $2(E_{pp} - E_{op})$ . From the curves in figure 28, it will thus be found that  $E_{op} - E_{oo}$  is 0.7 cal mole<sup>-1</sup> and  $E_{pp} - E_{oo}$  is 4.2 cal mole<sup>-1</sup> for the liquid. For the solid the corresponding values are 0.6 cal mole<sup>-1</sup> and 5.4 cal mole<sup>-1</sup>, respectively. The relative size of  $E_{pp} - E_{oo}$  as compared to  $E_{op} - E_{oo}$  suggests that most of the deviation from ideal solution laws is due to special effects between *o*- $H_2$  molecules.

From the scattering of the points plotted, it appears that ordinates are uncertain to 0.2 or 0.3 cal mole<sup>-1</sup> for the liquid and possibly to 1 cal mole<sup>-1</sup> for the solid. The use of the straight line for  $\Delta L/\Delta x$  in figure 29 is very nearly consistent with its use for  $\Delta E/\Delta x$  and is allowed within the scattering of the data. Combining the results for the dependence upon composition with the results of Simon and Lange for normal hydrogen, the latent heat of vaporization of liquid hydrogen in calories per mole is approximately

$$217.0 - 0.27(T - 16.6)^2 + 1.4x + 2.9x^2 \quad (9.3)$$

for any mixture of *o*- $H_2$  and *p*- $H_2$ , where  $x$  is the orthohydrogen mole fraction.

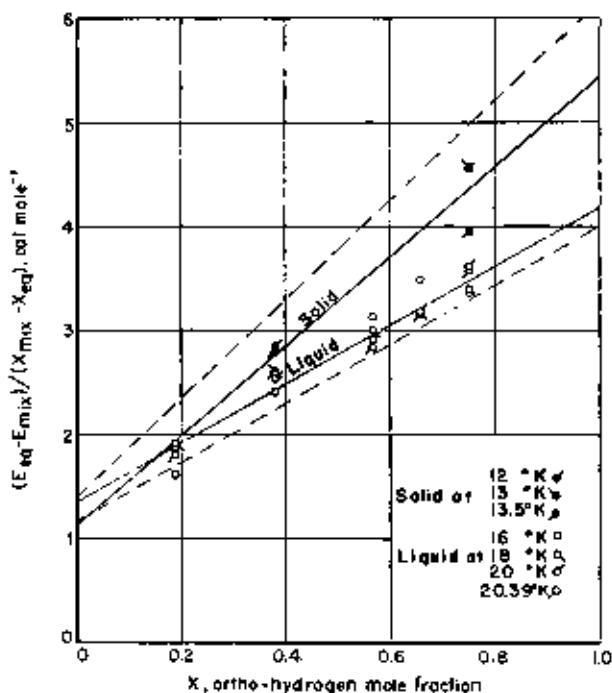


FIGURE 28. Dependence of internal energy of solid and liquid  $H_2$  upon the ortho-para composition.



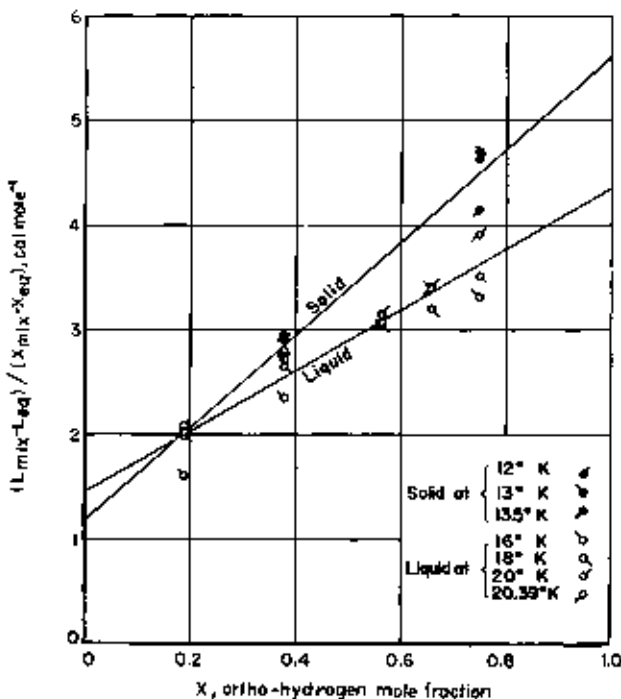


FIGURE 29. Dependence of latent heats of vaporization and sublimation of hydrogen upon the ortho-para composition.

The heats of fusion of para- and normal hydrogen are reported in table 38 as being equal within 0.03 cal mole<sup>-1</sup>. On the basis of the two distinct straight lines for liquid and solid hydrogen in figure 29, it would be expected that the difference would be about 0.7 cal mole<sup>-1</sup>. The reason for this discrepancy is not known, though it may suggest that the lines for the liquid and solid should be more nearly identical.

TABLE 38. Latent heats of fusion

Substance	Heat of fusion	T	P
	cal mole <sup>-1</sup>	°K	mm Hg
Normal hydrogen.....	28.0	13.95	54.0
Parahydrogen.....	28.0	13.91	52.8
Normal deuterium.....	47.0	18.72	128.5
Hydrogen deuteride.....	38.1	18.60	92.8

The manner in which the vapor pressures depend on composition and temperature has formed the basis for the treatment of latent heats of vaporization given in this section. Cohen and Urey [166] and Schäfer [164] have given theoretical discussions of the vapor pressures of ortho and

para H<sub>2</sub> and D<sub>2</sub>. Cohen and Urey did not expect deviations from the law of perfect solutions. Schäfer suggested that forces connected with rotation within the crystal lattice might account for vapor-pressure differences.

#### (c) Normal Deuterium

Clusius and Bartholomé [174] measured the heat of vaporization of normal deuterium, obtaining the value 302.3 cal mole<sup>-1</sup> at 19.70° K.

#### (d) Mixtures of *o*-D<sub>2</sub> and *p*-D<sub>2</sub>

The difference in latent heats of vaporization and the approximate difference in internal energies have been calculated from the vapor pressures of the normal and the 20.4° K equilibrium mixtures of ortho- and paradeterium measured by Brickwedde, Scott, and Taylor [149]. PVT data for deuterium as determined by Schäfer were also used in the calculation. As there are data for only two compositions, giving only one difference of composition, it is not possible either to correct for fractionation or to test for deviation from Raoult's Law. It seems improbable that the law holds for deuterium, as it does not hold for hydrogen. The indicated differences in latent heats of vaporization are smaller than for hydrogen. Thus,  $L_{norm} - L_{eq} = 0.3$  cal mole<sup>-1</sup> for the liquid and 1.0 cal mole<sup>-1</sup> for the solid. The same values are obtained for the differences in internal energies,  $E_{eq} - E_{norm}$ . Cohen and Urey [166] on the basis of their theoretical calculations, concluded that differences in binding energy between corresponding forms should be half as great for D<sub>2</sub> as for H<sub>2</sub>. Considering that the uncertainties in the data for D<sub>2</sub> are comparable with the magnitudes themselves, the data can not be said to conflict with the theoretical prediction.

#### (e) Hydrogen Deuteride

Brickwedde and Scott [146] measured the heat of vaporization of hydrogen deuteride, obtaining the value 257 cal mole<sup>-1</sup> at 22.54° K.

### 3. Latent Heats of Fusion

The latent heats of fusion of hydrogen, parahydrogen, normal deuterium, and hydrogen deuteride were measured by Simon and Lange [171], Clusius and Hiller [172], Clusius and Bartholomé [174], and by Brickwedde and Scott [150], respec-

tively, and are listed in table 38 with corresponding vapor pressures and temperatures.

## X. The Temperature-Entropy Diagram

### 1. Data

Data of several different types were used in determining the temperature-entropy diagram. For the vapor, and for the gas below a density of 500 Amagats, values of the various quantities were obtained by interpolation from tables 14, 22, and 23. The particular difficulties encountered in treating the liquid region will be evident from the

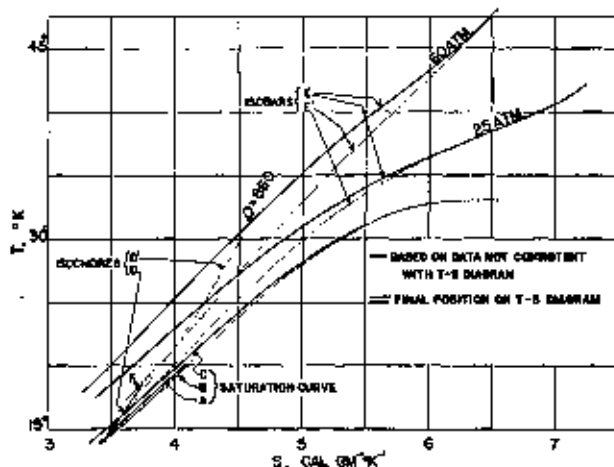


FIGURE 30. Discrepancies in the thermal data for  $H_2$  in the region of the liquid.

following discussion. Discrepancies between the various data for the liquid are shown in figure 30.

Between the triple point and the boiling point, the entropy of liquid normal hydrogen at saturation pressure was obtained using calorimetric data for the solid and liquid and adding a theoretical value for the entropy of mixing. The result is shown as line *B* in figure 30. The entropy of the liquid was also calculated using the theoretical entropy of the ideal gas, correcting to the state of saturated vapor and subtracting the latent heat of vaporization. The latent heat of vaporization was determined in two ways—by direct calorimetric measurement and by using vapor pressures and other data with the Clapeyron equation. Line *A* is based on calorimetric latent heats and line *C* on latent heats from vapor pressures. At 20° K, line *B* indicates values 0.03 cal deg<sup>-1</sup> g<sup>-1</sup> greater than line *A* and 0.08 cal deg<sup>-1</sup> g<sup>-1</sup> greater than line *C*.

Lines of constant density could be obtained for the compressed liquid by integrating  $C_p/T$ , beginning at line *B*. Values of  $C_p$  from figure 26 were used. The results indicate that these constant density lines are approximately parallel at a given temperature for densities less than 500 Amagats. Data of table 14 indicate that there is a similar parallelism for higher densities near the critical temperature.

Values of entropy of the liquid for various pressures along the 17.34° K and 19.28° K isotherms were obtained by integration of the equation

$$(dS/dP)_T = -(dV/dT)_P. \quad (10.1)$$

The values used for  $(dV/dT)_P$  were based on smoothed values of volume for the liquid as given in table 32 for the temperatures 16.43° K, 18.24° K, and 20.33° K. The constant of integration was chosen to fit line *B*. From the results, a set of constant pressure lines, of which the segment *F* is typical, was obtained for various pressures. In addition, a point that should have been on the 860 Amagat density line was obtained by interpolation and a line *D* was drawn through it and through the 860 Amagat density point on line *B* as determined by eq 8.1. The line marked *D'* represents the final correlation.

An unsatisfactory set of values of entropy for the liquid along constant pressure lines was obtained by integrating the  $C_p$  data of Gutsche, figure 27. Curves *E* are the results for 25 and 60 atm, while the final correlation gave curves *E'*.

### 2. Final Correlation

In the final correlation, the saturation curve *B* was accepted and the isochores were considered parallel. The isochores at high density were given by integration of  $C_p/T$ , beginning on line *B*. The isochores at intermediate density were obtained by interpolation between values at high density and values below 500 Amagats. The interpolation was made along the 35° K isotherm from an entropy-density plot extending from  $\rho=860$  Amagats to  $\rho=340$  Amagats.

The extension of curve *B* to temperatures higher than were given by calorimetric data for the liquid was made from the lower parts of the interpolated isochores and the temperature-density relations for the liquid at saturation pressure given by eq 8.1.

The constant pressure lines were determined mainly from the vapor-pressure equation and the equation

$$(dS/dV)_T = (dP/dT)_V. \quad (10.2)$$

At lower temperatures the lines were in fair agreement with Bartholome's PVT data, which served to locate them more closely.

The lines of constant enthalpy were determined from integrals of  $TdS$  under the constant pressure lines and were checked by integration along the isochores based on the equation

$$(dH/dT)_P = T(dS/dT)_V + V(dS/dV)_T. \quad (10.3)$$

The location of the curves within the dome is quite straightforward, as the fractionation of the

ortho-para mixture is too small to affect these curves significantly.

The resulting temperature-entropy diagram for normal hydrogen is presented in composite form in figures 31, 32, and 33. The thermal units used are based on the calorie, the Kelvin degree, and the gram, with pressures in atmospheres and densities in Amagat units.

The diagram shows lines of constant enthalpy, pressure and density and, in the region of coexistence of liquid and vapor, lines of constant "quality." The painstaking construction of the curves pertaining to the liquid region, amounting to a correlation of the data for the liquid, has been made by Robert N. Schwartz, who has also drawn the remainder of the diagram on the basis of the tables of this paper.

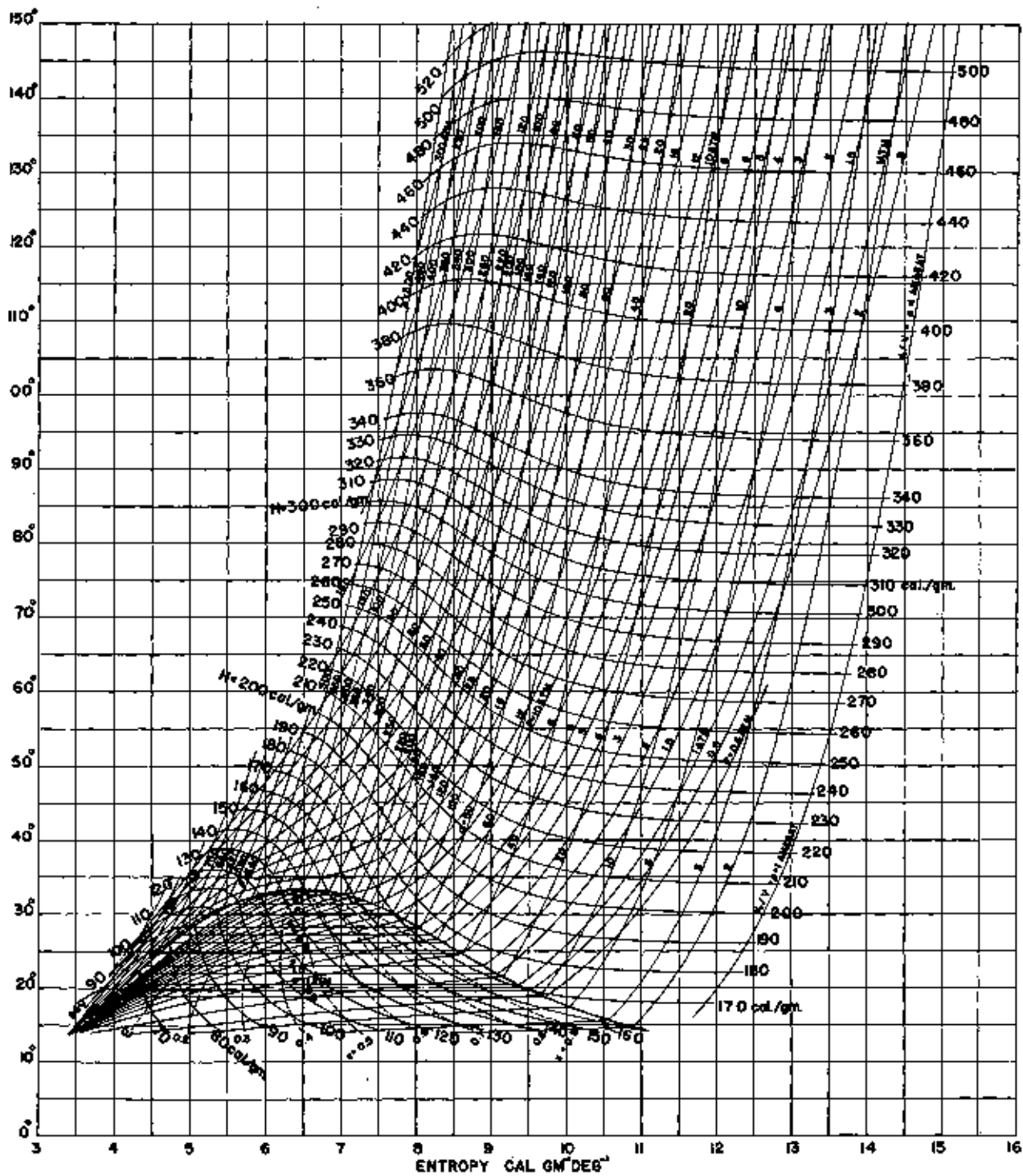


FIGURE 31. Temperature-entropy diagram for  $H_2$  in the region  $0^\circ$  to  $180^\circ$  K.

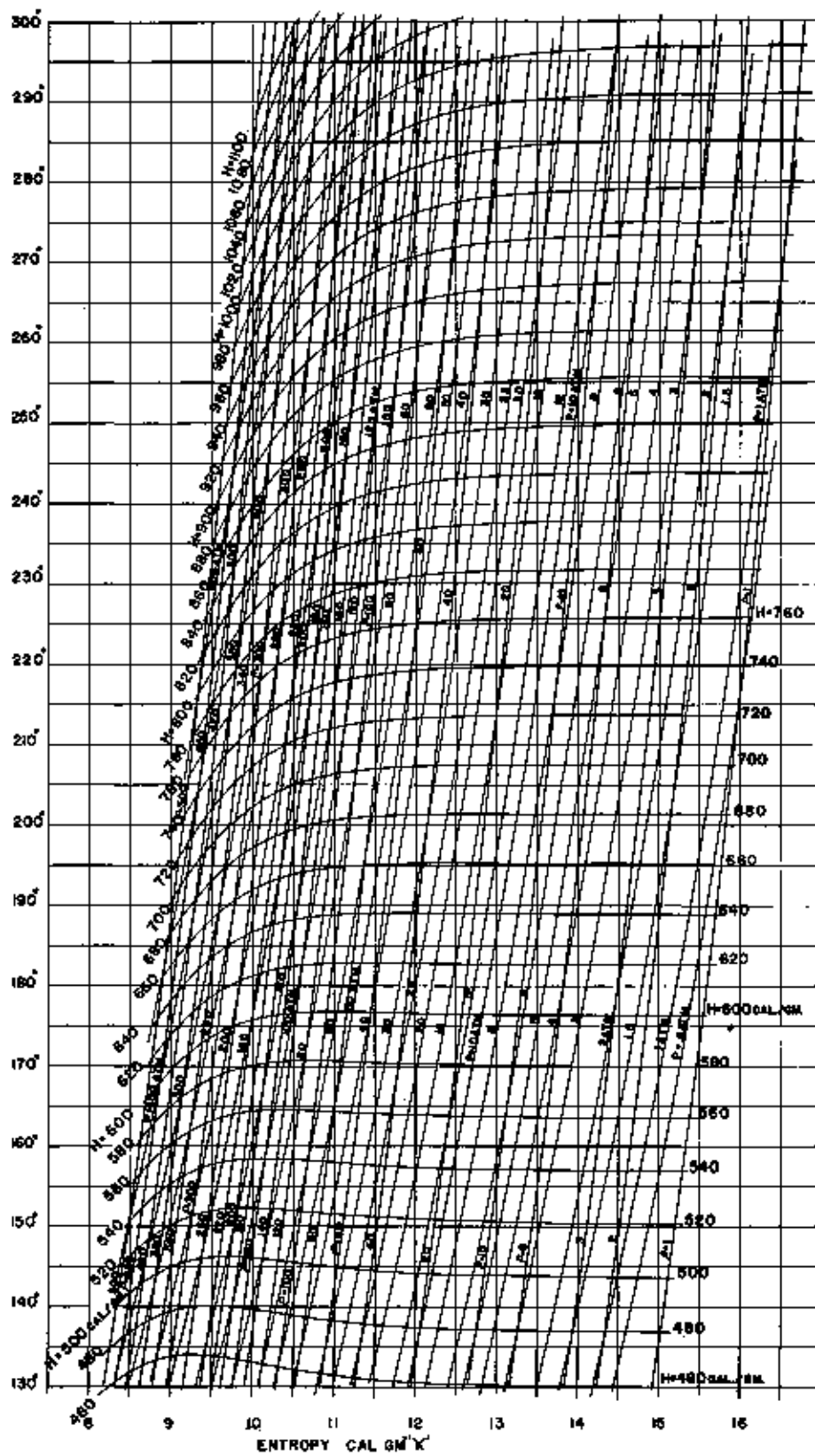


FIGURE 32. Temperature-entropy diagram for H<sub>2</sub> in the region 130° to 300° K.

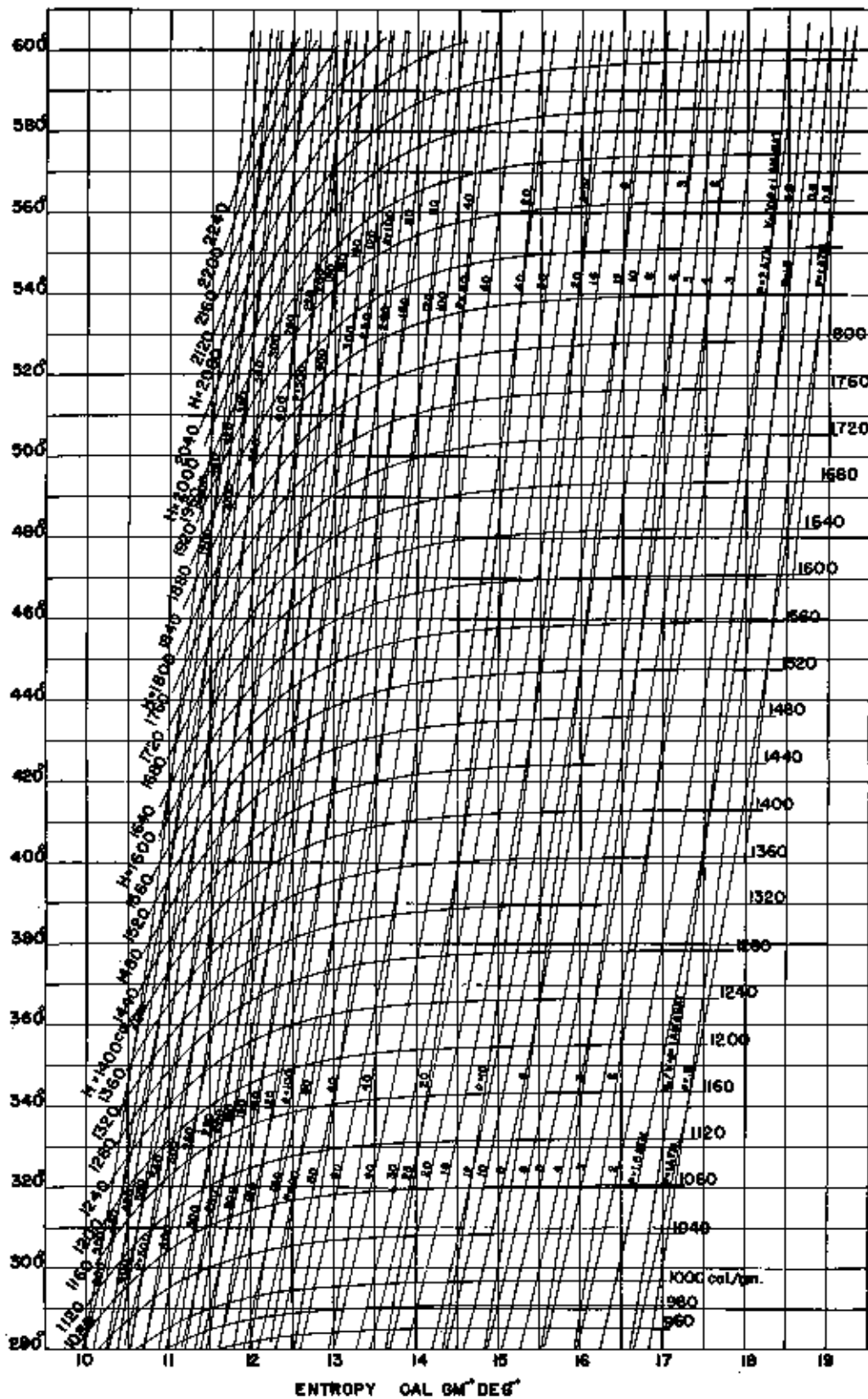


FIGURE 33. Temperature-entropy diagram for  $H_2$  in the region  $280^\circ$  to  $600^\circ$  K.

## XI. References

### I. Thermodynamic Properties of the Hydrogens in the Ideal Gas State

- [1] D. M. Dennison, *Proc. Roy. Soc. (London)* **115**, 483 (1927).
- [2] F. Rasetti, *Phys. Rev.* **34**, 367 (1929).
- [3] W. F. Giauque, *J. Am. Chem. Soc.* **52**, 4808 (1930).
- [4] W. F. Giauque, *J. Am. Chem. Soc.* **52**, 4816 (1930).
- [5] H. H. Hyman, *Phys. Rev.* **36**, 187 (1930).
- [6] H. H. Hyman and C. R. Jeppesen, *Nature* **125**, 462 (1930).
- [7] R. T. Birge and C. R. Jeppesen, *Nature* **125**, 463 (1930).
- [8] R. Rydberg, *Z. Physik* **73**, 376 (1931).
- [9] O. Klein, *Z. Physik* **76**, 226 (1932).
- [10] J. L. Dunham, *Phys. Rev.* **41**, 721 (1932).
- [11] R. W. Harkness and W. E. Deming, *J. Am. Chem. Soc.* **54**, 2850 (1932).
- [12] C. R. Jeppesen, *Phys. Rev.* **44**, 165 (1933).
- [13] H. C. Urey and D. Rittenberg, *J. Chem. Phys.* **1**, 137 (1933).
- [14] G. N. Lewis and M. F. Ashley, *Phys. Rev.* **43**, 837 (1933).
- [15] C. R. Jeppesen, *Phys. Rev.* **45**, 480 (1934).
- [16] K. Mie, *Z. Physik* **91**, 475 (1934).
- [17] C. O. Davis and H. L. Johnston, *J. Am. Chem. Soc.* **56**, 1045 (1934).
- [18] H. L. Johnston and E. A. Long, *J. Chem. Phys.* **2**, 389 (1934).
- [19] R. Wildt, *Z. Astrophysik* **9**, 176 (1934).
- [20] H. Beutler, *Z. physik. Chem. [B]* **27**, 287 (1934).
- [21] H. Beutler, *Z. physik. Chem. [B]* **29**, 315 (1935).
- [22] G. K. Teal and G. E. MacWood, *J. Chem. Phys.* **3**, 760 (1935).
- [23] Y. Fujioka and T. Wada, *Sci. Papers Inst. Phys. Chem. Research (Komagome, Hongo, Tokyo)* **27**, 210 (1935).
- [24] C. R. Jeppesen, *Phys. Rev.* **49**, 797 (1936).
- [25] I. Sandeman, *Proc. Roy. Soc. Edinburgh* **59**, 130 (1938-39).
- [26] R. T. Birge, *Rev. Modern Phys.* **13**, 233 (1941).
- [27] H. W. Woolley, *J. Chem. Phys.* **9**, 470 (1941).
- [28] D. D. Wagman, J. E. Kilpatrick, W. J. Taylor, K. S. Pitzer, and F. D. Rossini, *J. Research NBS* **34**, 143 (1945) RP1634.
- [29] G. N. Lewis and M. Randall, *Thermodynamics and the free energy of chemical substances* (McGraw-Hill Book Co., Inc., New York, N. Y., 1923).
- [30] P. S. Epstein, *Textbook on thermodynamics* (John Wiley and Sons, Inc., New York, N. Y., 1937).
- [31] F. H. Mac Dougall, *Thermodynamics and chemistry* (John Wiley and Sons, Inc., New York, N. Y., 1939).
- [32] S. Glasstone, *Textbook of physical chemistry* (D. Van Nostrand Co., Inc., New York, N. Y., 1940).

### 2. Thermal Measurements on Gaseous Hydrogen

- [33] O. Lummer and E. Pringsheim, *Wied. Ann.* **64**, 555 (1898).

- [34] M. Pier, *Z. Elektrochem.* **16**, 897 (1910).
- [35] N. Bjerrum, *Z. Elektrochem.* **18**, 101 (1912).
- [36] A. Eucken, *Sitzber. preuss. Akad. Wiss.* **1912**, 141 (1912).
- [37] K. Scheel and W. Heuse, *Ann. Physik* **40**, 473 (1913).
- [38] I. Langmuir and G. M. J. Mackay, *J. Am. Chem. Soc.* **36**, 1708 (1914).
- [39] I. Langmuir, *J. Am. Chem. Soc.* **37**, 417 (1915).
- [40] J. M. Crofts, *J. Chem. Soc.* **1915**, 290 (1915).
- [41] M. C. Shields, *Phys. Rev.* **10**, 525 (1917).
- [42] M. Trautz and K. Hebbel, *Ann. Physik* **74**, 285 (1924).
- [43] J. H. Brinkworth, *Proc. Roy. Soc. (London)* **107**, 510 (1925).
- [44] J. H. Partington and A. B. Howe, *Proc. Roy. Soc. (London)* **109**, 286 (1925).
- [45] F. A. Giacomini, *Phil. Mag.* **50**, 146 (1925).
- [46] R. E. Cornish and E. D. Eastman, *J. Am. Chem. Soc.* **50**, 627 (1928).
- [47] F. R. Bichowsky and L. C. Copeland, *J. Am. Chem. Soc.* **50**, 1315 (1928).
- [48] A. Eucken and K. Hiller, *Z. physik. Chem. [B]* **4**, 142 (1929).
- [49] E. J. Workman, *Phys. Rev.* **37**, 1345 (1931).
- [50] A. Eucken and O. Mücke, *Z. physik. Chem.* **18**, 167 (1932).
- [51] K. Wohl and M. Magat, *Z. physik. Chem.* **19**, 117 (1932).
- [52] A. Farkas, L. Farkas, and P. Harteck, *Proc. Roy. Soc. [A]* **144**, 481 (1934).
- [53] W. T. David and A. S. Lesh, *Phil. Mag.* **18**, 307 (1934).
- [54] D. Rittenberg, W. Bleakney, H. C. Urey, *J. Chem. Phys.* **2**, 48 (1934).
- [55] A. J. Gould, W. Bleakney, and H. S. Taylor, *J. Chem. Phys.* **2**, 362 (1934).
- [56] R. W. Fenning and A. C. Whiffen, *Phil. Trans. Roy. Soc. (London)*, **238**, 149 (1939).
- [57] H. L. Johnston, I. I. Bezman, and C. B. Hood, *J. Am. Chem. Soc.* **68**, 2367 (1946).
- [58] H. L. Johnston, C. A. Swanson, and H. E. Wirth, *J. Am. Chem. Soc.* **68**, 2373 (1946).

### 3. PVT Relations for Gaseous Hydrogens

- [59] H. Kamerlingh Onnes and C. Braak, *Commun. Phys. Lab. Univ. Leiden* **97a** (1906), **99a**, **100a** (1907).
- [60] H. Kamerlingh Onnes and W. J. de Haas, *Commun. Phys. Lab. Univ. Leiden* **127e** (1912).
- [61] P. Kohnstamm and K. W. Walstra, *Koninkl. Akad. Wetenschappen Amsterdam, Proc.* **17**, 203 (1914).
- [62] H. Kamerlingh Onnes, C. A. Crommelin, and P. G. Cath, *Commun. Phys. Lab. Univ. Leiden* **151c** (1917).
- [63] L. Holborn, *Ann. Physik* **63**, 674 (1920).
- [64] J. Palacios Martinez and H. Kamerlingh Onnes, *Commun. Phys. Lab. Univ. Leiden* **164** (1923).
- [65] H. Kamerlingh Onnes and F. M. Penning, *Commun. Phys. Lab. Univ. Leiden* **165b** (1923).
- [66] C. A. Crommelin and J. C. Swallow, *Commun. Phys. Lab. Univ. Leiden* **172a** (1924).
- [67] L. Holborn and J. Otto, *Z. Physik* **23**, 77 (1924).

- [68] F. P. G. A. J. van Agt and H. Kamerlingh Onnes, *Commun. Phys. Lab. Univ. Leiden* **176b** (1925).
- [69] F. P. G. A. J. van Agt, *Commun. Phys. Lab. Univ. Leiden* **176c** (1925).
- [70] L. Holburn and J. Otto, *Z. Physik* **33**, 1 (1925).
- [71] L. Holburn and J. Otto, *Z. Physik* **38**, 359 (1926).
- [72] G. P. Nijhoff and W. H. Keesom, *Commun. Phys. Lab. Univ. Leiden* **188d** (1927).
- [73] E. P. Bartlett, *J. Am. Chem. Soc.* **49**, 687 (1927).
- [74] E. P. Bartlett, H. L. Cupples, and T. H. Tremearne, *J. Am. Chem. Soc.* **50**, 1275 (1928).
- [75] G. P. Nijhoff and W. H. Keesom, *Commun. Phys. Lab. Univ. Leiden* **188e** (1928).
- [76] E. P. Bartlett, H. C. Hetherington, H. M. Kvalnes, and T. H. Tremearne, *J. Am. Chem. Soc.* **52**, 1363 (1930).
- [77] A. van Itterbeek and W. H. Keesom, *Commun. Phys. Lab. Univ. Leiden*, **216c** (1931).
- [78] A. van Itterbeek, *Commun. Phys. Lab. Univ. Leiden, Supp.* **70b** (1931).
- [79] A. Michels, G. P. Nijhoff, and A. J. J. Gerver, *Ann. Physik* **12**, 562 (1932).
- [80] W. E. Deming and L. E. Shupe, *Phys. Rev.* **40**, 848 (1932).
- [81] A. Michels and A. J. J. Gerver, *Ann. Physik* **16**, 745 (1933).
- [82] W. E. Deming and L. S. Deming, *Phys. Rev.* **45**, 109 (1934).
- [83] J. B. M. Coppock, *Trans. Faraday Soc.* **31**, 913 (1935).
- [84] G. E. Uhlenbeck and E. Beth, *Physica* **3**, 729 (1936).
- [85] K. Schäfer, *Z. physik. Chem. [B]* **36**, 85 (1937).
- [86] K. Schäfer, *Z. physik. Chem. [B]* **38**, 187 (1937).
- [87] J. de Boer and A. Michels, *Physica* **5**, 945 (1938).
- [88] R. Wiebe and V. L. Gaddy, *J. Am. Chem. Soc.* **60**, 2300 (1938).
- [89] F. G. Keyes, Gas thermometer scale corrections based on an objective correlation of available data for hydrogen, helium, and nitrogen; from: Temperature, its measurement and control in science and industry, American Institute of Physics, (Reinhold Publishing Corporation, 1941).
- [90] C. S. Cragoe, Slopes of the PV isotherms of some thermodynamic gases at pressures below two atmospheres; from: Temperature, its measurement and control in science and industry, American Institute of Physics (Reinhold Publishing Corporation, 1941); *J. Research NBS* **26**, 495 (1941) RP1393.
- [91] A. Michels and M. Goudekot, *Physica* **8**, 347 (1941).
- [92] A. Michels and M. Goudekot, *Physica* **8**, 353 (1941).
- [93] A. Michels and M. Goudekot, *Physica* **8**, 387 (1941).
- 4. Viscosity of Gaseous Hydrogen**
- [94] M. Trautz and P. B. Baumann, *Ann. Physik* **2**, 733 (1929).
- [95] M. Trautz and F. W. Stauf, *Ann. Physik* **2**, 737 (1929).
- [96] M. Trautz and W. Ludewigs, *Ann. Physik* **3**, 409 (1929).
- [97] M. Trautz and H. E. Binkele, *Ann. Physik* **5**, 561 (1930).
- [98] M. Trautz and A. Meister, *Ann. Physik* **7**, 409 (1930).
- [99] M. Trautz and R. Zink, *Ann. Physik* **7**, 427 (1930).
- [100] M. Trautz and F. Kurz, *Ann. Physik* **9**, 931 (1931).
- [101] M. Trautz and K. G. Sorg, *Ann. Physik* **10**, 81 (1931).
- [102] M. Trautz and R. Heberling, *Ann. Physik* **20**, 118 (1934).
- [103] B. P. Sutherland and O. Maass, *Canadian J. Research* **6**, 428 (1932).
- [104] H. Adzumi, *Bul. Chem. Soc. (Japan)* **12**, 199 (1937).
- [105] A. van Itterbeek and Miss A. Claes, *Nature* **143**, 793 (1938) and *Physica* **5**, 938 (1938).
- [106] A. van Itterbeek and O. van Paemal, *Physica* **7**, 265 (1940).
- [107] A. van Itterbeek and O. van Paemal, *Physica* **7**, 273 (1940).
- [108] W. H. Keesom and P. H. Keesom, *Physica* **7**, 29 (1940).
- [109] H. L. Johnston and K. E. McCloskey, *J. Phys. Chem.* **44**, 1038 (1940).
- [110] R. Wobser and F. Müller, *Kolloid-Beihfte* **52**, 165 (1941).
- 5. Thermal Conductivity of Gaseous Hydrogen**
- [111] A. Schleiermacher, *Wied. Ann.* **36**, 346 (1889).
- [112] A. Winkelmann, *Wied. Ann.* **44**, 177 and 429 (1891).
- [113] P. A. Eckerlein, *Ann. Physik* **3**, 120 (1900).
- [114] P. Gunther, *Dissertation, Halle* (1906).
- [115] A. Eucken, *Physik. Z.* **12**, 1101 (1911).
- [116] A. Eucken, *Physik. Z.* **14**, 324 (1913).
- [117] S. Weber, *Ann. Physik* **54**, 437 (1917).
- [118] E. Schneider, *Ann. Physik* **79**, 177 (1926).
- [119] E. Schneider, *Ann. Physik* **80**, 215 (1926).
- [120] H. Gregory and C. T. Archer, *Proc. Roy. Soc. [A]* **110**, 91 (1926).
- [121] K. F. Bonhoeffer and P. Harteck, *Z. physik. Chem. [B]* **4**, 113 (1929).
- [122] P. Harteck and H. W. Schmidt, *Z. physik. Chem. [B]* **21**, 447 (1933).
- [123] B. G. Dickens, *Proc. Roy. Soc. (London) [A]* **143**, 517 (1934).
- [124] W. G. Kannuluik and L. H. Martin, *Proc. Roy. Soc. (London) [A]* **144**, 496 (1934).
- [125] H. S. Gregory, *Proc. Roy. Soc. (London) [A]* **149**, 35 (1935).
- [126] W. Northdurft, *Ann. Physik* **28**, 137 (1937).
- [127] C. T. Archer, *Proc. Roy. Soc.* **165**, 474 (1938).
- [128] H. Spencer-Gregory and E. H. Dock, *Phil. Mag.* **25**, 129 (1938).
- [129] N. B. Vargaftik and I. D. Parfenov, *J. Exptl. Theoret. Phys. (U. S. S. R.)* **8**, 189 (1938).
- [130] W. G. Kannuluik, *Proc. Roy. Soc. (London) [A]* **175**, 36 (1940).
- [131] H. L. Johnston and E. R. Grilly, *J. Chem. Phys.* **14**, 233 (1946).
- 6. Viscosity and Thermal Conductivity of Gaseous Hydrogen at High Pressure**
- [132] D. Enskog, *Kungl. Svenska Vetenskaps Akademiens Handl.* **63**, No. 4 (1921).
- [133] H. B. Phillips, *J. Math. Phys.* **1**, 42 (1922).



- [134] J. H. Boyd, Jr., *Phys. Rev.* **35**, 1284 (1930).  
 [135] R. O. Gibson, Dissertation, Amsterdam (1933).  
 [136] E. W. Comings and R. S. Egly, *Ind. Eng. Chem.* **32**, 714 (1940).  
 [137] S. Chapman and T. G. Cowling, *The mathematical theory of nonuniform gases*, (Cambridge at the University Press, 1939).

### 7. Viscosity of Liquid Hydrogen

- [138] J. E. Verschaffelt and C. Nicaise, *Commun. Phys. Lab. Leiden* **151g** (1917).  
 [139] W. H. Keesom and G. E. MacWood, *Physica* **5**, 745 (1938).  
 [140] H. E. Johns, *Can. J. Research* **17** [A] 221 (1939).

### 8. Vapor Pressures

- [141] H. Kamerlingh Onnes and W. H. Keesom, *Commun. Phys. Lab. Univ. Leiden*, **137d** (1913).  
 [142] P. G. Cath and H. Kamerlingh Onnes, *Commun. Phys. Lab. Univ. Leiden*, **132a** (1917).  
 [143] J. Palacios Martinez and H. Kamerlingh Onnes, *Commun. Phys. Lab. Univ. Leiden*, **156b** (1922).  
 [144] F. Henning, *Z. Physik* **40**, 775 (1926).  
 [145] W. H. Keesom, A. Bijl, and Miss H. Van der Horst, *Commun. Phys. Lab. Univ. Leiden*, **217a** (1931).  
 [146] F. G. Brickwedde and R. B. Scott, *The vapor pressures of mixtures of ortho and para hydrogen* (Unpublished).  
 [147] E. Cremer and M. Polanyi, *Z. physik. Chem. [B]* **21**, 459 (1933).  
 [148] R. B. Scott, F. G. Brickwedde, H. C. Urey, and M. H. Wahl, *J. Chem. Phys.* **2**, 454 (1934).  
 [149] F. G. Brickwedde, R. B. Scott, and H. S. Taylor, *J. Research NBS* **15**, 463 (1935) RPS41; *J. Chem. Phys.* **3**, 653 (1935).  
 [150] F. G. Brickwedde and R. B. Scott, *Vapor pressures, specific heats, heats of transition and molecular volumes of liquid and solid hydrogen deuteride* (Unpublished).  
 [151] R. D. O'Neal and M. Goldhaber, *Phys. Rev.* **56**, 574 (1940).  
 [152] W. F. Libby and C. A. Barter, *J. Chem. Phys.* **10**, 184 (1942).

### 9. Melting Curves

- [153] H. Kamerlingh Onnes and W. van Gulik, *Commun. Phys. Lab. Univ. Leiden* **184a** (1926).  
 [154] W. van Gulik and W. H. Keesom, *Commun. Phys. Lab. Univ. Leiden* **192b** (1928).  
 [155] F. Simon, M. Ruhemann, and W. A. M. Edwards, *Z. physik. Chem. [B]* **6**, 331 (1929).  
 [156] W. H. Keesom and J. H. C. Lisman, *Commun. Phys. Lab. Univ. Leiden* **213e** (1931).

- [157] W. H. Keesom and J. H. C. Lisman, *Commun. Phys. Lab. Univ. Leiden* **221a** (1932).

### 10. PVT Relations for Condensed Phases

- [158] J. Dewar, *Proc. Roy. Soc. [A]* **73**, 251 (1904).  
 [159] H. Kamerlingh Onnes and C. A. Crommelin, *Commun. Phys. Lab. Univ. Leiden* **137a** (1913).  
 [160] H. Augustin, *Ann. Physik* **46**, 419 (1915).  
 [161] E. Mathias, C. A. Crommelin, and H. Kamerlingh Onnes, *Commun. Phys. Lab. Univ. Leiden* **154b** (1921).  
 [162] W. H. Keesom, J. de Smedt, and H. II. Mooy, *K. Akad. Wetensch. Amsterdam, Proc.* **33**, 8, 814 (1930); *Commun. Phys. Lab. Univ. Leiden* **200d** (1930).  
 [163] R. B. Scott and F. G. Brickwedde, *J. Research NBS* **19**, 237 (1937) RP1023.  
 [164] K. Schäfer, *Naturwissenschaften* **26**, 563 (1938).  
 [165] Helen D. Megaw, *Phil. Mag.* **26**, 129 (1939).  
 [166] K. Cohen and H. C. Urey, *J. Chem. Phys.* **7**, 157 (1939).

### 11. Thermal Properties of Condensed Hydrogen

- [167] W. H. Keesom, *Commun. Phys. Lab. Univ. Leiden* **137e** (1911).  
 [168] A. Eucken, *Verh. deut. Phys. Ges.* **18**, 18 (1916).  
 [169] A. Eucken, *Verh. deut. Phys. Ges.* **15**, 4 (1916).  
 [170] W. H. Keesom and H. Kamerlingh Onnes, *Commun. Phys. Lab. Univ. Leiden* **153c** (1917).  
 [171] F. Simon and F. Lange, *Z. Physik* **15**, 312 (1923).  
 [172] K. Clusius and K. Hiller, *Z. physik. Chem. [B]* **4**, 158 (1929).  
 [173] K. Mendelssohn, M. Ruhemann, and F. Simon, *Z. physik. Chem. [B]* **15**, 121 (1931).  
 [174] K. Clusius and E. Bartholomé, *Z. physik. Chem. [B]* **30**, 237 (1935).  
 [175] A. Pitt and W. J. Jackson, *Can. J. Research* **12**, 688 (1935).  
 [176] E. Bartholomé and A. Eucken, *Z. Elektrochem.* **42**, 547 (1936).  
 [177] E. Bartholomé, *Z. physik. Chem. [B]* **33**, 387 (1936).  
 [178] H. Gutsche, *Z. physik. Chem. [A]* **164**, 45 (1939).

### 12. Unclassified

- [179] G. Rutledge, *Phys. Rev.* **40**, 262 (1932).  
 [180] H. J. Hoge and F. G. Brickwedde, *J. Research NBS* **22**, 351 (1939) RP1188.  
 [181] *Mathematical Tables Project, Tables of Lagrangian Interpolation Coefficients*, (Columbia University Press, 1944).

WASHINGTON, August 7, 1947.